Geomorphological and Geophysical Investigation of the Effects of Active Tectonic Deformation on the Hydrogeology of North Culverden Basin, North Canterbury

A thesis
submitted in partial fulfillment
of the requirements for the Degree
of
DOCTOR OF PHILOSOPHY IN GEOLOGICAL SCIENCES
at the
University of Canterbury

by

MARK JAMES ARMSTRONG

University of Canterbury
2000

Frontispiece: Oblique aerial photograph looking northwards along the eastern margin of Culverden Basin

ABSTRACT

This thesis examines the complex interaction between the tectonic evolution of Culverden Basin and the Late Quaternary sediments, which form the aquifer-bearing deposits, using geological and geomorphological mapping as well as near-surface geophysical investigations.

Along the eastern margin of Culverden Basin, the deformation associated with the actively widening Australian-Pacific plate boundary zone, has resulted in the evolution of Culverden Basin and the progressive inversion of the basin floor. The eastern margin of the basin is structurally controlled by a NE trending, complexly segmented range-front fault system and associated thrust-propagated anticlines forming the basin boundary. Basin inversion is driven by the westward propagation of footwall imbricate thrusts and associated folds. The inversion of the basin floor lead to the creation of sub-basins within the larger basin, which have controlled the distribution and architecture of the Late Quaternary stratigraphy.

The Late Quaternary sedimentary record documents periods of climatically induced aggradation during cold conditions and degradation in the intervening warmer times. The interaction between the sedimentation and ongoing tectonic deformation has resulted in complex lithological relationships between the locally sourced alluvial fans and the glacial outwash deposits of the major rivers entering the basin.

The architecture of the aquifers is therefore controlled by the changing fluvial regime and its interaction with the evolving sub-basins. The progressive evolution of the sub-basins leads to increasing complexities in the facies relationships and to the confinement of the deposits into progressively smaller portions of the sub-basins. Once the basin boundaries become emergent, the basin becomes isolated, and potentially cut-off from its groundwater recharge source.

Leonard Mound is an actively evolving imbricate thrust system along the eastern margin of Culverden Basin that has isolated the Wynyard sub-basin from the central portion of Culverden Basin, during the Late Pleistocene and present. The emergence of Leonard Mound is preventing the recharge to the Wynyard sub-basin from the high yielding aquifers of the central portion of the basin. In the central portion of Culverden Basin, high natural recharge combined with an irrigation scheme has allowed for transformation of the basin into a major dairy farming centre. In contrast, the Wynyard sub-basin is still subjected to frequent summer droughts, making it desirable to find a better source of groundwater for the eastern margin of the basin.

The hydrogeological model provided by the Culverden Basin almost certainly has wider implications to the groundwater resources of other basins in similar active tectonic settings.

TABLE OF CONTENTS

LIST OF FIGURES

CHAPTER 1

CHAPTER 2

CHAPTER 3

CHAPTER 4

CHAPTER 5

APPENDICES

LIST OF TABLES

CONTENTS OF VOLUME 2

FIGURES

MAPS AND CROSS SECTIONS

GPR PROFILES

ACKNOWLEDGEMENTS

I would like to thank many people in the department for their help and support during the course of this thesis. Firstly there are my three supervisors, Jarg Pettinga, David Nobes and Jocelyn Campbell, who are gratefully acknowledged for all their assistance, especially in the final few months of the project. Many thanks to the Active Tectonics Research Group and Mason Trust whose funding made the project feasible. The Active Tectonics Research Group also supplied the Hilux 4WD vehicle, which thankfully was never dented/scratched during my time. I also wish to thanks Nicola Litchfield and Hamish Kellahan for discussions on North Canterbury tectonics. I must also thank Trevor Webb, Landcare Research for access to his unpublished soil maps of the basin.

All the farmers in the district are gratefully acknowledged for allowing access to their properties. In particular, I wish to thank Richard and Janine Ormond and Tom and Fiona Burrows for accommodation during my stays in the basin.

A huge thanks goes to all the technical staff in the department without whom theses could not be done. Namely Mike and John for all their computer help, Lee for drafting, Kerry for photo developing and occasional games of squash, Arthur for slides and installing the fear of damaging the Hilux into all of us, Rob for thin sections and the chopping board and Cathy for doing a fantastic job keeping the geophysical equipment well maintained and organised.

Due to the nature of the geophysical surveying, field assistants were required at various times. The data could never have been collected without them. I wish to thank the 1997 4^{th} year geophysics students whose project it was to survey various portions of Leonard Mound and the basin: Ashley, Stefan, Debbie, Amanda, Danny, Cameron, Andre, Mark, Norman, Anabel, Philippa and Marli. Cheers guys as it saved me a lot of time. I also wish to thank Phoebe and Sartan for their invaluable help. Phoebe is also thanked for various discussions on the usefulness of TEM in delineating different gravel packages.

A special thanks has to go to all the fellow students whom have graced me with their presence over the last few years. To the members of the SGS, Steve, Al, Rod, Rach, Phil, Richard and Jezza, thanks guys for some awesome times. In particular I wish to say a huge cheers to Steve, room-mate for 3 years, co-inventor of indoor softball and kart champion, Al for constantly twisting my rubber arm into a few not so quiet Blue Ducks at the Dux, Jezza for reminding us that all women are beautiful, and Richy Jongens for teaching me that stress never pays. I will always look forward to seeing you guys for a few more quiets at the Dux.

And finally to the people most dearest to me, without whom I could not have made it. First and foremost I wish to thank my parents for all their support and encouragement throughout my time at university, and without whom this would not have been possible. My two sisters are thanked for being there and offering plenty of encouragement when it was needed. To Paul and Kate many, many thanks for all the encouragement, meals and great times so far and long may they continue. Kate is also thanked for her help in the compilation of the thesis. And finally, a very special thank-you goes to Sonya for all her help throughout the course of my thesis, and for making the last 5 years absolutely fantastic.

THANKYOU ONE AND ALL!!!

CHAPTER 1

INTRODUCTION

1.1 BACKGROUND

Low annual rainfall and frequent summer droughts has led to traditional land use within Culverden Basin being limited to sheep and cattle grazing, requiring relatively low amounts of water. Over the last two decades the central portion of the basin has been transformed into a major dairy farming centre due to the development of an irrigation scheme in the late 1970's. Whilst the irrigation scheme has removed the dependency on the groundwater for the central portions of Culverden Basin, the non-irrigated eastern margin is still prone to summer droughts. Therefore, there is a need to find a greater source of groundwater for the landowners along the eastern basin margin, requiring the evaluation of the groundwater resource of Culverden Basin.

To evaluate the groundwater resource, a hydrogeological model for the basin needs to be developed. There are three steps involved in the development of a hydrogeological model (Stone, 1999): (1) compiling the basic geologic and hydrologic information, (2) characterizing the geologic setting and hydrologic system, and (3) synthesizing this information into a hydrogeologic model.

This thesis takes the first fundamental step in the process, which is the characterization of the geological setting of the northern portion of Culverden Basin, in particular the eastern margin of the basin. It was not in the scope of this study to determine the hydrologic properties (e.g. transmissivity, storativity, hydraulic conductivity etc.) of the system. They need to be the focus of future research to fully evaluate the groundwater resource. Although the northern portion of the basin has been mapped previously (Falloon, 1954; Gregg, 1964; Clayton, 1965 and 1968), the relationships arising from the interaction of an actively evolving imbricate thrust system superimposed on a complex fluvial architecture, have remained unrecognized and not studied by previous workers. These relationships are playing vital roles in the

groundwater regime, and hence must be understood if a hydrogeological model is to be devised.

In conjunction with the geological and geomorphological mapping, four geophysical techniques were used to confirm the geological and geomorphic interpretations, determine the thicknesses of the various units and gauge the amount of displacement across the structures. When started, this was one of the first theses to use two of the shallow geophysical techniques employed in this study (time–domain electromagnetics (TEM) and ground penetrating radar (GPR)) within New Zealand. Consequently, a fundamental objective was to determine the suitability of the methods in active tectonic and hydrogeologic studies and whether or not they would be valuable tools for future investigations.

1.2 THESIS OBJECTIVES

This thesis has the following objectives.

1. Using geological and geomorphological mapping, integrated with selected geophysical techniques, develop an understanding of the structural setting and evolution of north Culverden Basin.
2. Investigate, using detailed geomorphological mapping, the relationships between the active tectonic deformation, fluvial architecture and groundwater along the structurally complex eastern margin of north Culverden Basin.
3. Evaluation of the selected geophysical techniques, especially time domain electromagnetics (TEM) and ground penetrating radar (GPR), in hydrogeological and active tectonic investigations with respect to the North Canterbury fluvial setting in Culverden Basin.
4. Develop a conceptual hydrogeological model, based on north Culverden Basin, focusing on the effects of tectonic deformation on the aquifer systems of basins situated in active tectonic settings.
5. Consider issues concerning the future evaluation of the groundwater resource in Culverden Basin, with respect to the hydrogeologic model developed for north Culverden Basin.

1.3 REGIONAL SETTING

The New Zealand continent straddles the Australian-Pacific plate boundary, which may have initiated as early as 40 ma ago, after New Zealand separated from Antarctica and Australia about 75 ma (Pettinga et al., 1998). Progressive changes in the plate convergence direction, resulting from a south-westward shift in the pole of rotation, from about 10ma ago (Walcott, 1984), lead to the development of oppositely dipping convergent subduction systems at the northern and southern ends of the continent (Figure 1.1). The northern end of the continent saw the development of the eastward facing Kermadec-Hikurangi trench during the late Oligocene-Miocene, and later during the Pliocene the westward facing Puysegur trench developed to the south of the emerged land mass.

The transition between these two subducting systems is dominated by the Alpine Fault and the regional strike-slip faults of the Marlborough Fault System. There are four main faults in the Marlborough Fault System: Wairau, Awatere, Clarence and Hope Faults. It is well documented that activity on these four main faults decreases northward (Campbell 1973; 1992). Studies have also shown that these faults have formed sequentially from north to south (Lamb and Bibby, 1989; Cowan, 1992) indicating that the zone of oblique continental collision has progressively widened to the south since the inception of the present convergent plate boundary regime.

Traditionally the Hope Fault has been considered to be the southern boundary of the Marlborough Fault System, and is currently the most active of the faults. The Hope Fault is strongly segmented with slip rates varying from 14±3 mm/yr (Cowan, 1990) west of Hanmer basin to greater than 30 mm/yr to the east. Shear along the Hope Fault now appears to be confined to a narrow corridor, but indications of a once broader zone of disseminated strain are evident from folds dragged into and truncated against the fault. Further to the south, the developing Porters Pass-Amberley Fault Zone (PPAFZ) is a highly active zone of interconnected strike-slip faults, oblique thrusts and associated fault-propagated folds, and represents the juvenile stages of a future through-going strike-slip fault, reflecting the southward propagation of the Marlborough Fault System.

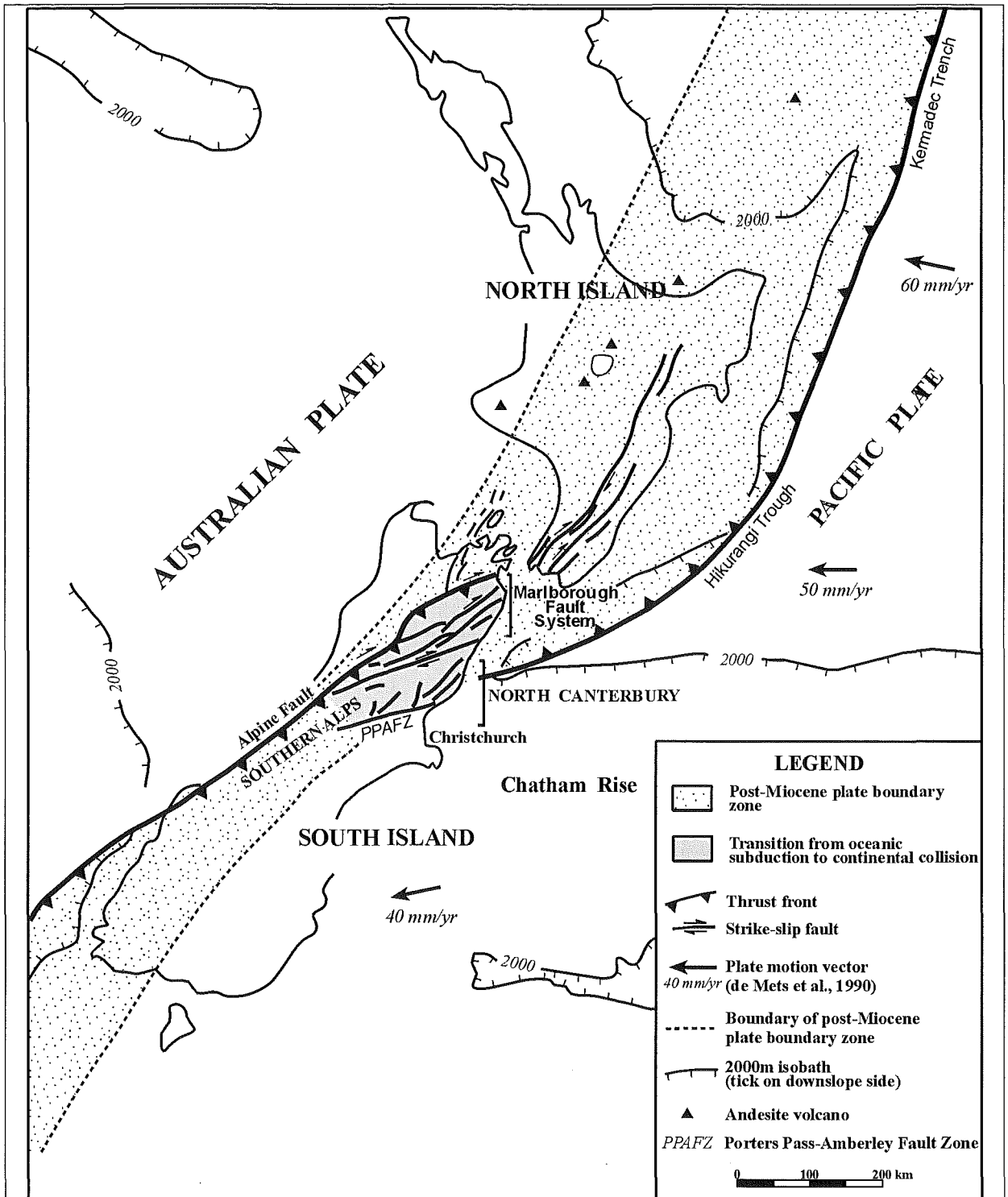

FIGURE 1.1. Elements of the Australia-Pacific plate boundary zone in New Zealand (after Cowan, 1990).

In North Canterbury and Marlborough, the transition from subduction to collision (Reyners and Cowan, 1993) has been responsible for crustal shortening and thickening. This has resulted in the formation of NE-SW striking thrusts and/or reverse faults and asymmetric folds (Yousif, 1987; Litchfield, 1996; Kellahan, 1998) which have accommodated 12-15 % (Nicol,

1991; Nicol et al., 1994; Cowan et al., 1996) of shortening during the Pleistocene. Seismicity studies have shown that this effect may be relatively thin-skinned extending down to 12-15 km in the crust (Reyners and Cowan, 1993).

Plate motion vectors (de Mets et al, 1990) and principal horizontal compression directions for the South Island (Bibby, 1970, 1976, 1981; Arabasz and Robinson, 1976; Rynn and Scholz, 1978; Walcott, 1978; Nicol and Campbell, 1990; Nicol and Wise, 1992; Pettinga and Wise, 1994) all predict a NE-SW trend of the faults in the North Canterbury region. However, along the southwestern margin (Nicol, 1991, 1992; Mould, 1992) a more northerly trend is observed, and in the Weka Pass area (Nicol, 1991, 1992) W-E trending structures are observed. The change in orientation of the faults and folds has been attributed to W-E oriented, north-facing normal faults that have been active from the Cretaceous to the present (Barnes, 1993) and have subsequently been overprinted by the Late Cainozoic deformation.

Since the Late Miocene, the rate of tectonism has increased dramatically reaching its maximum in the Pliocene (1-2 Ma) and continuing through to the present. It has become apparent that deformation in North Canterbury commenced within the last 0.5-1 million years (Nicol, 1991; Cowan, 1992; Mould, 1992; Nicol et al., 1994; Litchfield, 1995; Kellahan, 1998). The Late Cainozoic deformation was responsible for the rapid widening of the plate boundary zone and for the formation of the thrust and fold belt seen today.

The deformation associated with the active continental collision has produced 5 structural domains (Pettinga et. al., 1995), shown in Figure 1.2 and outlined below:

- *Domain 1 – Marlborough Fault Zone:* A major system of NE trending strike-slip faults including the Awatere, Clarence and Hope faults that splay at their SW and NE terminations producing imbricate thrust systems.

- *Domain 2 – West Culverden Fault Zone:* A zone of predominantly west dipping thrusts and/or reverse faults and associated fault propagated folds, inferred to represent back-thrusting off the Alpine Fault.

- *Domain 3 – Porters Pass-Amberley Fault Zone:* A Late Pleistocene hybrid system of ENE trending strike-slip faults, oblique thrusts and fault propagated folds interconnected by

transfer faults and ramp structures along the west margin of the Canterbury Plains. The juvenile system reflects the latest phase of plate boundary zone widening.

- *Domain 4 – North Canterbury Fold and Fault Belt:* A domain of east dipping thrusts extending southwest from Kaikoura through the NE part of the onshore Canterbury region, and offshore across the continental shelf. The thrusting has resulted in the development of asymmetric anticline/syncline pairs, producing Torlesse basement cored ranges and basins floored by Quaternary alluvium and Tertiary formations. These faults extend to within 5 km of the Hope Fault, indicating that the major strike-slip faulting is mainly restricted to the Hope Fault zone, and highly developed strain partitioning in the upper crust.

As is seen from Figure 1.2, Culverden Basin is situated between domains 2, 4 and 5 and represents a relatively undeformed piece of the upper crust preserving the Late Cretaceous to Tertiary strata as well as the extensive Late Quaternary fluvial and glacio-fluvial deposits.

1.4 LOCATION AND PHYSIOGRAPHY

Culverden Basin is the largest of three inland basins (Cheviot Basin, Culverden Basin and Lees Valley) in North Canterbury (Figure 1.3). Located 90 km north of Christchurch and 35 km inland, Culverden Basin is approximately 55 km long by 20 km wide and covers an area of 17,000 hectares. The basin is surrounded by steep rugged ranges composed of Torlesse basement rocks, up to 900 m in elevation, with low, rolling hills of Tertiary strata in front of the ranges.

Four major rivers (Waiau, Hurunui, Pahau and Waitohi) cut across the basin floor. Both the Waiau and Hurunui Rivers have cut gorges in the ranges on either side of the basin and are braided across the floor of the basin. The area has a mean average rainfall of 750 mm with frequent summer droughts which, prior to the 1970's, controlled the land use in the basin. Historically, land use in the basin has been 80 percent sheep grazing, 10 percent cattle grazing and 10 percent cropping (Close, 1987). However, with the development of an irrigation scheme in the late 1970's, the basin has seen a dramatic change in land use. Now dairying dominates the land use of the basin floor while sheep and cattle grazing still predominate on the hills and unirrigated areas. Due to the irrigation scheme, farmers have border dyked their

paddocks to reduce surface flooding which has destroyed most of the subtle geomorphic features that were visible on the older airphotos.

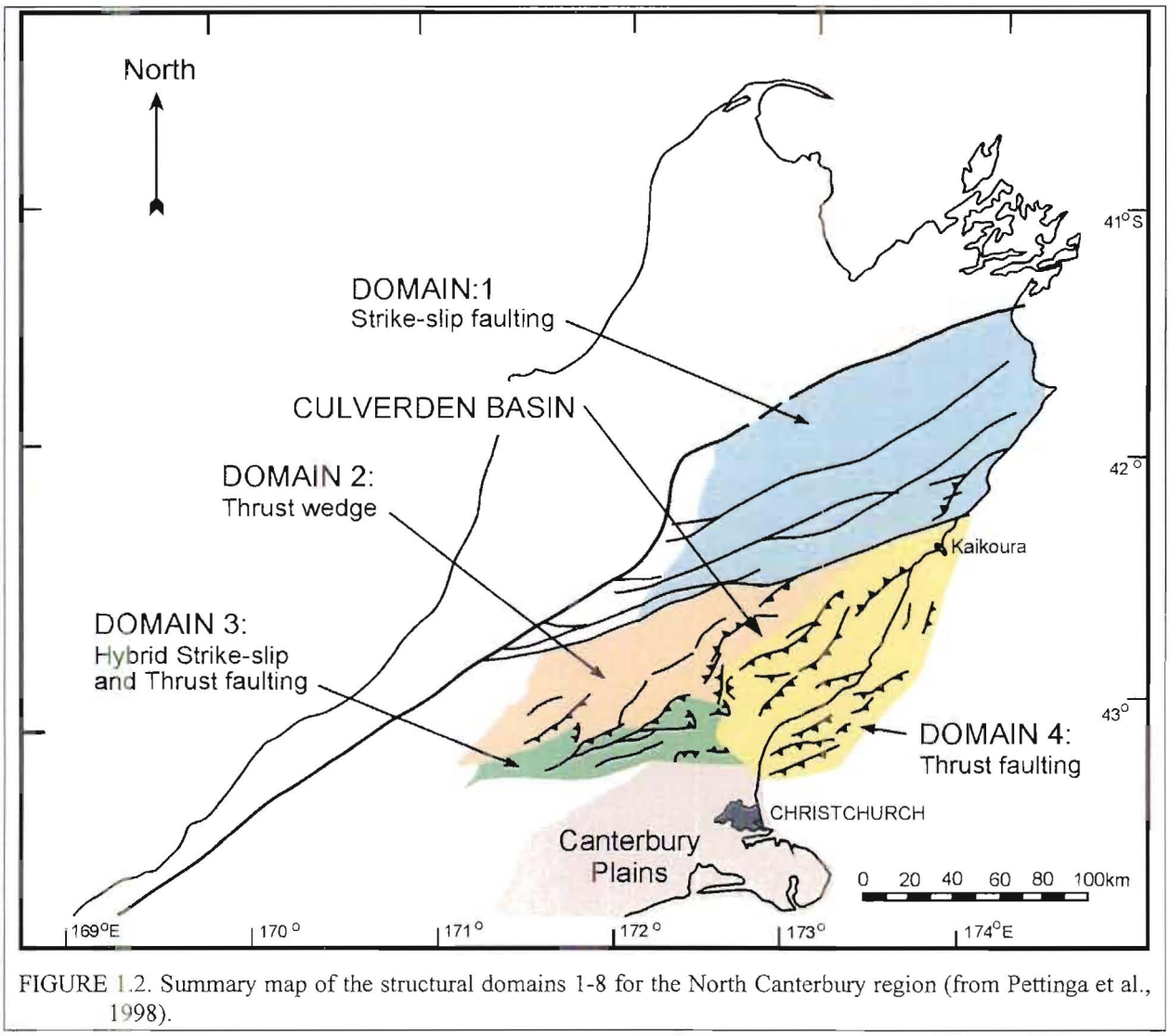

FIGURE 1.2. Summary map of the structural domains 1-8 for the North Canterbury region (from Pettinga et al., 1998).

The study area itself is essentially the eastern margin of the basin extending from the Waitohi River in the south to gridline 5845000N (NZMS 260) in the north. The crest of the Lowry Peaks Range marks the eastern boundary which was in part a common boundary with Litchfield (1996) and Kellahan (1998) (Figure 1.4). The study area incorporates the floor of the basin from the Waiau River southward to the Waitohi River. Figure 1.4 also shows the major topographic features of the field area that will be referred to throughout the course of this thesis. Reconnaissance mapping of the hills and ranges bounding the western and northwestern margins was carried out so as to understand the tectonic setting of the basin.

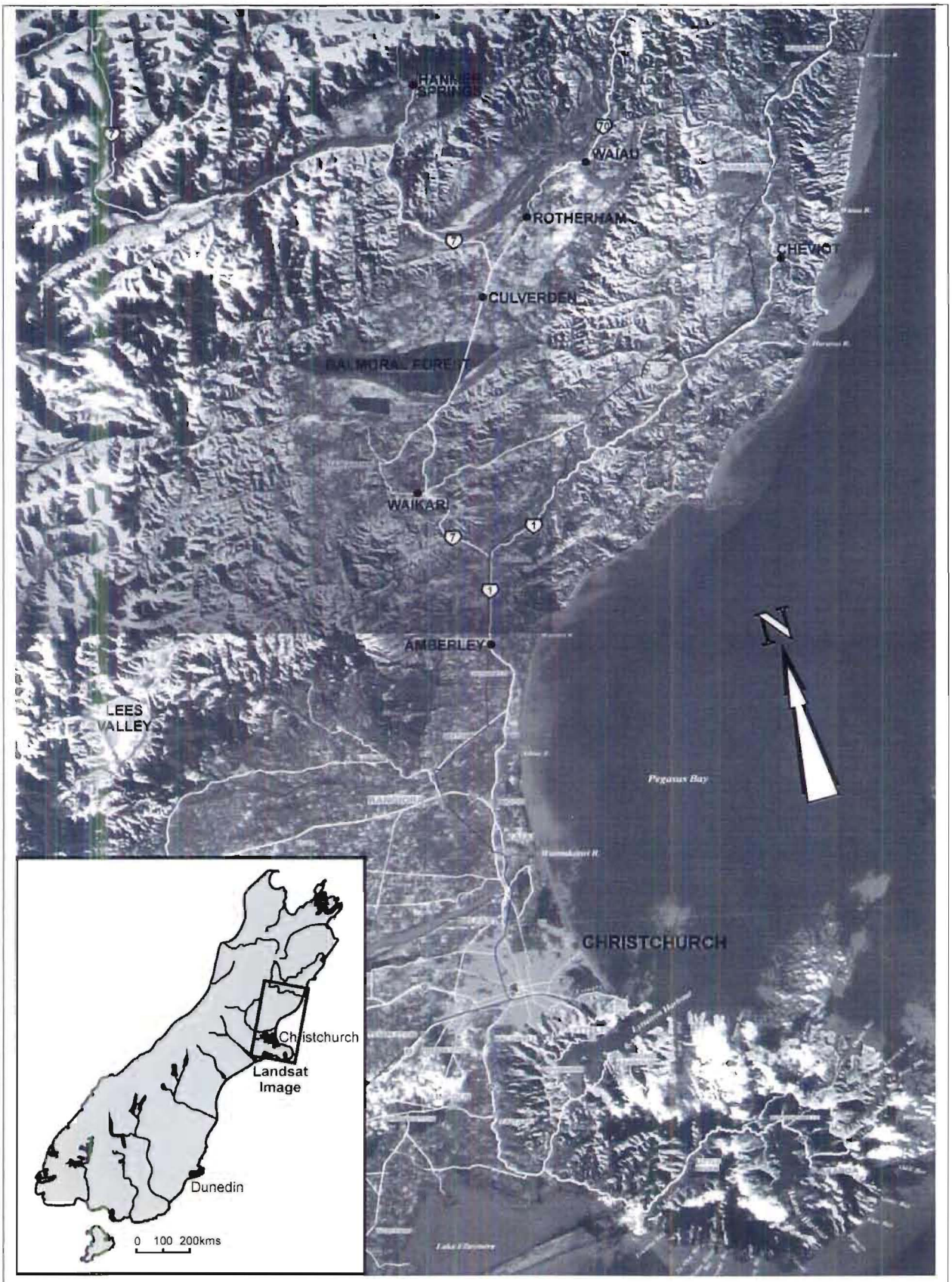

FIGURE 1.3. Landsat image of Banks Peninsula and North Canterbury. Culverden Basin is readily observed, bounded on the north and west by the mountainous areas of the Southern Alps and to the east by the North Canterbury Fold and Fault Belt.

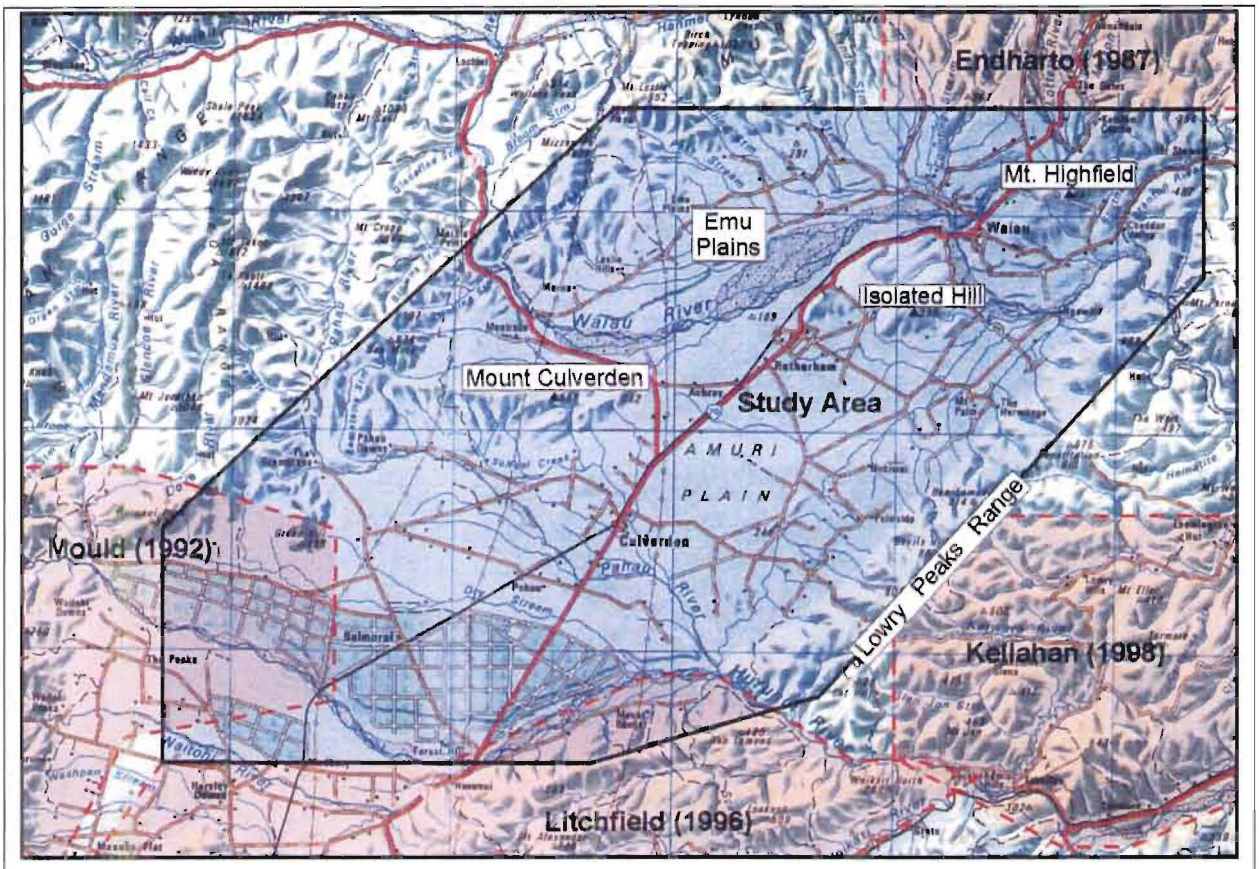

FIGURE 1.4. Locality diagram of study area and four recently completed M.Sc. thesis studies which lie adjacent to this thesis study.

1.5 PREVIOUS WORK

The early geologists (Buchanan, 1868; Haast, 1871a; 1871b ; 1879; Hutton, 1874, 1885, 1888; McKay, 1890, 1892) all focused on the stratigraphy and physical features of the region primarily north of Waiau and in the Waikari area. Early in the 20th century, Cotton (1913) was the first to suggest that the ranges are basement-cored anticlines and that the major rivers are antecedent. Following that Speight (1915 and 1926) concluded that the Culverden Basin was formed as a result of both faulting and folding in his study of intermontane basins in North Canterbury.

Several Ph.D. and M.Sc. theses have focused on areas in and around Culverden Basin. The first was by Schofield (1949) followed shortly by Hamilton (1950) and then Falloon (1954). Both Schofield and Hamilton focused on the Waikari area and in particular the stratigraphy with very little emphasis on the structure. Falloon (1954) was the first to study the entire Culverden Basin and by drawing on Hamilton's work correlated the units across the entire basin. The Late Pleistocene geology was mapped by Clayton (1965) who correlated the gravel

deposits on the floor of the basin and around the margins to the glacial deposits seen in the Hope River.

The glacial deposits of the Hurunui River were first described by Speight (1918), but it wasn't until Powers (1962), who described the terraces of the Hurunui River, that an understanding of the Late Pleistocene history of the basin was gained. Powers work was closely followed by a thesis by Read (1964) dealing with the glacial geology of the Hurunui River between Lake Sumner and the Mandamus River.

The stratigraphy and structure of the northern end of the basin has been addressed in four theses: Gregg, 1965; Lammerink, 1976; Coote, 1987; Endharto, 1987. Gregg (1965) mapped the pre-quaternary geology around Waiau township and was the first to map some of the major structural features. Part of the area was revisited by Lammerink (1976) who mapped in greater detail the structure of the Mount Highfield Fold and Highfield Folds. More recently Coote (1987) and Endharto (1987) studied the Cookson Volcanics and tectonics in the region between Waiau and the Hope Fault. Coote's thesis was the first to study in detail the petrography and petrology of the Cookson Volcanics and investigate their tectonic history. At the same time Endharto (1987) looked at the Wandle En Echelon Fold System developing in the shear belt between the Hope Fault and the Rahi Fault.

With the inception of the Active Tectonics Research Group, a number of Ph.D. and M.Sc. thesis have been completed in areas immediately adjacent to this field area. Although not within the field area, Nicol's (1991) thesis was the first to study in detail the folding style and kinematics in the North Canterbury region. Structural interpretation by Mould (1992) showed that the western margin of Culverden Basin is dominated by westward dipping reverse faults that are inferred to be back-thrusts off the Alpine Fault system. Litchfield (1995) mapped the southern end of the Lowry Peaks Range and the adjacent Waikari Valley. To the east of Culverden Basin, the Cheviot Basin is one of the series of inland basins across North Canterbury and was the focus of the most recent mapping thesis by Kellahan (1998). Although not strictly in the immediate area, Kellahan's work provided useful insights into the stratigraphy, which was so poorly exposed in the Culverden Basin.

Several workers (Andrews, 1960, 1963 and 1968; Browne and Field, 1985 and 1988; Field and Browne, 1989) have attempted to produce a lithostratigraphic correlation for the whole of North Canterbury. Gregg (1964) produced the 1:250,000 geological map of the Hurunui Region drawing mainly on Hamilton's 1950 mapping. As part of the Balmoral irrigation scheme several reports by Browne (1984a and 1984b) for the NZ Geological Survey studied the southern edge of Green Hill and the Balmoral Fault.

A number of surveys were conducted as part of the irrigation scheme. Southall and Rennie (1977) mapped the soils and tested their suitability for irrigation. Close (1985 and 1987) investigated the effect that the irrigation scheme will have on the groundwater levels within the basin. Close determined that the groundwater should rise on average 0.7 m/year once the irrigation scheme is fully implemented. Close also showed that the groundwater was uncontaminated, which is important for interpreting some of the geophysical results.

Geophysically, little work has been done in the basin prior to this thesis. Four gravity surveys have been run of which only two are of interest. Whiteford (1978) and Woodward and Carmen (1982) located a few gravity stations within the basin as part of transects run from Christchurch to the Westcoast. The most comprehensive gravity survey was by Dibble (1973) that showed the basin was deepest along its eastern margin. Another survey by Hicks (1989) as part of a gravity survey looking at the Canterbury Plains, concluded that Culverden Basin was a pull-apart basin based on its shape and gravity signature. This is clearly not the case based on this study and previous studies.

1.6 GEOLOGICAL AND GEOMORPHIC MAPS

A brief mention of the maps produced in this thesis is needed before the discussion of the various structures in later chapters. The geology and geomorphology has been mapped using aerial photographs blown up to a scale of approximately 1:7,000. Three maps were then produced:

Map 1 –Geological map of the study area (1:35,000)

Map 2 – Late Quaternary geology and geomorphology of the eastern margin (1:15,000)

Map 3 – Tectonic geomorphology of the Leonard Mound Fault System (1:10,000)

Throughout the thesis there are 3D rendered images of various parts of Culverden Basin. For some areas the corresponding vertical aerial photographs have been joined and draped over the 3D surface, and for the other areas a simple colour scheme has been used. The 3D rendering of the topography was done in WoolleySoft Visual Terrain 98® and the viewing in WoolleySoft Visual Animator 98®.

1.6.1 Classification of Fault and Fold Activity

The classification scheme devised by Pettinga et al. (1998) for fault and fold activity is adopted for this study. Three classes of activity were devised:

Activity Class I: faults and folds which cut or displace Holocene surfaces (i.e. younger than 10,000 years old);

Activity Class II: faults and folds which cut or displace deposits of the late last glaciation (i.e. younger than 25,000 years old), and where Holocene deposits are not displaced or proven displaced;

Activity Class III: faults and folds which are considered probably active but do not clearly affect geomorphic surfaces less than 25,000 years old.

The different classes will be denoted by different line colours on the maps, with red, blue and green representing the three classes respectively. Inactive structures will be represented by a black line.

1.7 THESIS STRUCTURE

Characterization of the geological setting of the northern portion of Culverden Basin was a three-step process:

1. geological mapping of the pre-Pleistocene stratigraphy and structure (Chapter 2),
2. geomorphic investigation of the Late Quaternary stratigraphy and deformation (Chapter 3), and
3. geophysical surveys to aid in the geomorphic and geologic interpretations (Chapter 4).

Chapter 5 reviews and synthesizes all of the acquired information in chapters 2, 3 and 4 into a conceptual hydrogeologic model, and concludes by examining the implications of the model to the groundwater resource of Culverden Basin and the groundwater resources of basins in active tectonic settings.

CHAPTER 2

PRE-QUATERNARY GEOLOGICAL SETTING OF CULVERDEN BASIN

2.1 INTRODUCTION

The structural evolution of Culverden Basin has been controlled dominantly by Pliocene-Pleistocene reverse faults/thrusts and corresponding folds, manifested in the formation of Torlesse Group basement cored ranges and intervening basins preserving the Late Cretaceous-Tertiary cover sequence. Culverden Basin is the largest inland basin in North Canterbury and is believed to represent a piece of relatively undeformed upper crust between two thrust dominated domains (Pettinga et. al., 1998). Clearly, the adjoining deformation is best observed around the margin of the basin on the ranges and low hills flanking the ranges. The floor of the basin is filled by a collection of Late Quaternary coalescing aggradation surfaces that have buried and hidden the incipient deformation occurring on the basin floor. Inliers of uplifted pre-Quaternary rocks, suggest that under the relatively thin Late Quaternary veneer, the floor of the basin may not be as structurally simple as the flat, undeformed basin floor would indicate.

The deformation of the basin floor is important from a hydrogeological perspective, as it has clearly controlled the deposition of the Late Quaternary aquifer-forming alluvium, and is presently partitioning the basin into sub-basins that have different hydrological properties.

This chapter examines the geology of the basin margins, focusing in particular on the eastern margin, to gain a better understanding of the geological structure of Culverden Basin. The majority of fault related structures described in this chapter are classified as either Class III or inactive based on the classification scheme (Pettinga et. al, 1998) outlined in Chapter 1. The Late Quaternary fluvial deposits and the structures affecting those deposits, will be discussed in Chapter 3.

2.2 STRATIGRAPHY

The rocks in the study area have been broadly split into three groups: the basement rocks comprising the Mesozoic Torlesse Supergroup; the cover sequence incorporating the Late Cretaceous to Pliocene sedimentary succession; and finally the Late Quaternary (Pleistocene to Holocene) glacio-fluvial and fluvial gravels. The succession is shown in the generalized stratigraphic column (Figure 2.1).

Around the extremities of Culverden Basin, late Cretaceous to Pleistocene marine siltstones, sandstones, limestones and conglomerates overlie Triassic to early Cretaceous basement rocks. The basin is floored by Late Pleistocene and Holocene fluvial gravels from the three major rivers, Waiau, Pahau, and Hurunui rivers, with several structural highs producing Tertiary inliers. Exposure of the Tertiary strata was limited to the low hills flanking the Torlesse composed ranges and the occasional inlier in the central portions of the basin. Even on the hills the exposure was limited to streams and limestone scarps which acted as good marker horizons.

2.2.1 Basement Rocks

The basement greywacke rocks in the study area are assigned to the Pahau Subterrane of the Torlesse Supergroup (Warren, 1967; Bishop et al., 1985). The rocks are dominated by well indurated, flysch deposited quartzofeldspathic arenites and argillites (comprising 99 % of the total lithology (MacKinnon, 1983)), bedded and interbedded on a variety of scales ranging from a few centimetres to tens of metres and regionally metamorphosed to prehnite-pumpellyite facies. Associated with the arenites and argillites are minor conglomerates, volcanics and cherts all of which are inferred to have been deposited in an accretionary prism setting during the Late Jurassic to Middle Cretaceous (Bishop et al., 1985).

The majority of the Torlesse cored ranges are steep and rugged. There are areas that show relatively smooth relief that in other areas of North Canterbury have been interpreted to represent the Cretaceous peneplain. It is interesting to note that these surfaces show very little weathering south of the Waiau River indicating that prior to the marine transgression which deposited the Late Cretaceous to Tertiary cover sequence the Torlesse was subjected to

erosion. In contrast to the north of the Waiau River there is a thick weathering zone present at the unconformity between the basement and cover sequence.

Detailed study and mapping of the Torlesse Supergroup was not undertaken in this thesis, however, the presence of resistant sandstone beds, as indicated by "strike-lines", aided in determination of the gross structure and generally suggest that the bedding strikes NE-SW.

2.2.2 Cover Rocks

The Late Cretaceous to Cenozoic cover sequence rocks comprise sandstones, mudstones, conglomerates, limestones and volcanogenic deposits that belong to the Eyre, Cookson Volcanics and Motunau groups.

2.2.2.1 Eyre Group (Late Cretaceous to Middle Oligocene)

The Late Cretaceous formations are only found to the north of the Waiau River on Mount Highfield (Map 1). To the south of the Waiau River, the absence of the Late Cretaceous formation lead to the proposal that a topographic high existed, the Hurunui High, to be discussed later in detail.

Stanton Conglomerate

First mentioned by Fyfe (1934) as a Cretaceous basal conglomerate and later named by Healy (1939), the Stanton Conglomerate was mapped and characterised by Gregg (1965) in the area to the north of Waiau. The unconformable contact with the underlying Torlesse basement rocks is sharp and undulatory. Gregg (1965) assigned a fluvial origin to the conglomerate and Browne and Field (1985) interpreted the Stanton Conglomerate as a fluvial facies deposited in a narrow fault-angle depression that trended NW-SE to the north of Waiau.

On the whole, the Stanton Conglomerate is matrix supported with rounded Torlesse, schistose, gneissic, quartzose and igneous clasts that are generally 5-10 cm in diameter. The exposures are generally massive, however, Gregg (1965) reported imbrication of the clasts indicating a northwest current direction.

GENERALISED AND SCHEMATIC STRATIGRAPHIC COLUMNS

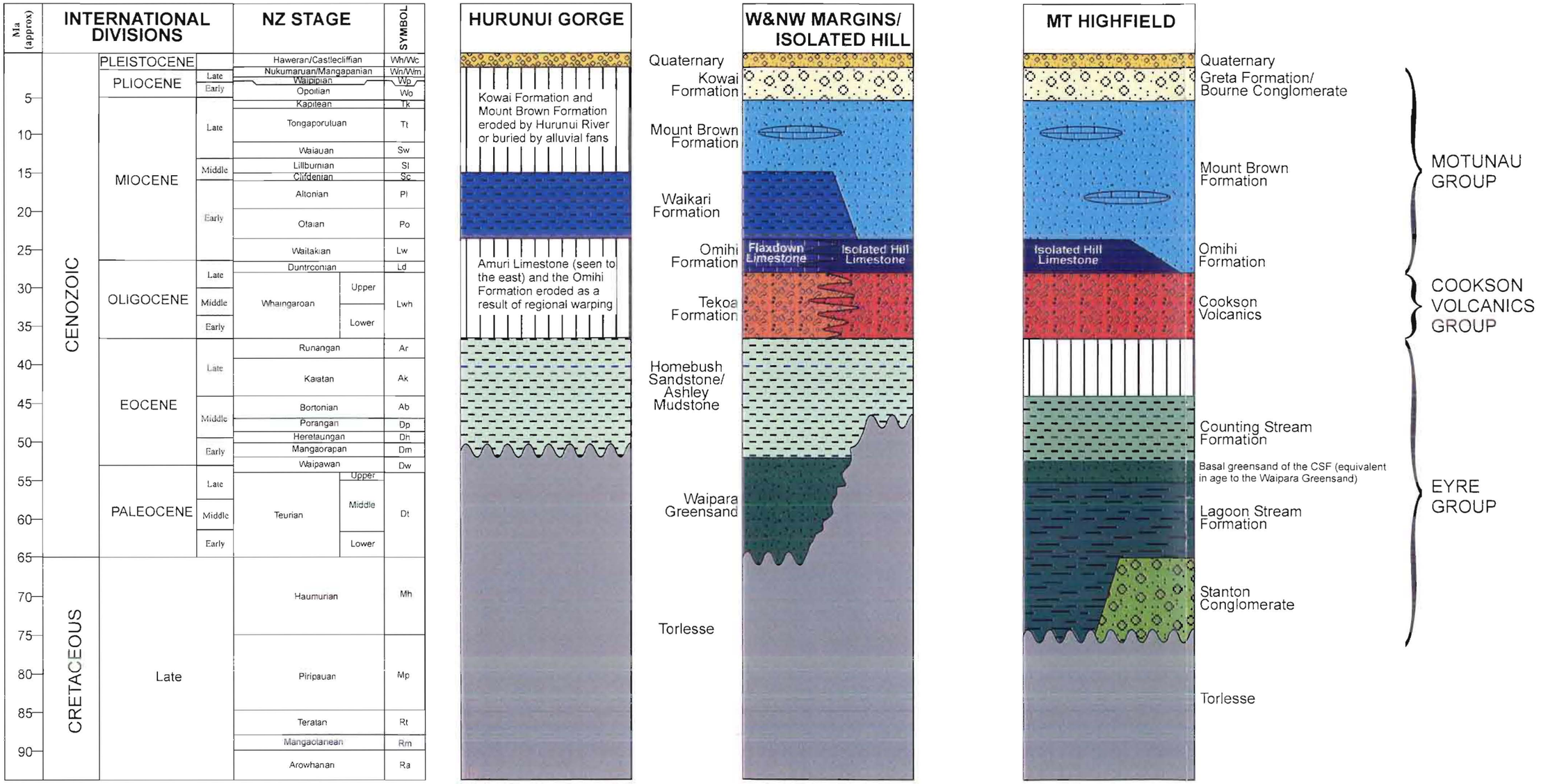

FIGURE 2.1: Stratigraphic columns for the different areas of Culverden Basin. Ages and nomenclature from Browne and Field (1985), Litchfield (1995) for the Hurunui Gorge, Mould (1992) for the SW margin, and Gregg (1965), Lammerink (1976), Coote (1987) and Endharto (1987) for Mount Highfield.

A maximum thickness of 60-70 m is reached in the core of the Mount Highfield Anticline and rapidly thins on the limbs of the fold. It is only seen in the northeastern portion of the field area. A Haumurian age was interpreted by Gregg (1965) based on stratigraphic grounds.

Lagoon Stream Formation

Located to the north of Waiau, the Lagoon Stream Formation conformably overlies the Stanton Conglomerate and unconformably onlaps the Torlesse basement. The lithologies comprising the Lagoon Stream Formation alternate between massive, yellow-brown, unconsolidated, well sorted, glauconitic sand and chocolate brown, weathered, flaky, laminated, sulphurous mudstone.

Where the Lagoon Stream Formation overlies the Torlesse basement there is a 1 m deep highly leached zone in the Torlesse. In contrast, the contact between the Lagoon Stream Formation and the Stanton Conglomerate is gradational over a 2 m thick zone with the number of pebbles decreasing in abundance. The zone is iron oxide enriched as a result of weathering and leaching. As with the Stanton Conglomerate the Lagoon Stream Formation reaches a maximum thickness in the core of the Mount Highfield Anticline of upto 100m.

It is believed that the Lagoon Stream Formation was deposited in a geographically restricted, poorly oxygenated shallow marine or lagoonal setting (Browne and Field, 1985). Based on pollen taxa from the top of the formation, Piripauan to Teurian ages have been reported (Browne and Field, 1985)

Counting Stream Formation

As with the Stanton Conglomerate and the Lagoon Stream Formation, the Counting Stream Formation occurs only to the north of Waiau. The basal part of the formation is a richly glauconitic greensand that is distinctive, by comparison with the underlying Lagoon Stream Formation. The greensand is equivalent in age to the Waipara Greensand seen to the south. Above the greensand, the formation consists of a light grey, slightly glauconitic, moderately indurated, generally massive mudstone.

The Counting Stream Formation conformably overlies the Lagoon Stream Formation with a sharp contact between the two. The unit reaches a maximum thickness to the north of the field area of 120 m (Endharto, 1987), but in the field area is only 10-20 m thick.

Ashley Mudstone

Only observed in the Ben Lomond Syncline, the Ashley Mudstone unconformably overlies the basement rocks. The Ashley Mudstone is dominated by blue-grey, massive, calcareous mudstone with interbedded friable to moderately indurated sandstones that can posses a high glauconite content.

The base of the formation is Teurian toWaipawan and the top is dated as Kaiatan by Foraminifera (Browne and Field, 1985)

Homebush Sandstone

The Homebush Sandstone is typically a white to pale grey, poorly indurated, massive, moderately sorted, mildly glauconitic, quartzose sandstone that underlies the Cookson Volcanics. Only in the Hurunui Gorge (Map 1) is the complex contact with the Ashley mudstone observed, even though it has been recorded in other areas (Lewis et al., 1979; Browne and Field, 1985; Barrel, 1989; Nicol, 1991; Litchfield, 1995; Kellahan, 1998). Lewis et al. (1979) attributed the complex relationship to diapirism from tectonic triggering before, or during, the formation of the unconformity between the Amuri Limestone and Omihi Formation.

Carlson et al. (1980) suggested a deltaic or tidal channel environment at its type section in the Coalgate area of mid Canterbury, whereas Browne and Field (1985) assigned a shallow marine environment further north. From stratigraphic relationships, an Arnold age seems most appropriate for the northern Canterbury localities (Browne and Field, 1985)

2.2.2.3 Cookson Volcanics Group

Predominately composed of tuffs and volcaniclastic breccia, with minor basaltic flows, basaltic dykes and intercalated limestones, the Cookson Volcanics make up the thickest (1200-1300m) mid-Oligocene volcanics in the country (Browne and Field, 1985). On the western margin of Culverden Basin the Cookson Volcanics are known locally as the Tekoa Formation. However, around Waiau they are still referred to as the Cookson Volcanics. Detailed work by Coote (1987) saw the Cookson Volcanic Group divided into three units:

I. Hossack Volcanics
II. Dog Hill Volcanics
III. Mason Hill Volcanics

Of these three only the Mason Hill Volcanics occur in the northern portion of the field area. The volcanics are only seen in the northern and western margins of the Culverden Basin. East of the Lowry Peaks Range in the Cheviot Basin, Kaiwara Valley and Waikari Valley, Cookson Volcanics have not been reported.

The Mason Hill Volcanics are principally comprised of volcanic breccia along with basaltic lavas, pillow lavas and volcanic sandstones. The breccia is red brown in colour and has basaltic clasts ranging from 1 cm to 40 cm set within a calcareous matrix. To the north of Mount Highfield the unit is more stratified, highlighted by the presence of calcareous bands that generally increase in abundance towards the top of the unit. South of Mount Highfield the breccia horizons become more massive with a higher calcareous content so that it forms resistant ridges which are easily traced. Towards the top of the volcanics up to 50 cm clasts of basalt are set in a calcareous matrix which then grades into the Isolated Hill Limestone. The Cookson Volcanics are conformably overlain by the Isolated Hill Limestone, and in turn disconformably overlie the Counting Stream Formation. The thickness of the unit within the field area is dramatically less than the 1200-1300 m observed on Mount Mason to the north. Generally the volcanics are around 10-20 m thick.

Associated with the Cookson Volcanics is a dyke that cuts the Homebush Sandstone and basement rocks on the southern edge of Isolated Hill. The dyke has a W-E orientation that is possibly reflective of a pre-existing weakness in the Torlesse.

Earliest volcanism was surtseyan (Coote, 1987), with strombolian and hawaiian type volcanism becoming prevalent as the setting became emergent. Coote (1987) believed that there were two vent areas for the Cookson Volcanics: one near Counting Stream and Lottery River and the other near Mason River and Lagoon Stream. A number of authors have assigned ages, based on the macrofossil assemblage, for the Cookson Volcanics ranging from Duntroonian to Waitakian (McKay, 1890), lower Kaiatan (Fyfe, 1934), Duntroonian (Schofield, 1951), and Whaingaroan to lower Waitakian (Gregg, 1965). Coote (1987) suggests that the volcanics range from Runangan to Duntroonian.

2.2.2.4 Motunau Group

Omihi Formation

Andrews (1963) divided the Omihi Formation into five members, which was later modified by Browne and Field (1985) to include six members:

I. Flaxdown Limestone
II. Weka Pass Stone
III. Gorries Creek Greensand
IV. Berrydale Greensand
V. Isolated Hill Limestone
VI. Marble Point Limestone

Of these six members only the Isolated Hill Limestone is present within the mapped portion of the field area. Along the western margin of the basin the Flaxdown Limestone crops out, which Mason (1949) believed to be a correlative of the Isolated Hill Limestone.

Isolated Hill Limestone Member

At its base, the Isolated Hill Limestone has a pinkish colour due to its gradational contact with the conformably overlain Tekoa Tuffs and Cookson Volcanics, and becomes light grey to creamy towards the top. The limestone is flaggy, bedded on a centimeter to decimeter scale, crystalline and very well indurated. The member extends from Isolated Hill, 4 km southwest of Waiau, northeast to Mount Highfield and onwards. At its type location, the Isolated Hill

quarry, the limestone is overlain by a phosphatised pebble band marking the conformable contact with the overlying Mount Brown Formation.

Browne and Field (1985) suggest that the Isolated Hill Limestone was deposited on the flanks of a submerged volcanic complex and from macrofossils Gregg (1965) reported a Duntroonian to Waitakian age.

Waikari Formation

Defined in 1963 by Andrews, the Waikari Formation can be divided in to 5 members as follows:

I. Glenesk Sandstone
II. Tommys Creek Concretionary Sandstone
III. Gowan Hill Sandstone
IV. Scargill Siltstone
V. Pahau Siltstone

The Scargill Siltstone is the only one of these members found in the field area and is in the core of the Ben Lomond Syncline.

The Scargill Siltstone is a blue-grey sandy siltstone with concretionary layers. The unit unconformably overlies the Homebush Sandstone/Ashley Mudstone in the Hurunui Gorge. Andrews (1963) reported a Waitakian to Otaian age for the Pahau Siltstone and an Otaian to Lilliburnian age for the Scargill Siltstone.

Mount Brown Formation

The Mount Brown Formation is by far the most extensive of the cover rock units found within the study area. Throughout the study area, the Mount Brown Formation exhibits a wide range of lithological variation. The dominant lithology is a medium brown, medium to fine, well sorted, moderately indurated, micaceous, massive to finely bedded sandstone (Figure 2.2). Interbedded with the sandstone are fossiliferous limestones, well indurated calcareous sandstones and siltstones.

Browne and Field (1985) suggest that the Mount Brown Formation was deposited in a rapidly subsiding basin at depths similar to those for the Omihi and Waikari Formations. The siltstone is believed to be hemipelagic sediment deposited between mass flows of sand. The upward change from the mass-flow dominated facies to the siltstone facies signifies a deepening of the basin culminating in the deposition of the Greta Formation. Browne and Field (1985) also believed that the Mount Brown was a tongue of sandstone separating two siltstone basins; the Tokama Siltstone to the south and the Greta Formation to the north.

FIGURE 2.2: Photo of the Mount Brown Formation exposed in the scarp adjacent to the Rotherham-Waiau Highway (State Highway 70).

Greta Formation

The Greta Formation consists of blue/grey, moderately indurated, micaceous, calcareous, bioturbated, fine to very fine sandy mudstone. Generally the mudstone is massive, however faint stratification is visible in some weathered sections. Locally it contains moderately indurated conglomerate beds composed of rounded Torlesse clasts upto 5 cm, with a fine to very fine sandy mudstone matrix that is commonly red/brown.

Brown and Field (1985) divided the Greta Formation into three sub-formational lithofacies: the Glenmount lithofacies, Koromiko lithofacies (both modified after Maxwell, 1964), and the Athol Glen Sandstone lithofacies (after Maxwell, 1964). In the Cheviot Basin the Greta Formation was divided into three constituent members by Kellahan, 1998: the Te Ngapari Siltstone (modified from Maxwell, 1964), the Homestead Siltstone, and the Koromiko Siltstone member (after Maxwell, 1964). For the purpose of this study, the Greta Formation was left undifferentiated as there was only a small section at the northern end of the study area. The unit conformably overlies the Mount Brown and unconformably overlies the Isolated Hill Limestone, Cookson Volcanics, and the Counting Stream Formation in the northeastern portion of the field area.

Deposition was believed to have been in quiet water, probably on the continental shelf or slope in a continually subsiding basin (Maxwell, 1964). Browne and Field (1985) assign an age of Tongaporutuan to Mangapanian for the majority of the unit, however around Waiau they assign an age of Clifdenian at the base and lower Wanganui Series for the top of the formation.

Kowai Formation (Nukumaruan to Castlecliffian)

As with the Mount Brown Formation, the Kowai Gravels occur extensively throughout the study area, in particular along the western and northern margins of the basin. The only occurrence of them along the eastern margin of the basin is on the southern end of Leonard Mound. Preservation of the formation has occurred on the downthrown blocks of the major faults (e.g. Isolated Hill Fault and Green Hill Fault). They reach a maximum thickness of 1600 m on Green Hill (Mould, 1992), but are generally less than 100 m where observed elsewhere along the basin margins.

As with the Greta Formation, the gravel clasts are composed of well rounded Torlesse arenites and argillites with a fine to coarse angular sandy matrix. Generally the gravels are massive to poorly bedded, but in places are well bedded. Interbedded with the conglomerate are sandstone and siltstone layers, which may be several metres thick. Although these layers where not found exposed in the study area, they have been found in adjacent areas (e.g. Kellahan, 1998) and are also observed in the geological logs of the boreholes throughout the

basin. The presence of the sandstone and siltstone layers was used to distinguish the Kowai gravels from the younger Late Quaternary deposits.

The similarity of the sandstone and siltstone beds with the Mount Brown Formation often makes it difficult to distinguish between the two formations. It was proposed by Mason (1949) that the first appearance of conglomerate should define the boundary between the two units, whereas Browne and Field (1985) argue that the contact should be defined by the last appearance of limestone in the Mount Brown Formation. For the purpose of this study, Mason's (1949) method is preferred as the first appearance of conglomerate represents a significant change in the tectonic setting of the source area and a change in energy of the depositional environment of the Kowai Formation.

At the base of the formation Maxwell (1964) reported features that are common to beaches, and in conjunction with marine fossils and glauconite, indicates that the basal portion of the Kowai Gravels are a shallow marine sequence. Browne and Field (1985) suggest that the Kowai Formation was deposited at inner to mid shelf depths, affected by periods of fluctuating eustatic sea-level associated with non-marine deposition.

2.2.3 Discussion

2.2.3.1 Basement-Cover Rock Unconformity

Throughout the majority of North Canterbury the regional unconformity between the Torlesse basement and the cover sequence spans the Middle Cretaceous and is marked by a distinct angular discordance between the Torlesse and cover rocks. The Torlesse bedding is steeply dipping as a result of the Rangitata II deformation event (Bradshaw, 1989) that uplifted and deformed the basement, in contrast to the moderately dipping cover sequence. Over the majority of the study area, the time span represented by the unconformity needs to be extended to the mid Eocene, as the Late Cretaceous Broken River and Conway Formations mapped to the south and east, are not present. Only in the northern part of the study area are Late Cretaceous strata present.

The degree of weathering of the Torlesse sandstones beneath the unconformity differs between the regions where the Late Cretaceous units are, and are not, present. Where the Late Cretaceous units are present the Torlesse rocks show a thick zone of weathering and leaching (Cowan, 1992). In contrast, over the majority of the study area there is very little or no weathering beneath the unconformity indicative of widespread erosion prior to the deposition of the Cainozoic marine sediments.

The Cretaceous peneplain onto which the marine transgression deposited the cover sequence is exposed at various localities surrounding Culverden Basin, and characteristically appears to be a subdued erosional surface compared with the normally steep and rugged morphology characterizing the basement cored ranges today.

Hurunui High

Controlling the sedimentation in the North Canterbury area from the Late Cretaceous through to the Middle Eocene was the Hurunui High (Figure 2.3). Browne and Field (1988) first proposed the Hurunui High based on the lack of the Late Cretaceous sediments and the presence of conglomeratic layers in the basal sections of the Conway, Waipara Greensand and Ashley Mudstone Formations. The topographic relief on the high was probably not much more than 100 m, but the slow sedimentation rates meant that it was not surmounted until the Eocene by the Ashley Mudstone.

The location of the Hurunui High has been well documented in the southern portion of the basin (Nicol, 1991; Mould, 1992; Litchfield, 1995) and further to the east (Kellahan, 1998). Mould (1992) suggested that the Hurunui High could extend as far north as Mount Culverden. Within the field area, the only Late Cretaceous sediments are found on Mount Highfield at the northern end of the basin. A few kilometres to the south, on Isolated Hill, and to the west on Emu Plains and Mount Culverden, the late Cretaceous sediments are absent indicating that these areas were part of the high, supporting Moulds hypothesis and the location inferred by Browne and Field (1985).

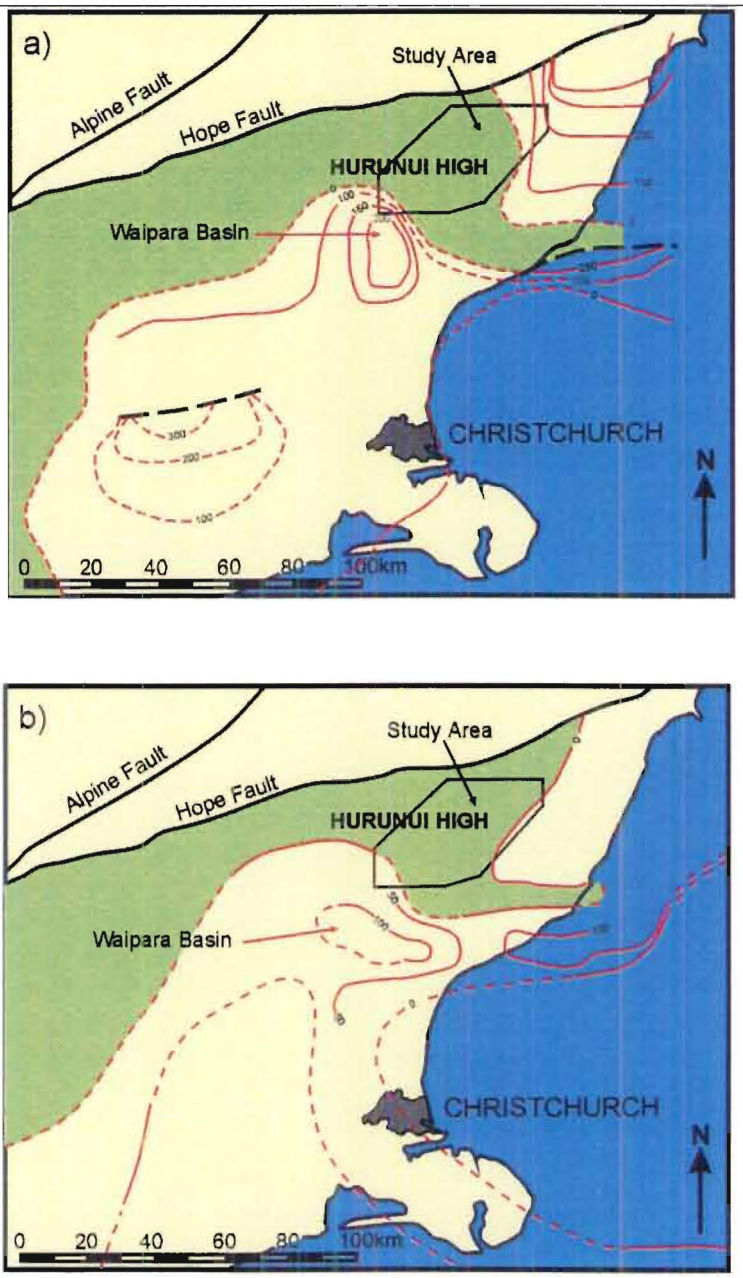

FIGURE 2.3: Lateral extent of the Hurunui High in terms of isopach maps of thickness (m) of sediments in North Canterbury during the Late Cretaceous (a) and Paleocene (b) (after Field and Browne, 1989).

2.2.3.2 Cover Sequence Deformation

The cover sequence records several periods of deformation since the Oligocene. Up until the Oligocene there was relative quiescence with slow transgressive sedimentation. Although not present in the study area, the Amuri Limestone is the most widespread of the Tertiary units in the North Canterbury region and separates the Eyre and Motunau Groups. It has been proposed by Lewis (1992) that the removal of the Amuri Limestone was the result of the initiation of the current plate boundary through New Zealand which, in North Canterbury, produced large scale warping in the mid-late Oligocene. Widespread volcanism in the Late

Oligocene along pre-existing zones of weakness in the basement also indicates that the Oligocene was a time when there was significant change in the tectonic setting of the region.

During the Miocene a relatively simple basin existed (Figure 2.4) into which deposition of the Waikari and Mount Brown Formations occurred. An influx of sediment during the Miocene was from the west, associated with the uplift of the Southern Alps along the Alpine Fault. At the end of the Miocene the continued deformation and uplift resulted in the culmination of the marine regression which saw the deposition of the Pliocene Greta Formation and the Kowai Formation, believed to be the onshore and lateral equivalent.

2.3 STRUCTURE

Culverden Basin is situated between two opposing thrust systems (Nicol et. al., 1995). The eastern margin of the basin (Figure 2.5) is dominated by westward facing reverse faults/thrusts that belong to the Domain 4 (North Canterbury Fault and Fold Belt). In contrast, eastward facing reverse faults/thrusts of Domain 2 are responsible for the structural evolution of the western edge of the basin. This thesis focuses on the eastern margin of the basin, as the relationships between the fluvial facies and active deformation are strongly influencing the hydrogeology, which is observable in the geomorphology. Reconnaissance mapping of the west and northwest margins was undertaken so as to gain an understanding of the overall tectonic setting of the northern part of the basin. It was also important for the interpretation of the geophysical data in the central and western portions of the basin that the style of deformation along the western margin be better known.

The proposed structures can be viewed in detail on Map 1 (and cross sections) and are summarised in Figure 2.5 and in tables 2.1 and 2.2.

2.3.1 East Culverden Fault Zone

The actively evolving imbricate thrust system along the eastern margin of the basin is dominated by the Lowry Peaks Fault (LPF) and associated folds which manifest themselves in the Lowry Peaks Range. The Lowry Peaks Range (Figure 2.6) is a typical example of the northeast-southwest oriented, fault controlled, basement-cored anticlinal ridges that are seen

throughout North Canterbury. For the majority of its length, there is no active trace associated with the LPF. The deformation is being accommodated by the Leonard Mound Fault (LMF) splaying obliquely off the LPF. The LMF and associated structures will be dealt with further in the following chapter when the geomorphic expression of the active deformation is examined.

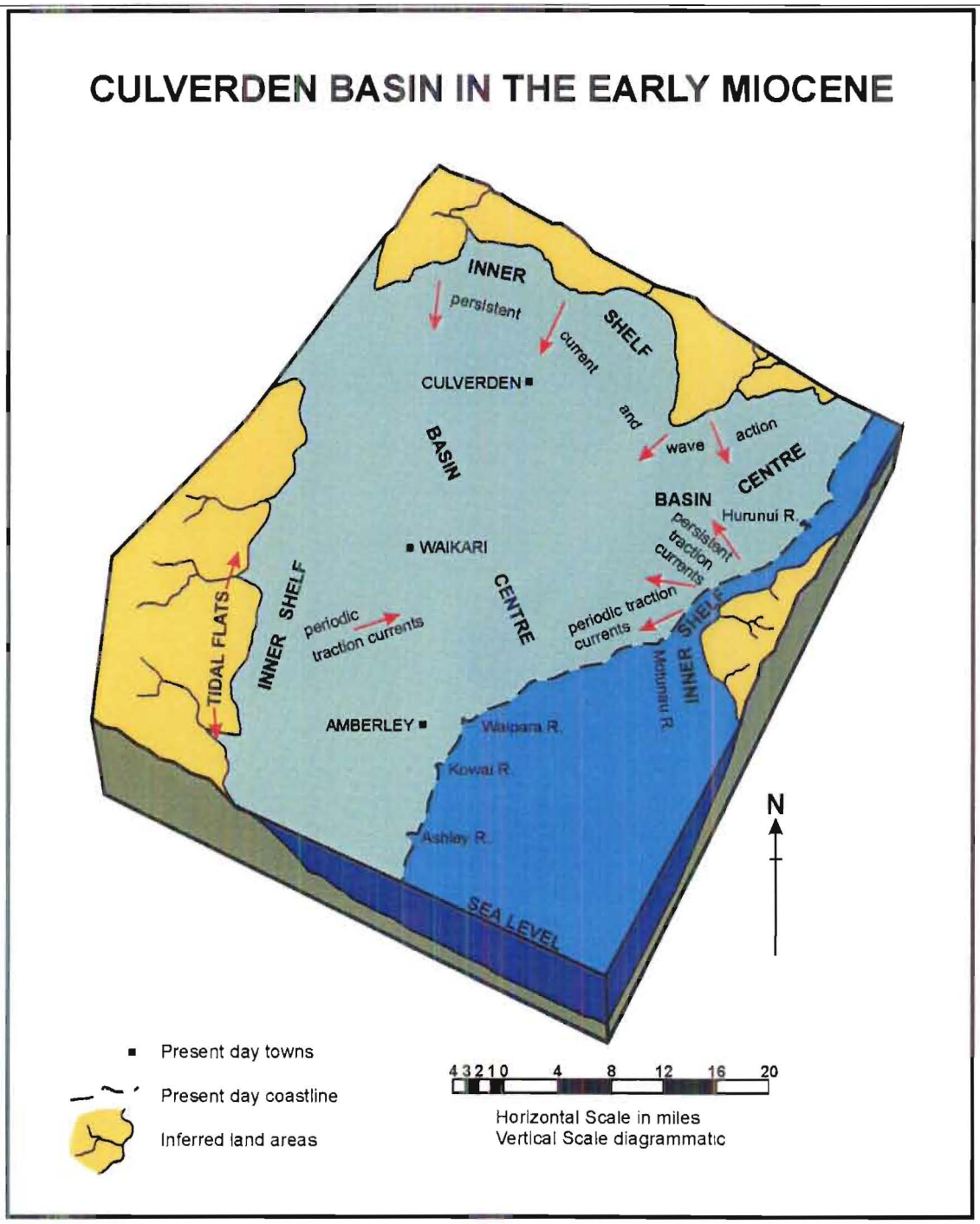

FIGURE 2.4: Diagrammatic sketch showing the reconstructed geography/bathymetry for Culverden Basin and North Canterbury during Miocene time (after Andrews, 1968).

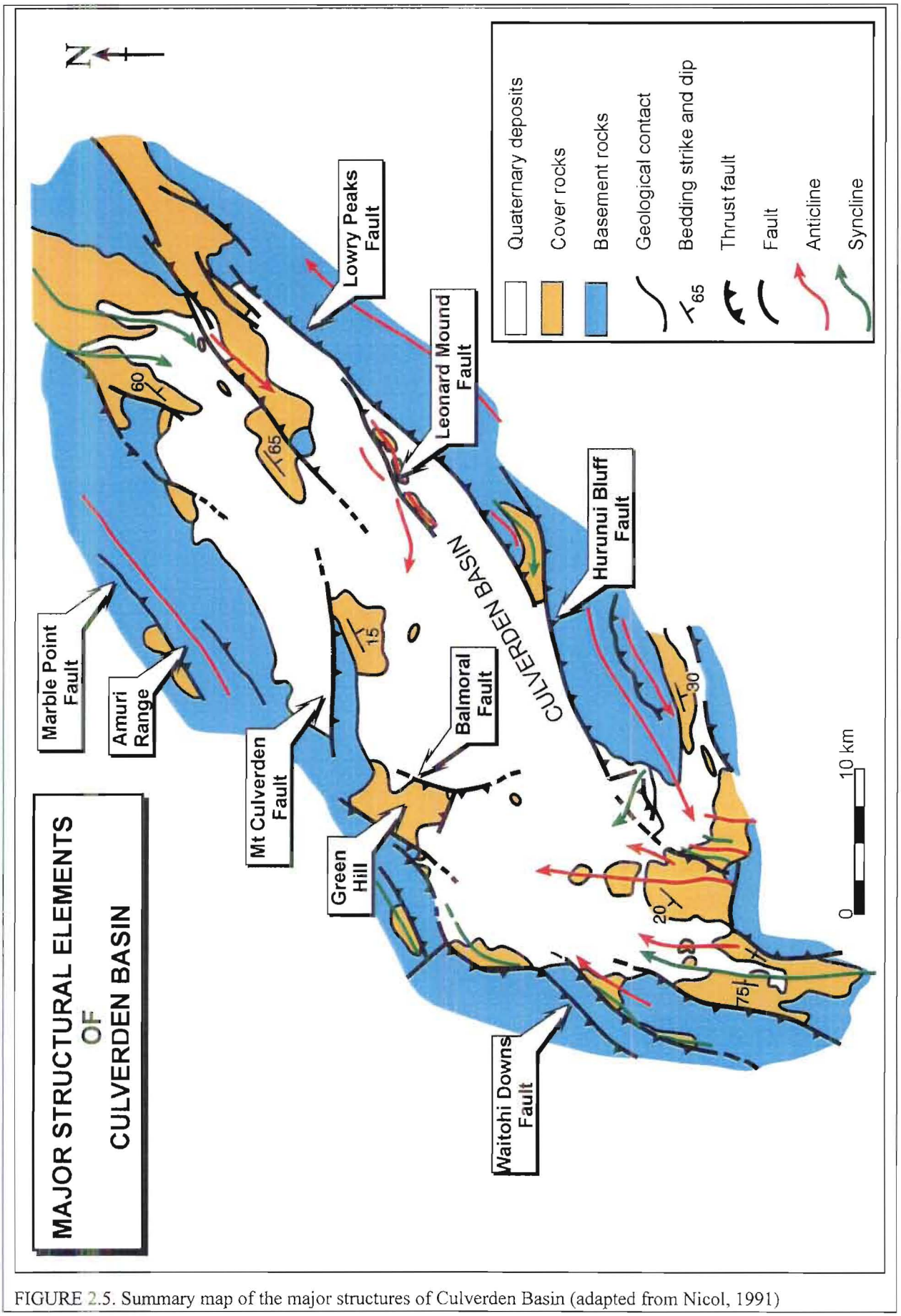

FIGURE 2.5. Summary map of the major structures of Culverden Basin (adapted from Nicol, 1991)

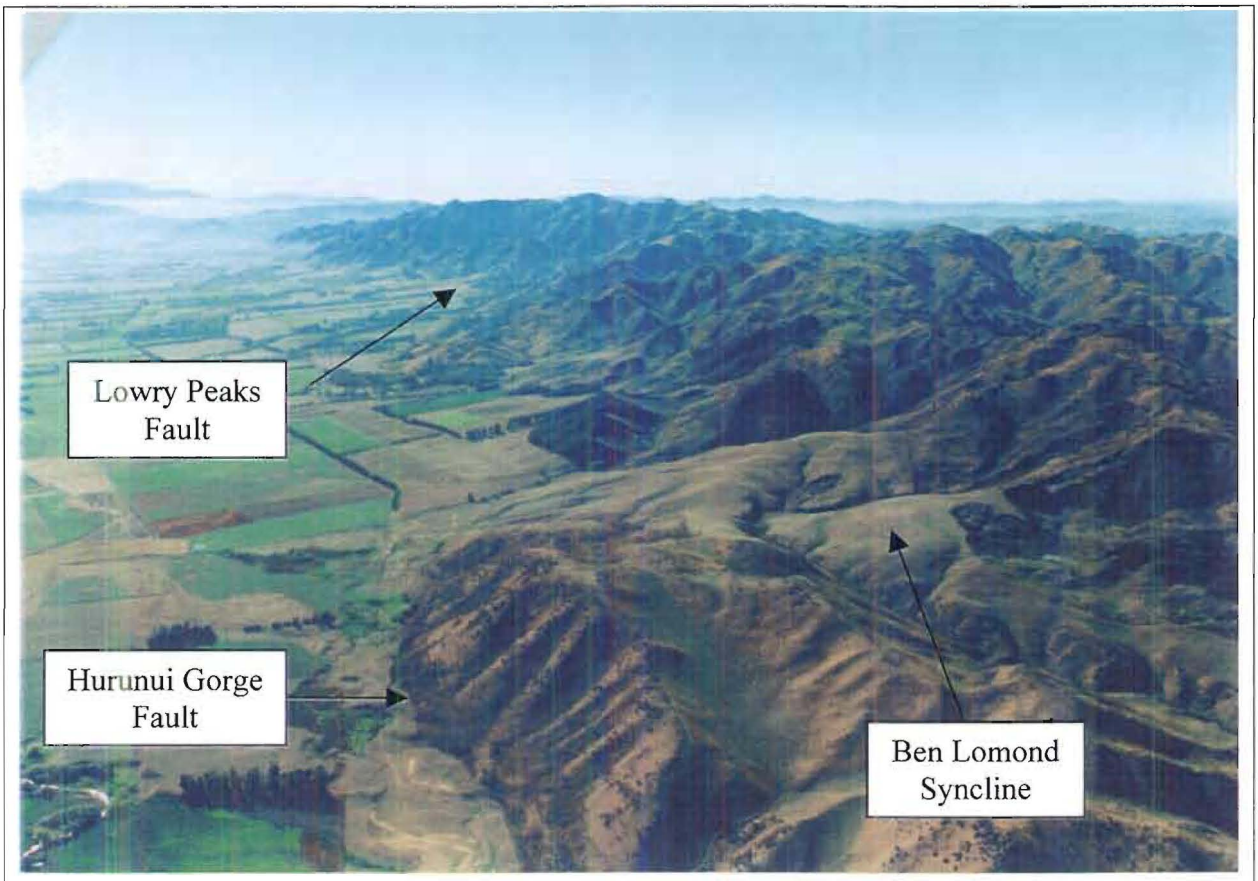

FIGURE 2.6. Oblique aerial photograph of the Lowry Peaks Range looking north from the Hurunui Gorge.

Falloon (1954) was the first to map the fault system, but interpreted the Lowry Peaks Fault as a high angle normal fault, which, based on present knowledge, is clearly not the case. Gregg's (1964) 1:250 000 scale geological map of the Culverden Basin, whilst correctly interpreting the structure, was not able adequately to show the complexity of the system. The first detailed mapping of the fault system was by Litchfield (1995) for the section to the south of the Hurunui River. Litchfield showed that the range-front could be characterised by two southward dipping listric thrust faults.

2.3.1.1 Range-front Faulting

The East Culverden Fault Zone (ECFZ) consists of a number of faults (Table 2.1) and folds with a typical NE-SW trend as seen in the North Canterbury fault and fold belt. The ECFZ can be divided into three main seismogenic segments (Pettinga and Yetton, 1998): south of the Hurunui River, between the Hurunui and The Hermitage station and north of The Hermitage station (Map 1). To the south the ECFZ is dominated by the Hurunui Bluff Fault (Litchfield,

1995) which trends approximately 065^0, whilst to the north the ECFZ is dominated by the Lowry Peaks Fault which trends approximately 045^0. The range-front of the southern section has been trimmed and modified by the Hurunui River, whilst the northern half is dominated by large alluvial fans building out from the Lowry Peaks Range. There has not been modification of these fans except by streams from the Lowry Peaks Range.

The central and northern sections are the primary focus for this study. The southern section was mapped by Litchfield (1995) and has been included as it is necessary for the understanding of the Lowry Peaks Fault Zone as a whole. The structures present in the southern section are only briefly described in the following discussions.

TABLE 2.1. Description of the major faults within the East Culverden Fault Zone.

Name	Location	Best Exposure	Orientation	Lateral Extent	Type	Comments
Hurunui Bluff Fault	N side of Lowry Peaks Range to S of Hurunui River	Gully west of Mt Benger Homestead. Hurunui River south of Ben Lomond Syncline	ENE-WSW	16km+	Thrust	Bounds the Lowry Peaks Range to south of Hurunui River. Responsible for uplifting a number of terraces associated with the Hurunui River.
Hurunui Gorge Fault	N side of Lowry Peaks Range across mouth of Hurunui Gorge	-	NE-SW	3km	Thrust	Assumes the range-bounding position once the HBF veers off to bound the eastern limb of the Ben Lomond Syncline.
Lowry Peaks Fault	N side of Lowry Peaks Range from Hurunui to Waiau Rivers	Crushed and sheared Torlesse in the Stanton River	Variable but dominantly NE-SW	21km	Thrust	As with HBF bounds SE margin of Culverden Basin. Complexly splayed and segmented. Responsible for uplift of Lowry Peaks Range.
Totika Fault	Bourne River	Where fault leaves Bourne River.	NE-SW	4.5km+	Thrust	Juxtaposes Torlesse against cover sequence strata.
Leonard Mound Fault	N side of Leonard Mound	-	NE-SW	15 km	Thrust	Presently accommodating the deformation along the range-front to the north of the Hurunui River

Hurunui Bluff Fault

The Lowry Peaks range-front to the south of the Hurunui River (Figure 2.7) is characterised by two southward-dipping listric thrust faults (Litchfield, 1995): i) the Hurunui Bluff Fault that bounds the range-front, and ii) the Hurunui Gorge Fault (Map 1). The Hurunui Bluff Fault bounds the entire range-front (Litchfield, 1995) until it veers into the range bounding the Ben Lomond Syncline (discussed below) at its eastern end, at which point the Hurunui Gorge Fault takes up the range-bounding position across the mouth of the Hurunui Gorge.

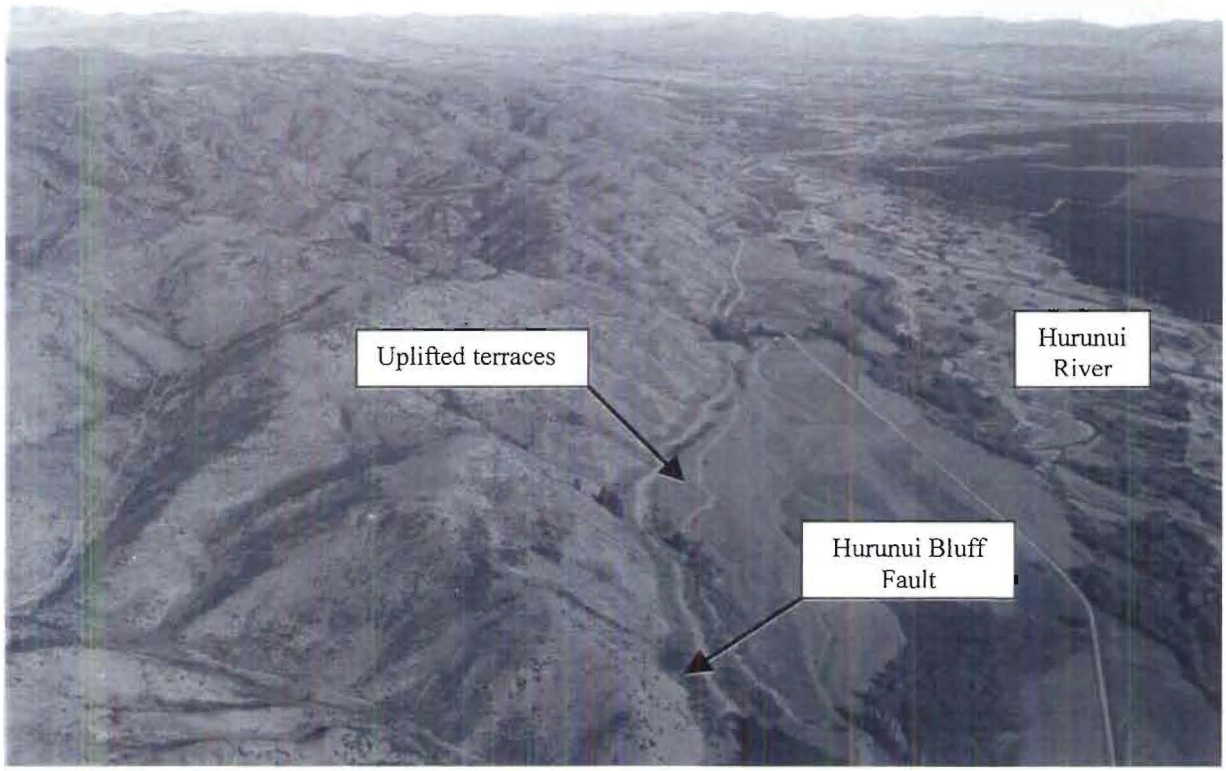

FIGURE 2.7: Photograph of the southern section of the East Culverden Fault Zone looking south along the Hurunui Bluff Fault and Hurunui Bluff Anticline, showing the uplifted terraces of the Hurunui River.

Along the range-front, direct evidence for faulting has either been removed by the Hurunui River, or buried by terrace deposits and alluvial fans. However, a series of river terraces that have clearly been uplifted and possibly back-tilted along the range-front (Figure 2.7), along with anomalous drainage patterns, clearly indicate that faulting has occurred at the eastern end of the range-front. In the Hurunui Gorge clear evidence for major faulting does exist with the

presence of large shear zones with reverse senses of shear. Other small faults also indicate the presence of back-thrusts.

Hurunui Gorge Fault

Named by Litchfield (1995), the Hurunui Gorge Fault is a splay of the Hurunui Bluff Fault, probably resulting from the change in strike of the overall fault system. In comparison to the HBF there has been significantly less uplift associated with the HGF as reflected in the relative elevation of the uplifted basement rocks. This uplift has been sufficient for the preservation of the Hurunui Gorge Syncline on the northern side of the Hurunui Gorge. The structure persists to the southern side of the Hurunui Gorge where basement rocks have been faulted up against the Tertiary sequence seen preserved in the syncline, but at a lower elevation.

Lowry Peaks Fault

In contrast to the Hurunui Bluff Fault, which is a single continuous fault along the southern section of the Lowry Peaks Range, the Lowry Peaks Fault is a complexly splayed and segmented fault. The Lowry Peaks Range along the southern section was also extensively modified by the Hurunui River, which flowed along its base trimming the range-front and producing a set of river terraces. To the north of the Hurunui Gorge there has been no trimming or modification of the range-front as Leonard Mound acted as a barrier to the Waiau River during the Late Pleistocene. As a result there are classical range-bounding alluvial fans extending out from the range burying any evidence of the fault that exists there.

The geomorphology of fault bounded range-fronts has been well documented (Wallace, 1978, Bull, 1984, Mayer, 1986, Wells et al, 1986 and Garlick, 1992). Wallace (1978) devised a model showing the sequence for fault controlled mountain fronts (Figure 2.8). Wallace's model shows that for mountain fronts with recent episodes of mountain uplift, development of triangular facets on the end of spurs, a straight mountain-piedmont junction and narrow valley floors occur. There will also be very little development of alluvial fans along the base of the mountain front. When the fault bounding the mountain front becomes inactive and fluvial

processes dominate, the mountain-piedmont junction becomes sinuous, the valley floors become broader and the development of extensive fans occurs.

For the most part, the Lowry Peaks Range front shows features that are consistent with D in the Wallace model. From this it is reasonable to assume that the Lowry Peaks Fault occurs near the base of the range and that there has been very little erosion of the range-front back from the fault. Around the Hurunui Gorge the range-front does become more sinuous as a result of the presence of the softer cover sequence rocks which are more easily eroded. Different splays and segments of the faults are often highlighted by a change in the elevation and morphology of the Torlesse bedrock on either side of the gorge, where the structures cross it.

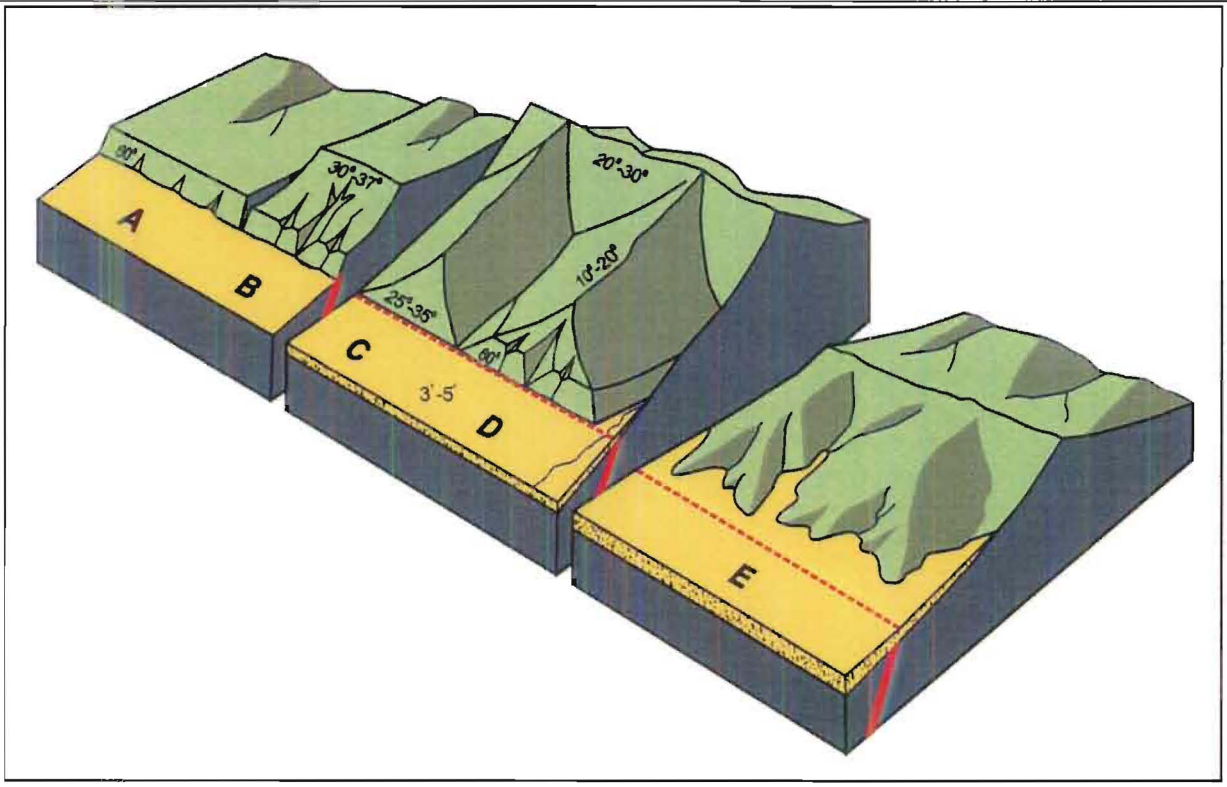

FIGURE 2.8. Block diagram showing the sequence of development of fault-generated landscapes for initial stage (A, B), maximum relief (C, D) and dominance of fluvial erosion during subsequent stage of tectonic quiescence (E) (from Wallace, 1978).

For a 12km section from Kaiwara Road northwards to "The Hermitage Station" (grid reference N32/145314) there appears to be no splaying, or segmentation, of the fault. To the north of The Hermitage, the fault becomes segmented with the most pronounced segmentation

occurring at the junction of the Lowry Peaks Fault with the Leonard Mound Fault. At that location there is approximately a 1km step in the range-front. Where there is segment termination and motion transfer onto adjacent structures, there is a corresponding decrease in the elevation of the Lowry Peaks Range. Where motion is transferred from one segment to another it is inferred that tear faults are acting as the transfer mechanism. The evidence for the tear faults are long straight stream gullies and a change in the attitude of the Torlesse bedrock on either side of the inferred faults.

On the northern side of the Waiau River the fault becomes splayed with three faults accommodating the deformation. The Lowry Peaks Fault (per se) continues up the Stanton River and is marked by crushed and sheared Torlesse bedrock in the river. The fault can be traced until the Stanton River changes to a WNW course that is controlled by another set of structures. This WNW set of lineaments parallel the strike of the Rahi Fault. North of the Stanton River there are numerous NNE trending lineaments, but determining which set is older than the other is not possible. It may well be that the WNW lineaments are related to the Late Cretaceous deformation and have been reactivated during the current tectonic regime. However, this is purely speculation at this stage. To the west of the Lowry Peaks Fault, the Totika Fault (described shortly) is observed in Bourne Stream, with a smaller, unnamed fault between the Lowry Peaks and Totika faults.

Totika Fault

The Totika Fault, named by Lammerink (1976), is one of three faults on the northern side of the Waiau River that are splays of the Lowry Peaks Fault. The Totika Fault is clearly marked as the Torlesse basement rocks have been uplifted against the Greta Formation. In Bourne Stream the basement is highly crushed and sheared. Unfortunately, the Holocene gravels in the valley floor have buried the trace of the fault, but the occurrence of the Isolated Hill Limestone and Cookson Volcanics at the mouth of the valley are evidence that the fault exists underneath the younger alluvium.

Approximately 2km from its southern end the fault leaves the Bourne Stream valley and veers up a side valley along which it continues until it merges with the Lowry Peaks Fault. Although there is no direct evidence for another fault to continue up Bourne Stream, the straight nature

of the valley, in conjunction with some N-S trending lineaments at the northern end of the stream, suggest that valley is fault controlled. As there is no direct evidence for the inferred faulting, the fault must predate the Late Pleistocene and Holocene gravels on the floor of the valley.

Leonard Mound Fault

The Leonard Mound Fault is the largest fault within the Leonard Mound Fault System (LMFS). Currently, the LMFS is accommodating the deformation observed along the NE margin of the basin. Traceable for 15 km, the thrusting is clearly expressed as a scarp that is up to 30 m high. The thrusting has involved the Tertiary cover sequence along with the Pleistocene and Holocene fluvial gravels and range-bounding fan gravels. The footwall of the fault is clearly imbricated as expressed by numerous smaller faults and small scale folding of the gravels.

2.3.1.2 Folding

There are four observable majors folds associated with the ECFZ (Table 2.2). The Lowry Peaks Range, bordering the eastern margin of the basin owes most of its elevation and topographic expression to folding and comprises three of the major folds: 1) the Hurunui Bluff Anticline to the south of the Hurunui River, 2) the Lowry Peaks Anticline to the north of the Hurunui River, and 3) the Ngawiro Anticline at the northern end of the range Map 1). The Hurunui Bluff Anticline, originally named the Lowry Peaks Anticline by Litchfield (1995), was renamed for this study so that it matched the dominant fault closely associated with its development. The fourth major fold is the Ben Lomond Syncline which has preserved a portion of the Tertiary sequence in the Hurunui Gorge. An important fold in the system, which is not described here, is the inferred syncline that has developed on the downthrown side of the Hurunui Bluff Fault and the Lowry Peaks Fault. Although there is no visible indication at the surface of the fold due to infilling by the Pleistocene gravel units, the formation of the Ben Lomond Syncline and other synclines on the downthrown footwall blocks of major thrusts, all suggest that a syncline should be present. This issue is addressed further in the geophysics chapter, which looks at the depth of the basin along the SE margin.

The different folds comprising the range are expressed by the cover sequence around the range, stream patterns and topographical and morphological changes in the Torlesse bedrock. The central portion of the range is characterised by steep, rugged Torlesse outcrop. In contrast, around the Waiau River and to the south of the Hurunui River, the Torlesse topography displays a smoother and more rounded appearance, believed to represent the Cretaceous peneplain surface onto which the cover sequence was deposited. The nature of this topographic contrast reflects the amount of uplift and erosion that has taken place, with the rugged central portion having undergone significantly more than either end of the range. This is important as it has dictated the amount of sediment available to the streams depositing range-bounding fans along the western side of the range.

TABLE 2.2. Description of the major folds of the East Culverden Fault Zone.

Name	Location	Trend	Axial Trace Length	Shape	Amplitude	Comments
Hurunui Bluff Anticline	Lowry Peaks Range to south of Hurunui Gorge	WSW-ENE	18km+	Asymmetric, sigmoidal, vergence to NW, open	~600m	Closely associated with the Hurunui Bluff Fault.
Ben Lomond Syncline	Near entrance to Hurunui Gorge	W-E to SW-NE	4km	Asymmetric, sigmoidal, vergence to S-SE, open	~300m	Closely associated with the Hurunui Bluff Fault.
Lowry Peaks Anticline	Lowry Peaks Range to north of Hurunui Gorge	NE-SW	17km	Asymmetric, vergence to NW, open	~700m	Closely associated with the Lowry Peaks Fault.
Ngawiro Anticline	Lowry Peaks Range around the Waiau River	NE-SW	8km	Symmetric, sigmoidal	~450m	Fold shape reflected in geomorphology of the range.
Leonard Mound Anticline	Leonard Mound	NE-SW	7km	Asymmetric	80m	Forms part of Leonard Mound along eastern margin. The most actively growing fold in the basin.

Hurunui Bluff Anticline

As with the Hurunui Bluff Fault, the Hurunui Bluff Anticline trends ENE-WSW with a slightly sigmoidal and largely symmetrical appearance. The symmetrical nature of the fold was attributed by Litchfield (1995), to at least one imbricate splay of the HBF and the very young (Late Pliocene to recent) age of the faulting along the range-front. Structure contouring

of the basement-cover sequence boundary by Litchfield showed the presence of three NNE-SSW trending cross folds and evidence for back-thrusting on the southern limb of the fold.

Lowry Peaks Anticline

The Lowry Peaks Anticline forms the central section of the Lowry Peaks Range. Geomorphically, the central section of the range is very distinctive from the southern and northern sections, reflecting the structural history of the range. The Torlesse basement has been highly eroded producing a very steep and rugged appearance to the range. In contrast, the Torlesse basement of the other two sections is morphologically "smooth" and subdued, which has been attributed to representing the Cretaceous peneplain (Cowan, 1992, Litchfield, 1995, and Kellahan, 1998) in other parts of North Canterbury. Topographically, the central portion of the range is significantly higher, and combined with the above morphological differences, indicates that the central section of the range has undergone greater uplift, and is probably older, than the northern and southern sections.

The amount of erosion makes structure contouring of the basement more difficult for the Lowry Peaks Anticline, than for the Hurunui Bluff Anticline, as it is difficult to determine how far below the basement/cover sequence contact the range now sits. The structure contours (Figure 2.9, Volume 2) indicate that the Lowry Peaks Anticline is a doubly plunging, asymmetric anticline with a steeper dipping western limb, and gentler dipping eastern limb. The asymmetry may be reflecting a lack of imbricate splays and back-thrusts of the Lowry Peaks Fault, and possibly an older age of uplift of part of this range, than the Litchfield (1995) documented to the south of the Hurunui River. In plan view, the fold is slightly sigmoidal, with the projected trace of the axial plane becoming difficult to define at either end of the fold. The plunging nature of the fold is reflecting the transfer of displacement from one segment of the Lowry Peaks Fault to another. At the southern end, it is the displacement transfer between the Hurunui Bluff Fault, Hurunui Gorge Fault and Lowry Peaks Fault that has resulted in the structural low, which the Hurunui River has exploited. At the northern end, the transfer of displacement is from the central segment to the northern segment of the Lowry Peaks Fault, which has controlled the development of the Ngawiro Anticline.

Ngawiro Anticline

Named after Ngawiro Station (Map 1), the Ngawiro Anticline is a plunging, symmetrical fold that is located at the northern end of the Lowry Peaks Range. The folding is clearly expressed in the rounded shape of the range, as there has been relatively little erosion of this section, to degrade the smooth surface of the Cretaceous peneplain. The symmetry of the range, lower elevation and relatively uneroded surface (Figure 2.10), indicates that the Ngawiro Anticline is probably the youngest and structurally most immature of the folds comprising the Lowry Peaks Range.

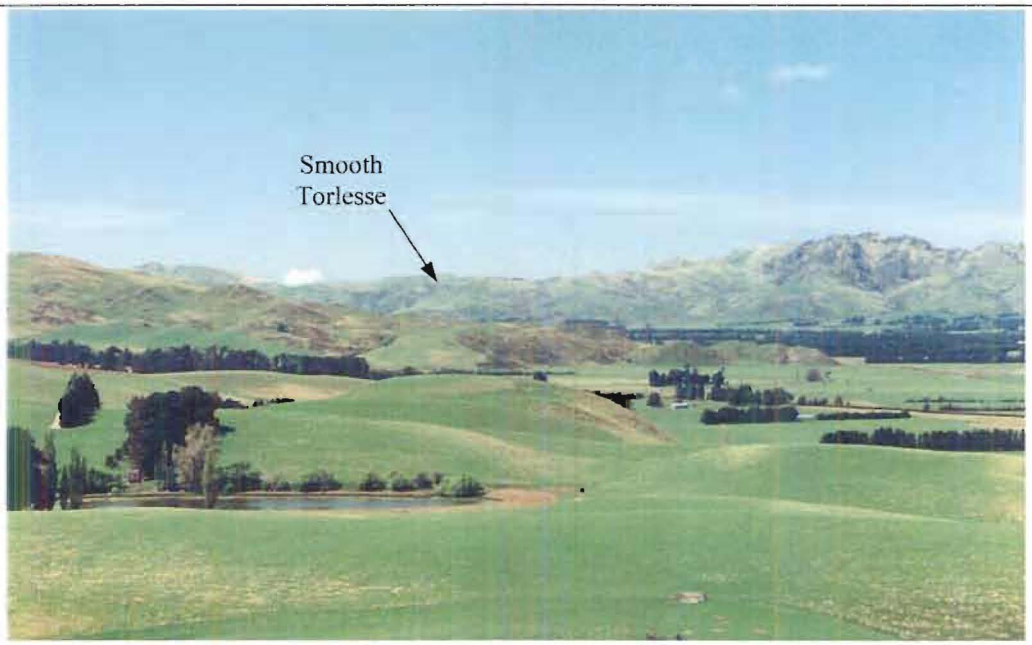

FIGURE 2.10. Photograph of Lowry Peaks Range (background) showing the smoother morphology of the Torlesse at the northern end of the range. The photo is taken from Isolated Hill looking east.

Ben Lomond Syncline

Formed on the downthrown block of the Hurunui Bluff Fault the Ben Lomond Syncline (Hamilton, 1950) trends NE-SW and preserves a small section of the otherwise eroded cover rock sequence on the western side of the Lowry Peaks Range. Only two units of the cover sequence are found in the syncline. Unconformably overlying the basement rocks is the Ashley Mudstone, overlain in turn by the Waikari Formation. The syncline is best exposed on the southern side of the Hurunui River (Figure 2.11) as an asymmetric, southward verging syncline. To the north of the Hurunui River the syncline continues until it is truncated by a transfer fault juxtaposing basement rocks against the younger cover rocks. Outcrop to the

north of the Hurunui River is limited to one or two gullies and the head scarp of the Hurunui Gorge Landslide that has developed on the softer cover sequence. The nature of the range-front at Kaiwara Station suggests that the units seen in the syncline were present but have subsequently been eroded. The presence of the Hurunui Gorge Fault has protected the syncline from erosion immediately north of the Hurunui River.

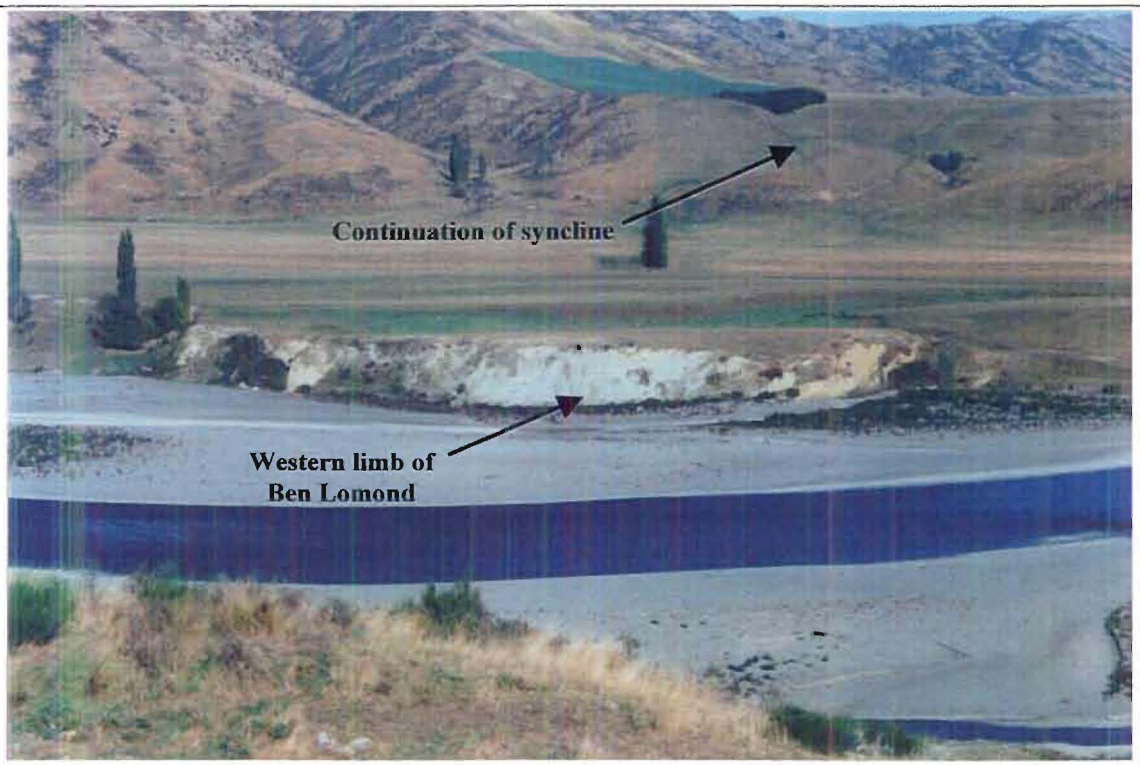

FIGURE 2.11. Photograph looking southwards of the Waikari Formation (grey) overlying the Homebush Sandstone (brown) in the western limb of the Ben Lomond Syncline, exposed in the southern banks of the Hurunui River, Hurunui Gorge (grid reference: N33/030184). The smooth topography of the low hills marks the continuation of the syncline.

It appears from the presence of anomalously thick river gravels (Litchfield, 1995) in terrace scarps to the south of the Hurunui River that the river has preferentially scoured the softer cover rocks. As will be shown in Chapter 3, the Hurunui River has exploited a structural low where displacement transferred from the Hurunui Bluff Fault to the Lowry Peaks Fault. The presence of the softer cover rocks allowed the river to establish its current course.

2.3.3 Isolated Hill

Located on the southern side of the Waiau River, Isolated Hill consists of a number of westward facing thrusts and their corresponding folds (Map 1). The largest of the faults is the Isolated Hill Fault that has uplifted and folded the Torlesse basement and cover sequence rocks into the Isolated Hill Anticline that forms the highest section of Isolated Hill. On the crest of the hill, the Mount Brown Formation and Kowai Formation have been eroded off leaving the hill capped by the Isolated Hill Limestone. To the west, on the downthrown block of the Isolated Hill Fault, the preservation of the Mount Brown and Kowai formations is compatible with Dibble's (1973) gravity data indicating that the deepest portion of the Culverden Basin occurs in the hinge of the Isolated Hill Syncline.

On the eastern and western margins of Isolated Hill, two other faults occur, both with substantial displacements. To the east is the Cranford Downs Fault which sees the Torlesse basement faulted against the younger Mount Brown Formation and to the west is the Rotherham Fault that has produced a 60m high scarp of Mount Brown Formation alongside the Rotherham-Waiau Highway. Neither of these two faults, nor the Isolated Hill Fault have deformed the Late Pleistocene glacial outwash surface on the southern side of Isolated Hill, under which the faults were inferred, and later confirmed by the geophysics, to project.

2.3.3.1 Isolated Hill Fault

Running through the centre of Isolated Hill (Figure 2.12) are a number of faults of which the most significant is the Isolated Hill Fault (IHF). On the whole the Isolated Hill Fault runs NE-SW and dips to the SE, but a cross-fault has divided the fault into two distinct segments. The southern segment displays the greatest amount of movement associated with any of the faults on Isolated Hill, juxtaposing Torlesse basement against the Kowai Formation. Based on gravity data (Chapter 4) and the straight trace of the fault, the fault appears to be dipping steeply to the SE. In contrast the northern segment of the Isolated Hill Fault has thrust Isolated Hill Limestone over the Kowai Formation. While this segment still dips to the SE the dip appears to be moderate rather than steep.

There is no exposure of the fault, but to the west of the Isolated Hill Quarry, Isolated Hill Limestone can be seen within a few metres of deformed Kowai Formation gravels. A change

in the slope angle and a morphological change in the hillslope is also observed, which pinpoints the location of the fault. Once the fault runs into the quarry it is difficult to locate due to the landslide in which the quarry is located.

In a zone, approximately 1 km to the west of the Isolated Hill Fault, are several faults reflecting footwall imbrication of the Isolated Hill Fault. These faults are marked by stream gullies and on the ridges between the gullies, the Mount Brown Formation is sub-vertical.

The cross fault that divides the IHF trends NNE-SSW and displays a sinistral sense of movement. The fault can be traced distance of 2.5km until it disappears under the basin floor gravels. The fault has quite clearly partitioned the central portion of Isolated Hill into two parts. The fault runs up a steep gully to the west of the contact between the Torlesse and overlying cover sequence.

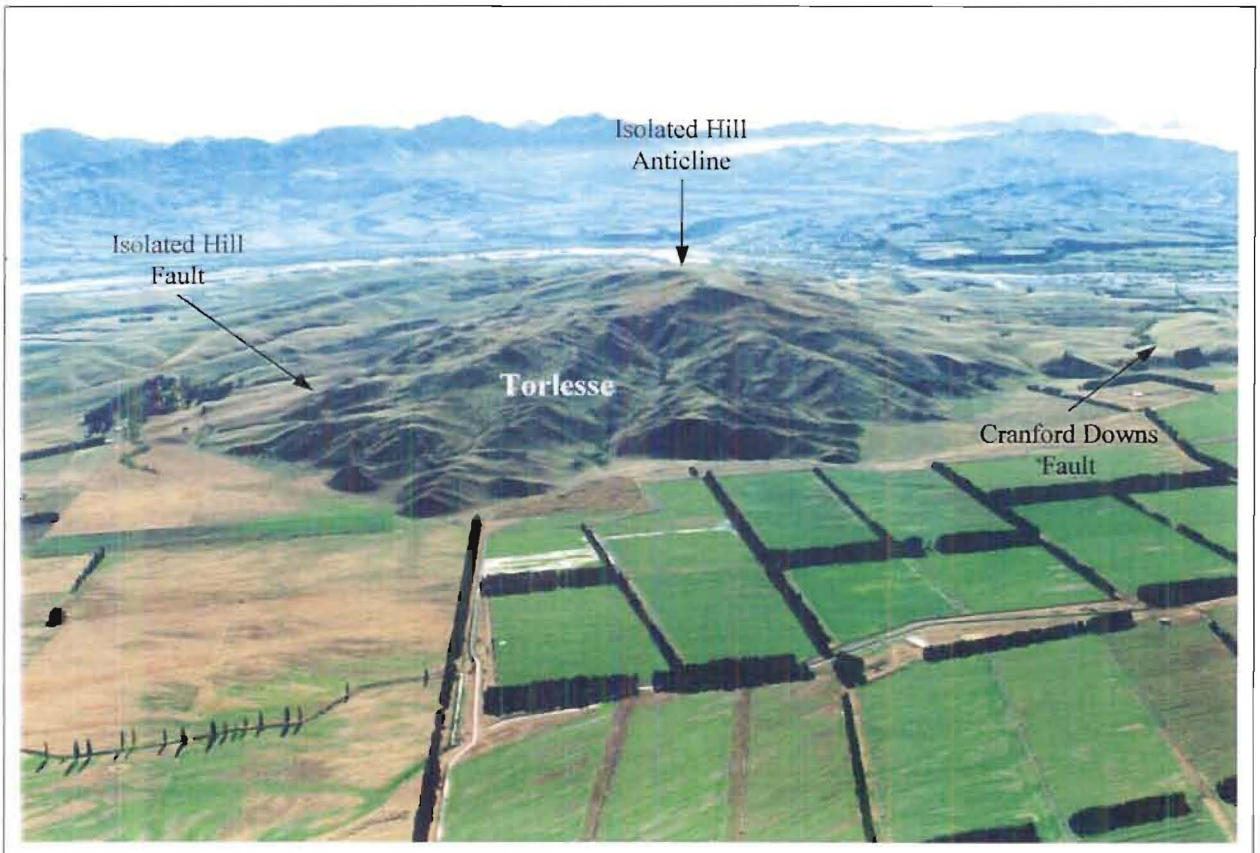

FIGURE 2.12. Aerial photo of Isolated Hill looking northward towards Mount Highfield and Emu Plains.

2.3.3.2 Cranford Downs Fault

As with the Isolated Hill Fault no exposure of the fault has been found. Based on the stratigraphic relationships on either side of the fault, it is clear that there has been significant uplift on the Cranford Downs Fault as Torlesse basement rocks have been uplifted against Mount Brown Formation. The Cranford Downs Fault has a similar northeast-southwest trend to the Isolated Hill Fault and other major faults in the region, and is only visible for 1-1.5km. The southwestern end is buried under the Late Pleistocene gravels of the Burnham Formation, whilst the northeastern has been eroded and buried by the streams that cut across its trace. The age of the Cranford Downs Fault is hard to determine but is assumed to be similar to that of the Isolated Hill Fault, which postdates the Kowai Formation and predates the Burnham Formation.

2.3.3.3 Rotherham Fault

Alongside the Rotherham to Waiau Highway is a scarp composed of Mount Brown Formation that is up to 60m high. The scarp is associated with the Rotherham Fault that has uplifted the western edge of Isolated Hill. Unfortunately, the Waiau River has trimmed the scarp making the precise location of the fault difficult to determine.

Within the fault scarp the Mount Brown Formation can be seen to be dipping 20-25° to the southeast. Just north of Cranford Station, tilted gravels overlie the Mount Brown Formation approximately 30m above the floor of the basin. These gravels are part of the older Kowai Formation gravels, and dip 10-15° to the southeast. In this region, the Mount Brown is crushed and indicates that the Rotherham Fault is in close proximity.

It is also interesting to look at the boreholes (N32/0035, N32/0036, N32/0147 and N32/0212, Appendix 1) placed on either side of the inferred fault especially at the northern end of Isolated Hill. To the east there is only a 3m covering of gravels overlying the Mount Brown Formation, whereas to the west the wells indicate that there is at least 20m and the geophysics (Chapter 4) would suggest that there is significantly more than that. The faulting has produced a structural low into which the Waiau River, along with the rivers and streams entering the basin form the north have deposited a thick succession of gravels.

The fault is easily traceable until it reaches the Waiau River at which point all evidence has been removed. On the northern side of the Waiau River on the high terrace composed dominantly of Woodlands Formation, several scarps are seen on a strike parallel to the Rotherham Fault and in line with the inferred location. The origin of these scarps is uncertain, but they may well be fault scarps related to the Rotherham Fault. If they are, then they suggest that the youngest movement on the fault postdates the Woodlands Formation, but predates the Burnham Formation as no sign of the faulting is seen in the Burnham Formation.

2.3.3.4 Isolated Hill Anticline

Capping Isolated Hill is the Isolated Hill Limestone, which clearly defines the Isolated Hill Anticline on the northern end of the hill. At the southern end of the hill, the cover sequence has been stripped away exposing the Torlesse basement in the core of the fold. The fold reaches its maximum amplitude at the Isolated Hill trig station and plunges to the northeast, forming a structural low between Isolated Hill and Mount Highfield, which the rivers have exploited.

The folding is best expressed by the rounded morphology of the hill-crest, because a series of small-scale faults have disrupted the limestone, giving it the appearance of being tilted to the southeast rather than folded. These faults are sigmoidal in plan view and have trace lengths of a few hundred metres. In the areas between the faults, Mount Brown Formation is still preserved.

2.3.2.5 Isolated Hill Syncline

A gravity survey by Dibble (1973) showed that one of the largest negative anomalies (Chapter 4) within the basin occurs on the NW side of Isolated Hill. The axis of the anomaly parallels the major faults observed in the vicinity and is interpreted to coincide with the axis of a syncline developed on the downthrown block of the Isolated Hill Fault. In the core of the syncline Kowai Formation gravels have been preserved. As with the anticlines in the region, the gravity data indicates that the fold is asymmetric, with the eastern limb being steeper than the western limb. On the ground the western limb dips at 20-25° SE as expressed in the

Mount brown Formation. The eastern limb on the other hand is not observed and is believed to have been faulted out by the imbricate faults of the Isolated Hill Fault.

2.3.4 Mount Highfield

Within the study area, Mount Highfield is unique. The presence of the Late Cretaceous to Early Eocene formations, which are not seen to the south, indicates that the northern boundary of the Hurunui High occurs between Mount Highfield and Isolated Hill (Map 1). Mount Highfield itself, is a plunging asymmetric anticline, that unlike the other folds in the area, has an overturned forelimb. Controlling the development of the Mount Highfield Anticline is the Mount Highfield Fault along the northwestern edge of Mount Highfield.

The majority of the faults described here have been mapped previously by several different workers: Falloon (1954), Gregg (1964), Gregg (1965), Lammerink (1976) and Endharto (1987). These workers suggested that the faults were steeply dipping and upthrown to the east.

2.3.4.1 Mount Highfield Fault

Running along the northwestern edge of Mount Highfield, the Mount Highfield Fault has been responsible for the development of the anticline that constitutes Mount Highfield. Although not exposed, the location of the fault can be determined from the stratigraphic relationships and the deformation of the units in close proximity. On the SE side of the fault, the uplifted units have been folded into an anticline whose fore-limb has been overturned and is dipping steeply to the southeast. In contrast, those units on the relatively downthrown side of the fault dip moderately to the northwest.

The fault can be traced along the edge of Mount Highfield a distance of approximately 5km. At the northern end the fault is juxtaposing Torlesse against Torlesse. To the west of the fault the Stanton Conglomerate is observed overlying the Torlesse in the terrace scarp at Highfield Station. Southward the fault can be traced to Waiau township at which point the rivers have conspired to remove its trace. To the south of the Waiau River, there is the Isolated Hill Fault which may represent the continuation of the Mount Highfield Fault.

Capping the terrace at Highfield Station are gravels that, for simplicity, have been correlated with the Windwhistle Formation (Gregg, 1964) even though they are not glacial outwash deposits (Chapter 3). These gravels show no sign of displacement or disruption indicating that since the early last glaciation there has been no significant movement on the fault.

2.3.4.2 Rahi Fault

Located at the northern extremity of the study area, the Rahi Fault was first mapped by Gregg (1964), followed by Gregg (1965), and named by Lammerink (1976). To the north of the fault the Late Cretaceous-Tertiary strata are folded into a plunging anticline as part of the Upper Highfield folds. Across the fault the strata have been significantly displaced juxtaposing the Torlesse basement and the Late Cretaceous-Tertiary strata against the Greta Formation. This truncation of the units to the north of the fault is most clearly highlighted by the sinuous Isolated Hill Limestone ridge.

Both Gregg (1964) and Lammerink (1976) have tentatively correlated the units to the north of the fault with those seen in the terrace to the north of Waiau. This leads to a dextral strike separation of approximately 5.6km. The fault becomes buried by the Pleistocene gravels once it crosses the Mason River, and its probable connection with the footwall of the Iho Fault. It seems more probable from the general structural style, that this separation, while a dextral component of slipping may be needed, is largely a product of overturning of the southern strike extension of the footwall units.

2.3.4.3 Other Faults

Three other faults (Iho, Paku and Ngaro) all trend NE-SW and lie between the Totika and Rahi faults on Mount Highfield. The location of all three faults can be readily identified. The Iho Fault has faulted the Torlesse basement rocks against the Late Cretaceous to Eocene conglomerates and marine sediments near the Mason River. The Iho Fault appears to be the best candidate as the continuation of the Mount Highfield Fault seen to the south. The Stanton Conglomerate near the fault is highly sheared and crushed. Unfortunately, due to the nature of the outcrop it is not possible to examine it in detail. From the closest vantage point, approximately 20m away, from the other side of the gully up which the fault runs, the

deformation in the gravels indicates that the fault is steeply dipping in the near surface. Further to the NE a slice of basement has been faulted into the Greta Formation as a result of movement on both the Iho and Paku Faults. The SW end of the fault is marked as a gully in the Torlesse basement.

The Paku and Ngaro faults are both marked by straight stream gullies. The Ngaro Fault occurs on the western side of the Mount Highfield trig station and has produced some scarp-like features on the ends of the small spurs of Torlesse. As with the Paku Fault the NW side of the faults have been upthrown relative to the SE sides. In contrast the other faults in the area have their SE sides upthrown relative to their NW sides. The Paku and Ngaro faults are possibly back-thrusts off the Iho and Rahi faults. Although not exposed, the faults are assumed to be sub-vertical in the near surface.

2.3.4.4 Mount Highfield Anticline

The Mount Highfield Anticline is unique within the field area in that the Late Cretaceous to Tertiary strata have been preserved on both limbs of the fold. The cover sequence formations are observed to reach their maximum thicknesses in the core of the fold and thin out rapidly onto the limbs of the fold. The Isolated Hill Limestone, that caps Mount Highfield, pinches out rapidly to the south and is absent around the nose of the anticline. The Mount Brown Formation, around the nose of the fold, unconformably overlies the Cookson Volcanics. In contrast to the Isolated Hill Limestone, which pinches out south of the trig on Mount Highfield, the Cookson Volcanics thicken markedly, indicating relief at the time of deposition. The nose of the fold is overlain by the Pleistocene gravels derived from the Mason and Lottery rivers.

Not only is the fold unique for the preservation of the strata on the fore-limb, but the strata shows that the fore-limb is overturned and is dipping steeply to the SE. Mapping of the stratigraphy indicates that the fold is plunging to the southwest. As with the other folds in the region the forelimb is steeper than the back-limb, which dips at 20-25° SE.

2.4 INLIERS

Within the basin there are several inliers which provide valuable insights into the deformation occurring beneath the floor of the basin. The most notable of these is Leonard Mound along the eastern margin of the basin. The faults of Leonard Mound and the associated fault system responsible for its development will be covered in the following chapter. Along with Leonard Mound there are two other inliers. Immediately to the west of Culverden is the Culverden Inlier, whilst to the south, by the Hurunui River, is the Hurunui Inlier.

2.4.1 Culverden Inlier

Situated 1.5-2km west of Culverden, the Culverden inlier is an upthrown block of Early Pleistocene gravels and Tertiary strata (Figure 2.13). The uplift has produced an asymmetric anticline that plunges to the southeast. Although not seen, the fault responsible for the uplift is assumed to be a NW-SE trending, high angle reverse fault based on the morphology of the inlier. The NW-SE trend is orthogonal to the trend of the majority of structures seen not only in and around the Culverden Basin, but also North Canterbury. The trend is similar to the orientation of the cross faults on the western end of Mount Culverden and may represent an extension of one of these faults.

On the NE side of the inlier, Isolated Hill Limestone is exposed in a quarry and is dipping moderately to the southeast. Faults with up to 1m wide gouge zones are also present which strike sub-parallel to the crest of the inlier and dip steeply to the southeast. It is believed that these faults represent the orientation of the main fault controlling the inlier. At the base of the quarry, blocks of basalt and greensand are present which are part of the Cookson Volcanics that underlie the Isolated Hill Limestone. There is no sign of the Mount Brown Formation that conformably overlies the Isolated Hill Limestone on Mount Culverden to the north. To the west of the limestone quarry, another quarry has been established to obtain the gravels that cap the inlier. The gravels are composed of weathered, rounded Torlesse clasts. The gravels are stratified and are dipping approximately 10° to the southeast. From the degree of weathering and the dip, these gravels appear to be early Pleistocene and most likely part of the Kowai Formation.

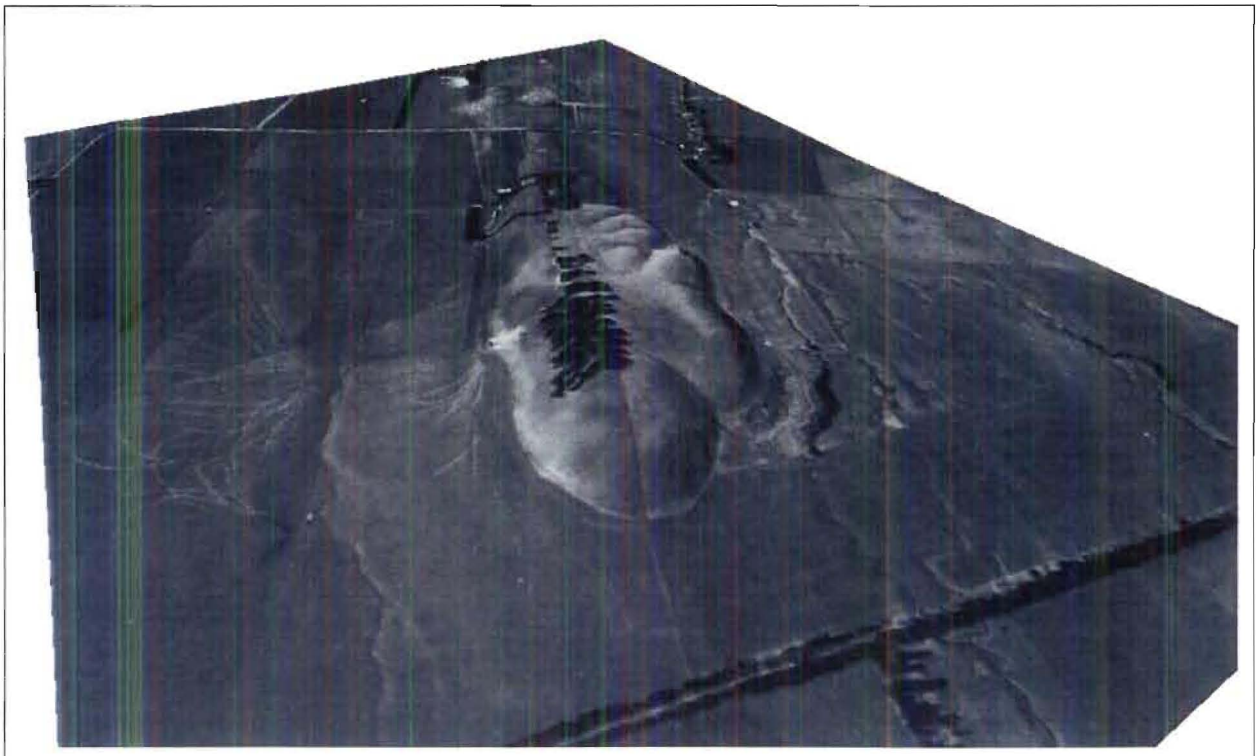

FIGURE 2.13. 3D rendered aerial photograph looking southeast along the Culverden Inlier.

Capping the inlier is a thick soil upto 4m thick on the crest and the southern flank and only 150cm on the northern flank. Surrounding the inlier are Late Pleistocene gravels of the fan complex from the Pahau and Hurunui Rivers (see Chapter 3.). There has been no deformation of the Late Pleistocene gravels.

On the southern side of the inlier, the soil and gravels have been dissected by several small streams that only flow during the winter months. These streams flow in a south-southeast direction indicative of the southeast plunge of the fold. The source of water for the streams is most likely the underlying limestone rather than surface runoff.

2.4.2 Hurunui Mound Inlier

First mapped by Gregg (1964), followed by Browne (1984) and finally Mould (1992), the Hurunui Mound Inlier, or Balmoral Forest Inlier (Browne (1984), is a series of NE trending tight anticlines and synclines. Mount Brown Formation sandstones and limestones are involved in the deformation surrounded by the Pleistocene gravels of the Burnham Formation

and younger outwash gravels belonging to the St Bernard Formation (Gregg, 1964). All these gravels are capped by 1-3m of loess (Browne 1984).

The asymmetric nature of the folds (Figure 2.14) tend to suggest that the faults controlling their development is a SW facing reverse fault related to the faults seen on the western margin of the basin.

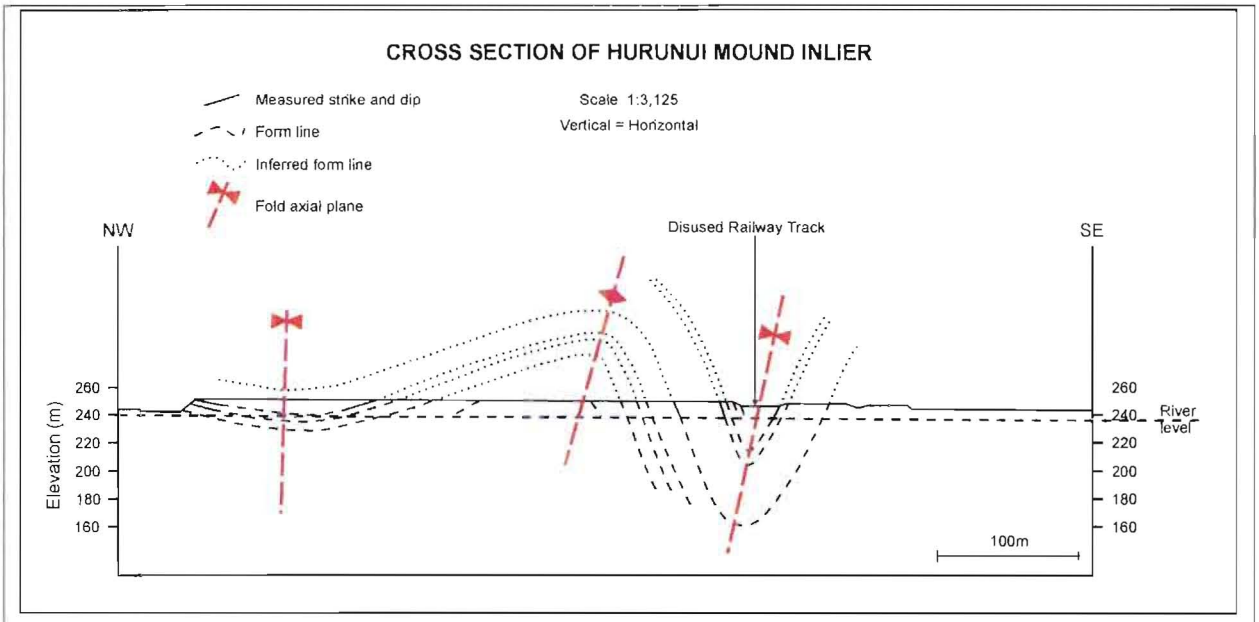

FIGURE 2.14: A schematic cross section of the Hurunui Mound Inlier. Form lines are derived from marker horizons in the Mount Brown Formation (from Mould, 1992).

2.5 OVERVIEW OF THE WEST AND NORTHWEST MARGINS

Reconnaissance mapping of the western and northwestern basin margins was carried out so as to:

1. gain an understanding of the structural setting of the basin,
2. aid in the modelling of the TEM and gravity data.

The structures discussed in this section are shown in Figure 2.15 (Volume 2).

2.5.1 Western Margin

The mapping of a significant portion of the western margin was by Mould (1992). Mould showed that the western margin was controlled by a series of eastward facing reverse faults/thrusts believed to be back-thrusts off the Alpine Fault. There are three faults principally involved in the deformation along the western margin: Waitohi Downs Fault, Green Hill Fault and Balmoral Fault.

To the south of the Hurunui River, Mould (1992) mapped the Waitohi Downs Fault and showed it to be the most laterally extensive of the major faults along the western margin of the basin. At its type location, Flaxdown Quarry to the north of the Hurunui River, Torlesse sandstones have been thrust against the Flaxdown Limestone. North of Flaxdown Quarry the fault is expressed as an alignment of saddles within the Torlesse basement. In some stream gullies the fault can be seen dipping at moderate angles to the NW.

Gravity data (Dibble, 1973; Hicks, 1989) indicates the presence of a significant basin beneath the Hurunui River between the Hurunui Mound and the southern edge of Green Hill. Adjacent to this basin, the Waitohi Downs Fault undergoes a swing in strike from N to NE, suggesting that the basin may have controlled the location of the fault, this, however, is geometrically impossible. Rather, a structural high is required to produce the concave SE jog in the strike of the fault. Mould (1992) attributed the jog to the presence of a weak zone within the Torlesse which the fault exploited. Along the western margin several N-S lineaments are observed (next section) giving rise to the very straight basin margin and the zone of weakness that the Waitohi Downs Fault exploited.

To the east of the Waitohi Downs Fault is the Green Hill Fault. Where exposed the fault is typically a steeply dipping reverse fault that has juxtaposed Cookson Volcanics against the Kowai Formation suggesting significant uplift since the Early Pleistocene. The fault is best exposed in Cascade Stream and is seen to be dipping to the NW at 70°. To the north of Cascade Stream the fault is easily identifiable as it has thrust Torlesse rocks over the Tertiary succession. As the fault approaches the Pahau River it becomes highly splayed and is responsible for the wedging out of the Tertiary sequence in the Pahau River. The splays are marked by saddles and can also be observed again juxtaposing basement against the cover

sequence in the banks of the Pahau River. Where visible these splays appear to be dipping at a lower angle than Mould observed for the fault to the south.

The final of the three faults, the Balmoral Fault, is the only fault with an obvious Holocene surface trace along the margin. Mould (1992) mapped the fault and showed that there has been up to 5.75m of vertical displacement and 14m of horizontal displacement (Figure 2.16). The active nature of the Balmoral Fault indicates that the western range-front is propagating eastward into the basin. The fault has been responsible for the uplift of the eastern edge of Green Hill on which up to 1600m of Kowai Formation gravels have been preserved in the Green Hill Syncline. The fault is traceable along the eastern edge of Green Hill and appears to connect with a fault mapped on the northern side of the Pahau River which has thrust Torlesse over Cookson Volcanics and Isolated Hill Limestone.

Associated with the faulting are three fault related folds which trend parallel to the faults. To the south of the Hurunui River is the Waitohi Downs Syncline formed on the downthrown block of the Waitohi Downs Fault. To the north of the Hurunui River are the Flaxdown Quarry Anticline and Green Hill Syncline. The later two folds are both poorly exposed and preserved. All three folds are asymmetric with the axial planes dipping steeply in the same direction as the nearby macroscopic faults.

2.5.2 Mount Culverden Fault

Anomalous to the trend of the other major structures in the region, the Mount Culverden Fault has an orientation due east-west. Essentially straight, the fault can be traced along the base of the Mount Culverden Range (Figure 2.17) for 12km at which point it splays. One splay continues on the east-west orientation up Countess Stream whilst the other splay heads off on a WSW trend marked by a line of saddles across which a change in the morphology of the Torlesse based topography is observed. On the northern side of the fault the topography is steep and rugged compared with smooth on the southern side. The eastern end of the range becomes saw-tooth like in appearance, which may be indicating near surface segmentation of the fault. The fault is inferred to be a high angle reverse fault with the southern side uplifted relative to the northern side. Its strike may well suggest that it is a reactivated Late Cretaceous normal fault, similar to those documented by Nicol (1991, 1993) and Barnes (1993).

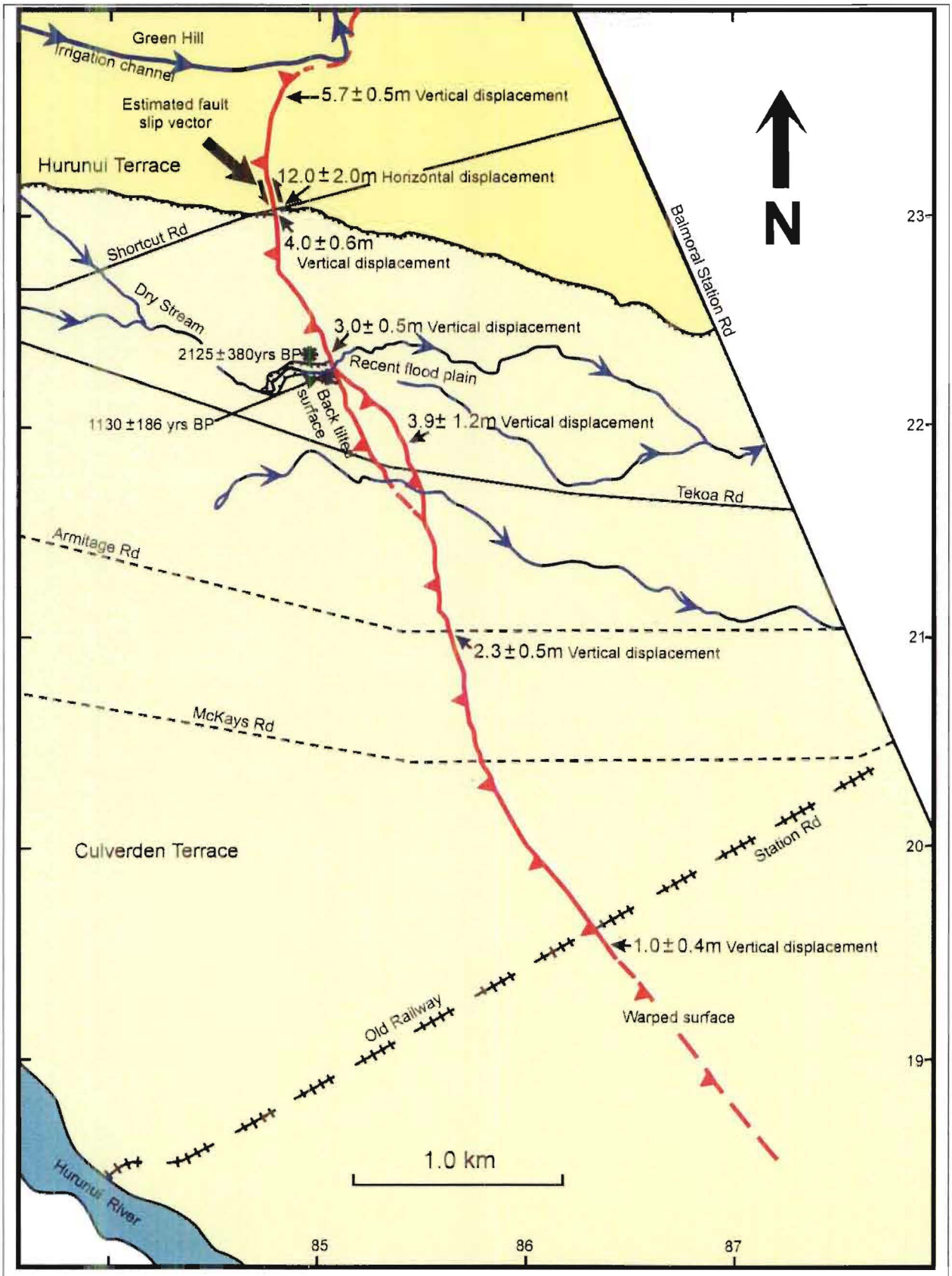

FIGURE 2.16. A map of the active Balmoral Fault showing vertical and horizontal displacements. Also shown (asterix) are the sites from which weathering rinds were collected for constraining the age of ground rupture (from Mould, 1992).

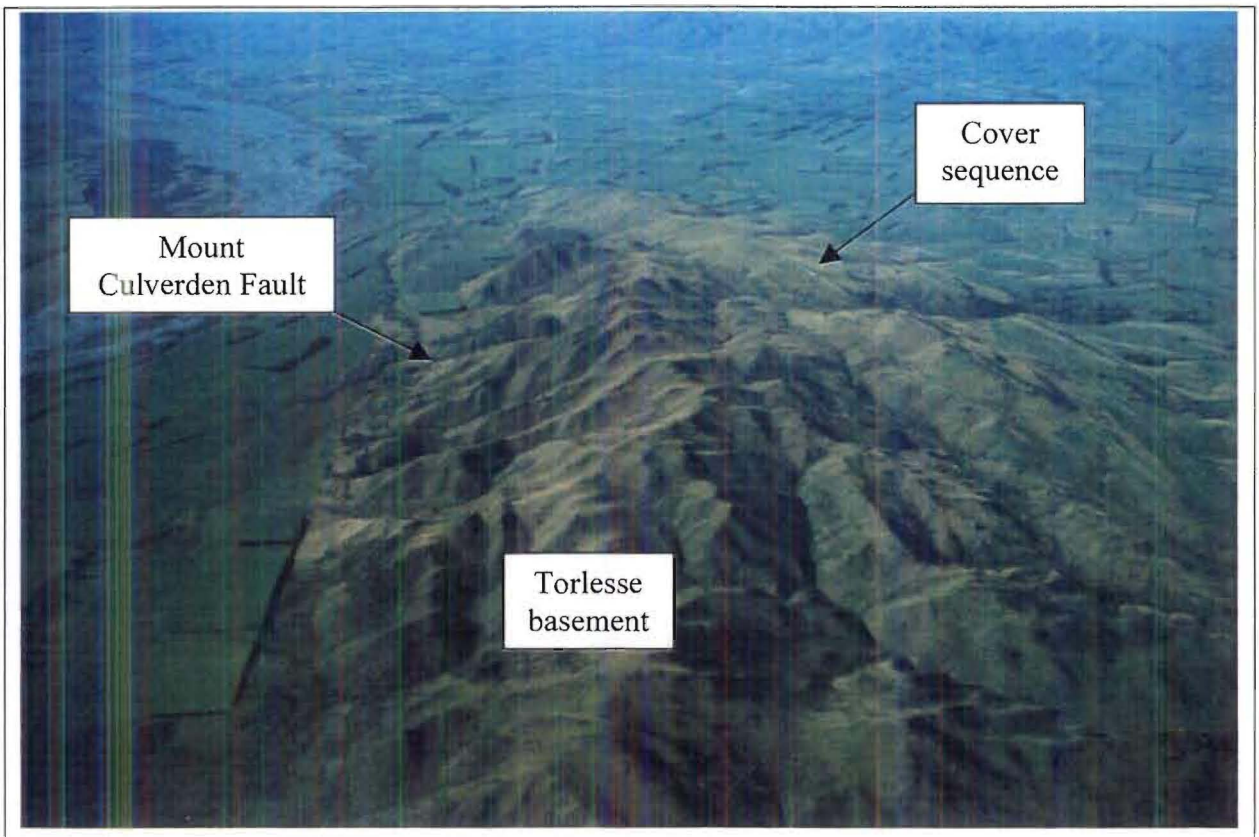

FIGURE 2.17. Photo of Mount Culverden looking east along the Mount Culverden Fault (Photo courtesy of Jarg Pettinga).

Cover sequence rocks are exposed on the southern side of Mount Culverden and are dipping southwards whilst on the northern side the cover sequence has been eroded off leaving the Torlesse basement exposed. Stratigraphically, the Tertiary succession on the southern flank of Mount Culverden is similar to that seen on Isolated Hill.

Based on the geology and geomorphology, an estimate of the amount of vertical displacement associated with the Mount Culverden Fault is difficult. Based on the elevation of the range (upto 400m above the basin floor) and the thickness of the tertiary strata exposed on the southern flank of Mount Culverden, there may well have been 700-1000m of vertical uplift.

Towards the western end of Mount Culverden there are a number of NW-SE trending faults that are most clearly visible on the southern flanks of Mount Culverden. These faults are marked by straight streams across which a change in the attitude of the Torlesse and displacement of the Tertiary strata is observed. The orientation of these faults is similar to the Cabbage Tree Fault and the cross faults seen dissecting the Amuri Range to the north.

Although the fault planes are not exposed, it is inferred, based on the Cabbage Tree Fault, that these faults are SW dipping reverse faults with a sinistral sense of horizontal motion. It is also suspected that one of these faults may be responsible for the uplift of the Culverden Inlier.

Mount Culverden also marks a boundary between the dominantly eastward facing thrusting observed along the western margin and the westward facing thrusting responsible for the Amuri Range to the north. This may suggest that the Mount Culverden Fault existed prior to the current period of deformation and has partitioned the strain along the northwestern margin into two parts. Further work and detailed mapping around the junction of the Mount Culverden Fault with the structures to the north and south needs to be carried out to gain a better understanding of the kinematics of the deformation in this region.

2.5.3 Emu Plains

To the north of Mount Culverden a similar style of faulting is seen as that along the eastern margin of the basin. Known as Emu Plains, the area is characterised by uplifted Torlesse basement on westward facing reverse faults and by the development of a broad terrace of predominantly Burnham Formation. Very little of the cover sequence has been preserved on and around Emu Plains. The majority has been eroded off to leave relatively smooth Torlesse based topography on the lower slopes of the range. Upslope the morphology of the Torlesse abruptly changes to the more characteristic steep and rugged topography indicative of a longer period of erosion.

Essentially the Amuri Range is another basement-cored asymmetric anticline that plunges to the SW, for which the major range-bounding fault is the Marble Point Fault. Mapped by Syme (1991), the Marble Point Fault is a northeast striking oblique thrust system that merges with the Hope Fault at it northeastern end and is truncated by the Cabbage Tree Fault at its southwestern end. The faulting has resulted in the formation of a tight train of folds in the footwall of the Marble Point Fault, expressed in the Tertiary strata. Surface ruptures, recent downcutting and gradient anomalies on the Waiau River all indicate that activity is ongoing.

Several tear faults, orthogonal to the trend of the thrusts, exist along the NW margin that are segmenting the Amuri Range. The best exposed of the tear faults is the Cabbage Tree Fault

that was mapped by Syme (1991). The Cabbage Tree Fault (CFT) is a NNW striking fault that truncates the western end of the Marble Point Fault to the NW of the study area. Deformation associated with the CFT indicates that the fault is acting as a transfer fault with a component of reverse motion (Syme, 1991, Pettinga, 1997). The other tear faults are not exposed but are clearly delineated by streams on the range and by the termination of the NE-SW striking structures.

Deforming the SE flank of the Amuri Range are a number of hanging wall imbricate thrusts that parallel the trend of the Marble Point Fault. As a result of the cross-faults, these thrusts tend to be relatively short in extent. These faults have their own asymmetric plunging anticlines which verge to the NW.

The northern end of Emu Plains is dominated by relatively large alluvial fans extending out from the Amuri Range. In contrast to the fans along the eastern margin of the basin, the streams on the fans are incised into the fans as a result of erosion, by the Waiau River, into the toe of the fans.

2.5.4 Lineaments

Visible most clearly on the landsat image of North Canterbury (Figure 1.1) are a number of N-NNE trending lineaments along the western margin of Culverden Basin. The straight western margin is a continuation of the longest lineament that runs from Mount Grey in the south, through to the Hope Fault to the north. Mould (1992) reported that the Mandamus Igneous Complex lies along the lineament. Mould also noted that to the west of the Mount Grey-Hope Fault lineament, the Torlesse contains uncommonly high occurrences of spilitic volcanics. To the east there are several more of the lineaments along which the Pahau River and Ramatama Stream flow.

From the decrease in altitude of the Torlesse it appears that the eastern side of the lineaments are downthrown relative to the west. From the evidence Mould (1992) suggested that the Culverden Basin could be overprinting an older set of N-S structures which have been exploited by the Mandamus Igneous Complex and the Waitohi Fault.

2.6 SUMMARY

The eastern margin of Culverden basin is structurally controlled by the East Culverden Fault Zone, comprising a complexly segmented range-front fault system and associated fault-propagated anticlines. The Lowry Peaks Range, bordering the eastern margin of the basin, is the surface manifestation of the deformation and is composed of three anticlines with differing structural styles, reflecting the relative ages of the folds. The transfer of displacement from one segment of the fault to another, has created structural lows which the rivers have exploited.

Mount Highfield and Isolated Hill are both part of the fold and fault belt. The Mount Highfield/Isolated Hill structures are the westward propagating footwall imbricate thrusts and associated folds of the range-front fault system of the ECFZ. These structures represent the onset of basin inversion at the northern end of Culverden Basin. As a result of the deformation, it is envisaged that Culverden Basin is becoming partitioned into small sub-basins, whose ongoing tectonic evolution will influence the distribution and architecture of the Late Quaternary deposits described in the following chapter.

The majority of the deformation along the eastern margin is being accommodated on the Leonard Mound Fault System. The Leonard Mound Fault is an imbricate splay of the LPF and shows that the eastern margin is actively propagating westward into the basin. The western margin of the basin is also propagating into the basin as is evident from the active Balmoral Fault. As with the eastern margin, reverse faults/thrusts dominate and have been inferred to be back-thrusts off the Alpine Fault to the west. The faults appear to be overprinting an older set of structures that have produced a structural low along the western margin of the basin.

CHAPTER 3

LATE QUATERNARY GEOLOGY AND GEOMORPHOLOGY

3.1 INTRODUCTION

The Quaternary is defined by climatic changes strong enough to cause ice ages (Bull, 1991). The climate changes have been preserved in the landscape by the hills, streams, alluvial deposits and soils, revealing the geomorphic processes associated with the changing conditions. Hydrogeologically, the alluvial deposits are the most important stratigraphic units within the basin, as they are the aquifer bearing units from which the groundwater is extracted. Due to the different depositional environments, there is a range of lithologic facies within the deposits, whose interaction will strongly influence the near surface groundwater flow. Superimposed on that fluvial architecture, is the active earth deformation that is clearly disrupting the aquifers and consequently needs to be considered in the hydrogeological model.

The previous chapter essentially dealt with the broad scale structure of Culverden Basin, which has played an important role in controlling the deposition of the Late Quaternary alluvium. As was shown, the majority of those structures do not clearly cut or displace the late last glaciation and Holocene deposits classifying them as either probably active (Class III) or inactive based on the classification scheme devised by Pettinga et al. (1998). As a result, they will have very little effect on the near surface groundwater flow, which is occurring predominantly within the deposits assigned to the last glaciation. The structures investigated in detail in this chapter are those which have disrupted deposits younger than 25,000 years and are accordingly classified as either Class I or II. The main focus is the actively evolving imbricate thrust system (Leonard Mound Fault System) along the eastern margin of the basin and its associated structures. Geomorphically, the system has been pristinely preserved allowing for detailed geomorphic mapping, which has aided in the understanding of the tectonic development of the east basin margin, and the effects of that deformation on the groundwater system.

This chapter describes the Late Quaternary fluvial and tectonic features within the study area. The proposed fluvial and tectonic features can be viewed on Maps 2 and 3 respectively (Volume 2). The relationships between the different fluvial and tectonic facies, and their roles in the hydrogeologic setting, are examined in Chapter 5 once the geophysical investigations (Chapter 4) have been discussed.

3.2 ALLUVIAL DEPOSITS

The Late Quaternary stratigraphy of Culverden Basin can be broadly divided into glacial versus non-glacial deposits. The glacial deposits consist of glacial outwash sheets deposited by the major rivers (Waiau, Pahau and Hurunui) flowing into the basin from the west during the Late Pleistocene. The non-glacial deposits are either those deposited by non-glaciated rivers (e.g. Mason and Lottery rivers), the range-bounding alluvial fans (e.g. Lowry Peaks fans) or are clearly Holocene in age (e.g. modern river gravels).

Exposure of the deposits, especially to the south of the Waiau River, was limited to a few stream banks and pits dug by the farmers. From those limited exposures and bore logs of the water wells in the basin, it is difficult to map the different deposits based on their lithological characteristics alone, as they are often very similar. The mapping of the alluvial deposits has been based on the *geomorphic surfaces* of the different alluvial deposits, as each surface has distinctive geomorphic features. A geomorphic surface, as defined by Ruhe (1956) and Bull (1991), is a mappable landscape element that has been formed during a discrete time period; it has distinctive materials, topographic features, soil profile and weathering characteristics. The correlation of the different deposits is based on the map relationships and comparison with the timing of aggradation events in nearby catchments (e.g. Charwell River), whose deposits have been dated.

Differentiation of the Pliocene gravels from the younger fluvial and glacio-fluvial Quaternary aggradation gravels can be difficult. In places the older gravels can dip up to 35° (e.g. Isolated Hill) whereas the later Quaternary gravels on the whole are sub-horizontal. It was also found that the Pliocene gravels have interbedded sandstones and siltstones, up to several metres thick, which are absent from the younger gravels. This was particularly useful in delineating the Pliocene versus Quaternary gravels in some of the boreholes in the basin.

3.2.1 Glacial Stratigraphy

The floor of the Culverden Basin is covered by coalescing glacial outwash sheets deposited by the three rivers flowing into the basin from the west. The deposits from the three rivers are clearly distinguishable, and have been mapped previously by Powers (1962), Gregg (1964) and Clayton (1965 and 1968). Powers mapped the terraces of the Hurunui River, Clayton mapped the deposits associated with the Waiau River, and Gregg correlated the glacio-fluvial deposits with the glacial chronology established in other South Island regions (Figure 3.1).

Based on soil profiles, surface elevations and geomorphic features, Clayton (1965 and 1968) recognised and mapped (Figure 3.2) four glacial advances (all within the last Otiran/Hope Glaciation) and established a local glacial chronology for the Waiau Valley. The oldest of the four is the Leslie Hills Advance, which has been correlated with the Windwhistle Formation. The following three advances were correlated with the Burnham Formation mapped by Gregg (1964). Of the three, the oldest advance (Glenhope) is found on Emu Plains on the northern side of the Waiau River. The braid channels, which are so characteristic of the Burnham Formation to the south of the Waiau River, are much more subdued on Emu Plains, which Clayton attributed to representing an older surface. To the south of the Waiau River, Clayton distinguished two advances (Glynn Wye and Lewis) due to a scarp that runs from the eastern end of Mount Culverden eastwards to Mount Palm Road, at which point it dies out.

Clayton based his interpretations on observations he made of the glacial stratigraphy in the Lower Hope Valley to the west of Hanmer Basin. More recent work (Knuepfer, 1984 and Cowan 1989) reinterpreted Clayton's stratigraphy, in which Cowan identified three successive stadials of the Hope Glaciation (between 70 000 and 14 000 yr BP): Glenhope Advance (70 000-25 000 yr BP), Glynn Wye Advance (22 000-16 000 yr BP) and Dismal Advance (15 000-14 000 yr BP).

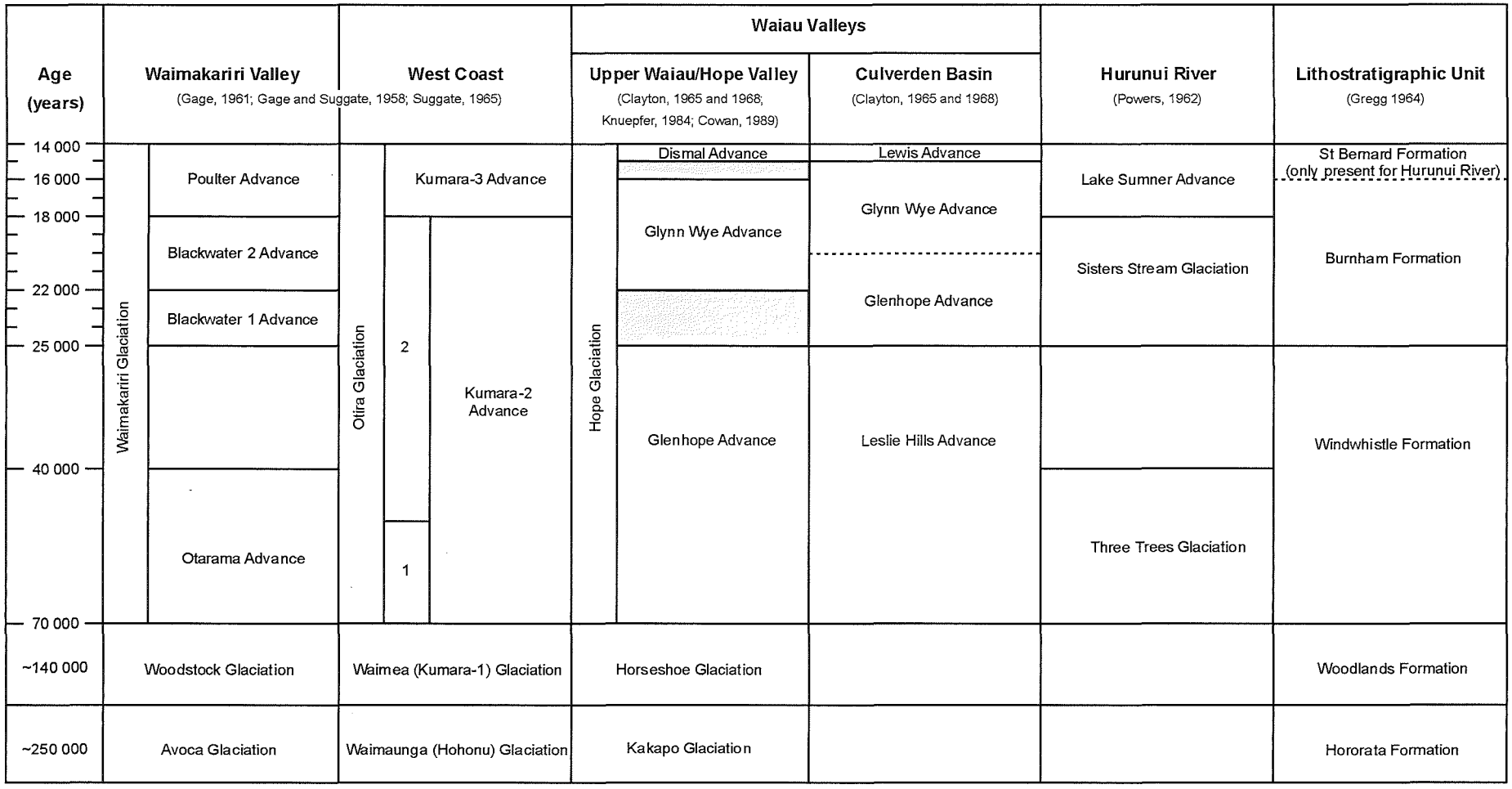

FIGURE 3.1. Correlation of the Late Pleistocene glacial chronology of Culverden Basin with other South Island chronologies. Shaded areas denote periods of ice retreat documented by Cowan (1989).

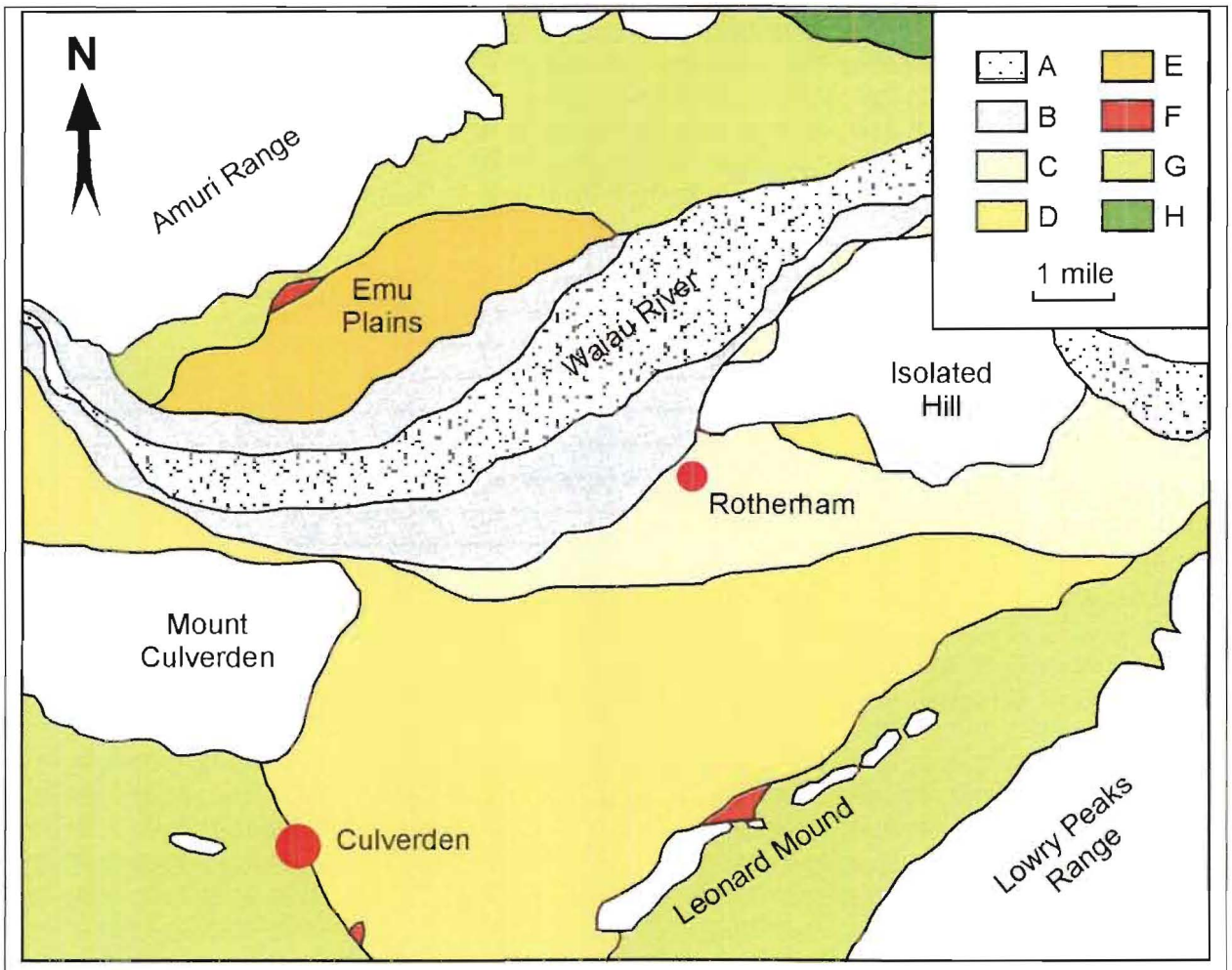

FIGURE 3.2. Clayton's (1965) map of the Late Pleistocene glacial stratigraphy of the northern Culverden Basin. (A) modern floodplain, (B) post-glacial deposits, (C) Lewis Advance, (D) Glynn Wye Advance, (E) Glenhope Advance, (F) Leslie Hills Advance, (G) Alluvial fans of Hope Glaciation age, (H) Alluvial fans of Horseshoe Glaciation age.

After examination of the glacial stratigraphy within Culverden Basin during this study, Cowan's nomenclature has been adopted for the Waiau River glacio-fluvial deposits. The Glenhope advance only occurs in scattered remnants along Emu Plains and to the southeast of Culverden. The Glynn Wye Advance forms the extensive outwash sheet that covers the floor of the basin to the north of Culverden, and has been called the Culverden Surface. I found no evidence to distinguish the three surfaces that Clayton mapped. Lithologically there is no difference in Clayton's Lewis, Glynn Wye and Glenhope advances. To the south of the Waiau River, the geomorphic features of the deposits also suggest that they are a single advance rather than two. The subdued nature of the braid channels on the Emu Plains surface, compared to those on the Culverden Surface, is believed to reflect the amount of time the

Waiau occupied the surface. The thin to absent soil cover on the Culverden Surface indicates that the Waiau River was probably active on the surface until the end of the Hope Glaciation.

The Dismal Advance can be traced down the Hope and Waiau Valleys to the Hanmer Basin where it forms remnant terrace surfaces at the entrance to the Waiau Gorge, which can be traced through the gorge to the Culverden Basin. Once out of the gorge, the terraces merge very quickly with the main basin surface making it very difficult to trace the deposits out onto the floor of the basin. Hence within the study area no deposits associated with the Dismal Advance have been recognised.

The glacial chronology established by Powers (1962) for the Hurunui River has been adopted for this study. Three terraces were mapped by Powers and later named by Mould (1992) and correspond to the four glacial advances that powers identified in the Hurunui Valley. The three terraces from highest to lowest are the Hurunui, Culverden and Medbury terraces and are underlain by deposits from the Three Trees glaciation, Sisters Stream glaciation and Lake Sumner Advance respectively.

In contrast, the Pahau River deposits have not been examined to the same degree as those for the Waiau and Hurunui rivers. Gregg (1964) mapped the deposits (Figure 3.3), however, a recent unpublished soil map of the basin (pers. comm., T. Webb, Landcare Research, 1998) indicates that there needs to be a revision to Gregg's mapping. On the northern side of the Pahau River Gregg mapped the deposits as dominantly St Bernard Formation. Whilst the St Bernard Formation exists, it does not form the majority of those deposits. Based on the soils and aerial photographs, the glacio-fluvial deposits from the Pahau River have been reassigned in this study.

The equivalent aged deposits from the three rivers all display very similar lithological and geomorphic characteristics. Hence, for the mapping of the deposits the lithostratigraphic nomenclature has been used. The remainder of this section describes the lithological and geomorphic features of those formations.

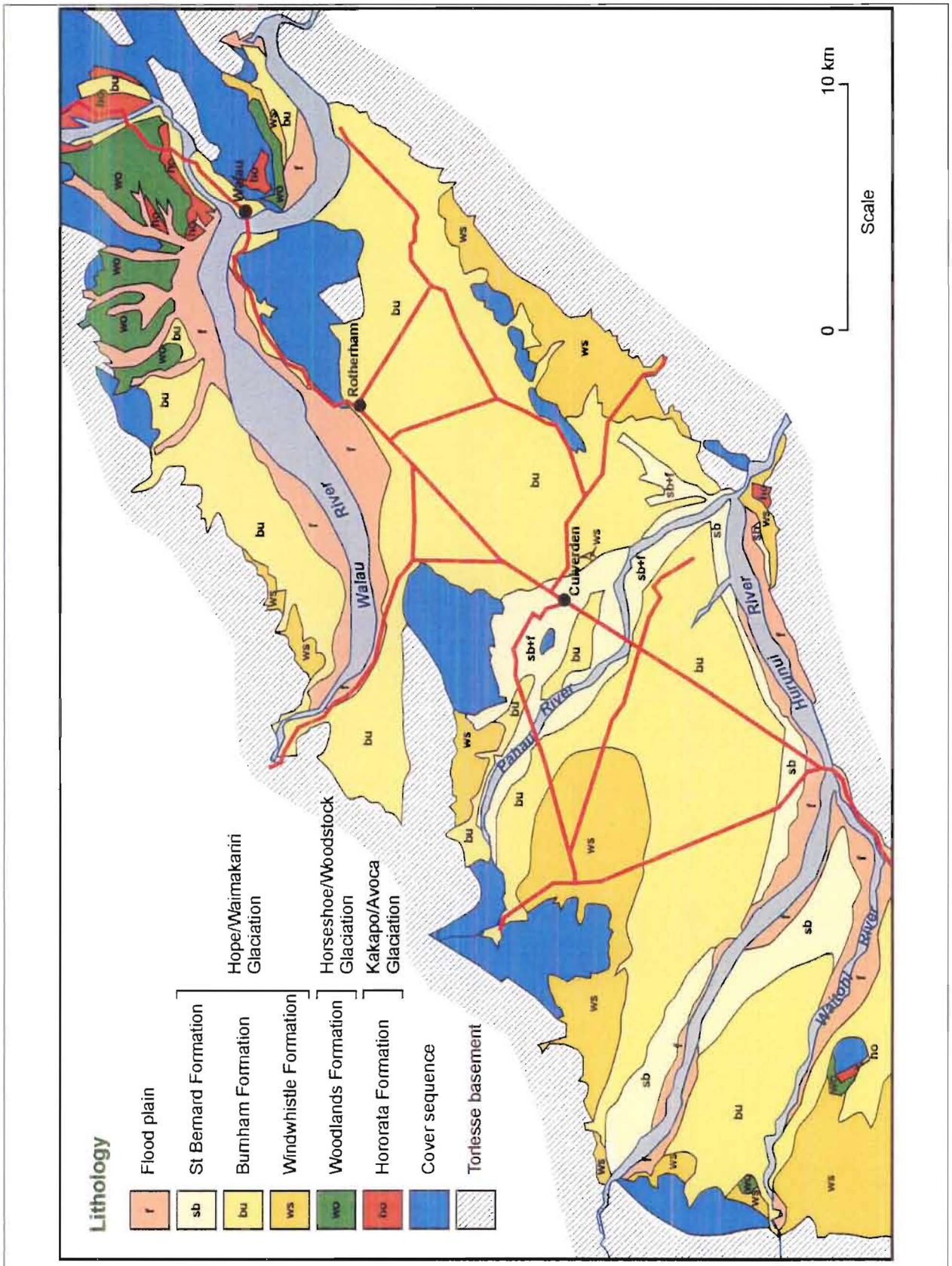

FIGURE 3.3. Gregg's (1964) map of the geology of Culverden Basin. The Late Cretaceous-Early Pleistocene stratigraphy has been simplified as it does not feature significantly in the discussion of the glacial chronology. It is important to note that whilst the Woodlands and Hororata Formations were correlated with the glacial chronology for simplicity by Gregg, they are not glacial outwash deposits (refer to Chapter 3.2.2).

3.2.1.1 Windwhistle Formation

The Windwhistle Formation is the oldest of the glacial deposits found within the basin. The Waiau River has removed all but two scattered remnants of the deposit at the northern end of the basin, whilst it forms approximately half of the mapped Pahau River deposits. The amount of degradation is clearly related to the size of the river that deposited the formation and subsequently eroded it. After deposition there was a major period of degradation during which time the Waiau and Hurunui rivers were able to cut major strath surfaces into the Windwhistle Formation onto which the Burnham Formation was deposited during the following glacial advance. In contrast, the Pahau River, which has significantly lower water flows, was unable to degrade the formation.

The Windwhistle Formation is composed of rounded clasts of Torlesse greywacke up to 8 cm in diameter. The interstitial material is dominantly coarse sand, but the bore logs do show clay and silt bound gravels which may represent waning flow conditions, overbank deposits, or the infiltration of loess into the underlying gravels. Generally only the matrix sands display any sign of weathering, with the clasts retaining a fresh, clean appearance, with minor limonite staining.

3.2.1.2 Burnham Formation

The Burnham Formation is the most easily identifiable of the Late Quaternary deposits due to its distinctive geomorphic expression. On aerial photographs the old braid channels of the rivers are clearly visible due to the very thin soil profile developed on the surfaces. Not only do the braid channels make the Burnham Formation very distinctive, but they also indicate from which river the deposits were derived. This is particularly useful for the delineating the deposits from the Hurunui and Pahau rivers, where the outwash surfaces merge with no clear topographic boundary separating them.

The Burnham Formation is typical of braided river deposits, displaying a range of lithologies relating to channels, bars and overbank flood units (Boggs, 1984). In exposure and bore logs, the old channel deposits are fresh blue-grey, moderately imbricated, loose, fine to coarse, Torlesse greywacke gravels generally in a coarse sand matrix. Fine sediments are absent within these gravel layers. Fine-grained silts and clays with minor gravel are commonly

present as discontinuous sheets and lenses representing flood and overbank sediments deposited by a waning current following a high flow period. During such deposition events the river may have overtopped its cut channel, depositing alluvium over a significant area of the surface and subsequently forming a new river channel.

3.2.1.3 St Bernard Formation

The St Bernard Formation by all appearances is identical to the modern alluvium on the river floodplains. In consists of fresh, well rounded Torlesse greywacke clasts and sandy matrix. It occurs as a relatively narrow border along the Hurunui and Pahau rivers and several of the smaller streams.

3.2.2 Non-glacial Deposits

3.2.2.1 Mason and Lottery River Deposits

In contrast to the glacial deposits where none of the units pre-dated the last glaciation, at the northern end of the basin deposits equivalent in age of the two previous glaciations (Horseshoe and Kakapo) are found. The climatic conditions controlling the glacial cycles in the catchments of the Waiau and Hurunui rivers, also controlled the cycles of deposition in the Mason and Lottery rivers. For simplicity Gregg (1964) correlated the deposits with the glacial chronology, and that nomenclature will be used in this study. The oldest of the two is the Hororata Formation (approximately 250 000 years old) and the younger is the Woodlands Formation (approximately 140 000 years old). Along with those older deposits, units of equivalent age to the glacial deposits are also found, but comprise a relatively small portion of the stratigraphy. The source of these units have been the Mason and Lottery rivers flowing into the basin from the north.

The Hororata Formation is found on the southern end of Mount Highfield and in relic surfaces on the western side of the Mason River. The Woodlands Formation is also found on the southern end of Mount Highfield, and forms a broad flat terrace on the western side of the

Mason and Lottery rivers. The Hororata Formation can be distinguished from the younger Woodlands Formation on the basis of four criteria:

1. degree of weathering
2. degree of stream dissection,
3. thickness of soil cover, and
4. attitude of the gravels.

Whereas the younger glacial outwash deposits on the basin floor generally appeared fresh and unweathered, these older formations are weathered to a dark yellow-brown colour. The degree of weathering and iron oxidation generally increases with age, as does the thickness of the soil cover and amount of stream dissection. On the southern end of Mount Highfield, both formations are tilted to the southeast in response to the Mount Highfield Fault. On the western side of the Mason River only the Hororata Formation are tilted (10° SE); the Woodlands Formation are sub-horizontal.

Close to the present level of the rivers, gravels of equivalent ages to the deposits of the Hope Glaciation are seen. These deposits are very limited in extent as the continued downcutting of the Mason and Lottery rivers degrades the surfaces. On the high surface of Woodlands Formation to the west of the Mason River, there are several NE-SW oriented scarps that are believed to be tectonic in origin. The scarps are in line with the inferred trace of the Rotherham Fault, and suggest that the last movement on the Rotherham Fault post-dated the deposition of the Woodlands Formation.

3.2.2.2 Eastern Margin Alluvial Fans

Modern alluvial fans form in areas of high relief, commonly at the base of a mountain range, where an abundant supply of sediment is available (Boggs, 1987). They have been defined as a cone-shaped deposit of coarse stream sediments, sheet flood deposits, and debris flows that forms where a narrow canyon stream suddenly disgorges into a flat valley (Prothero and Schwab, 1996). Sediment structures and textures are a function of the change in the hydraulic potential of the stream/river from a higher gradient valley catchment to the flatter valley floor; a steeper fan slope provides greater hydraulic potential resulting in an overall larger grain size than an equivalent gentle slope.

In longitudinal profile, alluvial fans can be divided into distinct parts (Figure 3.4). The proximal fan, or fanhead, has the steepest slope. The deposits are coarse and very poorly sorted, mainly of debris-flow origin. Streamflow in the proximal fan tends to be confined to a single channel. The midfan is characterised by more gentle slopes, finer sediments and a branching network of channels, which feed the different parts of the midfan. Midfan deposits include both extensive streamflow sediments and possibly debris-flow units. Furthest from the range-front is the distal fan, or fanbase, which makes up the toe of the fan, and is characterised by the gentlest slopes, finest sediment and lack of well-defined channels. Distal fan sediments are largely sand and silt of sheetflood origin, formed by surges of sediment-laden water that spread out from end of a stream channel onto a fan. Fans often have stream channels that are incised into the fan surface. Incision is deepest at the fan head and decreases down-fan until the stream channel and fan surface intersect (Lecce, 1990). This point on the fan surface is called the intersection point (Wasson, 1974).

Alluvial fans can be used as useful indicators to the rate of tectonism along the range-fronts. Bull (1977b) demonstrates that along tectonically active mountain fronts fans are deposited adjacent to the mountain front, whereas in tectonically stable areas the streams get entrenched in the fans shifting deposition out from the mountain front (Figure 3.5).

The gravels of the basin floor and the northern margin of the basin have been classified using the glacial chronology. Unfortunately, the gravel packages along the eastern margin are not so easily classified. The eastern margin has a potpourri of different gravel packages, associated with the classic range-bounding fan systems building out from the Lowry Peaks Range. Correlation with the glacial chronology is difficult given the current lack of absolute ages for the gravels. Presently, the ages are inferred based on their stratigraphic relationship with the glacial outwash surfaces, in particular the Burnham Formation which is geomorphologically very distinctive, aggradation events dated in nearby areas (e.g. Charwell River area) and estimates of the soil profile age (pers. comm., T. Webb, Landcare Research, 1998).

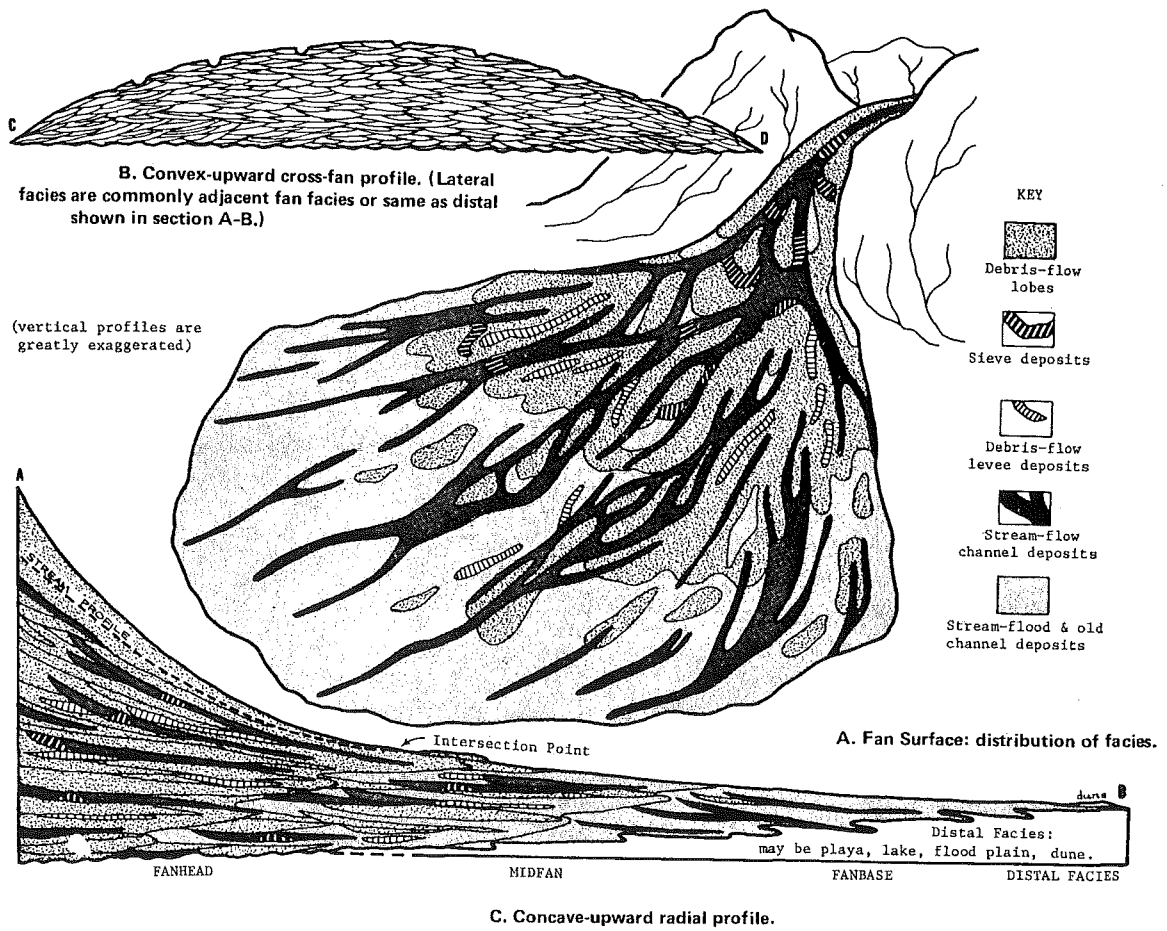

FIGURE 3.4. Typical surface features and cross-sectional profiles of alluvial fans. A. Fan surface. B. Profile across the fan. C. Longitudinal profile (Boggs, 1987)

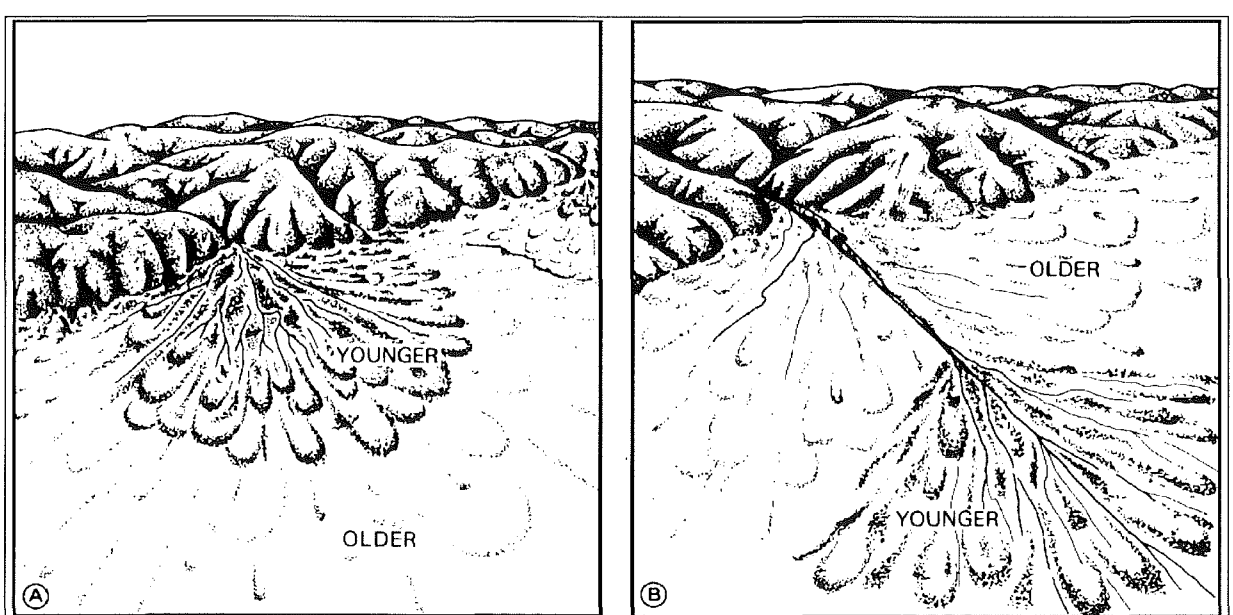

FIGURE 3.5. Alluvial fan morphology: (A) deposition adjacent to mountain front and (B) deposition shifted downfan as a result of fanhead entrenchment (From Bull, 1977b).

The Lowry Peaks Range has been the source area for all of the alluvial fans along the eastern margin, except for the small and localised fans shed off Leonard Mound. Four major sets of fans can be recognised along the margin (Figure 3.6), and will be described in the order given: (A) the central Lowry Peaks fans are those to the east of the Leonard Mound Fault and to the south of the junction of the Lowry Peaks Fault and Leonard Mound Fault, (B) the western Lowry Peaks fans are those from the same catchments as the central fans, but are being deposited to the west of Leonard Mound, (C) the northern Lowry Peaks fans, as the name indicates are those to the north of Leonard Mound, along the northern portion of the Lowry Peaks Range and (D) the Leonard Mound fans are the small and localised fans shed off Leonard Mound. Table 3.1 summarizes the main lithologic and geomorphic characteristics of the different fan surfaces and shows the correlation of the different fan surfaces based on their features.

The fans have been labeled according to which set they belong to and their relative ages. The letter denotes which set they are a member of (C = central Lowry Peaks fans, N = northern Lowry Peaks fans, W = western Lowry Peaks fans and L = Leonard Mound fans), and the number refers to the relative ages of the fans within each set, with 1 being the oldest.

Central Lowry Peaks Fans

The central fans are the most extensive of the four sets of fans. They occur between the Leonard Mound and Lowry Peaks faults, from the junction of the Lowry Peaks Fault and Leonard Mound Fault, southwards along the central portion of the Lowry Peaks Range. It is important to keep in mind that, although for the purpose of this discussion the central Lowry Peaks Fans are those on the uplifted side of the Leonard Mound Fault, they would have extended to the west of the fault. It is believed that the composite surface is composed principally of the oldest fans within this set.

Four different aged fan surfaces (C_1-C_4) can be distinguished based on their morphology, deposits and geographic position relative to the range-front. The oldest (C_1) fans occur at the northern end of the central portion of the range. The fans have very steep gradients and have been deeply incised by the streams flowing off the Lowry Peaks Range. Where exposed the gravels are typical of proximal fan deposits i.e. they are composed of poorly sorted, poorly

stratified, angular Torlesse greywacke clasts upto 5 cm in size. In contrast to the glacial gravels to the west, the fan gravels have a significantly higher fines content, and the matrix and clasts are extensively weathered to a brown colour.

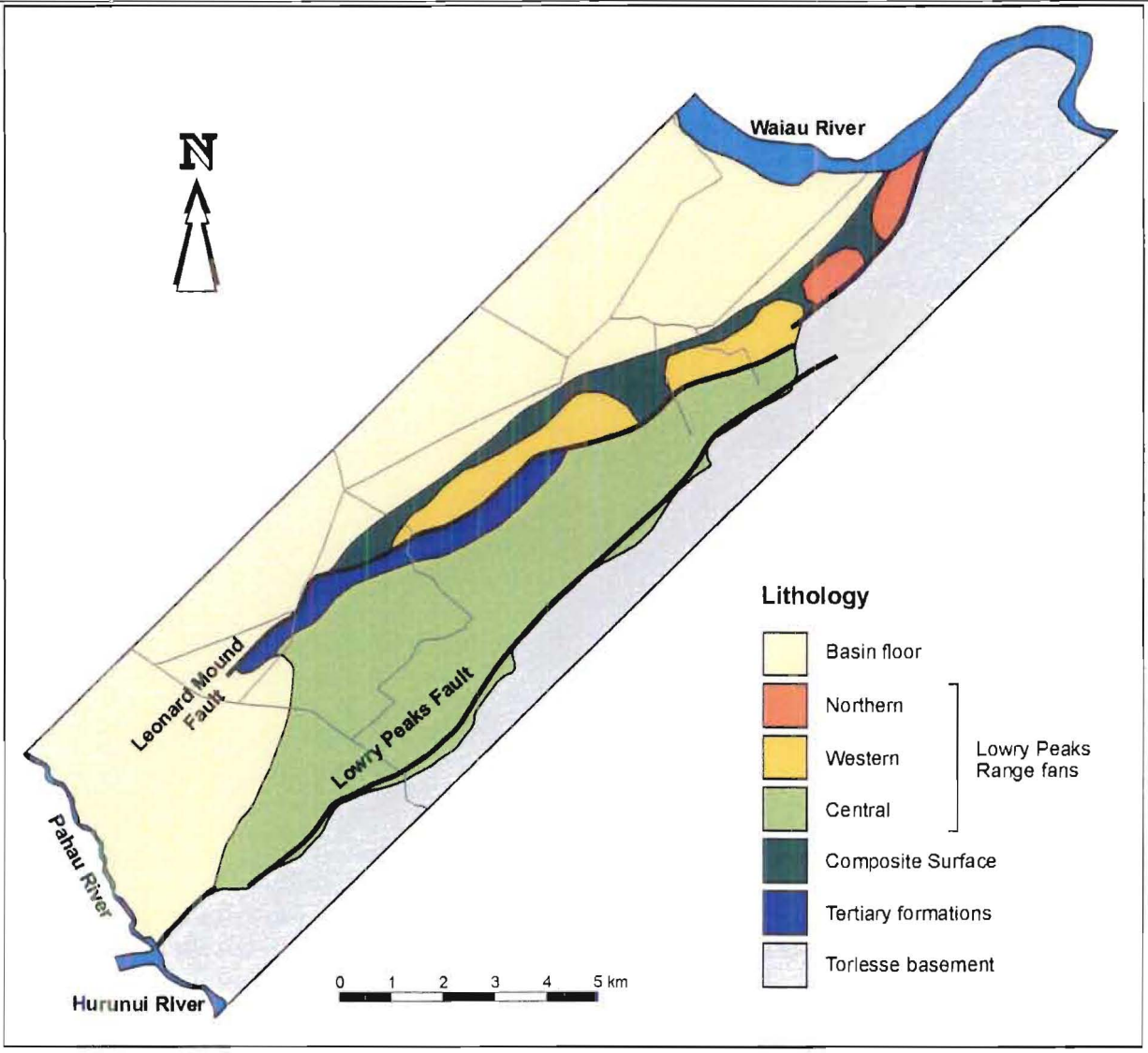

FIGURE 3.6. Summary map of the different alluvial fans of the eastern margin of Culverden Basin.

The C_1 fans occur dominantly to the north of Palmside Road. To the south of Palmside Road, in the Wynyard sub-basin, the streams have eroded the majority of the fans leaving remnant surfaces surrounded by the younger C_2 fans (Figure 3.7). A distinct morphological change in the fan surfaces is observed on the C_2 fans. To the north of Palmside Road, the equivalent aged fans are found on the western side of Leonard Mound, and have hence been described under the western Lowry Peaks fans. The C_2 fans are characterised by gentle slopes, smooth

surfaces and a single stream confined to a narrow, shallowly incised channel. The deposits are much better sorted than those of the proximal fans, and become well stratified by the time they reach Leonard Mound. In an exposure in a terrace on the western side of Leonard Mound (grid reference: N33/083283), the gravels are well stratified with layers of fine gravel (clasts less than 1 cm), sands and silts. Where studied (pers. comm., T. Webb, Landcare Research, 1998), a moderately deep silt loam, known locally as the Culverden soils, has developed on the fans. Culverden soils are found on the alluvial fans around the margin of the basin and may be upto 65 cm thick (Southall and Rennie, 1977).

The Holocene fans ($C_{3 \text{ and } 4}$), in contrast to the older Late Pleistocene fans ($C_{1 \text{ and } 2}$), are significantly smaller in extent and are being deposited up to 2 km out from the range-front. Both C_3 and C_4 fans are characterised by a fine network of dendritic streams (Figure 3.8) and the absence of a soil cover. During the Holocene the climatic conditions were not as severe as during the Late Pleistocene. As a result, there was not the large amount of material available to the streams, which is reflected in the smaller size of the fans and the lithology of the deposits. The Holocene fans are composed mainly of fine sand and silt and reworked older fans. The current sites of deposition tend to be wet and swampy as the fine material is restricting the drainage of the surface water.

Table 3.1. Correlation and brief description of the Lowry Peaks Range fans.

Fan Surface			**Characteristics**	
Central	**Western**	**Northern**	**Lithologic**	**Geomorphic**
C_4	W_3	N_3	Mainly fine sand, silt and clay with some reworked older fan material.	Fine network of dendritic streams. Ground is typically wet due to poor drainage. No soil cover.
C_3	W_2	N_2	Very similar to younger fans except have more coarse material from reworking of older fans.	Fine network of dendritic streams. No soil cover. Not as poorly drained as younger fans.
C_2	W_1	N_1	Weathered clasts of Torlesse greywacke which reduce in size away from range-front, and the sorting and stratification improve away from range-front. Clasts weathered due to weathering of Torlesse on range and not after deposition.	Low gradients with streams confined to a single, narrow, shallowly incised channel. Covered by Culverden soils that may be upto 65 cm thick.
C_1			Poorly sorted, poorly stratified, coarse alluvial fan gravels with Torlesse greywacke clasts upto 5 cm in size. Clast and matrix weathered to brown.	Very steep gradient and highly dissected. Upto 2 m of loess.

FIGURE 3.7. Photograph of the relic C_1 fans surrounded by the younger C_2 fans along the base of the Lowry Peaks Range immediately north of Kaiwara Road (visible centre right side of photo).

Western Lowry Peaks Fans

The western Lowry Peaks fans, in conjunction with the northern Lowry Peaks fans, form an apron of deposits along the western edge of Leonard Mound and the Lowry Peaks Range. The western Lowry Peaks fans are those to the south of the junction of the Lowry Peaks and Leonard Mound faults. The fans extend as far south as "Blakiston" (N33/067273) past which point the streams from the Lowry Peaks Range have been unable to incise through the ridge, preventing the deposition of fans on the western side of Leonard Mound.

Three fan surfaces (W_1-W_3) can be found along the western edge of Leonard Mound. The fans have the same morphological and lithological properties as the C_2-C_4 fans, leading to the belief that they are of the same age and from very similar catchments, in terms of size, rock-type, precipitation rates, vegetation, etc. This is, of course known to be the case as both sets of fans are derived from the central portion of the Lowry Peaks Range, which is lithologically and morphologically consistent along its length. The only difference between the central and

western Lowry Peaks fans, is the presence of the older C_1 fans to the east of Leonard Mound. It is believed that the C_1 fans constitute the majority of the composite surface, based on the stratigraphic position of the composite surface relative to the fans and Burnham Formation.

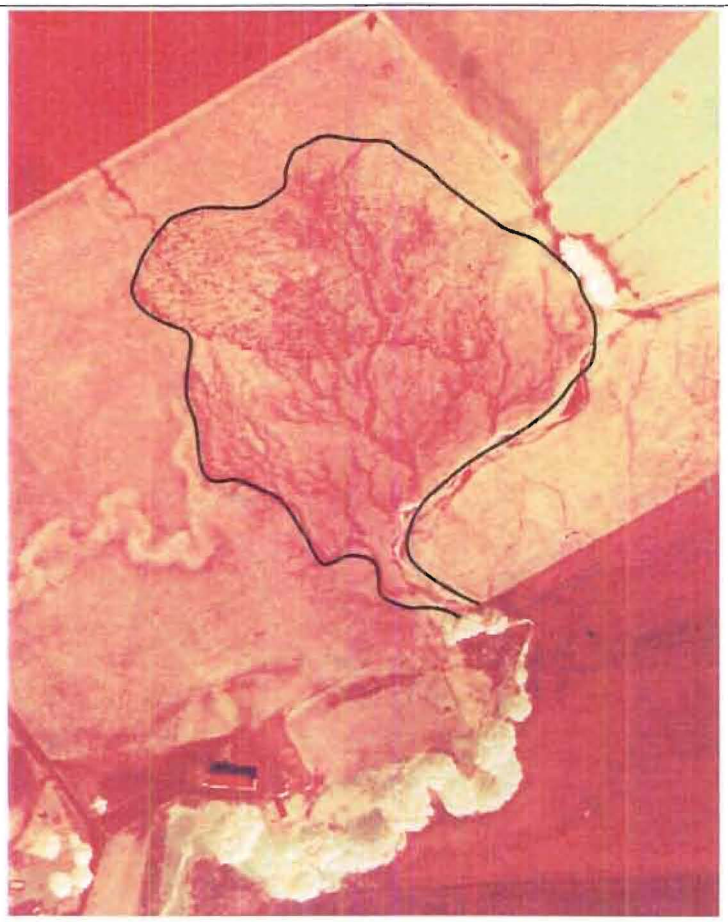

FIGURE 3.8. Infrared image of an active fan showing the fine dendritic network of streams (grid reference: N33/067278). Photo courtesy of T Webb, Landcare Research.

Northern Lowry Peaks Fans

Located along the northern section of the Lowry Peaks Range, the northern Lowry Peaks Fans reflect the morphological change between the central and northern sections of the range. As with western fans, three fan surfaces (N_1-N_3) are observed and they have the same lithological and morphological characteristics. However, they are noticeably smaller in size.

As was shown in Chapter 2, the northern section of the Lowry Peaks Range is relatively smooth and rounded compared to the central section. From that observation, it is clear that

there has been relatively little erosion of the range-front, resulting in substantially less material for the fans and hence smaller fan sizes.

Leonard Mound Fans

Along the base of the Leonard Mound Fault scarp there are fans derived from material shed off the scarp and from the streams that do not originate from the Lowry Peaks Range. In comparison to distal fans of the Lowry Peaks Range, these fans are small and very localised, and are composed of the older fan material.

Composite Surface

The composite surface is very distinct from the glacial deposits and the alluvial fans, which it separates. The zone is a topographic low between the glacial outwash deposits, which dip eastward and the alluvial fans, which dip westward. As a consequence it is the natural place for water to accumulate, whether that water be from the streams or the ground. The streams coming off the range and across the fans abruptly change direction and flow parallel to the range once they reach the composite surface. Due to the very low gradient of the surface, the streams are tightly meandering and are only able to carry very fine sediment that they consequently deposit and build up the composite surface. Those fines in conjunction with the high clay and silt content of the C_1 fan gravels believed to compose the surface are adversely affecting the drainage. Along the length of the surface, springs (discussed in Chapter 5) occur due to the tectonic deformation and interaction of the different fluvial sequences. As a result, the composite surface is very wet and swampy, especially in comparison to the very well drained gravels of the Burnham Formation.

The composite surface is split into two areas by the southern end of Leonard Mound. As with the western Lowry Peaks fans, the composite surface is only found to the west of Leonard Mound where the streams have been able to incise through the ridge, i.e. to the north of "Blakiston". This indicates that the composite surface is composed of the oldest C_1 fans, which the Leonard Mound Fault clearly displaces through the Mount Palm section of the Leonard Mound Fault System. That uplift has not only affected the drainage network developed on those fans, but it has also helped to preserve them from degradation by the

streams. As was seen earlier, to the south only relic surfaces of the C_1 fans remain, and as will be shown in the next section, the distance between the Lowry Peaks and Leonard Mound faults almost doubles at the southern end of Leonard Mound. Clearly this separation has affected the fluvial system, which will be addressed in the hydrogeological model of the margin (Chapter 5).

3.2.2.3 Modern Alluvium

The most recent deposits in the basin are the Holocene floodplain deposits, confined to the river and stream channels, and consisting of rounded, moderately well sorted fresh Torlesse basement derived gravels and sand.

3.2.3 Age Correlation of the Fluvial Deposits

So far, the lithological and geomorphic characteristics of the Late Quaternary deposits have been described, with only the ages for the glacial outwash surfaces discussed. To briefly recap, three advances of the last (Hope) glaciation were recognised in the Waiau/Hope Valleys (Knuepfer, 1984 and Cowan, 1989). From radiocarbon dates and weathering rind data, Knuepfer and Cowan assigned ages of 70 000-25 000 yrs BP (Glenhope Advance), 22 000-16 000 yrs BP (Glynn Wye Advance) and 15 000-14 000 yrs BP (Dismal Advance) for the three advances. In Culverden Basin, the Glynn Wye Advance constitutes the majority of the gravels covering the floor of the basin to the north of Culverden, with only remnants of the older Glenhope Advance remaining. The Dismal Advance can be traced down the Waiau River to the entrance of the basin, at which point it rapidly merges with the Glynn Wye Advance and can not be followed out into the basin. The advances have been correlated with the Windwhistle, Burnham and St Bernard formations respectively from oldest to youngest. In contrast the ages for the eastern margin alluvial fans have not been accurately determined. Their ages are inferred based on their stratigraphic relationships with the glacial deposits, geomorphic features and comparison with the extensively studied and dated aggradation events in the Charwell River area (Bull, 1991) to the north of Culverden Basin.

Before correlating the deposits, its is worth briefly outlining the factors which will control the reaction and response times of the streams within a fluvial system. Bull (1991) listed two sets

of variables (Table 3.2): the *independent* variables exert primary control on the fluvial system and are the result of processes occurring outside the fluvial system; the *dependent* variables result from process interactions within the system and are controlled by both the independent and other dependent variables. Watersheds with similar factors tend to have synchronous times of aggradation and consequently similar geomorphic characteristics. The most important variable, especially in relatively slow tectonic areas such as the Lowry Peaks Range, is the climate. Changing climatic conditions have globally dictated the Quaternary glacial versus interglacial periods and consequent cycles of aggradation and degradation. Bull (1991) showed mountain ranges in New Zealand had maximum sediment yields during times of full-glacial climates and hillslope sediment reservoirs became more stable during the Holocene. In an area such as the Charwell River where the Hope Fault is moving very quickly (30-40 mm/yr), tectonics will play a significant role. In contrast along the Lowry Peaks Range the rate of uplift is relatively slow (<1 mm/yr) and any tectonic signature is hidden by the climate response.

TABLE 3.2. Partial list of the independent and dependent variables of a fluvial system for a time span of more than 1000 years (Bull, 1991).

Independent Variables	**Dependent Variables**
Climate	Drainage basin area
Total relief (function of uplift and erosion)	Hillslope morphology
Base level of mouth of drainage basin	Soil profile development
Lithology	Vegetation
Geological structures	Water and sediment yield from hillslopes
	Stream channel slope/patterns

In the Charwell River area, Bull (1991) has recognised five Late Pleistocene aggradation events: Quail Downs, Dillondale, Flax Hills, Stone Jug and Dog Hills. For the purpose of this study, only the Flax Hills (48-31 ka), Stone Jug (26-14 ka) and Dog Hills (<12 ka) aggradation events are of interest as they of last glaciation and Holocene age. Figure 3.9 shows the correlation of the glacial surfaces and fan surfaces within the north part of Culverden Basin with the aggradation events proposed by Bull. There are of course problems with attempting to correlate the ages of Bull's events with the eastern margin alluvial fans, as the factors controlling the fluvial systems vary between the two areas. The Charwell River area is at a higher elevation, placing it close to the snowline level during the late Pleistocene. Consequently, the bedrock was subjected to greater erosion from freeze/thaw processes than

that on the Lowry Peaks Range. The Charwell River is also located in the Seaward Kaikoura Mountains that have a higher rainfall than the eastern margin of Culverden Basin, adding to the erosive power of the streams. Both fluvial system are situated on the Torlesse bedrock, however, the Torlesse bedrock in the Charwell River area is probably more sheared and crushed, due to the Hope Fault, making it more susceptible to erosion. Despite these differences, the climatic changes were so severe that the reaction times of the streams to those changing conditions would have been very similar in both areas, making it possible to use Bull's ages for constraining the ages of the eastern margin alluvial fans.

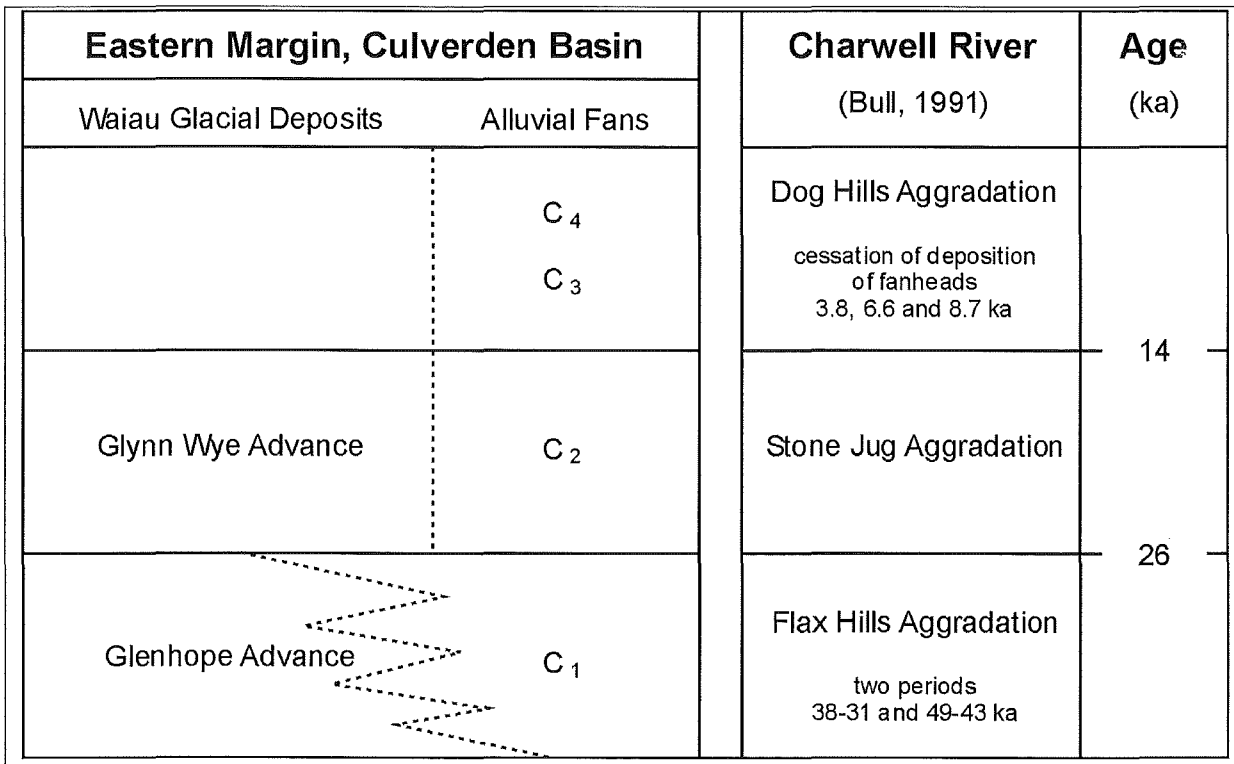

FIGURE 3.9. Correlation of the eastern margin alluvial fans with the glacial stratigraphy and aggradation events documented in the Charwell River area by Bull (1991). The fans of the eastern margin are represented by the central Lowry Peaks fans. For the correlation with the western and northern fans, please see Table 3.1.

3.3 TECTONIC DEFORMATION

Superimposed on the fluvial architecture is the tectonic deformation, which serves to further complicate the hydrogeology. The previous chapter dealt with the deformation occurring along the basin margins which is generally inactive. The structures in this section have been classified as either Class I or Class II (after the classification scheme of Pettinga et. al., 1998,

Chapter 1) activity as they clearly disrupt the deposits that are younger than 25 000 years old. The focus of this section is the actively evolving Leonard Mound imbricate thrust system splaying obliquely off the northern end of the Lowry Peaks Fault. The young age of the deformation, combined with very low rainfall have aided in the preservation of the geomorphic expression of the deformation, making it possible to examine in detail the style of deformation.

As will become apparent during this discussion, these structures are playing pivotal roles in controlling the near surface groundwater flow. The deformation has clearly disrupted the aquifers resulting in springs and the ponding of surface water on the relatively downthrown side of the faults and folds. As it turns out, the geomorphology is the main tool for investigating the effects of the active deformation on the groundwater regime due to the lack of success of the geophysical investigations in this regard.

3.3.1 Leonard Mound Fault System

Situated on the eastern margin of Culverden Basin, Leonard Mound is an active thrust driven asymmetric anticlinal ridge propagating obliquely into the basin. Leonard Mound extends for approximately 15km and rises to a maximum height of 70m above the floor of the basin. The Leonard Mound Fault System is dominated by the Leonard Mound Fault that has accommodated the majority of uplift associated with the Leonard Mound Fault System. Along the length of the fault system there a distinct changes in the elevation and character of the ridge indicating that the Leonard Mound Fault is a segmented and structurally complex system.

Recognition of the Leonard Mound Fault first occurred as part of a mapping thesis of Culverden Basin by Falloon (1954). Falloon attributed displacements seen to normal faulting which, based on this study, can clearly be shown not to be the case. Since Falloon no more investigations of the southeastern margin of Culverden Basin have occurred until this thesis. Initially, it was thought that the Leonard Mound Fault was a relatively simple single trace with an associated anticline on its upthrown side. However, detailed mapping has revealed that the deformation is being accommodated, not on a single fault but on numerous faults, some of which have resulted in gentle warping of the surface with no surface rupture.

Leonard Mound can be divided into five distinct sections (named after the farm properties on which they are located) based on the expression of the tectonic deformation (Figure 3.10). Streams generally divide the sections, as the segmentation of the fault has produced structural lows, which the streams have exploited. Only the Leonard Mound Fault is traceable through all of the sections, with the footwall imbricate structures generally restricted to a particular section. The first three sections (Southern, The Willows and Pukeiti) make up approximately the southern half of Leonard Mound and are characterised by the development of an anticline above the fault. In contrast, at the northern end of Leonard Mound, comprising the Kilsyth and Mount Palm sections, a fold has not developed, instead the strata have been tilted to the SE in response to the uplift across the Leonard Mound Fault. The five sections will be discussed separately in the following sections.

Geomorphically, the structures have been pristinely preserved allowing for detailed mapping of the fault system (Maps 3A-D, Volume 2). Along with the geomorphic mapping, geophysical investigations were carried out to confirm the geomorphic interpretations, look at the deformation within the gravels, and to try and determine the amount of uplift across the faults and folds comprising the LMFS. The results of the geophysical surveys are discussed in Chapter 4.

3.3.1.1 Southern Section (Map 3A)

Leonard Mound reaches its greatest elevation of 70m above the floor of the basin in the southern section. The ridge has three distinct surfaces at elevations of 15 m, 45 m and 70 m elevation above the basin floor (Figure 3.11). At its highest point, the deformation has resulted in the development of a symmetric fold where both limbs dip at 35° (inferred from the slope gradient) which has caused small slips on the eastern limb. Due to the limited extent of the middle surface, it is difficult to determine whether the gravels have been folded or not. The eastern limb of the ridge has a gradient of 18° SE, reflective of the dip of the underlying gravels and intermediary between the upper and lower surfaces. The lowest of the three surfaces shows no sign of folding, instead the uplifted deposits are tilted 8° to the southeast. At the southern end of Leonard Mound, the ridge was clearly trimmed by the Waiau River during the Late Pleistocene, as is evident from the braid channels visible on the aerial photographs (Figure 3.12). The two lowest surfaces represent old erosion surfaces of the

Waiau River during the Pleistocene, documenting several periods of movement of the Leonard Mound Fault.

Geomorphically it is apparent that the Leonard Mound Fault strikes along the base of Leonard Mound on the northwestern side. The faulting has produced a scarp that has been subjected to very minor erosion, still preserving the geomorphic expression of the deformation. Due to the lack of outcrop it is difficult to gauge the attitude of the fault. The geometry of the fault and fold will be discussed in Chapter 5, however, it appears that the Leonard Mound Fault is a shallow SE dipping fault that may steepen in the near surface.

The footwall of the fault is imbricated with a smaller fault occurring to the west of the main fault. This smaller fault has produced a scarp against which two ponds have formed. The scarp is upto 2.5m high and can be traced from the junction of The Mound Road and Isolated Hill Road southwards until it dies away leaving the surface warped rather than faulted. The faulting disrupts the Burnham Formation gravels which have been deposited against the fault scarp of the Leonard Mound Fault. There are no deposits younger than the Burnham Formation to gauge more accurately when the last movement on the faults occurred as no streams have been able to incise through this section of Leonard Mound.

Off the southern end of Leonard Mound there are multiple warps of the surface which represent the southward continuation of the LMFS. These folds are asymmetric with a steeper NW limb and on the downthrown side of the folds water has ponded highlighting the folding. The folds extend from Leonard Mound across Lowry Peaks Road and some distance south. Although these folds appear to be restricted to a relatively narrow zone, the geophysical results (Chapter 4) indicate that the zone of deformation associated with the LMFS may be substantially broader.

The ages of the gravels capping the southern section are somewhat enigmatic. Clearly they pre-date both the gravels on the floor of the basin to the west and the fan gravels under which they disappear to the east. There are three possible alternatives:

1. an older Lowry Peaks fan surface,
2. a pre-Burnham Formation glacial deposit, or
3. part of the Kowai Formation

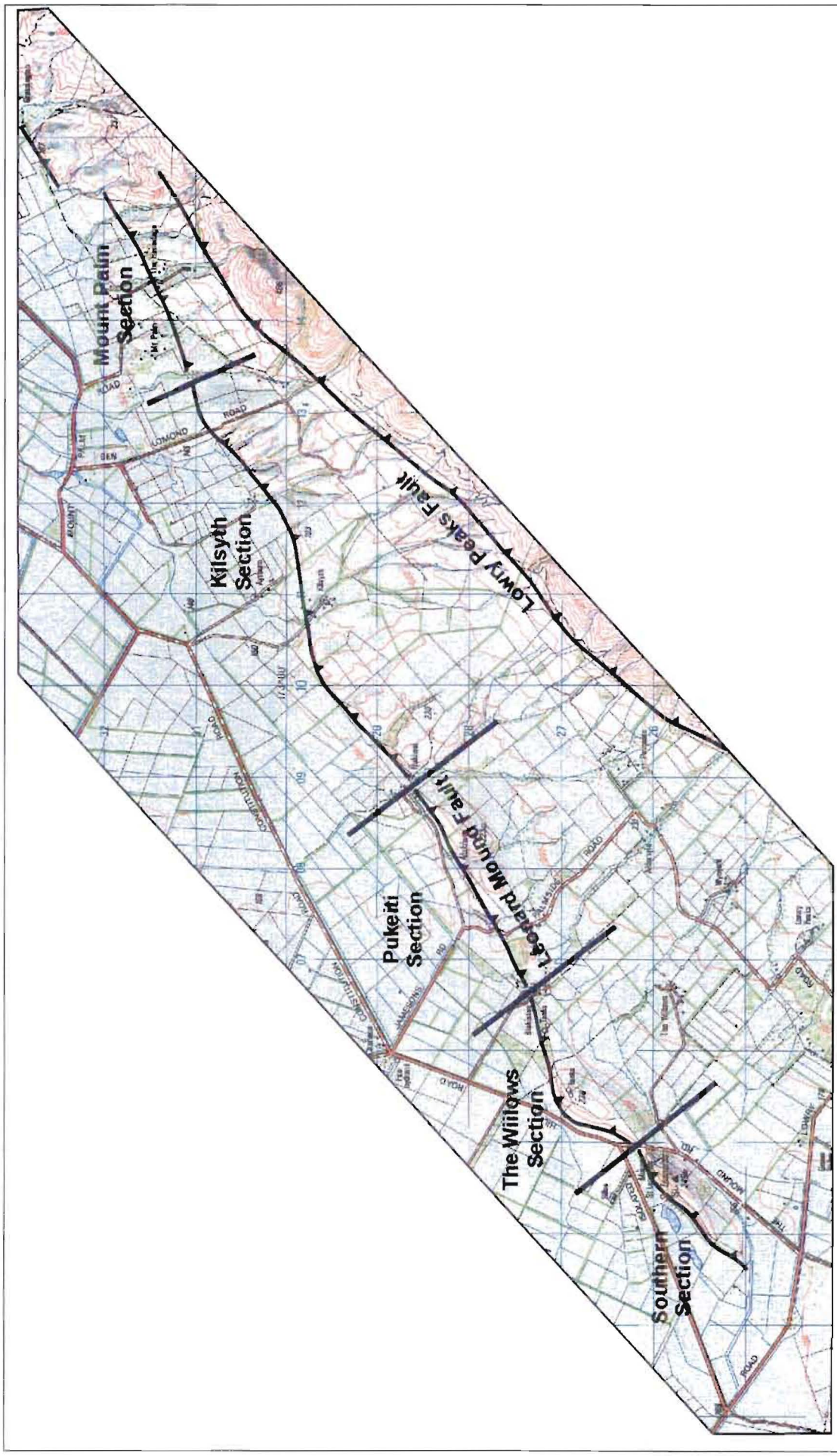

FIGURE 3.10. Map showing the five sections of Leonard Mound.

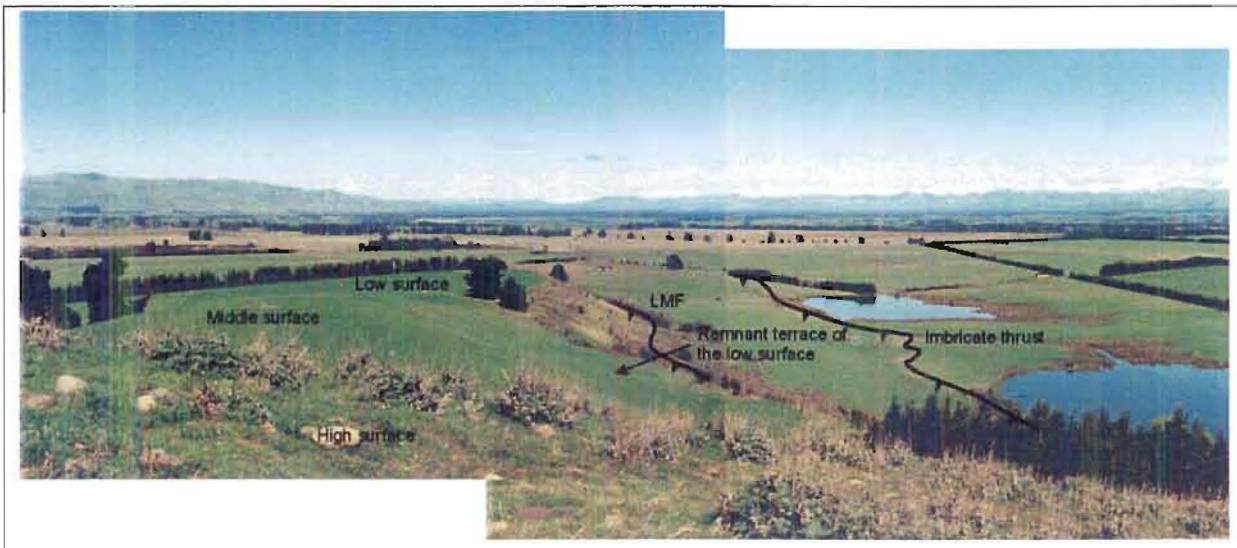

FIGURE 3.11. Photograph looking southwest along the Southern section of Leonard Mound showing the three surfaces, Leonard Mound Fault and the imbricate fault (highlighted by the ponds).

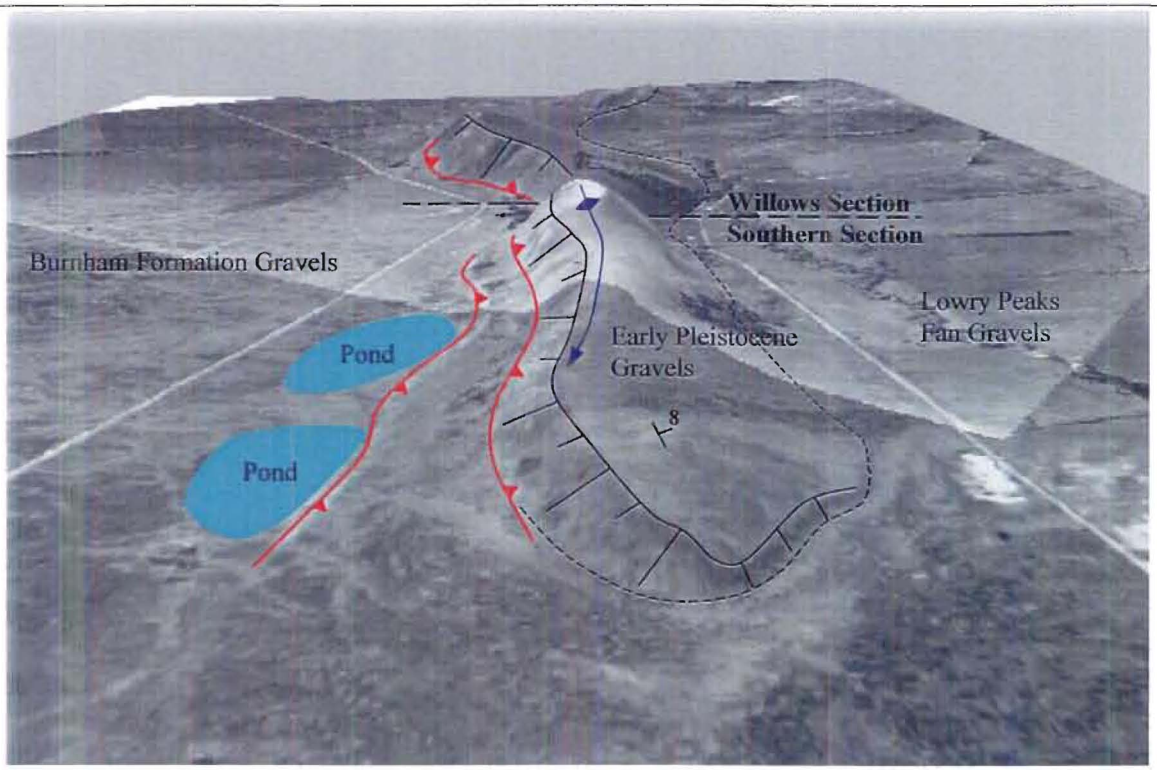

FIGURE 3.12. 3D rendered vertical aerial photograph looking northeast along the Southern section of Leonard Mound.

In the next section of Leonard Mound, the gravels are exposed in a small quarry, and as will be shown, the source of the gravels was to the northwest and not the Lowry Peaks Range. To the west of Leonard Mound two boreholes (N33/0011 and N33/0045, Appendix 1) show the Burnham Formation to be 28 m and 18 m thick respectively. Underlying the Burnham

Formation are sands and sandstones, believed to be part of the Kowai Formation, suggesting that the gravels capping the ridge are Kowai Formation and hence inferred Early Pleistocene in age.

3.3.1.2 The Willows Section (Map 3A)

The Willows section is dominated by a doubly plunging asymmetric anticline that reaches a maximum height of 40m above the basin floor. The fault has a typical bow shape (Elliot, 1976 and Wilkerson, 1992) indicating more displacement in the centre of the section than at the ends. At either end of the section the gravels have been uplifted and tilted to the 15° SE and not folded. As mentioned in the previous section, the gravels have been exposed in a quarry at the north end of the section. Lithologically these gravels are very similar to the gravels deposited by the major rivers, as opposed to the fan gravels from the Lowry Peaks Range. In conjunction with cross-bedding structures which indicate a source to the northwest, and the boreholes mentioned in the previous section, it suggests that these gravels are Early Pleistocene in age and are assigned to the Kowai Formation.

Geomorphically, the fold structure has been beautifully preserved (Figure 3.13) and is expressed by the rounded morphology of the ridge crest. The Leonard Mound Fault can easily be traced through the Willows section as a scarp up to 30m high has been formed. The scarp dips 30-35° W and the gravels capping the NW limb of the fold appear to dip in the order of 40° W (Figure 3.14). Although no bedding is exposed, after a dry summer the vegetation patterns revealed the general strike of bedding on the steep (western) limb of the fold. The slope gradient of the eastern limb is approximately 10° E, which seems to be indicative of the attitude of the gravels. A portion of the deformation has been accommodated on a back-thrust which has subtly folded the eastern limb of the Leonard Mound Fold, oversteepening the mid-slopes of the limb. A line of four tunnel gullies marks the slope break between the over-steepened surface and undeformed lower slope of the eastern limb.

On the scarp, three benches have been cut. There are two possible origins for these benches:

1. they are relic terraces of the Waiau River or streams and have been uplifted above the floor of the basin, or
2. the core of the anticline has been partially eroded leaving the more resistant beds.

Origin two is the preferred as there is no evidence that streams were present to create the benches. The alignment of the benches is also consistent with the attitude expected of the bedding in a plunging fold. This is also supported to the north in the next section (Pukeiti) by the presence of two resistant ridges resulting from the erosion of the fold core.

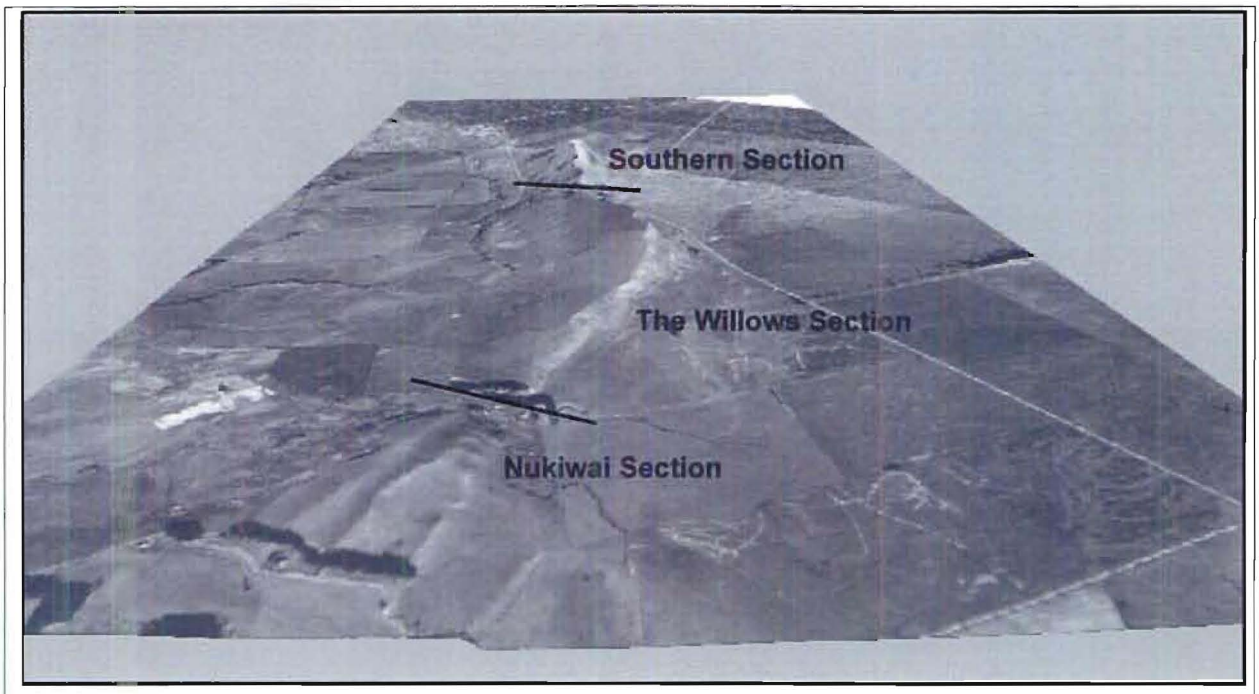

FIGURE 3.13. 3D rendered aerial photograph looking south of the Pukeiti, Willows and southern sections of Leonard Mound

Although the Leonard Mound Fault and associated fold are a classic example of a fault controlled fold, the most interesting feature of the Willows section is the development of a series of leading edge folds to the west of the Leonard Mound Fault. These smaller amplitude folds are generally no more than 2 m high and, as with the main fold, are asymmetric with relatively steeply dipping western limbs and horizontal to shallowly dipping eastern limbs. Ground penetrating radar (GPR) profiles (Chapter 4) clearly show that the gravels have been folded supporting the inferences that these features are leading edge folds, and not fluvial features. It is believed that these folds represent footwall imbrication of the Leonard Mound Fault. On the whole these folds trend sub-parallel to Leonard Mound but some do veer off and head towards Culverden. None of the faults controlling the development of these folds have broken through to the surface producing a scarp. It is noticeable that where these folds exist, the height of Leonard Mound has been reduced as a component of the deformation is being

accommodated on these secondary structures. As with the ponds in the southern section, water has accumulated in the downthrown side of some of the folds highlighting the folding.

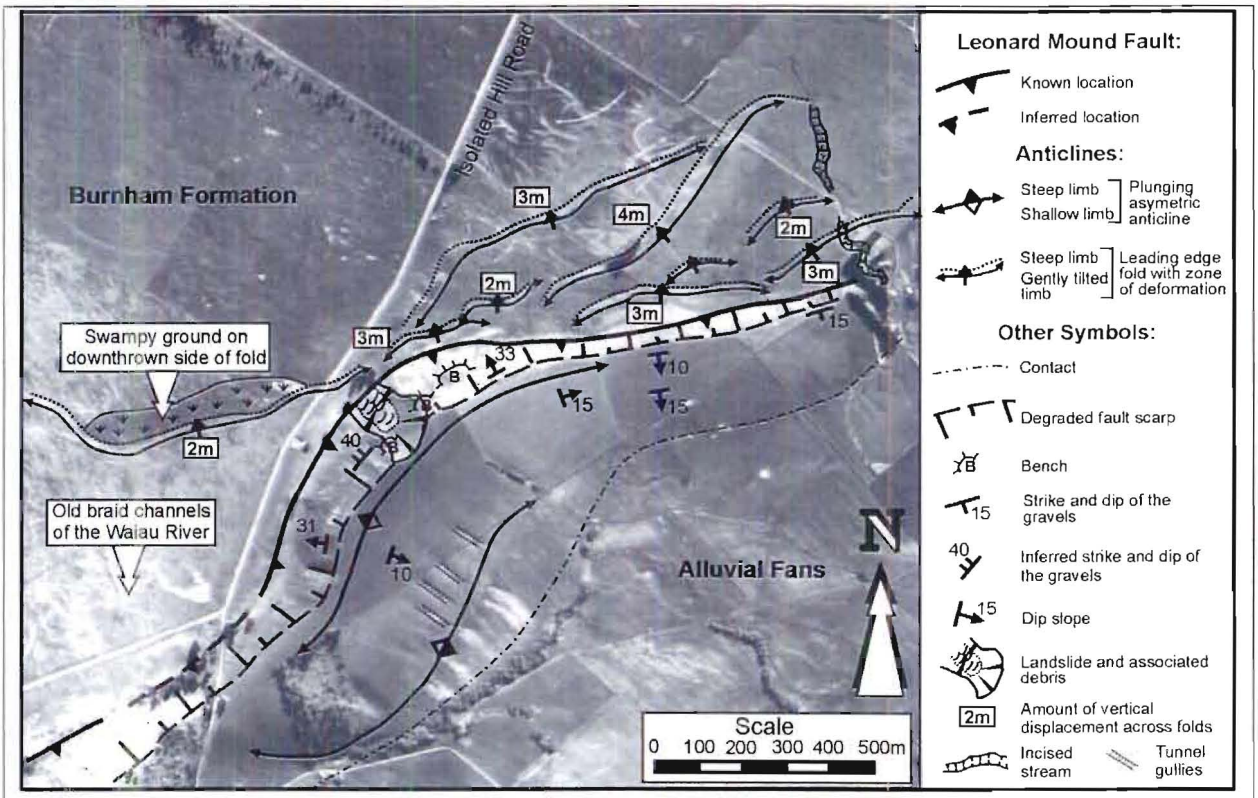

FIGURE 3.14. Vertical airphoto showing the geomorphology of the Willows section, Leonard Mound.

3.3.1.3 Pukeiti Section (Map 3B)

The Pukeiti Section of Leonard Mound is structurally and erosionally dissimilar to the rest of Leonard Mound. In the other sections, imbrication of the Leonard Mound Fault occurs in the footwall, and the deformation in the hanging wall is expressed as either a single fault-propagated anticline or an uplifted and back-tilted block. Three ridges are observed in the Pukeiti section, believed to be the result of two thrust/fold relationships. It is inferred that the two western ridges are of the same fold, which has had its core eroded leaving two resistant beds. The merging of the ridges at the northern and southern ends of the section implies that the fold is a doubly plunging asymmetric anticline, whose axis lies between the two ridges. Siltstones, believed to be the Mount Brown Formation, exposed in the stream gullies on the northern side of Palmside Road, show that the forelimb of the fold is steeply dipping to the northwest. In contrast the eastern of the two folds has not been eroded and still displays an asymmetric, plunging morphology that is restricted to the southern half of this section. It is

inferred that the Leonard Mound Fault is the western of the two thrusts and that the eastern thrust is a hanging wall, or piggy-back, imbricate thrust, making it unique from the other imbricate structures.

To the west of the Leonard Mound Fault, a scarp runs parallel to Leonard Mound for the length of this section from Blakiston to Nukiwai. The scarp is 5 m high and is the product of two imbricate thrusts of the Leonard Mound Fault. A step-over occurs where the faults cross Palmside Road (Map 3B), which has unfortunately destroyed some of the geomorphic expression. The step-over suggests that, as well as the obvious reverse motion, there is also a component of oblique motion on the fault.

The terrace formed between the LMF and the afore mentioned imbricate faults is composed of well stratified fine gravels with clasts of Torlesse sandstone upto 1cm in diameter. The terrace surface has been tilted very gently to the east, which is reflected in the very low dips observed in the gravels. The stratification and clast size indicates that these gravels are more likely to have been deposited by the streams flowing off the Lowry Peaks Range rather than the Waiau River. It is believed that these gravels belong to the C_2 fans, which points to a Holocene age of movement on the imbricate faults.

3.3.1.4 Kilsyth Section (Map 3C)

The most significant contrast between the Kilsyth section and the other sections of Leonard Mound is the presence of Mount Brown Formation sandstone and shelly horizons exposed in the fault scarp. The ridge does not show the fold morphology as seen to the south. This is supported by the attitude of the Mount Brown Formation, which dips moderately to the SE. The trace of the Leonard Mound Fault is quite clearly defined along the base of the fault scarp which is up to 20 m high and dips 40° NW. This section has a higher number of landslides, and generally larger landslides degrading the fault scarp.

As in the previous sections there is imbrication of the footwall represented by several smaller faults to the west of the Leonard Mound Fault. These footwall faults have ruptured the surface and produced scarps that are up to 5 m in elevation. The most significant of these secondary faults is the Boundary Fault which starts in this section and continues northwards for a

distance of 3-4 km, veering away from the Leonard Mound Fault. The name (from this study) derives from the geophysical surveys, which indicate that the fault is a significantly larger structure than the geomorphology would suggest, and appears to mark the western boundary of the deformation associated with the Leonard Mound Fault System. Since it appears to be a major structure, it warrants separate discussion in a following section. On the uplifted fan gravels to the west of the Leonard Mound Fault, the secondary faulting has gently folded the gravels producing asymmetric folds with more steeply dipping NW limbs and horizontal to gently dipping SE limbs.

It is notable that in the three sections to the south, there has been very little deposition of material to the west of Leonard Mound from the streams dissecting the mound. In contrast, to the west of the Kilsyth section and especially the Mount Palm section to the north, there is an extensive array of alluvial fans extending out from the base of Leonard Mound. In this region it is noticeable that the ridge is more highly dissected by the streams flowing off the Lowry Peaks Range. It is also evident that the degree of ridge dissection by the streams is related to the distance the LMF is away from the LPF.

3.3.1.5 Mount Palm Section (Map 3D)

Geomorphically, the faulting is not as well expressed in this section when compared to the south. In the southern sections, a scarp upto 30 m high has developed that has been subjected to very little degradation. In contrast, the uplifted C_1 fan gravels are extensively dissected and eroded by the streams draining the Lowry Peaks Range, leaving very little of the fault scarp (Figure 3.15). In addition to the amount of degradation, the streams responsible for the degradation have deposited the Late Pleistocene and Holocene alluvial deposits of the western Lowry Peaks fans, burying the lower portion of the scarp. It is important to observe that the faulting has not disrupted these fan surfaces, only the oldest of the Lowry Peaks fans, ruling out Holocene displacement on this section of the fault.

The fans have also buried any trace of structures immediately to the west of the Leonard Mound Fault. Unlike further south where the footwall imbricates occurred within a zone no more than 500 m wide from the Leonard Mound Fault, the closest fault is the Mount Palm Fault over 1 km away. The Mount Palm Fault is very similar in appearance to the Boundary

Fault. It has a NNE-SSW strike, veering it away very quickly from the Leonard Mound Fault, which changes to a more ENE-WSW strike at its northern end. Where it changes strike it becomes highly splayed with each splay having no more than 2 m of displacement, manifested as leading edge folds, typical of the Leonard Mound Fault System.

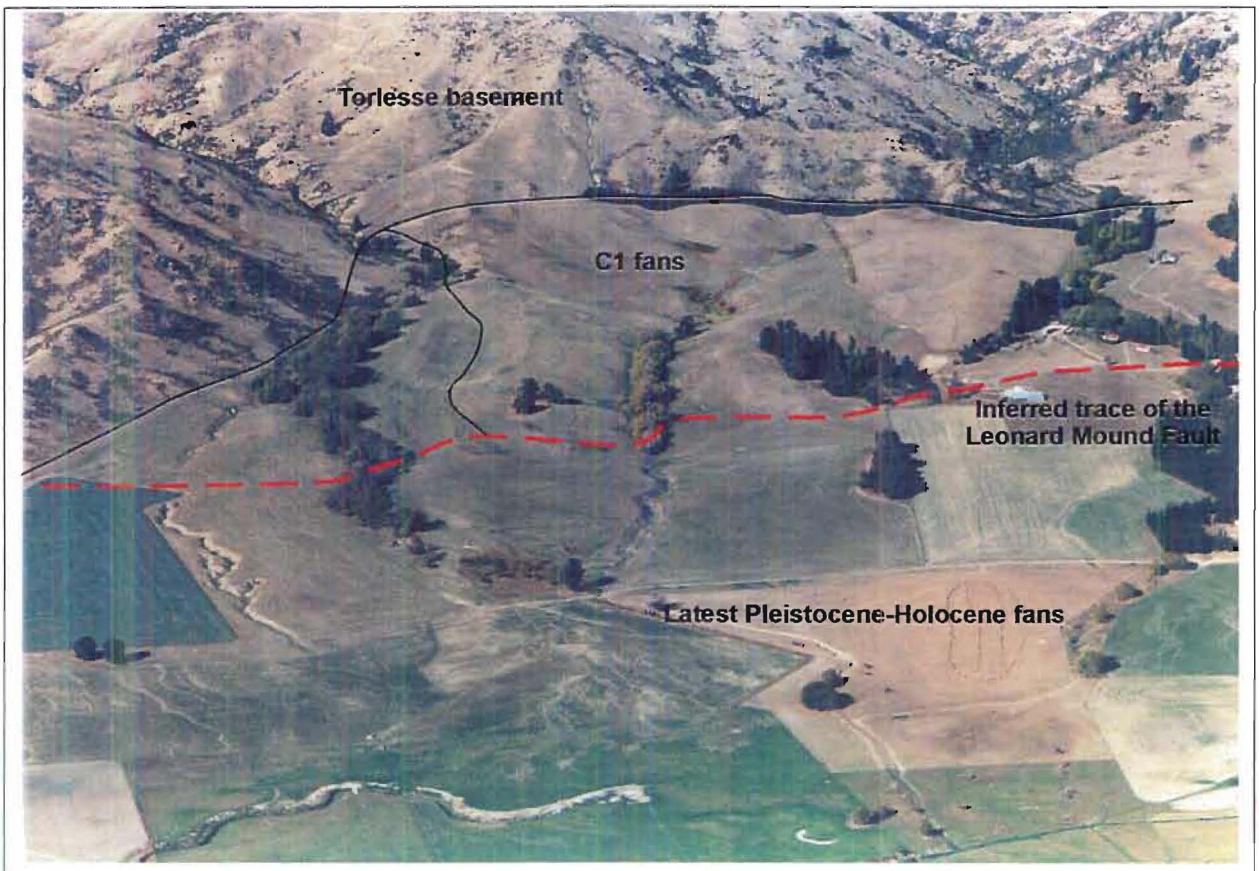

FIGURE 3.15. Photograph of the northern end of Leonard Mound showing the highly dissected nature of the uplifted fan gravels and the highly degraded fault scarp.

3.3.2 Boundary Fault (Map 3D)

Lying between Isolated Hill and the Lowry Peaks Range, the Boundary Fault has warranted a separate mention as it is some distance out from Leonard Mound and the other features associated with the LMFS. Although it starts within the Kilsyth section, as described earlier, its more northerly orientation veers it away from Leonard Mound and the Lowry Peaks Range (Map 3D, Volume 2).

In its southern portion, a scarp has developed that can be traced from Kilsyth to a few hundred metres north of Mount Palm Road and appears to be a splay off the Leonard Mound Fault.

North of Mount Palm Road the surface trace of the fault is lost, however, as the geophysical results show in Chapter 5, the fault can be traced further north. In the banks of the Waiau River, an outcrop of Mount Brown Formation also lends support to the continuation of the fault at least as far as the Waiau River, and it may well link with the Totika Fault seen in Bourne Stream, north of the Waiau River.

Geophysically this fault marks a sharp boundary in the basin between the SE margin associated deformation and the relatively undisturbed central basin, hence the naming of Boundary Fault. Geologically and geomorphically the fault also defines distinct areas. To the south of Mount Palm Road, the fault marks the boundary between the Burnham Formation to the west and the Lowry Peaks Range derived fan material to the east. The deposits to the east have been uplifted and tilted to the SE. On the downthrown side of the fault, a swampy patch of ground has developed in which there are relatively younger soils than the surrounding soils.

North of Mount Palm Road the Burnham Formation has buried any trace of the fault. The fault also marks the NW limit of any visible evidence of active faulting on an orientation similar to that associated with the LPFS and LMFS.

3.3.3 Hemmingford Fault

The Hemmingford Fault (new name) occurs between the Lowry Peaks Fault and the southern end of the Leonard Mound Fault (Map 1). It is named after the Hemmingford Station, located to the east of the fault. The trace of the fault, quite clearly seen on aerial photographs (Figure 3.16), extends for approximately 2.5km with a typical NE-SW trend. The southern end of the Hemmingford fault becomes buried under an alluvial fan from one of the streams off the Lowry Peaks Range, whilst the northern end of the trace dies out shortly after crossing the Lowry Peaks Road. The faulting has produced a scarp upto 4 m high and a characteristic asymmetric fold with a steeply dipping NW limb and gently dipping SE limb.

Although, geomorphologically the fault appears to be only a minor structure in terms of accommodating the deformation in the area, geophysical results indicate that it is more significant in terms of the deformation. As will be shown in Chapter 5, there may well have been several hundred metres of vertical displacement across the Hemmingford Fault. The

other significant aspect of the Hemmingford Fault is that it is active which, if it is part of the LPFS, shows that portions of the LPFS have been active during the Late Pleistocene. It is interesting to note that the Hemmingford Fault exists where the Leonard Mound Fault System dies out at its southern end, suggesting that the LPFS is still accommodating the deformation in the region to the south of the LMFS. In contrast, to the north it is apparent that the LMFS is accommodating the majority, if not all, of the deformation with no visible deformation occurring on the Lowry Peaks Fault.

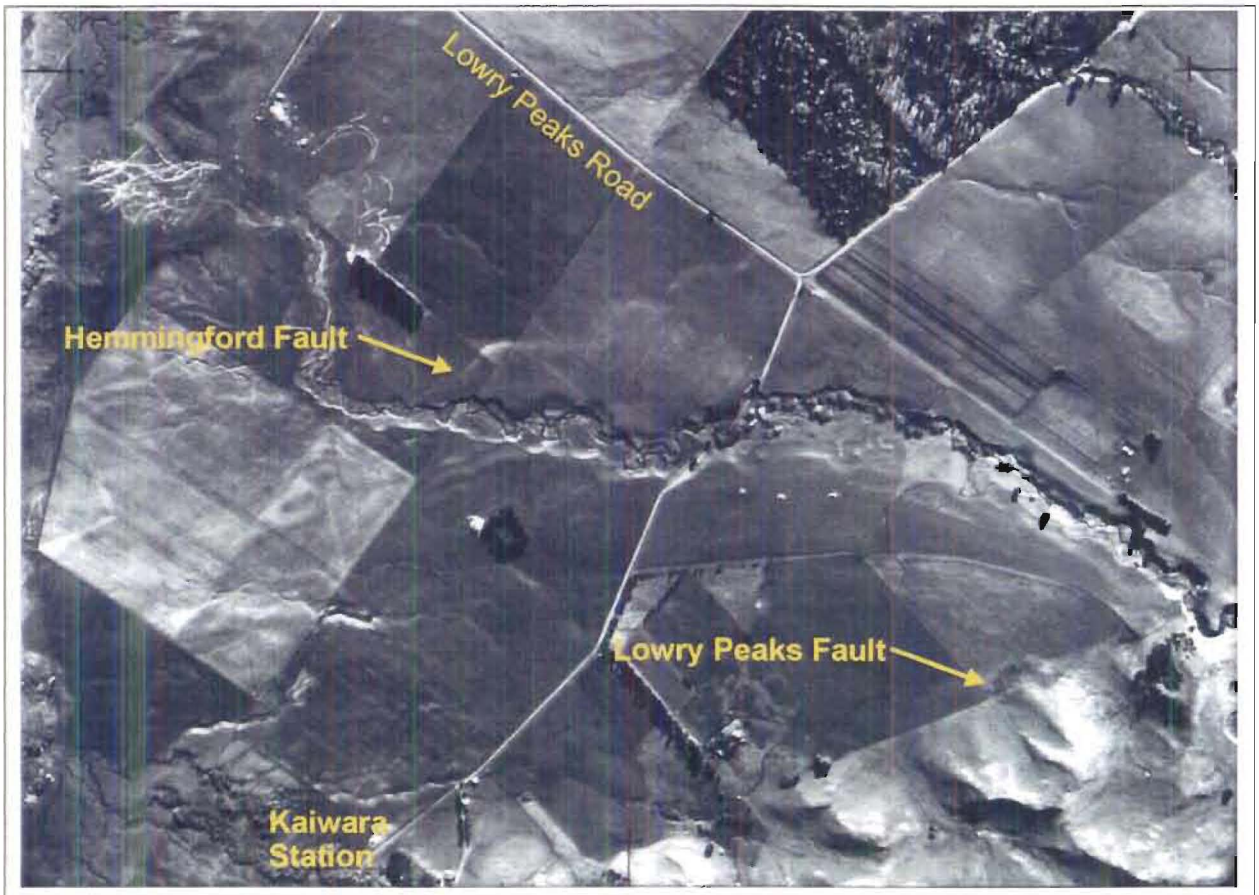

FIGURE 3.16. Vertical aerial photograph of the Hemmingford Fault (grid reference N33/053230). The trace of the fault can be seen at the base of the scarp and also by the change in the morphology of the streams dissecting the scarp.

3.3.4 Basin Floor Folds

Though technically not part of the Leonard Mound Fault System, the majority of these folds (Figure 3.17, Volume 2) appear to splay off from the Leonard Mound Fault System. The basin floor folds comprise a number of small leading edge anticlinal warps that generally have up to 2 m of relief. Geomorphically these folds have a typical leading edge fold character: steep

front limb and shallow dipping to horizontal back limb. The majority of the faults that are controlling the development of these folds have not ruptured the surface. Generally the folds have NE-SW trends, with a few trending E-W. The orientation and location of these folds is inferred to be being controlled by larger structures in the underlying cover sequence and basement rocks, and may be indicating the E-W partitioning of the basin.

To the east of Culverden a set of these folds is observed trending NE-SW. As will be shown in the following chapter, the gravity and TEM surveys show the Isolated Hill Fault to continue as far south as Culverden and possibly further, and projecting directly beneath the position of these folds. Therefore, these small folds are interpreted as representing Holocene displacement on a segment of the Isolated Hill Fault.

3.3.5 Age of Features

Along the length of the inferred trace of the Leonard Mound Fault, there is no clear evidence that the fault has moved during the Holocene. Across the valley mouths there has been no disruption or displacement of the latest Pleistocene and Holocene alluvial fan gravels shed off the Lowry Peaks Range. At the southern end of the system, the Burnham Formation has been deposited against the fault scarp and also shows no sign of having been deformed. The youngest age of movement that can be documented for the Leonard Mound Fault occurred after the deposition of the oldest Lowry Peaks range-bounding fans, which have clearly been uplifted at the northern end of the system. From the correlation with the deposits in the Charwell River area to the north of Culverden Basin, the inferred age of these fans is somewhere between 48-31 ka.

In contrast, the imbricate structures developing to the west of the Leonard Mound Fault are clearly Holocene in age. They have uplifted and folded the deposits of the Burnham Formation and the range-bounding alluvial fans. At the present time there is no way of more accurately defining the last period of movement on these structures, as no precise ages are available for the deposits.

3.4 DRAINAGE NETWORK

For many decades workers (e.g. Campbell, 1896; Hobbs, 1901; Zernitz, 1932; Adams, 1980; Burnett and Schumm, 1983; Bull, 1984; Ouchi, 1985; Bull and Knuepfer, 1987; Rhea, 1993) have used drainage patterns in active tectonic studies, and have shown how sensitive rivers and streams can be to even small movements across tectonic structures. Characteristics of the drainage network (e.g. drainage patterns, catchment size and shape, river and stream flow paths etc.) provide information on the lithological and structural setting of the drainage network.

3.4.1 Rivers

The floor of the Culverden Basin is comprised of gravels derived from the major rivers that flow across the basin in antecedent courses. Whilst the overall flow direction is towards the SE, the courses and morphologies reflect the control that different structural elements have on the rivers. Along the course of a large river, the morphology of that river will vary depending on several factors such as sediment load, sediment size, flow velocity, differing geological units and ongoing tectonic deformation. Four main types of rivers are recognised based on river morphology (Figure 3.18) of which straight and anastomosing are uncommon in the Culverden Basin.

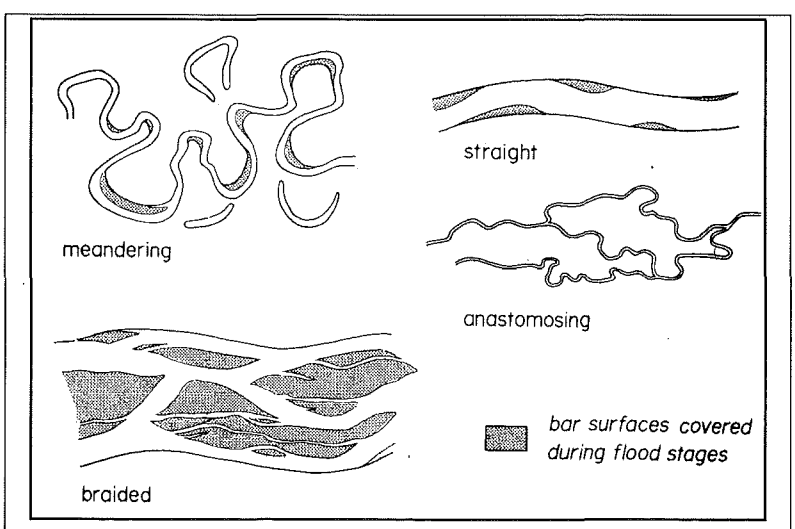

FIGURE 3.18. Principal types of rivers (from Miall, 1977).

Braided rivers are best developed in the distal parts of alluvial fans, on glacial outwash plains and in the mountainous regions of river systems where sediment is abundant and water discharge is high. Braiding occurs as a result of rapid, large fluctuations in river discharge, abundance of coarse sediment, a high rate of supply of sediment and easily erodable banks (Cant, 1982). In contrast meandering rivers have a much greater sinuosity, lower gradients and finer sediment load. They are generally confined to a single channel with banks that are difficult to erode.

The three large rivers that traverse Culverden Basin all possess a very similar morphology. Across the floor of the basin they are braided with floodplains whose width, ranging from 100m for the Pahau River to nearly 3km for the Waiau River, is dependant on the size of the river. Once they leave the basin they become confined to steep narrow gorges. The general flow direction of the rivers is to the SE parallel to the regional topographic gradient. However, the rivers have been forced to alter from their NW to SE flow direction in response to the deformation occurring within the basin and along the basin margins. The structures responsible for those changes are not always visible on the surface making the rivers a very good indicator of the subsurface deformation.

The Waiau River is the largest of the rivers (Figure 3.3). It plays a vital role in the hydrogeology of the northern portion of the basin as it supplies the majority of the natural recharge to the aquifer system, and water is drawn from the river for the irrigation scheme. Therefore, any structures that have, and are currently affecting its course will also be affecting the groundwater regime and hence need to be identified. The same is also true for the Hurunui and Pahau rivers to the south, and whilst these rivers will be described, the main focus is the Waiau River and the northern part of the basin.

During the Late Pleistocene the Waiau River clearly had a substantially broader active floodplain than it does at the present. The Late Pleistocene was a time of aggradation with the rivers supplying vast quantities of gravel into the basin whose floor was beneath the base level of sedimentation. In contrast the dramatic change in the climatic conditions at the end of the Pleistocene has resulted in the Holocene being a period of extensive degradation during which the rivers have incised into their present channels. The Glynn Wye Advance of the Hope Glaciation saw the Waiau River covering the majority of the basin floor to the north of

Culverden. The thin to absent soil cover on the Burnham Formation indicates that the river was active on the Culverden Surface up until the end of the Glynn Wye Glacial Advance (~16 000 yrs BP), and possibly to the end of the Hope Glaciation (~14 000 yrs BP). During that time the river had three main branches. The first flowed along its present path on the northern side of Isolated Hill and out through the gorge. The second and third branches flowed to the south of Isolated Hill with one branch rejoining the northern branch on the east side of Isolated Hill, whilst the other branch flowed south and merged with the Pahau River and went out through the Hurunui Gorge.

The question then, is why did the Waiau River adopt its present position and not take, what appears to be, the easier path to the south of Isolated Hill during the Holocene? Two opposite facing terrace scarps to the southeast of Rotherham (grid references: N32/060322 and N32/060334) may indicate that the Waiau River tried to cut a path to the south of Isolated Hill, but was subsequently forced to the north. Clearly, therefore, the structures mapped on Isolated Hill and Mount Culverden affected the present position of the river. The Isolated Hill and Rotherham faults do not have any clearly identifiable Holocene displacements adjacent to Isolated Hill. However, as discussed in an earlier section, the small folds observed to the east of Culverden may well represent Holocene movement on the continuation of the Isolated Hill Fault. If this is the case then it indicates that the Isolated Hill Fault has been active during the Holocene, and that those movements have controlled, in part, the present location of the Waiau River.

During the previous (Glenhope) glacial advance, the scattered remnants of Windwhistle Formation suggest that the river probably followed a similar course as to its course during the following (Glynn Wye) advance. In the Hope River, Cowan (1992) documented a period of ice retreat and erosion between the Glenhope and Glynn Wye Advances (25 000-22 000 yrs BP). In the Culverden Basin this period is represented by the widespread degradation of the Windwhistle Formation by the Waiau River.

Prior to the Hope Glaciation, the history of the Waiau River is more enigmatic. The only possible evidence that the Waiau River was active in the basin during that time, occurs along the eastern flank of the Amuri Range, bordering Emu Plains. As is described in Chapter 2, the lower slopes of the Amuri Range are composed of the morphologically "smooth" Torlesse

basement. Preserved in some of the stream gullies are packets of highly weathered gravels composed of angular to sub-rounded clasts of Torlesse set in a sandy matrix. The origin of these gravels is unclear, but from the altitudinal relationship with Windwhistle and Burnham formations, they are clearly older than those. However, whether they are from the Waiau River or are alluvial fans of the Amuri Range is uncertain. The smooth nature of the Torlesse may indicate that the Waiau River was active on this surface prior to it being uplifted on the thrusts at the boundary between the smooth and rugged morphologies.

The Pahau is the smallest of the three rivers that flow across the basin (Figure 3.3). Unlike the Waiau River, the tectonic features controlling its path are not as easily identifiable. Along its course it takes a number of sharp changes in flow direction indicative of structural control. Its course through the western ranges is controlled by a N-S trending lineament that can be seen on the landsat image of North Canterbury (Figure 1.1). On the floor of the basin the river undergoes two major bends. The first is where it crosses State Highway 7 and the second is 2-3 km to the east of the highway. The first bend is believed to be in response to the continuation of the Isolated Hill Fault and associated fold. As will be shown in Chapter 4, the crest of the structural high projects to the position of the bend in the river, and the presence of small folds to the east of Culverden, inferred to be the active traces of the Isolated Hill Fault, also indicates that the bends are structurally controlled. The second bend is believed to be the river correcting itself back to its preferred SE flow direction.

The Hurunui River, from the western ranges to the Lowry Peaks Range, displays the straightest flow path of the three rivers. It is evident from the terrace scarps on the southern side of the river that during the Late Pleistocene the river has migrated northwards. The structures responsible for the northwards migration of the Hurunui River are manifested as the Hawarden Anticline and the Trig C structures (Litchfield, 1995) at the southern end of the Lowry Peaks Range. Once the river reaches the Lowry Peaks Range it swings to the north and continues along the base of the range until exiting out through its gorge. Litchfield proposed that the Hurunui River once took a more direct route to the sea until uplift on the southern end of the Lowry Peaks Range, prior to the last glaciation, breached the river forcing it to flow northwards along the Hurunui Bluff Fault.

The courses of the major rivers once they leave the basin are anomalous in the sense that they cut straight across the major anticlines which coincide with the actively forming the ranges. Earlier workers (Cotton, 1913; Speight, 1915b and 1918; Thompson, 1920; Cotton, 1938; Powers, 1962) proposed that the rivers first established consequent paths to the sea on a coastal plain, of upper Kowai Formation, formed during the first stages of uplift on the major fault systems. The rivers then became sufficiently entrenched that they maintained their courses during the subsequent uplift of the ranges. However, in her thesis, Litchfield (1995) showed that the Kowai Formation had not been uniformly distributed over the entire area and that rivers are highly sensitive to uplift on even moderately small structures. It is now evident that the locations of the two gorges are structurally controlled.

The current position of the Hurunui Gorge is controlled by a structural low, resulting from displacement transfer between the Hurunui Bluff Fault and Hurunui Gorge Fault (Chapter 2). Earlier phases of faulting have preserved the softer Tertiary strata that the river exploited. Through the ranges the Hurunui River has a straight path in comparison to the Waiau River. The course of the Waiau River is sinuous and is controlled by both bedding within the Torlesse and differential uplift across faults and folds. As is shown in Chapter 2, the northern end of the Lowry Peaks Range is structurally lower than the southern end due to segmentation of the Lowry Peaks Fault. The Torlesse basement is "smooth" and has patches of gravels on the range crest suggesting that the Waiau, Mason and Stanton rivers have been flowing along their paths since the inception of the range-front faulting.

3.4.2 Streams

Streams are much more sensitive than the rivers to changes in the slope gradient due to their smaller size. Even a few metres of uplift across a fault/fold can change the morphology and course of a stream. Consequently, the streams are very good indicators of the more subtle deformation that may otherwise not be readily observed.

3.4.2.1 Drainage Patterns

Drainage patterns have been widely used in the study of active tectonics throughout North Canterbury (Campbell and Yousif, 1985; Litchfield, 1995), New Zealand (Bull and Knuepfer,

1987; Norris, 1998) and worldwide (Adams, 1980; Deffontaines et al., 1982; Ouchi, 1985; Harvey and Wells, 1987; Friederking, 1989; Pubellier et al, 1994). Recognition of various types of drainage patterns and the change in the rivers and streams morphology aids in the understanding of the tectonic and sedimentary environment of an area. From numerous studies many different types of drainage have been recognised of which those seen within the study area are shown in Figure 3.19.

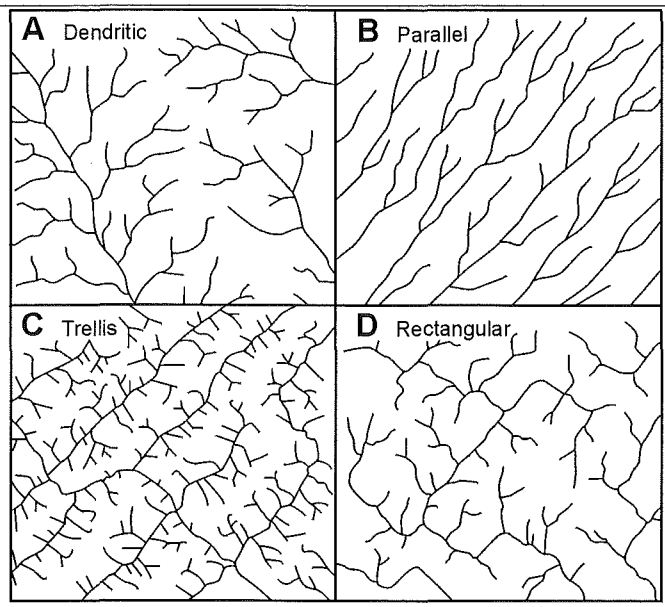

FIGURE 3.19. Basic drainage patterns (modified from Howard, 1976; and Bloom, 1991).

Drainage basins originate and spread in a variety of ways according to the history of the land surface on which they develop (Dunne, 1980). Earlier authors (e.g. Horton, 1945; Chorley, 1957; Strahler 1958) emphasize that initiation of stream channels and the resulting drainage networks are related to elements that control surface runoff processes, such as relief, vegetation, lithology and faulting. Whilst the surface runoff processes play a significant role in the development of the drainage network, a factor that was overlooked by those earlier workers was the effect of the shallow groundwater flow. It was demonstrated by Bunting (1961), Kirkby and Chorley (1967), Dunne (1980), Berger and Aghassy (1982), Higgins and Coates (1990) and LaFleur (1984, 1999) that the presence and movement of near-surface groundwater can promote continuous corrosion of bedrock and soil and thus create new drainage networks. From numerous studies of mountain ranges and flume table experiments, Talling et al. (1997) show how the setting of a region controls the development of the

drainage network (Figure 3.20). The drainage network on mountain ranges develops during the initial stages of range growth. The type of network developed will depend primarily on the slope of the land surface at that time and the subsequent tectonic influences.

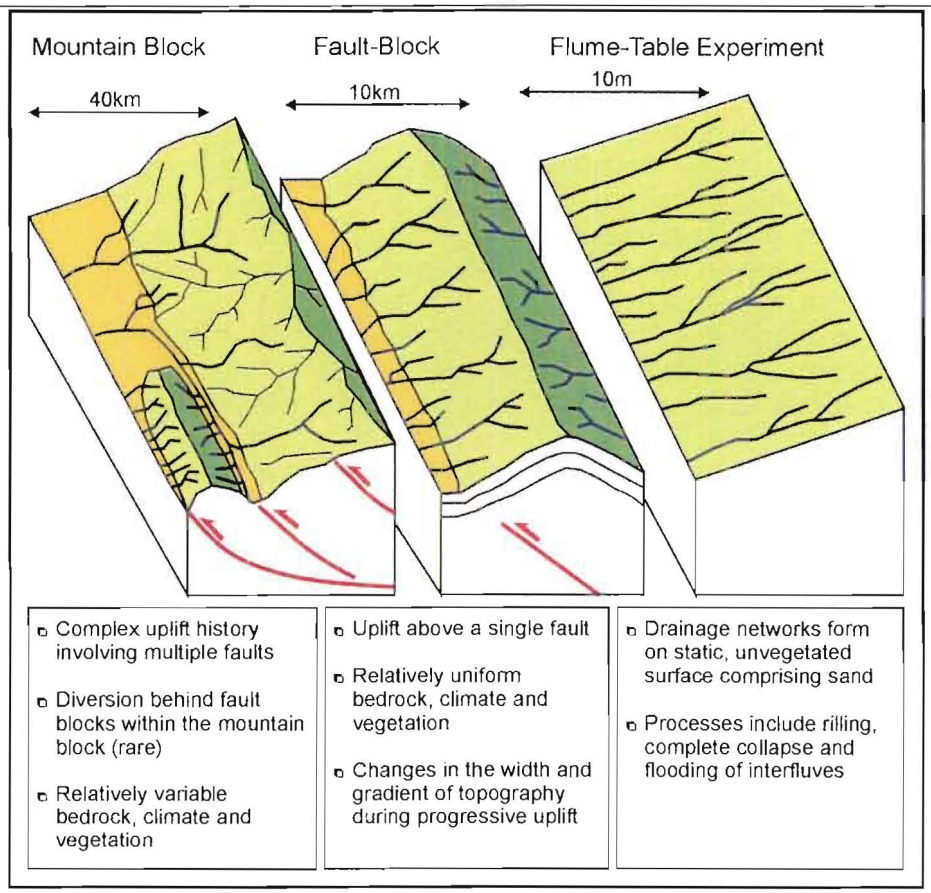

FIGURE 3.20. Schematic drawings summarising the different processes affecting drainage network growth in mountain belts, on fault blocks and in flume table experiments (Talling et al., 1997).

The streams have been ordered according to a hierarchical system devised by Strahler (1957). In this system all streams start as a first order stream. Where two streams of n^{th} order join they form a stream of n^{th+1} order. For example, where two first order streams join a second order stream is formed which becomes a third order stream once it joins with another second order stream etc. The major rivers in this study have not been classified according to this system as the majority of their catchments lay well outside the field area. The major trunk streams are those which reach an order of 4 or greater, whilst the small streams are those with a maximum order of 3.

As can be seen in Figure 3.21 very few of the streams reach an order of magnitude 4 or greater along the eastern margin of the basin. In comparison, on the other margins of the basin, the streams commonly attain a magnitude of 5 (Figure 3.22). This difference is directly attributable to the tectonic setting of the streams. On the western margin of the basin and to the south of the study area in the Waikari Valley, a trellis drainage pattern is observed with the major streams utilizing the downthrown blocks of the major faults. As the eastern limb of the Lowry Peaks Anticline demonstrates, major streams are also found on the gently dipping back-limbs of folds, as the catchments are substantially larger than those on the steeper fore-limbs. In contrast to those major streams on the downthrown blocks of major faults, the streams on the back-limbs of folds more commonly display a dendritic pattern reflecting the regional slope gradient.

Along the eastern margin of the basin the streams do not reach a magnitude of four or greater for two reasons:

(A) they are located on the steep fore-limb of the Lowry Peaks Anticline, and consequently have small catchments in comparison the back limb of the fold, and

(B) on the downthrown block of the Lowry Peaks Fault the alluvial range-bounding fans have infilled the synclinal depression, which has also been partially destroyed by the Leonard Mound Fault System, removing a valley which a major stream may have utilized.

One of the few streams that does reach a fourth order of magnitude is Bourne Stream to the north of the Waiau River. The location of Bourne Stream is controlled by the Totika Fault which has uplifted Torlesse and cover sequence units against the SE limb of the Mount Highfield Anticline. The majority of the streams feeding Bourne Stream are located on the shallowly dipping eastern limb of the Mount Highfield Anticline, and consequently have a larger network of streams able to combine to form a major stream.

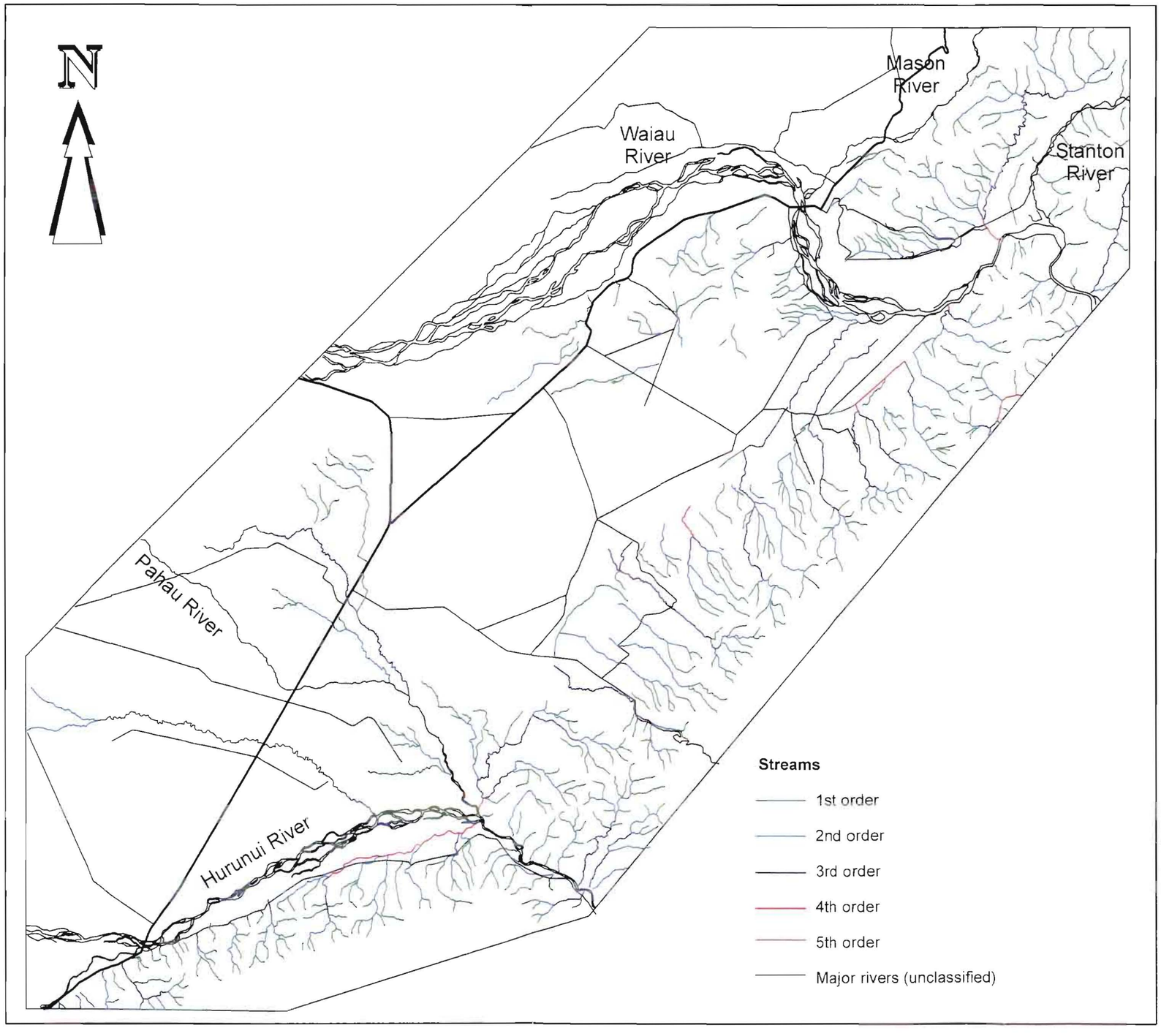

FIGURE 3.21. Map of the streams classified according to stream order.

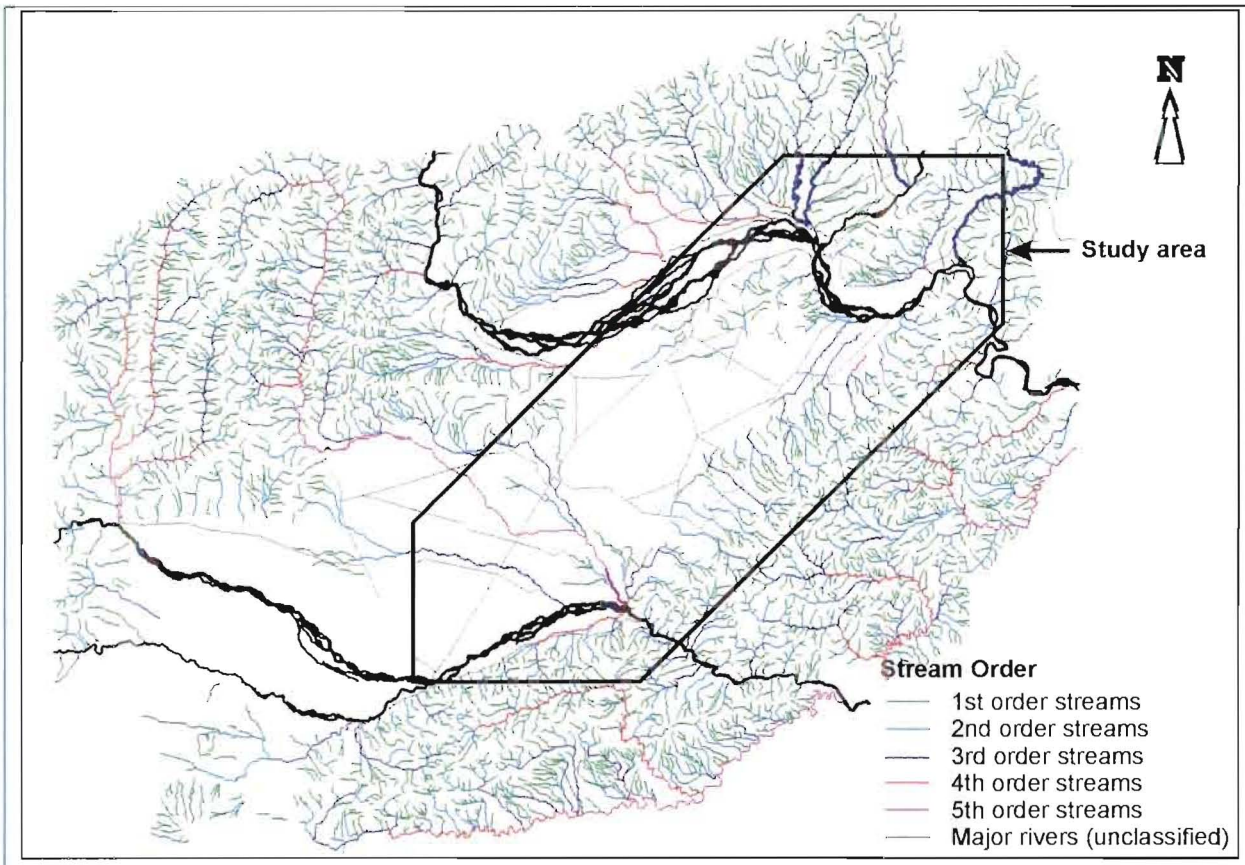

FIGURE 3.22. Comparison of the streams in the study area with those on the other margins of the basin.

The small streams have a range of patterns depending on the geological setting of the streams. It is clear that the characteristic pattern of flow on a dipping surface is dendritic, which does feature prominently in the drainage. There are, however, notable exceptions which are attributed to two controls, namely lithology and structure. The effects of lithology on the drainage patterns of the area can be divided into two types: (i) effects due to the differences in lithology between the major units, and (ii) effects due to the presence of resistant beds within the major units, in particular the Torlesse.

For the purpose of this discussion the streams of the different areas of the eastern margin will be compared to see the effect of the geological setting. The different areas are defined by the lithologies and structures and are:

- the Lowry Peaks Range,
- the eastern margin alluvial fans,
- the basin floor.

Lowry Peaks Range

On the Lowry Peaks Range, the streams have features that are characteristic of rapidly uplifted fault and mountain blocks. The streams have cut steep narrow gullies, which is reflected in the short narrow catchments of the streams. For the southern portion of the Lowry Peaks Range, Litchfield (1995) described a rectangular drainage pattern, which is mainly due to the presence of resistant beds within the Torlesse, but is also in part due to two sets of structures at high angles to each other. There is a N-S trending set of streams that Litchfield interpreted to represent a fracture control, and a WSW-ENE set that she interpreted as imbricate splays of the Hurunui Bluff Fault.

To the north of the Hurunui River on the central portion of the range, the streams possess a very similar drainage pattern to those seen on the southern section. There are three orientations of the streams related to structural control (Figure 3.23):

- NE-SW (sub-parallel to the range-front)
- NW-SE (perpendicular to the range-front)
- E-W

The NE-SW and NW-SE trending streams represent similar controls to those inferred by Litchfield, i.e. imbricate thrusts (NE-SW set) and cross-faults (NW-SE set). The slight change in orientation from those to the south in Litchfield's area is due to the change in the overall strike of the Lowry Peaks Fault System on either side of the Hurunui River. Although the streams inferred to be caused by the cross-faulting flow parallel to the gradient, and hence parallel to many of the other streams flowing off the range, they have distinctive, straight paths.

The third orientation of the streams is poorly expressed on the western limb of the Lowry Peaks Anticline, however, they form some of the major streams on the back (eastern) limb of the fold. These streams have an east-west trend, also believed to reflect structural control related to a pre-existing older set of Cretaceous structures that Nicol (1991, 1993) and Barnes (1993) documented in other areas of North Canterbury and offshore. It is also believed that the Mount Culverden Fault, on the west side of the basin, may be a reactivation of one of these east-west striking faults.

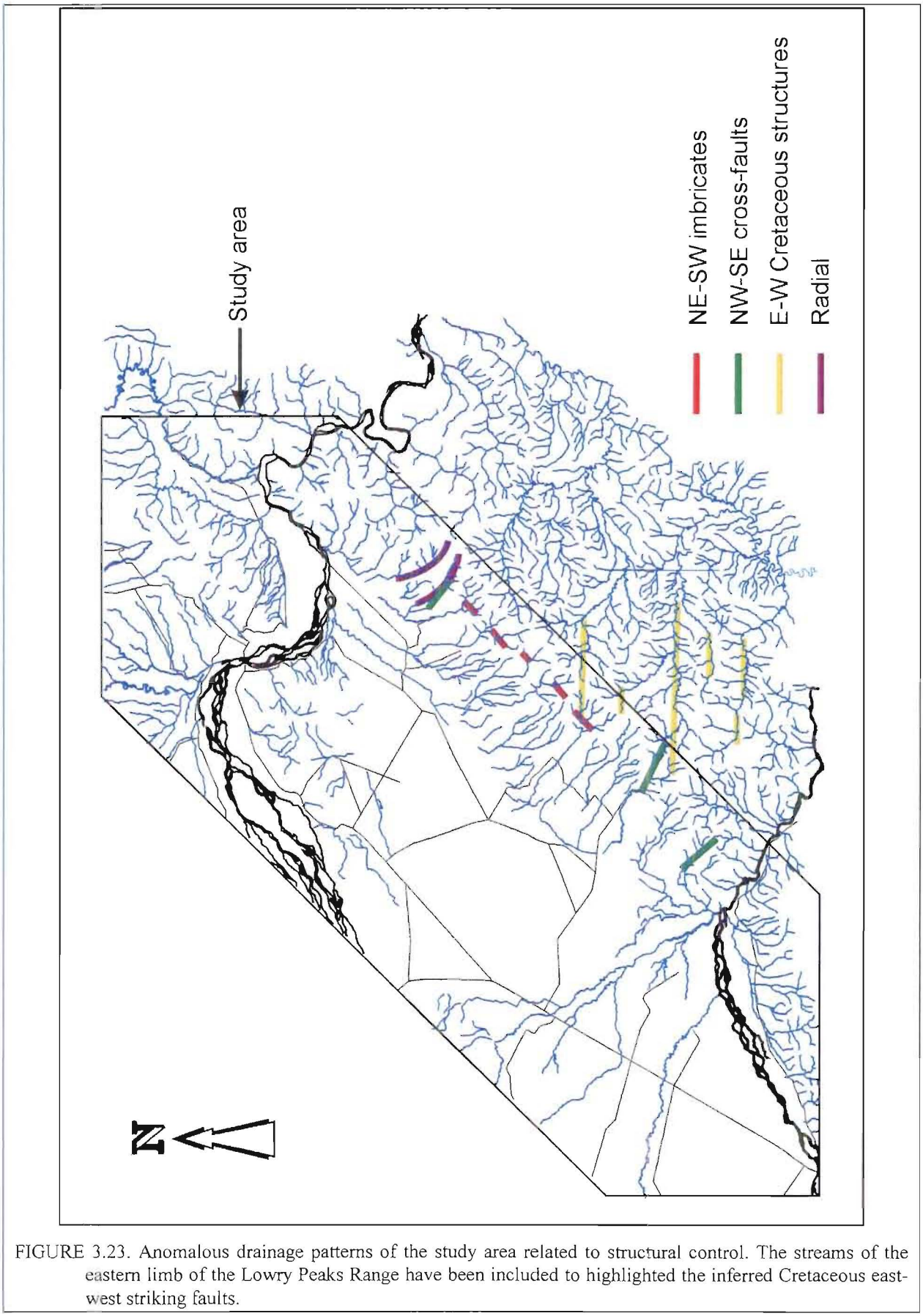

FIGURE 3.23. Anomalous drainage patterns of the study area related to structural control. The streams of the eastern limb of the Lowry Peaks Range have been included to highlighted the inferred Cretaceous east-west striking faults.

At the northern end of the range on the relatively smooth Torlesse, the streams possess a dendritic pattern. There has not been the same amount of erosion of this section of the range, hence the streams patterns are not yet reflecting the nature of the underlying bedrock. Two streams on this section are worthy of mention, and have been highlighted in Figure 3.23. Both streams have a curved path, which is highlighting the southern end of the southward plunging Ngawiro Anticline. The smaller streams feeding those larger streams display a radial pattern clearly delineating the nose of the fold.

Eastern Margin Alluvial Fans

The streams on the eastern margin alluvial fans display both the least dense and most "erratic" style of drainage and conversely some of the densest drainage within the study area. The most erratic drainage occurs on the composite surface, where the streams are generally short, discontinuous, and tightly meandering which directly reflects the lack of power of these streams as they flow over a very low gradient surface. These streams all flow perpendicular to the NW-SE regional gradient (parallel to the major structures) as they are trapped between the oppositely dipping glacial outwash surfaces and the Lowry Peaks fans. The streams are feed not only by the streams flowing off the alluvial fans, but also by groundwater springs related to the fluvial and tectonic relationships that will be examined in Chapter 5. Due to their low power, they are only able to carry very fine sediment that they deposit onto the composite surface, resulting in the poor drainage that characterizes the surface.

In contrast, at the northern end (Kilsyth and Mount Palm sections) of Leonard Mound, some of the densest drainage is found on the oldest (C_1), uplifted Lowry Peaks fans. These streams display a sub-parallel pattern related to the relatively steep gradient of the fan surfaces. The streams are all deeply incised as a result of the uplift of the fan surface by the Leonard Mound Fault, and the need for the streams to downcut to their equilibrium positions. The streams are highly variable in size, with the size of the stream proportional to the size of the catchment on the Lowry Peaks Range. The sizes of the streams are also clearly reflected in the widths of the valleys they have carved, and the size of the fans they have deposited to the west of the Leonard Mound Fault. Whilst these larger streams have carved relatively broad channels with flat floors, the majority of the streams are contained in narrow V-shaped gullies which are not sourced from the Lowry Peaks Range. The different processes that may be responsible for the

development of these streams are examined in Chapter 5, as the drainage network development may well be being controlled by the near surface groundwater flow within the fans.

The streams on the younger (C_{2-4}, W_{1-3} and N_{1-3}) Lowry Peaks Range fans are actively down-cutting into a single narrow channel and flow parallel to the slope of the fan. In comparison to the older fans, there is only one stream per fan. Once the streams leave the confines of their channels, they rapidly spread laterally producing a very fine network of streams, which is one of the characteristic geomorphic features of the Holocene fans. Clearly, during the Holocene the streams have not been as powerful as they were during the Late Pleistocene. This is best demonstrated by the streams at the southern end of Leonard Mound, which carved relatively large channels through the ridge, and were able to deposit material on the western side of Leonard Mound. Presently, water is starting to pond behind (eastern side) the ridge indicating that the streams are struggling to keep up with the continued uplift of Leonard Mound. Some of the streams are unable to keep up and have been forced to flow southwards, eventually finding their way to the Pahau River. One stream in particular, that flows through "The Willows", is in line with a saddle on Leonard Mound suggestive that the stream once flowed over the mound, however, the origin of the saddle is unclear and may well be the result of differential uplift of the ridge by the Leonard Mound Fault and its footwall imbricates (Figure 3.24). The streams behind the crest of the Leonard Mound all have meandering paths reflective of the very low gradient of the surface.

Basin Floor

The floor of the basin is noticeably devoid of streams, especially on the Culverden Surface to the north of Culverden. There are only a handful of streams that occur dominantly between Culverden and the Pahau River. These meandering streams are sourced from the southern flanks of Mount Culverden, and their meandering paths are reflective of the very low gradient of the basin floor. The streams located on the eastern end of Mount Culverden and Isolated Hill have very small catchments in low rainfall areas, and there is very little water available to the streams. What water is available will rapidly percolate into the water table once it strikes the very well drained gravels of the basin floor.

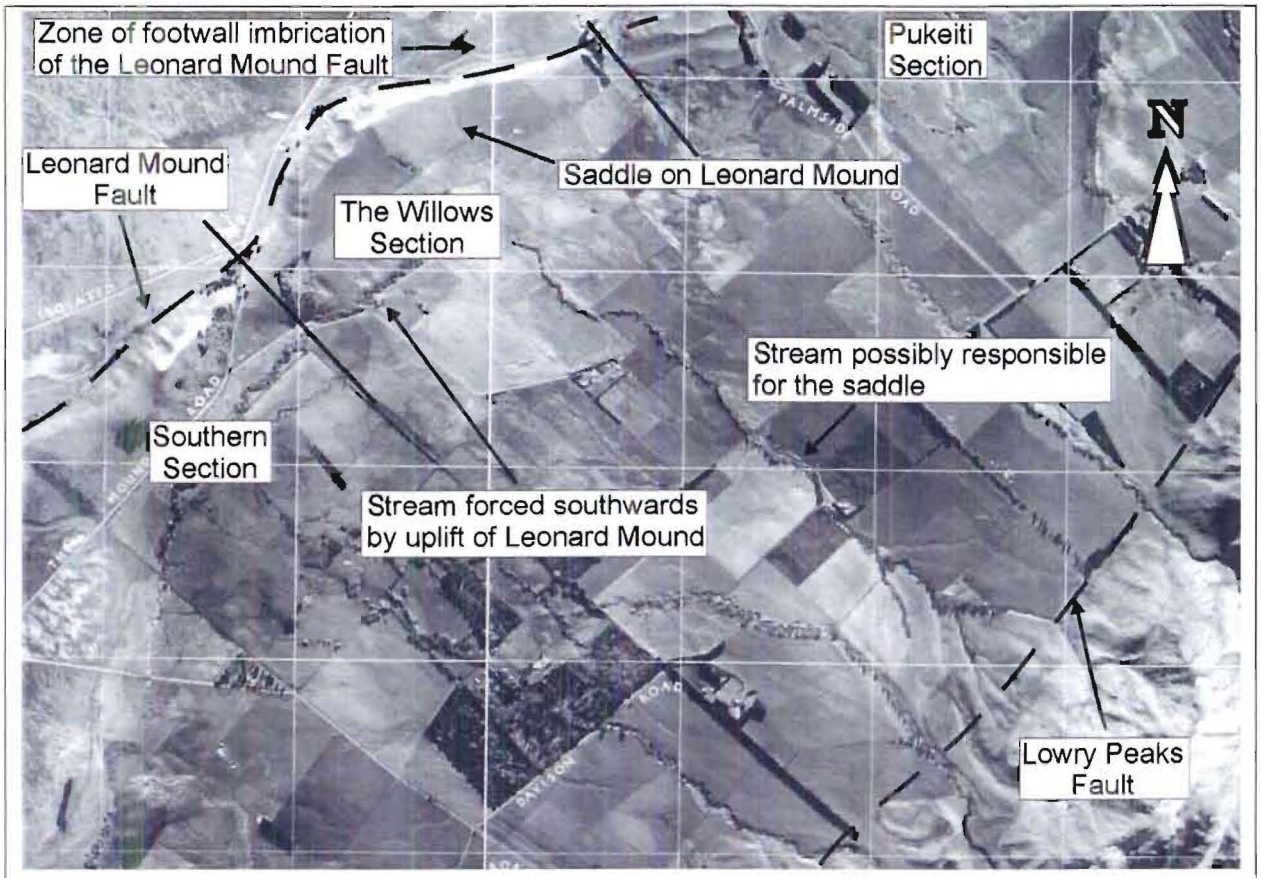

FIGURE 3.24. Vertical aerial photograph of the saddle in The Willows section of Leonard Mound formed by either the stream flowing off the Lowry Peaks Range, differential uplift of Leonard Mound by the Leonard Mound Fault and its imbricate structures, or a combination of both.

3.5 SUMMARY

Stratigraphically, the extensive Waiau, Pahau and Hurunui River aggradation deposits forming the major fill fans/terraces are related to the Late Quaternary periods of colder climate. During periods of warmer climatic conditions, fluvial degradation predominates, with the progressive dissection (degradation) from the level of aggradation to a subsequent tectonically controlled strath surface, associated with the present-day coarse of the rivers. The minor degradational terrace treads (including minor straths, fill-cut terraces, and fill terraces) record the complex responses of the various river systems traversing Culverden Basin to the reduced (interglacial) sediment supply, the regional active tectonic control on base-level, as well as the locally superimposed signature reflecting the response of the fluvial system to individual active structures.

Basin margin deposits are dominated by alluvial fan development. In northeast Culverden Basin the coalescing series of rangefront alluvial fans, derived from the Lowry Peaks Range,

interfinger basinwards with the fluvial aggradational deposits. This relationship is further complicated by the wide zone of active earth deformation associated with the development of the Leonard Mound Fault Zone.

The relationship between the sedimentation and ongoing tectonic deformation is crucial with respect to the groundwater aquifer system. The rate of deformation, expressed by fold growth and thrust related uplift along the northeast margin of Culverden basin, is relatively slow, with maximum estimated uplift rates along the Leonard Mound system of ~1m/kyr. Thus, during periods of rapid aggradation active structures within the basin, as well as along the margins of the basin, are likely to be overwhelmed by aggradational deposits, and become at least partially buried. Examples include the southward projected extension of the Isolated Hill structure, as well as the southern elements of the Leonard Mound structure. Equally, parts of each of these active fault zones have clearly remained emergent above the general level of aggradation, and thus has played an important part in influencing the sediment distribution and fluvial drainage patterns with north Culverden basin.

The rates of landscape emergence and modification by tectonic activity are poorly constrained because of the absence of reliable dating of the gravel sequences and inherent uncertainties in Late Quaternary glacial correlations in North Canterbury. Sediment sources during the cold-climate episodes were dominated by the fluvio-glacial system of the Waiau, and to a lesser extent by the Hurunui-Pahau, whilst the Lowry Peaks Range continued to provide fan materials which interfingered with the fluvio-glacial deposits. The fluvial architecture of the Culverden Basin is therefore dominated by complex facies associations generated under cold-climate conditions, with subsequent reworking and fines redeposition during interstadial or interglacial conditions.

This model has obvious implications for the hydrogeology of the Basin, and indicates a potentially complex groundwater flow pattern controlled by the distribution of the gravel aquifer units on which has been superimposed a NE-trending structural overprint.

CHAPTER 4

GEOPHYSICAL INVESTIGATIONS

4.1 INTRODUCTION

In this thesis three geophysical methods were used:

I. time-domain electromagnetics (TEM) to map the aquifers, quantify the amount of displacement across the structures mapped and assess the suitability of the TEM method in hydrogeological and active tectonic investigations in the North Canterbury region,

II. gravity to examine the gross structure of the basin and determine the amount of vertical movement across the major faults mapped on the basin margins, and

III. ground penetrating radar (GPR) to look at the near-surface deformation associated with the active structures.

There are many other geophysical techniques widely used in geological and groundwater investigations (e.g. Reynolds, 1997), such as seismic refraction/reflection, resistivity, magnetics, very low frequency (VLF) electromagnetics, large offset loop-loop frequency domain electromagnetics, magnetotellurics (MT) and controlled source magnetotellurics (CSAMT). The methods used in this survey were chosen primarily because of their availability, as they are either owned by the University of Canterbury (TEM and GPR) or readily available (gravity). The cost of hiring the seismic, other EM methods or MT equipment eliminated their use in this survey.

In all approximately 150 TEM soundings were performed, 150 gravity stations were surveyed and 20 GPR profiles of varying lengths were acquired. Four TEM and gravity transects were run across the basin along the same lines so that the TEM models could help constrain the gravity modelling. The GPR profiles are in Volume 2. The locations of the TEM soundings, gravity stations, GPR lines and resistivity soundings are shown on Map 4 (Volume 2). This chapter presents the results and interpretations of the geophysics surveys. For a description of the theory, survey design and processing behind each method, see Appendix 2.

4.1.1 Previous Geophysical Surveys

Prior to this thesis only gravity surveys had been run in and through Culverden Basin. The most extensive of the surveys (Whiteford, 1978; Woodward and Carman, 1982; Dibble, 1973; Hicks, 1989) was by Dibble (1973) (Figure 4.1) which located the major tectonic features of the basin. Hicks (1989) suggested from the gravity and the proximity of the basin to the major faults of the Ports Pass-Amberley Fault Zone and the Marlborough Fault System, that the Culverden Basin is a composite pull-apart basin related to strike-slip faulting, which is clearly incorrect based on this study and previous studies in the North Canterbury region. The other two surveys were by Whiteford (1978) and Woodward and Carmen (1982) as part of Christchurch to West Coast transects, from which no interpretations of the basin structure could be made.

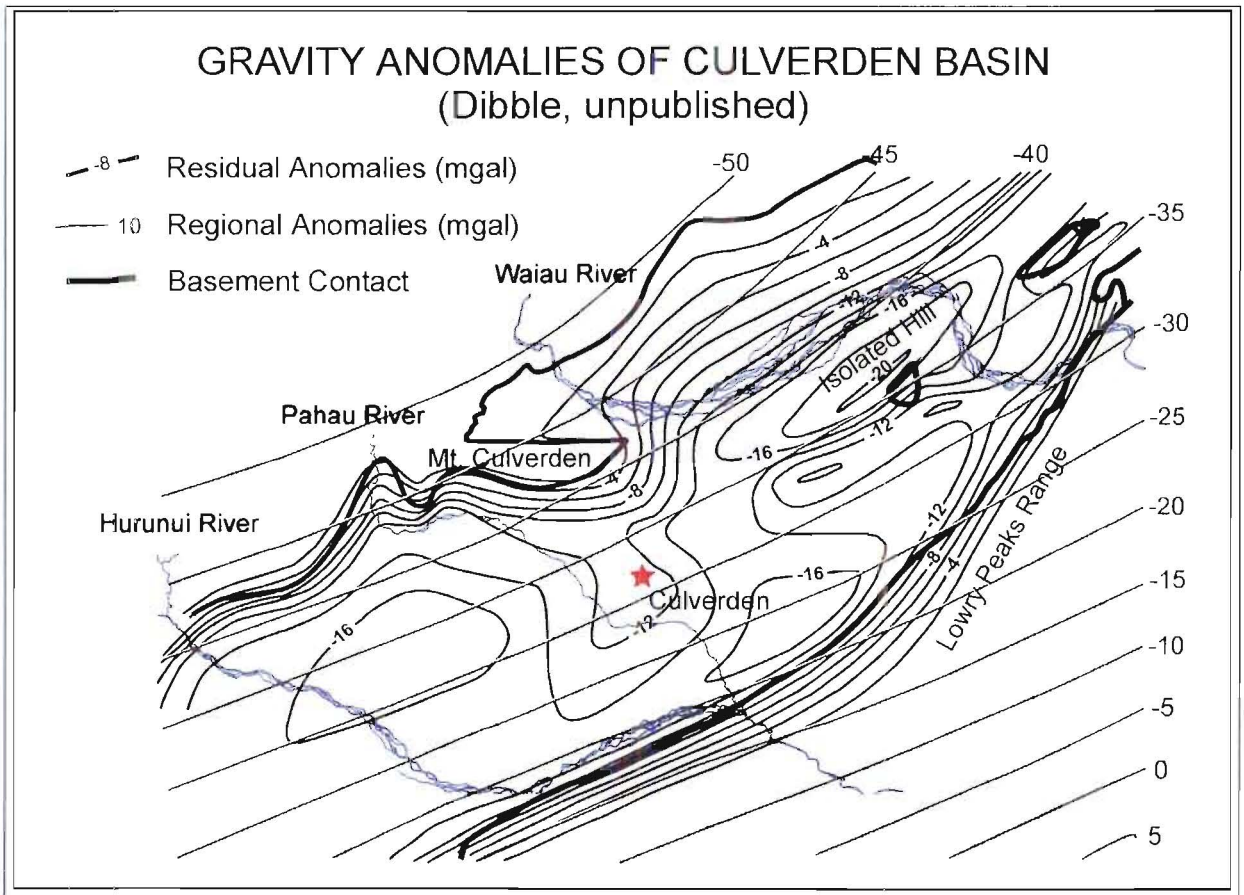

FIGURE 4.1. Dibble's (1973) gravity anomaly map of Culverden Basin related to the major structural elements mapped and described in the previous chapters. The greater the negative anomaly, the greater the depth to the Torlesse basement.

Before moving onto the surveys run in conjunction with this study, it is first interesting to look at the main features of Dibble's survey. The key points to note from Dibble's survey are:

- overall the basin is asymmetric being deeper along the eastern edge;
- the northern end of the basin appears more tectonically deformed than the southern end;
- a syncline has developed on the downthrown block of the Lowry Peaks Fault which appears to be plunging to the SW;
- along the eastern margin the basement reaches it greatest depth around the southern end of Leonard Mound;
- the largest negative gravity anomaly occurs on the western side of the Isolated Hill Fault possibly indicating the greatest depth to basement in the basin; and
- the Isolated Hill structures extend well into the basin.

4.1.2 Data Modelling and Constraints

The lack of deep boreholes throughout Culverden Basin made it difficult to constrain the geophysical models for both the TEM and gravity. Consequently, it became important to ensure there was internal consistency within the gravity and TEM lines, consistency between the gravity and TEM, consistency between the gravity data collected for this thesis and Dibble's (1973) gravity data, and finally consistency with the geological mapping. The data were modelled as follows (see Appendix 2 for a full description of the data processing procedures):

1. The TEM was modelled first using the limited number of boreholes as constraints. For those stations adjacent to the boreholes, the resistivities of the different layers were determined which were then used for the other stations. Along each profile, adjacent stations were checked to make sure there was lateral consistency between the layer thicknesses and resistivities. If there were differences the data were remodelled if those differences could not be accounted for by a geologically reasonable explanation:
2. The first check of the processed data gravity was to compare it to Dibble's (1973) gravity anomaly map to make sure that the anomalies observed in the data collected for this thesis correlated with those of Dibble's. There was very good agreement between both the location of the anomalies and the relative size of the anomalies, giving greater confidence in the data:

3. The thicknesses of the gravel deposits obtained from the TEM models were used as the initial constraint for the gravity modelling. All of the gravel units (Kowai Formation, glacial deposits and Lowry Peaks Range fan deposits) were modelled as a single layer as it was believed there was insufficient density contrast between them to be modelled separately. The geological mapping was used to help constrain the thickness of the cover sequence, particularly for the Mount Palm Road (MPR) profile run to the south of Isolated Hill. Once the profiles were modelled, an internal check was performed to make sure that where the transects intersected, the depths modelled were the same. If not, the data were remodelled until the depths were internally consistent, and the models were in agreement with the geological mapping:
4. Once the gravity data was modelled it was compared to the TEM models again. If there were discrepancies between the modelled thicknesses of the units, then both the TEM and gravity data were re-examined to eliminate those discrepancies.

4.2 TIME-DOMAIN ELECTROMAGNETICS

The TEM surveys had the following objectives:

I. Determine the amount of displacement across the mapped structures, described in chapters 2 and 3, which have controlled the distribution of the Late Quaternary deposits;
II. Detect any buried structures with no surface expression, that have also affected the distribution of the Late Quaternary deposits;
III. Determine the vertical and lateral extents of the different gravel formations within the basin which are potential sources of groundwater; and
IV. Map the aquifers and examine the effects of the active tectonic deformation (Chapter 3) on the aquifer architecture.

For TEM to detect a geological contact, there has to be a sufficient contrast in the electrical properties of the units above and below that contact. The electrical properties are dependent on the clay content, water content and water quality of the units (McNeill, 1990). Generally, it is expected that coarser deposits will be more electrically resistive than finer deposits, and water-saturated deposits will be less resistive than dry deposits. Unfortunately, this is further

complicated for gravels by the degree of weathering, varying clast lithology and matrix size and composition.

For the interpretation of the data, geo-electric sections were made showing the electrical structure with depth. On the geo-electric sections, a distinction has been made between contacts and boundaries. A contact is the shallowly dipping interface between two layers of differing resistivities (Figure 4.2). A boundary represents a vertical zone across which there is a change in the electrical structure. The most common cause of a boundary is faulting. Where the corresponding fault is seen on the surface it is shown on the profile as a red line. A boundary is replaced by a transition zone where either the change in the electrical structure is not as abrupt, or the data are noisy and can not be modelled adequately.

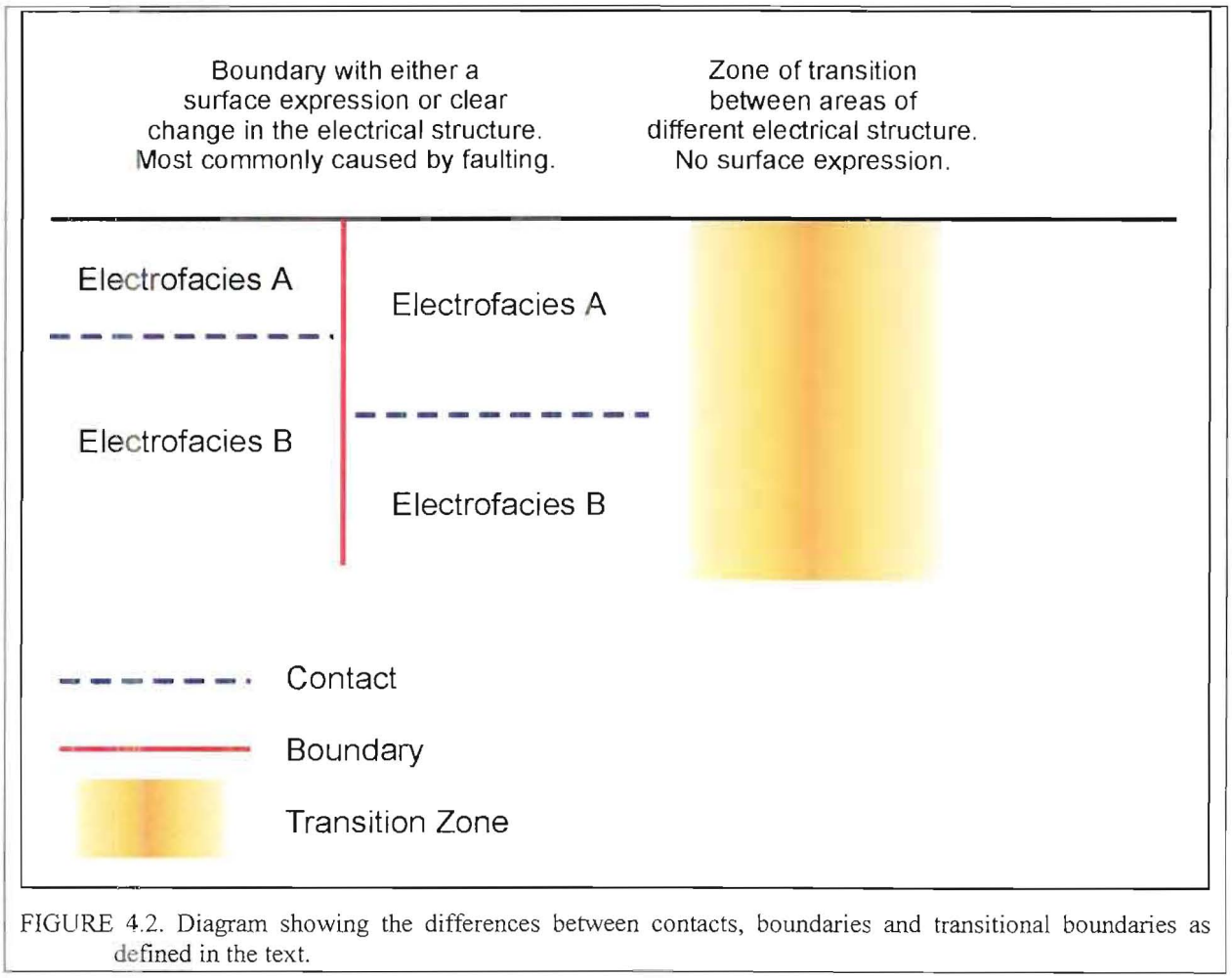

FIGURE 4.2. Diagram showing the differences between contacts, boundaries and transitional boundaries as defined in the text.

It must be stressed that an electrical contact need not be a geologic contact. There are many factors that control the electrical properties, which may or may not relate to a change in lithology. Consequently, the contacts drawn on the geo-electric sections represent a contact between two electro-facies and not lithological contacts. As will be shown, there was generally a strong correlation between the electro-facies and the major lithologies. In Chapter 5, the geology and geomorphology will be integrated with geophysics to construct geological cross sections.

4.2.1 Groundwater Investigations

TEM has been successfully used in groundwater exploration and aquifer mapping throughout many regions of the world (Fitterman et al., 1986; Fitterman, 1987; van Lissa et al., 1987; Hazell et al., 1988; McNeill, 1990; Taylor et al., 1992; Young et al., 1998). The presence of groundwater normally increases the conductivity (lowers the resistivity) of the host rock. As TEM excels at resolving conductive layers, it is, in principle, ideal for groundwater exploration. In practice, this has not proven to be the case for the North Canterbury environment. Where TEM has been used successfully for groundwater exploration overseas, the aquifers have been located within fractured bedrock and in arid areas.

It became apparent very early on in the thesis that the TEM was not going to be a useful tool for delineating the aquifers within the basin. However, it did prove very useful for delineating the major aquifer-bearing gravel deposits, such as the Burnham and Kowai formations, at depth. There are several reasons as to why the method proved unsuccessful for mapping the aquifers, not only in Culverden Basin but also in Waipara Basin to the east (Loris, 2000):

1. Within the main portion of the basin (i.e. to the west of Leonard Mound) the irrigation scheme has artificially raised the groundwater level to the very near surface. The raising of the water level has effectively removed any physical and resulting electrical contrast between the dry versus saturated gravels that the TEM would have detected,
2. On the alluvial fans along the eastern margin, due to the higher percentage of fines in the gravels, the gravels have a significantly lower resistivity than those seen to the west. Due to the lower resistivities, the contrast between the dry and saturated gravels is not enough to be detected and hence identified with the TEM,

3. By their nature, aquifers within braided river deposits and alluvial fans tend to be restricted to the old flow channels and streams. As a result they are confined to narrow, laterally restricted zones and may only be a few metres thick. Loris (2000) showed that wells only 100-200 m apart can be extracting water from different aquifers, even though they are at the same depth. As TEM is only recording data over discrete areas and volumes, it will not be able to adequately resolve the lateral and even vertical boundaries of the thin aquifers.

Due to the lack of success in mapping the aquifers, the remainder of the interpretations will focus on the stratigraphic and tectonic features of the basin.

4.2.2 Resistivity Determinations

To constrain the modelling and then relate the electro-facies to the geology, it is essential to determine the resistivities of the different subsurface units. To do this, TEM soundings were run adjacent to boreholes (Appendix 1) that clearly found either the Kowai Formation or the Mount Brown Formation. Unfortunately, there were only a few such boreholes. Two boreholes are along Lowry Peaks Road whilst the others are on the northern side of Isolated Hill. In the Lowry Peaks Road boreholes (N33/0011 and N33/0045), the Kowai Formation is found at depths of 28 m and 18 m respectively in the wells. On the northern side of Isolated Hill, wells N32/0036 and N32/0036 indicate that the Mount Brown Formation is at a depth of 3 m.

Soundings 17 and 14 (Figure 4.3) of the Lowry Peaks Road TEM transect were located adjacent to wells N33/0011 and N33/0045. Using the depth to the Kowai Formation to constrain the modelling, it was found that the overlying Burnham Formation gravels have very high resistivities (>500 ohm-m) compared to the Kowai gravels (~150 ohm-m). A low resistivity layer was found to exist beneath the Kowai Formation with a resistivity of 20-30 ohm-m, which is believed to represent the Mount Brown Formation.

On the northern side of Isolated Hill, two soundings were run to find the resistivity of the Mount Brown Formation. From boreholes (N32/0035 and N32/0036) it was known that there was only 3-4 m of Holocene river gravels overlying the Mount Brown Formation. The

equivalence models, shown in Figure 4.4, indicate that the Mount Brown Formation has a resistivity of 20-30 ohm-m, confirming the inference from the Lowry Peaks Road transect.

The resistivities found for the Late Pleistocene glacial deposits, Kowai Formation and Mount Brown Formation are valid for those stations that are located on the glacial outwash surfaces. On the alluvial fans along the eastern margin, the influence of the clay and silt within the gravels has lowered the resistivities making it impossible to correlate the electro-facies with the lithologies. There are also no good deep boreholes to use for constraining the TEM modelling.

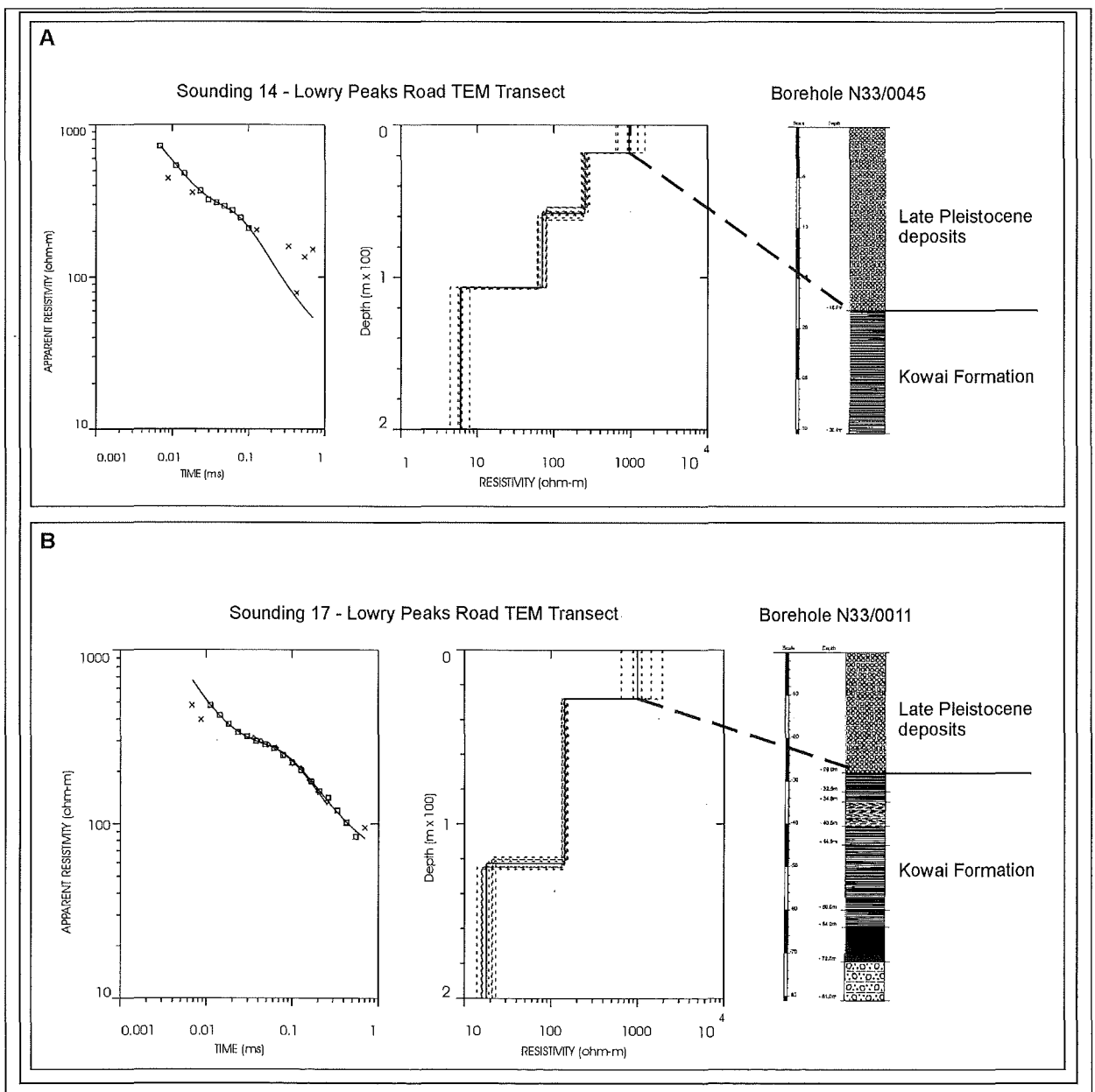

FIGURE 4.3. Well logs and corresponding TEM models for boreholes N33/0011 and N33/0045.

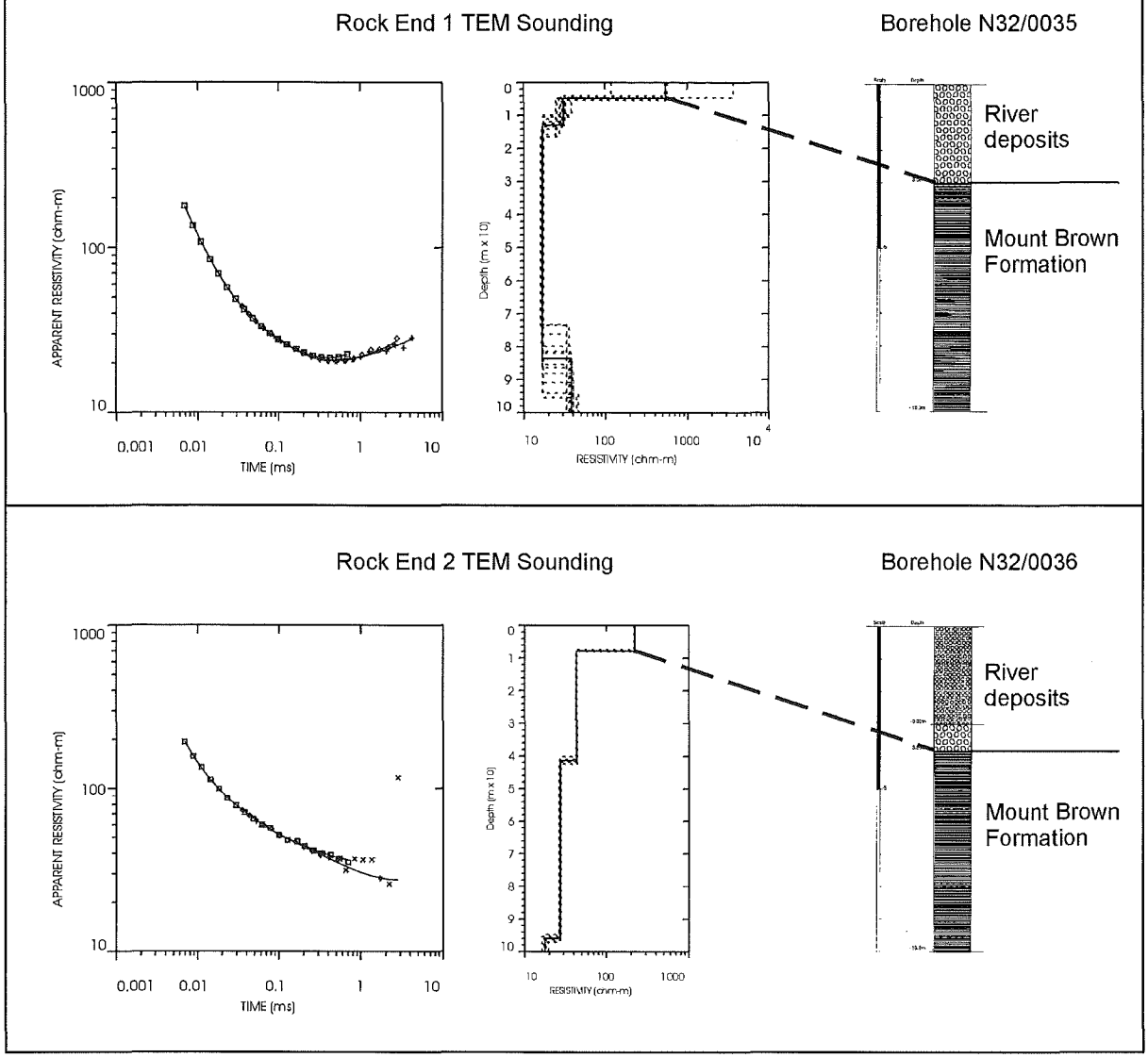

FIGURE 4.4. Well logs and corresponding TEM models for boreholes N32/0035 and N32/0036.

4.2.3 Basin Transects

Four transects were run across the basin and will be discussed in order from north to south. As has been mentioned, geo-electric sections were made to examine the subsurface electrical structure. However, it was often more useful to look at the change in the shape of the apparent resistivity curves as an indicator of a change in the subsurface electrical properties. The shape of the apparent resistivity curve is indicative of the electrical structure. Hence a sudden change in the curves, indicates an abrupt change in the subsurface. Likewise, poor data quality, in the absence of cultural interference (e.g. powerlines, electric fences, machinery etc) may also be indicative of rapid lateral changes in the resistivity, most commonly caused by faulting.

4.2.3.1 Mount Palm Road Transect

The Mount Palm Road transect (Figure 4.5) runs NE adjacent to Mount Palm Road from Leonard Mound to the Waiau River. Unfortunately, due to the nature of the topography on Leonard Mound it was not possible to start the profile to the east of the Leonard Mound Fault. However, some interesting features related to the Leonard Mound Fault System were still identifiable which can also be seen on the shorter Mount Palm lines to the north.

The only fault that crosses the transect, with a surface expression, is the Boundary Fault (Figure 4.5). At the location of the fault, there is an abrupt change in the electrical structure. On the eastern, or upthrown side of the fault, the Mount Brown Formation is observed, both in the TEM and borehole N32/0171, to come within 12 m of the surface. On the western side, the Mount Brown is at a depth of 110-120 m. Another abrupt change in the electrical structure is observed to the east of the Boundary Fault, and may well reflect another imbricate fault of the Leonard Mound complex.

To the west of the Boundary Fault the apparent resistivity curves for soundings 4 to 8 all have a very similar shape. When modelled, a 110-120 m thick layer, with a resistivity of approximately 300 ohm-m, overlies the Mount Brown Formation. The resistivity was intermediary between that for the Kowai Gravels and the Burnham Formation, raising uncertainty as to the lithology governing the electrical response. Care must be taken though, as a change in the electrical resistivity does not necessarily correspond to a lithological change. However, the difference in the electrical resistivities between the Burnham and Kowai formations versus the undifferentiated gravels are large enough, that a lithological change is considered the most likely reason for the change. On saying that, in the Mount Palm Road TEM transect, these deposits are found where Burnham Formation is known to exist on the surface, from the geological and geomorphological mapping, which is not indicated on the transect. This raises the possibility that the layer represents both the Burnham and Kowai formations, and that the modelling was unable to distinguish the two formations due to the data being noisy. In the Palmside Road transect, the layer is present, along with the Kowai and Burnham formations, suggesting that it is a separate layer. It is believed that another gravel deposit does exist giving rise to the modelled layer, but that noisy data in the Mount Palm Road transect precludes the distinction of the different layers. The origin of the 300 ohm-m layer is uncertain, and for the purposes of these discussions has been labeled as

undifferentiated deposits. The origin of the layer will be discussed further in Chapter 5. The very low resistivities modelled in the lowest layers of the transect, are probably down in the noise range of the equipment and must be treated with scepticism, if not discarded.

In contrast, from sounding 9 onwards, although the quality of the data is good, interpretation of the results is more difficult. A number of thin electro-facies are required for the calculated response to fit the measured response. At the present the origin of these thin layers is unclear. The layers could either be related to the thin Tertiary units (Isolated Hill Limestone, Cookson Volcanics etc) seen on Isolated Hill or thin gravel layers. The layers all appear to dip in the opposite direction of the underlying low resistivity (~25 ohm-m) layer suggesting that they may be the Late Pleistocene gravels deposited after the formation of Isolated Hill.

Between soundings 13 and 14 and also between soundings 15 and 16, boundaries in the electrical structure are evident. The especially noisy data in sounding 15 are believed to be indicative of the Isolated Hill Fault which, from mapping, is expected to project through this section of the profile. Stations 18 to 21 are all affected by anthropogenic noise from Rotherham. However soundings 21 and 22 indicate, through the relatively high resistivities, that there may be approximately 150 m of Late Pleistocene gravels overlying the Kowai Formation.

4.2.3.2 Palmside Road Transect

The data collected along Palmside Road (Figure 4.6) turned out to be the best collected within the basin. As shown in Chapter 3, during the Late Pleistocene there were two major depositional settings within the basin. The Palmside Road transect can be broadly divided into two regions separated by Leonard Mound. To the east of Leonard Mound, there are the large alluvial fans from the Lowry Peaks Range, and to the west the floor of the basin is covered by the Burnham Formation. This change is reflected in the resistivities. The alluvial fans have a higher percentage of clay and silt and therefore have lower resistivities than the sandy gravels on the basin floor.

MOUNT PALM ROAD TEM TRANSECT

APPARENT RESISTIVITY CURVES

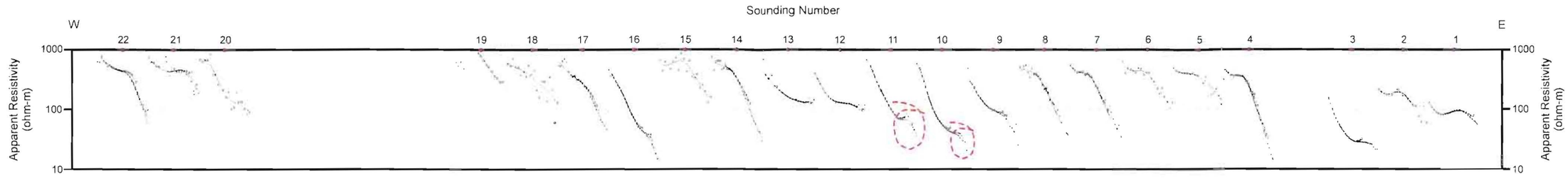

GEO-ELECTRIC SECTION

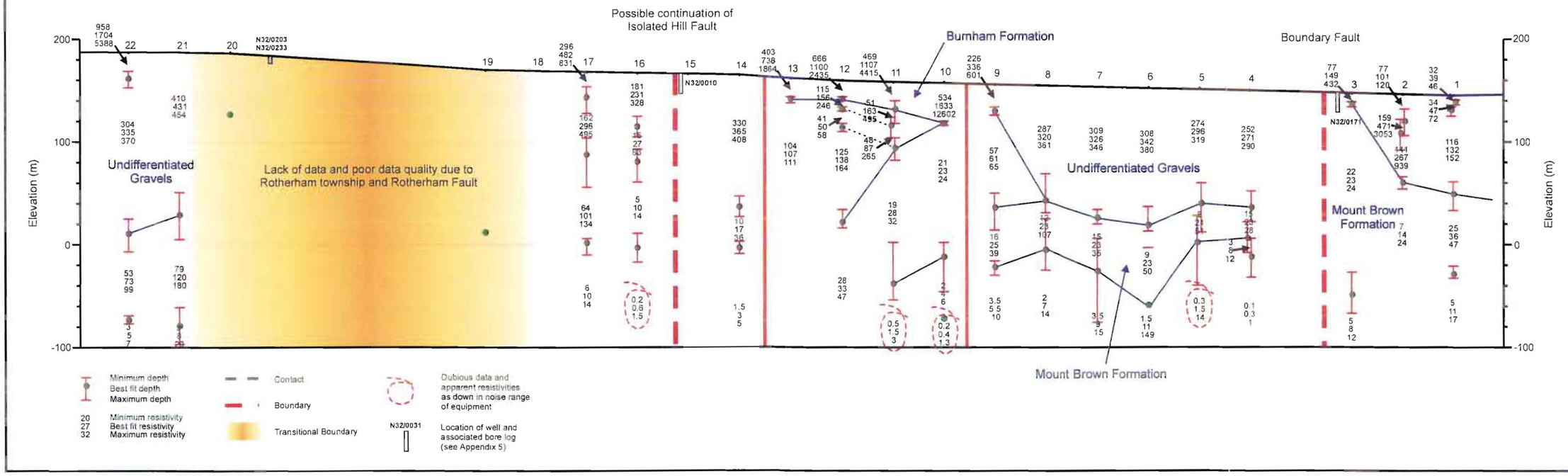

FIGURE 4.5. Mount Palm Road TEM transect.

PALMSIDE ROAD TEM TRANSECT

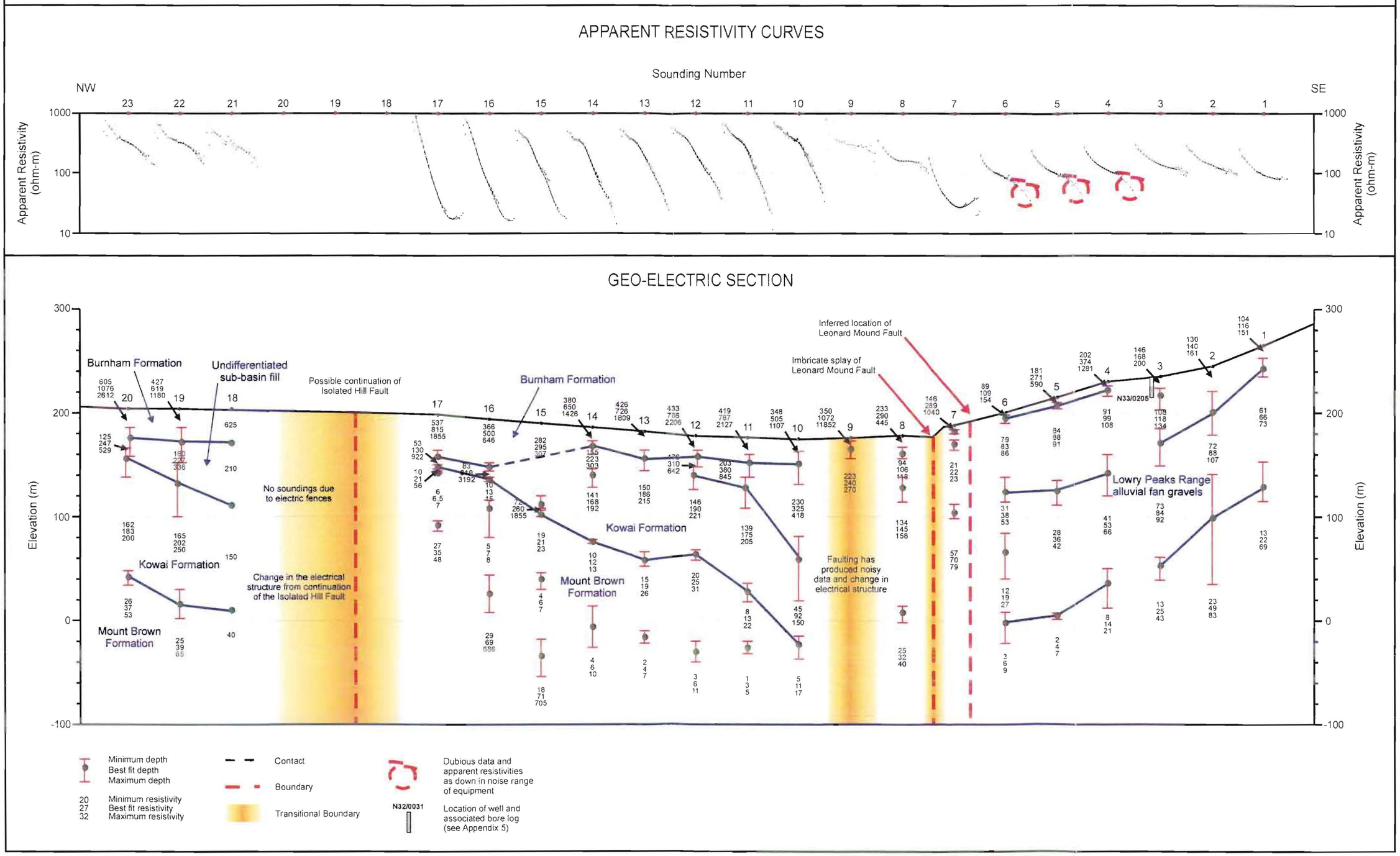

FIGURE 4.6. Palmside Road TEM transect

Structurally, between the LPFS and the LMFS it is expected that the Tertiary to Pleistocene deposits will be folded into a syncline as a result of the Lowry Peaks Fault. To the west of Leonard Mound it was expected that a syncline has developed on the downthrown side of the Leonard Mound Fault and from there westward the units would gently rise as the basin shallows.

Starting with section of the transect to the west of Leonard Mound, it can be seen that the units do in fact dip eastward as expected, however, the folding and thinning of the strata observed in soundings 16 and 17 was unexpected. Unfortunately, data were not collected between sounding 17 and sounding 18 due to electric fences, which the farmers were not prepared to turn off. In the region between soundings 17 and 18, a fault was also inferred from the gravity data, and is believed to be the continuation of the Isolated Hill Fault, mapped to the north on Isolated Hill. As with the Mount Palm Road transect, the top of the Mount Brown is readily identifiable by an abrupt decrease in the resistivity.

To the east of Leonard Mound, the shape of the apparent resistivity curves indicate that the resistivity does not vary substantially with depth. The curves show a slow decrease in the apparent resistivity with time compared with the rapid decrease seen in soundings 10 to 17. In contrast with the soundings to the west, where the Mount Brown Formation stood out clearly, there is not a strong contrast between the gravels and the Mount Brown Formation. Consequently, the electro-facies can not be related to the geological units. A subtle change is observed in the modelled resistivities between soundings 3 and 4. It is believed that this difference arises from the modelling differences at the tail of the apparent resistivity curves (as circled).

4.2.3.3 Lowry Peaks Road Transect

Compared to the majority of TEM soundings recorded in Culverden Basin, the soundings along Lowry Peaks Road (Figure 4.7) were of much poorer quality, especially in the area to the south of Leonard Mound. The quality of the data restricted interpretations regarding the thicknesses of the various units and displacement across the tectonic features, however, other conclusions can be drawn as to why the data quality is poor.

LOWRY PEAKS ROAD TEM TRANSECT

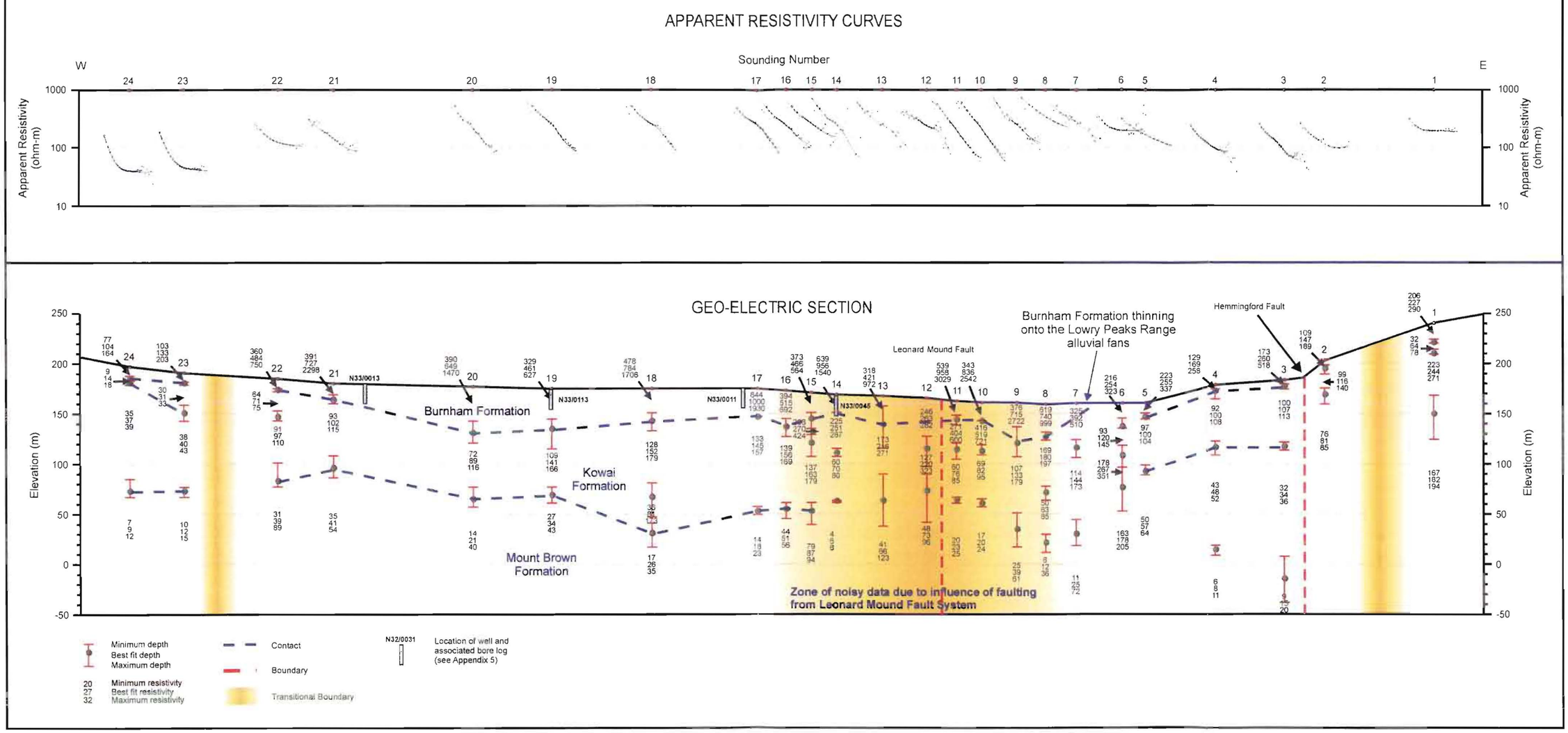

FIGURE 4.7. Lowry Peaks Road TEM transect

From the geomorphic mapping, the Leonard Mound Fault System can be seen to extend across Lowry Peaks Road as a series of leading edge folds. The deformation associated with the folding will produce significant lateral variation in the resistivities leading to a reduction in the data quality. From the data it appears that the zone of deformation associated with the Leonard Mound Fault System is approximately 3 km wide between soundings 7 and 15.

To the west of sounding 15 the quality of the data improves and shows layers dipping gently to the east. Likewise, to the east of sounding 7, the data are again of better quality, but interpretation of the electrical structure is still difficult. Between soundings 3 and 5, the electrical structure is consistent. The Hemmingford Fault cuts between soundings 2 and 3; sounding 2 is on the relatively upthrown side. The quality of the data is not as good in sounding 2, indicating that the faulting could be producing lateral resistivity variations at depth, which is expected across a fault. Despite that, there still appears to be a change in the electrical structure across the fault. Sounding 1 shows that the resistivity varies little with depth suggesting that there is a thick succession of gravels.

4.2.3.4 Pahau Reserve Road Transect

The final transect is situated to the south of the Pahau River and runs along Pahau Reserve Road and Long Plantation Road (Figure 4.8). This transect was run as part of a fourth year geophysics field exercise. After examination of the data, it was decided that further stations would not be of benefit, hence only eight soundings were performed. Dairying was established in this part of the basin first, therefore there is a lot of noise from electric fences and other cultural sources, which played havoc with the data. Unlike the transects to the north where the noisy data was used to infer the presence of buried structures, this is not the case for this transect. From Dibble's (1973) gravity data, it appeared that this section of the basin was relatively undeformed in comparison to the northern end of the basin. It was also believed to be one of the deepest parts of the basin.

Soundings 1-5 all display a very similar electrical structure. The relatively slowly decaying apparent resistivity curves indicate that the resistivities remain relatively high with depth, and that there is not a low resistivity layer within the depth range of the equipment. A small change is observed between soundings 5 and 6 that is due to improvement in the data quality.

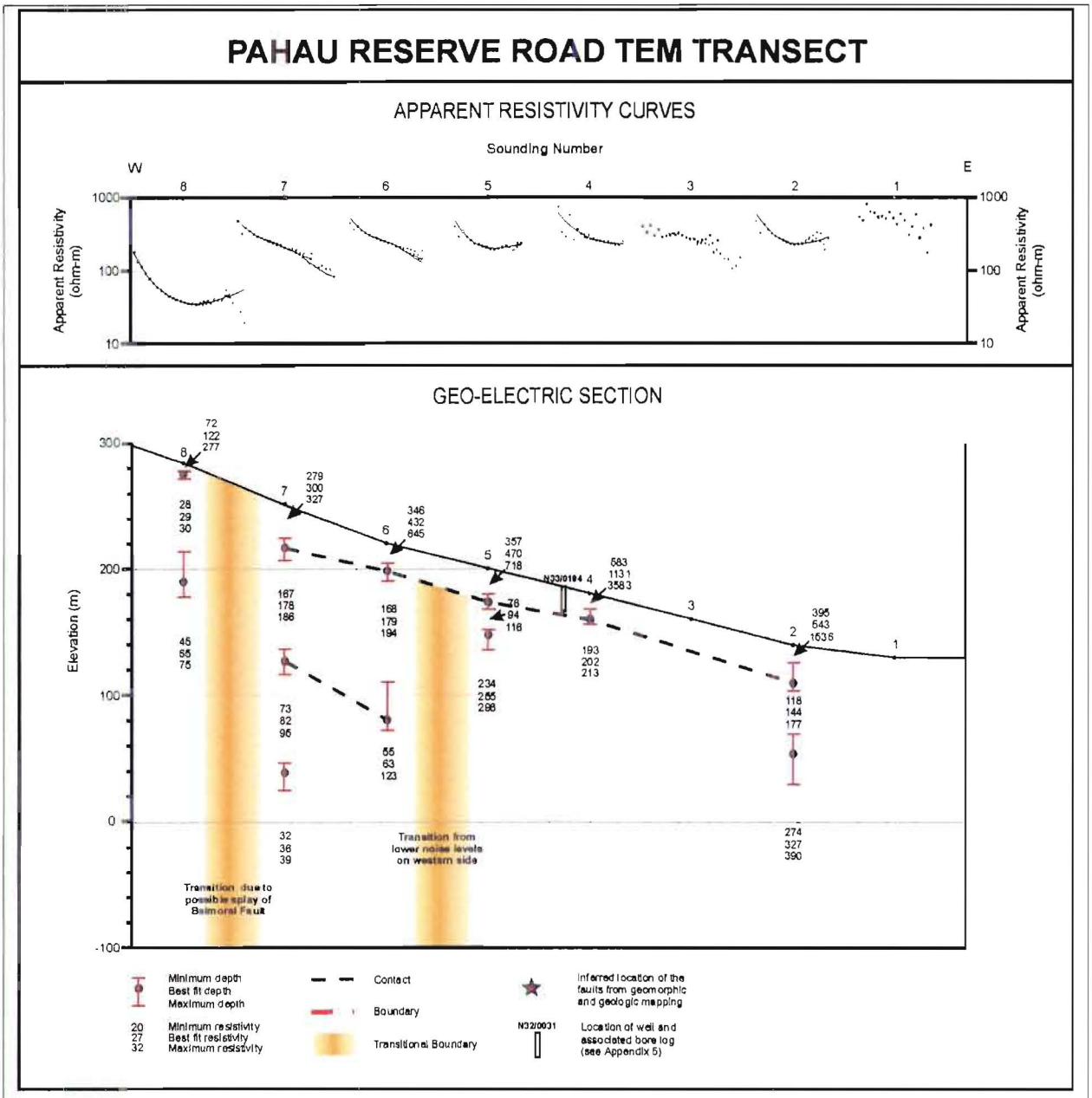

FIGURE 4.8. Pahau Reserve Road gravity transect.

Between soundings 7 and 8, there is a change in the electrical structure. In sounding 8, low resistivity layers are found within 20 m of the surface. Immediately to the west, the Balmoral Fault has uplifted the eastern edge of Green Hill, exposing the Waikari Formation. The Waikari Formation has very similar geologic characteristics to the Mount Brown Formation. Hence, its resistivity should also be similar. It is inferred on the TEM transect that the low resistivity layers correspond to the Waikari Formation, and that there is another fault between soundings 7 and 8 which has uplifted it from an altitude of 210 m in sounding 7 to the near surface in sounding 8. This fault is probably a splay of the Balmoral Fault.

4.2.4 Short Lines

In conjunction with the basin transects, short lines and clusters of soundings were located at various locations to study the stratigraphy and deformation at sites of interest.

4.2.4.1 Rock End Soundings

Nine soundings (Figure 4.9) were recorded at Rock End on the northern side of Isolated Hill. The soundings were performed to (a) determine the resistivity of the Mount Brown Formation, and (b) examine the faulting observed to Isolated Hill. The results of (a) were shown earlier, and show that the Mount Brown Formation has a resistivity of 20-30 ohm-m compared with over 100 ohm-m for the river gravels. The resistivity of the Tertiary strata does vary amongst the nine soundings, which will be caused by weathering and lithological changes. On Isolated Hill, the composition of the Mount Brown Formation varies from siltstone to limestone. The faulting observed has clearly disrupted the stratigraphy so that the lithologies change over short distances. It is interesting to note that the faulting has not affected the quality of the data as it has along the basin transects. This suggests that the faulting is juxtaposing units of very similar resistivities, which in turn indicates that the Mount Brown Formation maybe in excess of 200 m thick in this region.

4.2.4.2 Cranford Downs Lines

The Cranford Downs lines are located on the southern side of Isolated Hill.

Line 1

The apparent resistivity curves all display a very similar appearance, and indicate that the resistivity is decreasing with depth. In soundings 1-3 (Figure 4.10), a near-surface relatively high-resistivity layer overlies layers of moderate to low resistivities. It is inferred from the mapping on Isolated Hill that the moderate to low resistivities correspond to the Torlesse basement. The resistivity of those layers decreases towards the east, and is believed to be reflecting the weathering of the Torlesse underlying the Tertiary succession.

ROCK END TEM SOUNDINGS

Sounding 1

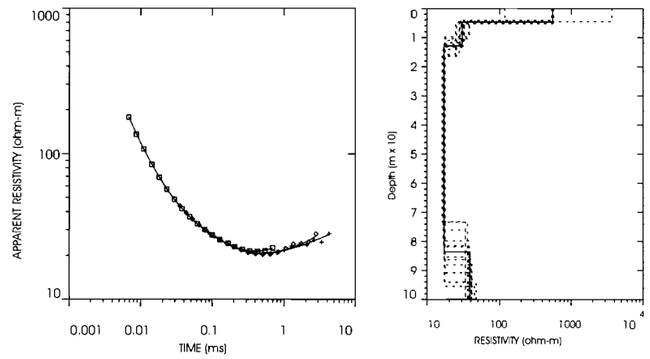

Sounding 2

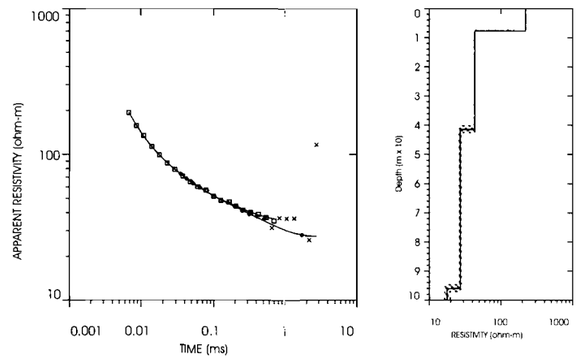

Sounding 3

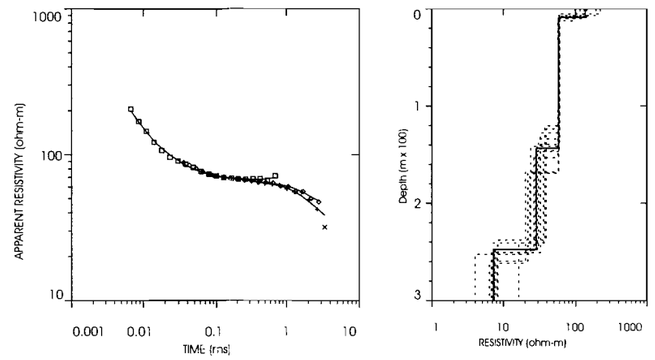

Sounding 4

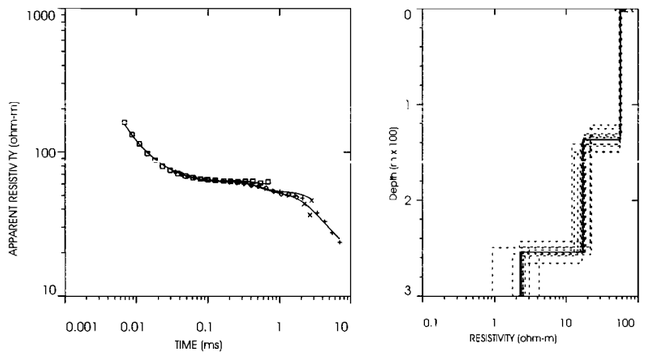

Sounding 5

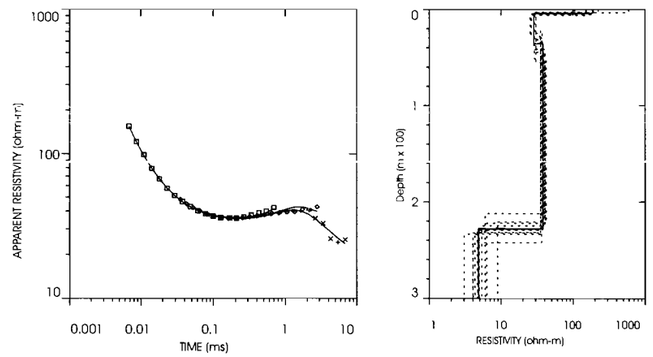

Sounding 9

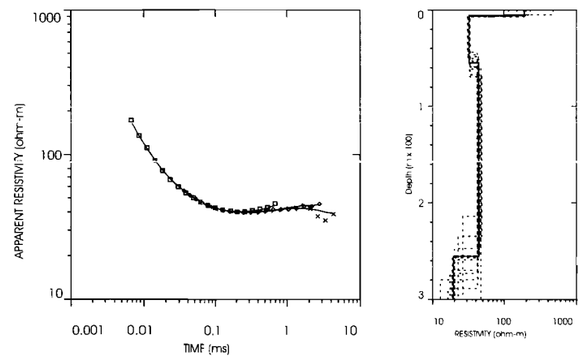

Sounding 6

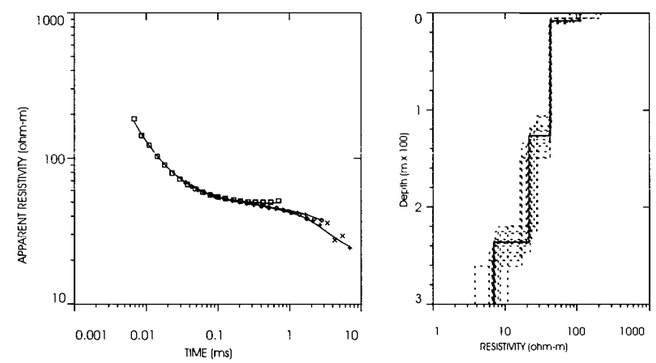

Sounding 7

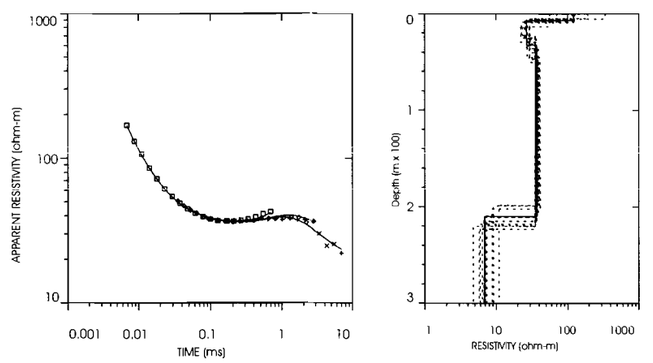

Sounding 8

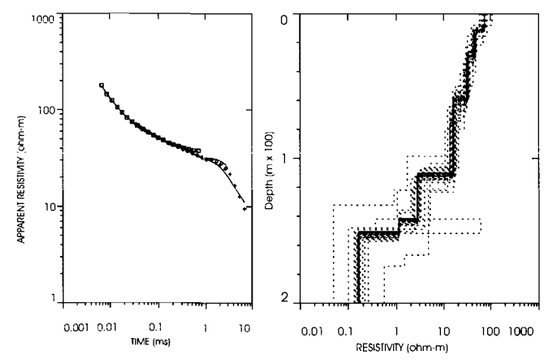

FIGURE 4.8. Rock End TEM soundings.

Sounding 4 displays a slight change in form, correlating with a low resistivity layer overlying a layer with a resistivity similar to those found in the first three soundings. From station 5 onwards, only the low resistivity layers are observed, corresponding with the Tertiary succession observed on Isolated Hill. From the geological mapping, the contact between the Torlesse and the Tertiary sequence occurs between soundings 3 and 4. Hence, it is believed that sounding 4 has detected the contact between the Tertiary and basement, and is able to resolve the contact as it is dipping at a relatively shallow angle of 20-25°. If the contact had been steeply dipping then the TEM would likely not have been able to resolve it.

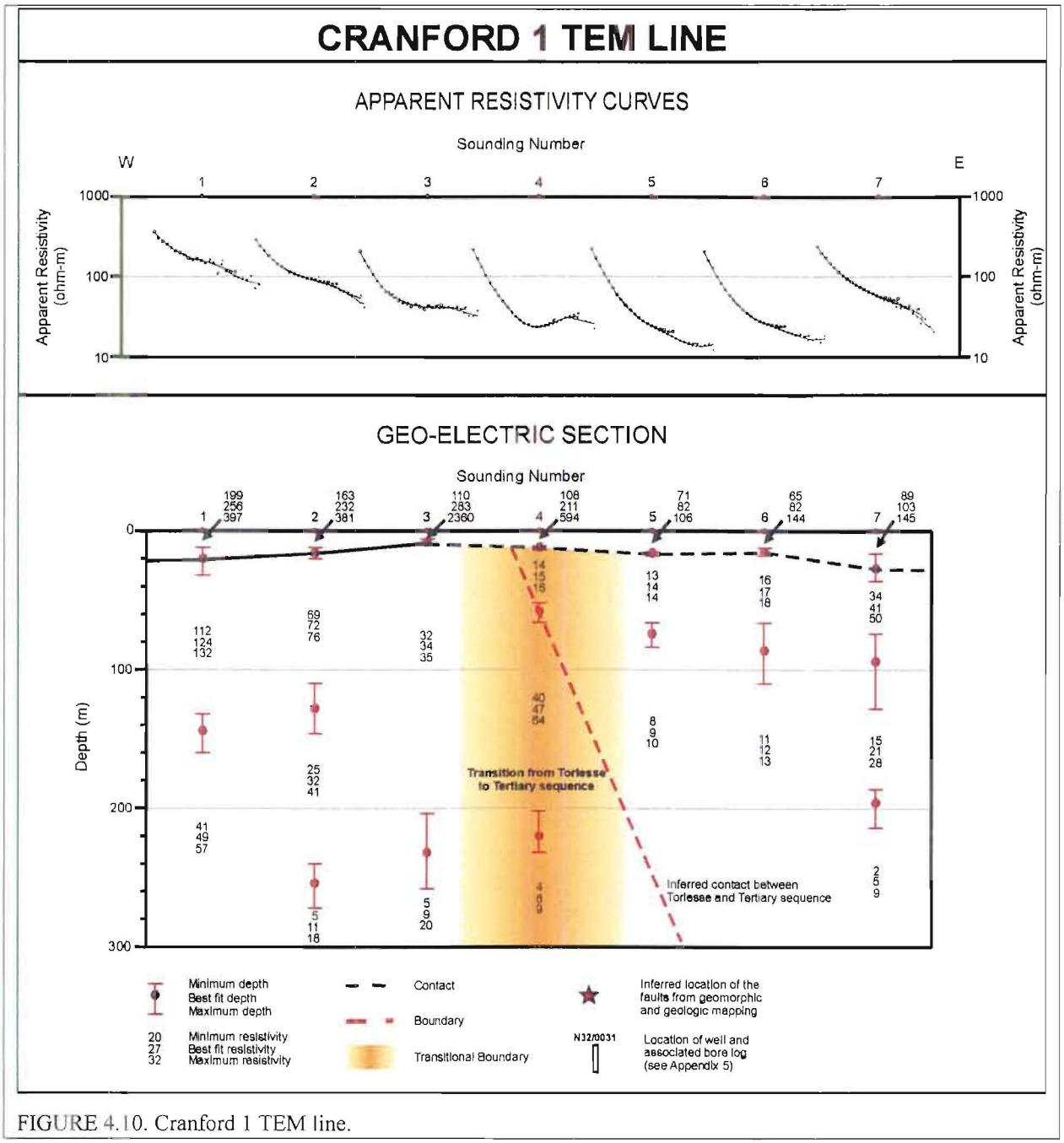

FIGURE 4.10. Cranford 1 TEM line.

Line 2

Line 2 was run with the aim of determining whether or not the Isolated Hill Fold continues under the basin floor, and if so, is it plunging to the south. The geo-electrical structure (Figure 4.11) indicates that the Tertiary strata overlying the Torlesse dips southwards at approximately 25° suggestive of a plunging fold. As with Cranford line 1 it is apparent that the resistivity of the Torlesse changes quite markedly both vertically and laterally.

4.2.4.3 Delamere Downs Soundings

Three soundings were run next to boreholes N32/0037 and N32/0038 on the southern side of Isolated Hill (Figure 4.12). The boreholes showed there to be 6-8 m of the Late Pleistocene glacial deposits overlying a cemented gravel which in turn overlies blue clay. In borehole N32/0037, the Late Pleistocene deposits are a brown silty clay compared with gravel in N32/0038. This change is reflected in the lower resistivities recorded in soundings 2 and 3 which were close to N32/0037. From the bore logs and TEM results, it is difficult to deduce whether the cemented gravels and clay are part of the Mount Brown Formation observed on Isolated Hill to the north, the Kowai Formation or a pre-Burnham Formation glacial deposit. The 18-21 ohm-m layer observed in sounding 1 suggests that they may be part of the Mount Brown Formation.

4.2.4.4 Mount Palm Lines

The purpose of these lines was to try to deduce the vertical displacement on the Leonard Mound Fault and to see whether or not other splays of both the LMFS and LPFS exist under the Late Pleistocene to Holocene fans. As shown in Chapter 2, only one trace can be mapped for the Leonard Mound Fault in this region, but another fault, the Boundary Fault, exists 2 km to the west which is inferred to mark the boundary between the deformed SE margin and relatively undeformed central basin. Lines 1 and 3 both start to the east of the mapped position of the Leonard Mound Fault and extend some distance to the NW. Unfortunately due to the dissected nature of the uplifted deposits, no station was possible to the east of the fault for line 2.

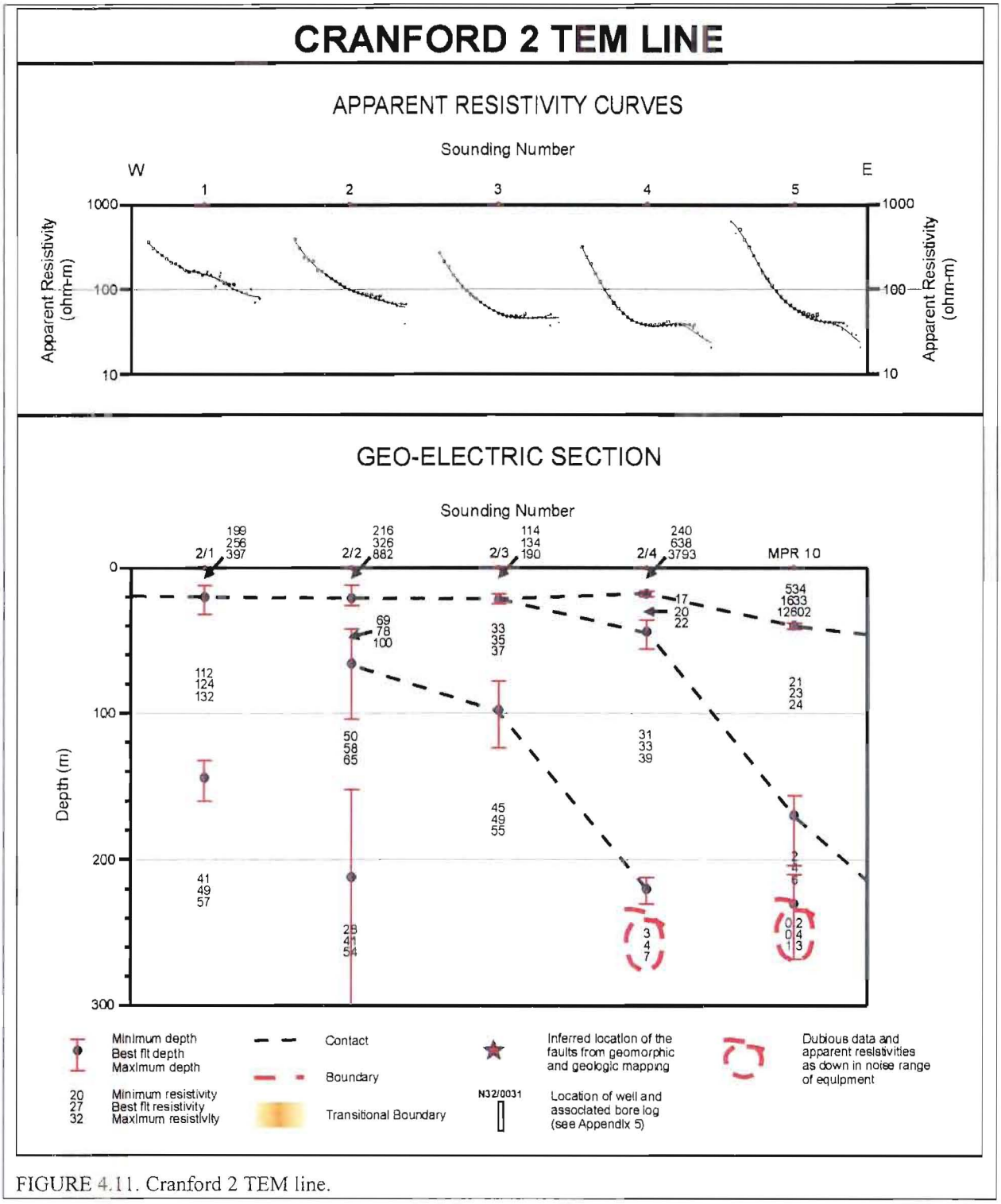

FIGURE 4.11. Cranford 2 TEM line.

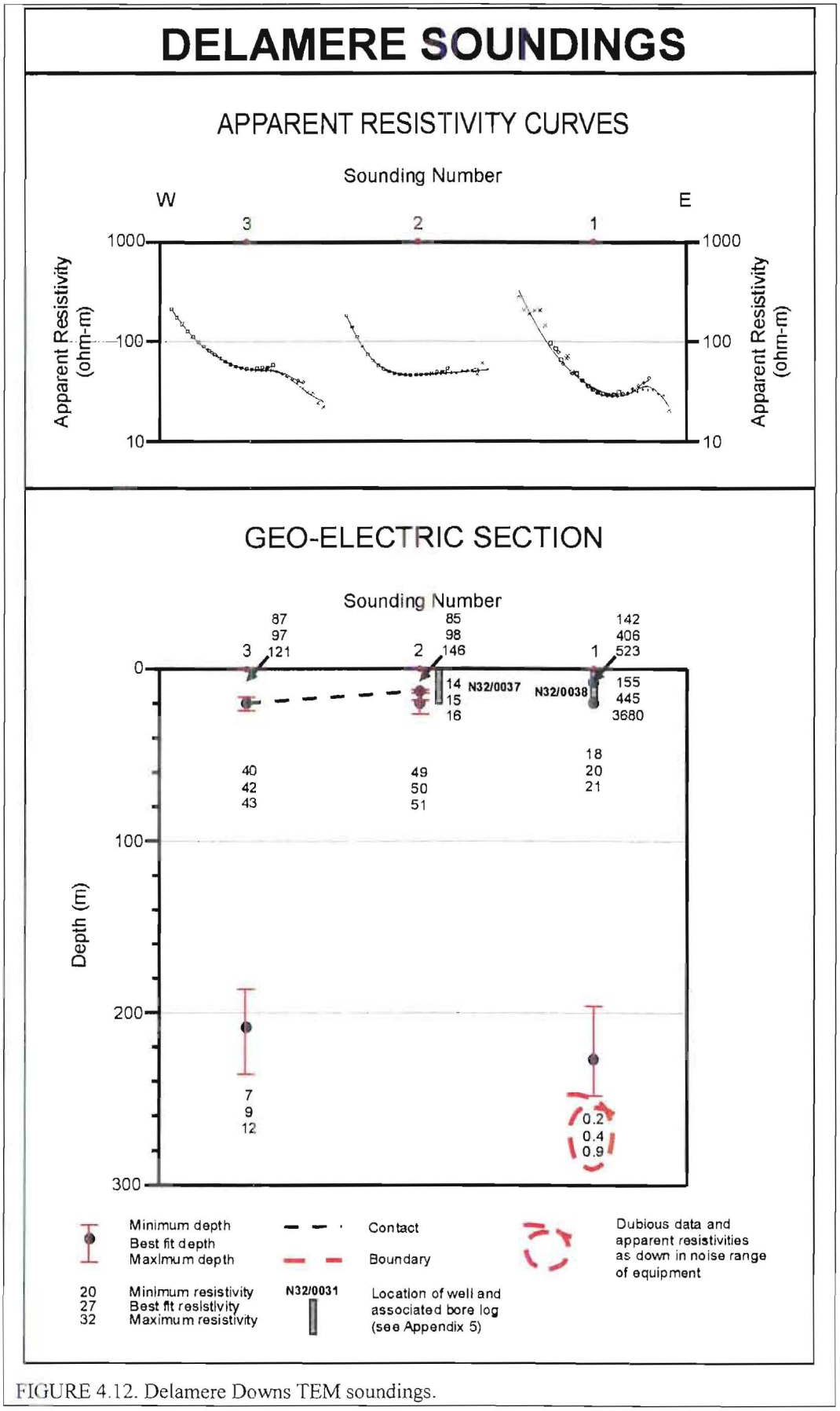

FIGURE 4.12. Delamere Downs TEM soundings.

In the three lines (Figures 4.13, 4.14 and 4.15), there are distinct electro-facies that relate to the major lithological units. The upper layer has a resistivity in excess of 100 ohm-m. The resistivity for that layer matches well with those soundings performed on the large Lowry Peaks fans to the south on Palmside Road and Lowry Peaks Road. Clearly all the fans have a significantly higher fines percentage than the glacial deposits to the west. Consequently, the fan deposits have significantly lower resistivities than the glacial deposits. That upper layer is only 30-40 m thick and in places overlies a layer with a higher resistivity, and in other places overlies layers with significantly lower resistivities. Based on the resistivities, it is inferred that the higher resistivities correspond to another gravel package, possibly the Kowai Formation, whilst the lower resistivities are the Tertiary sequence.

4.2.4.5 The Willows Soundings

The Willows soundings (Figure 4.16) were located on either side of Leonard Mound. Across the mound, there is an obvious change in the electrical structure and in the quality of the data. The soundings collected on the eastern side of the mound are of better quality than those to the west. Whether the difference in the noise level is resulting from geological or cultural sources is unclear. To the west of Leonard Mound there is extensive dairying with associated electric fences, whereas to the east dairying has not begun as the irrigation scheme does not extend into that portion of the basin. Geologically, imbricate splays of the Leonard Mound Fault are known to exist, and from the gravity surveys there appears to be another significant fault a short distance to the west of Leonard Mound. Therefore it is feasible that there is a highly disrupted zone to the west of the Leonard Mound Fault that is giving rise to the poorer data quality.

4.2.4.6 Southern Leonard Mound

Four soundings were performed across the southern end of Leonard Mound (Figure 4.17). Soundings 1 and 2 were to the east of the Leonard Mound Fault and soundings 3 and 4 were to the west. Sounding 3 was located between the Leonard Mound Fault and an imbricate splay against which the ponds have formed.

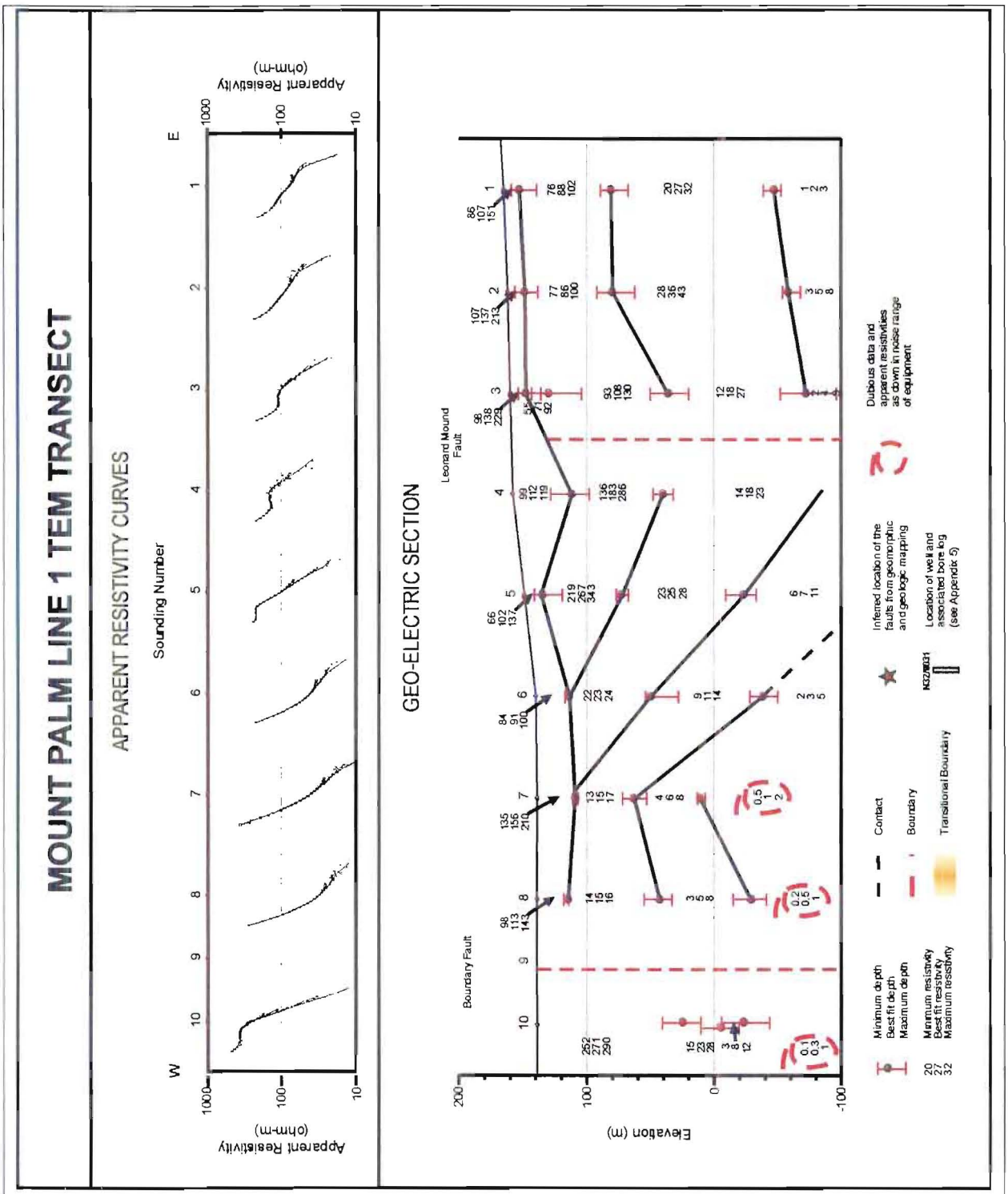

FIGURE 4.13. Mount Palm Line 1 TEM transect.

Sounding 3 has a completely different electrical structure to the other 3 soundings. The near surface layer is still the same, but the underlying layer differs markedly from the other soundings. In soundings 1 and 4, the second layer still has a high resistivity indicative of relatively clean sandy gravels. In contrast, sounding 3 has a low resistivity layer underlying

the upper layer before passing into a layer with a high resistivity. The origin of the low resistivity layer is uncertain but is almost certainly resulting from the imbricate thrust observed to the west. The thrusting may well have uplifted the Tertiary sequence to the near surface, or it has produced a disrupted zone that may have a higher water and clay content giving rise to the lower resistivities.

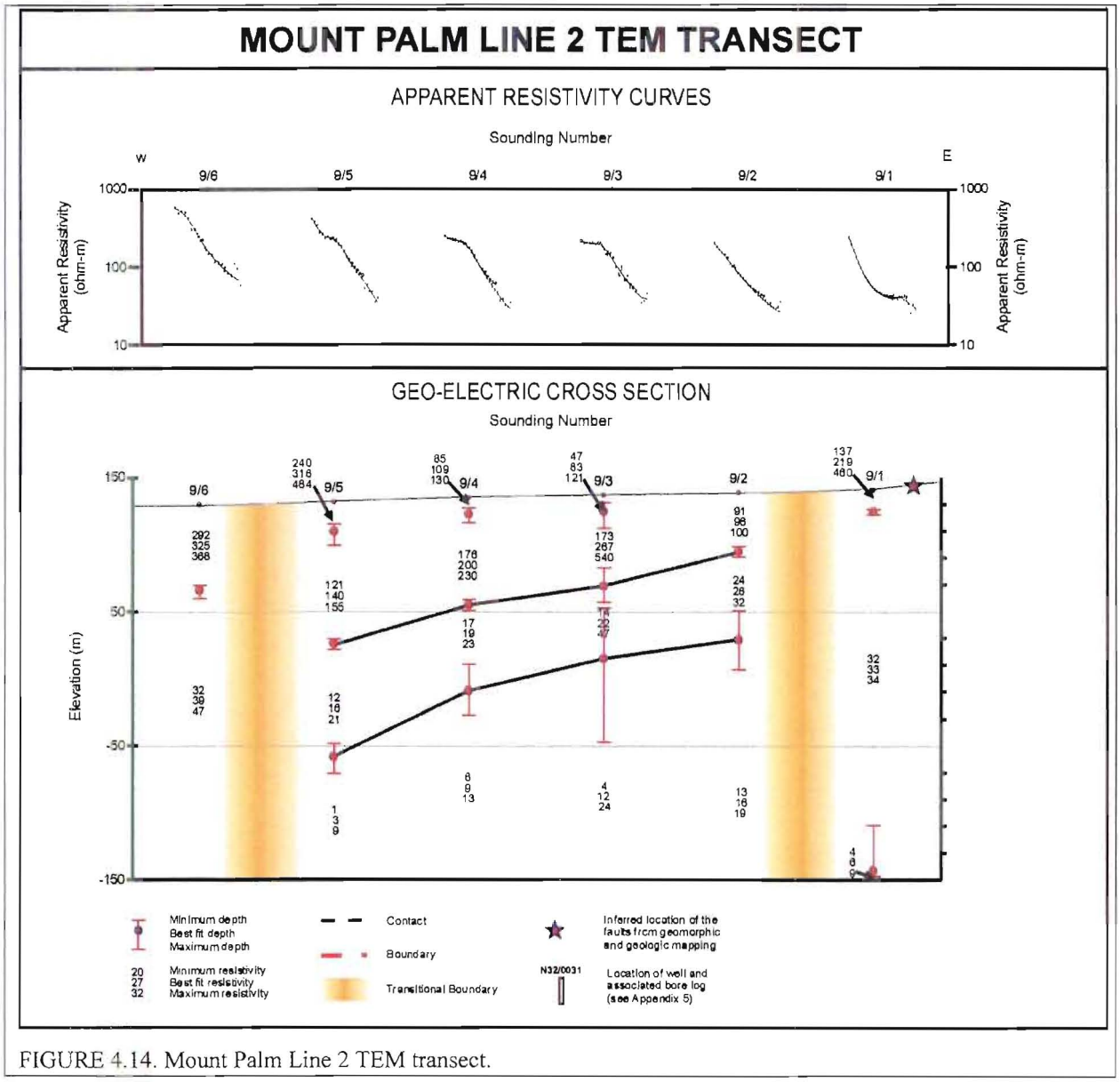

FIGURE 4.14. Mount Palm Line 2 TEM transect.

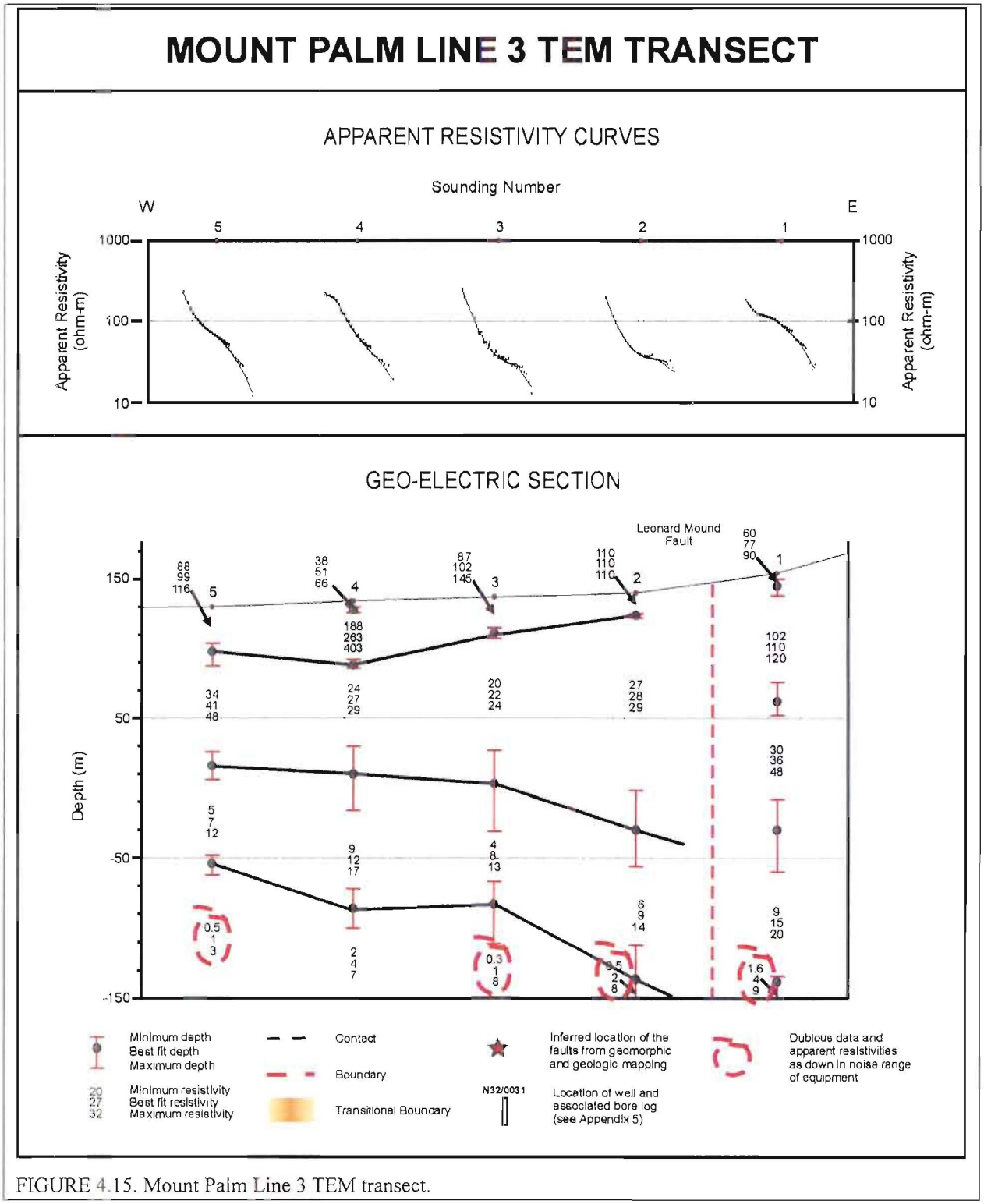

FIGURE 4.15. Mount Palm Line 3 TEM transect.

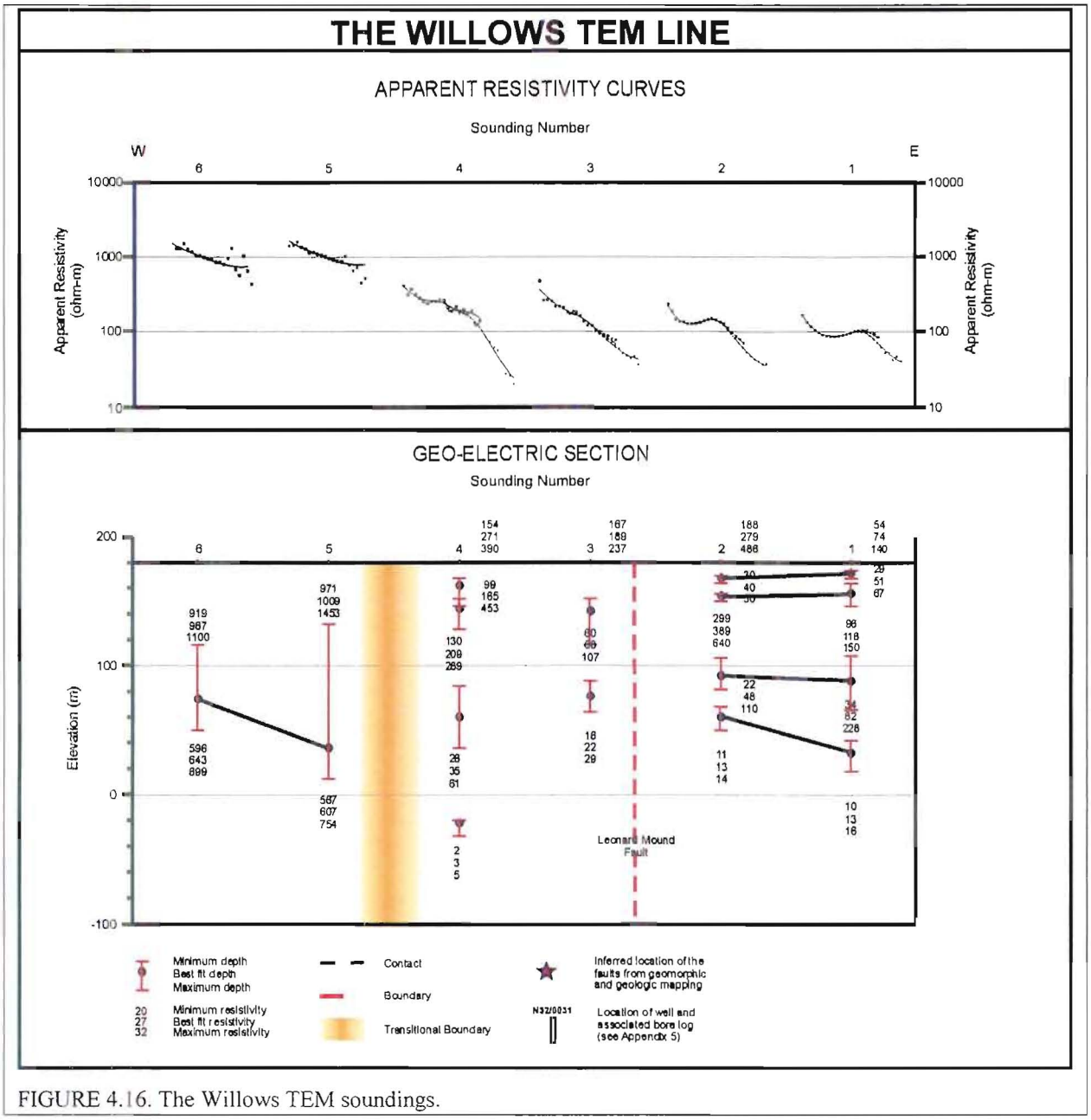

FIGURE 4.16. The Willows TEM soundings.

4.2.5 Summary

The TEM proved successful at delineating the lateral and vertical extents of the major aquifer-bearing gravel units within the basin, however, it was not successful at mapping the individual aquifers within those units, as discussed earlier. From the TEM models three aquifer-bearing units were delineated on the basis of their resistivities: Burnham Formation, Kowai Formation and undifferentiated sub-basin fill. The resistivities of the units primarily reflect changes in the composition of the gravels and the degree of weathering. The Burnham Formation is a clean, sandy gravel, with a correspondingly high resistivity. In contrast, the other units are

generally silty, weathered gravels, which consequently have a significantly lower resistivity than the Burnham Formation.

The Burnham Formation appears to form a veneer of uniform thickness (approximately 30 m) across the floor of the basin, to the west of Leonard Mound. As will be shown in Chapter 5, this is important in the hydrogeological model, as the Burnham Formation provides a conduit of recharge for the deeper aquifers. In contrast, the location and thickness of the other units vary substantially reflecting the structural control on their distribution, related to the partitioning of Culverden Basin into three distinct sub-basins.

4.3 GRAVITY

Although it was never intended to run a gravity survey at the onset of this thesis, when the chance arose to borrow the Otago University gravity meter a survey was run to examine the broad scale deformation occurring within the basin. The basin appears to be relatively simple due to the veneer of Late Pleistocene glacial outwash gravels covering the floor of the basin. However, a few inliers of Tertiary strata within the gravels suggest that the Tertiary succession may be substantially more deformed than first appearances would indicate.

As with the TEM, there was very little subsurface information about the thicknesses of the different geologic units to help constrain the modelling. This problem was further hindered by the lack of good density data on the units, especially for the gravels whose densities can vary substantially depending on the composition, percentage of fines, porosity, water content and weathering. Constraints for the modelling were from three sources. The first constraint was from the geologic mapping around the margins of the basin, which provided an estimate of the thickness of the various geologic units present. The second was the TEM, which provided the depth to the top of the Mount Brown Formation at various locations. Thirdly, checking for consistency in the thickness of the layers and general shape of the basin between profiles, especially where profiles crossed, provided an internal control for the modelling. It is stressed that, even though there are these constraints, without more control on the thickness of the cover sequence, there is still a large degree of uncertainty in the modelling. However, the models depict the gross basin structure and have located additional structures, which were not known to exist, but which are significant for the tectonic interpretations and the deeper

groundwater regime. If more subsurface information becomes available at a future date through boreholes or additional geophysical work, the gravity data can be remodeled incorporating that information.

Three layers (basement, cover and gravels) were used in the modelling. The lower layer is the Torlesse basement with typical crustal density of 2670 kg/m^3. The middle (cover) layer consists of the Late Cretaceous to Late Miocene formations from the basement to the top of the Mount Brown Formation. The upper (gravels) layer is composed of the Pliocene and Pleistocene gravels of the Kowai Formation, glacial outwash surfaces and eastern range-front fans. Densities of 2000 kg/m^3 and 2400 kg/m^3 respectively, were chosen for the gravel and cover layers based on density tables in various geophysical text books (e.g. Parasnis, 1986; Telford et al., 1976; Milsom, 1989), the densities of a wide range of New Zealand rock types (Whiteford and Lumb, 1975) and a recent gravity survey in the Waipara Basin to the east (Loris, 2000).

The cross-basin profiles will be discussed in order from north to south followed by the north-south running profiles that all tie the profiles together.

4.3.1 Morses Road

Located on Emu Plains, Morses Road runs from the Waiau River into the Amuri Range. A borehole to the south indicates that there is 90 m of Late Pleistocene gravels overlying the Torlesse basement with only a few metres of the Tertiary succession present. Mapping of the Amuri Range shows that more of the Tertiary succession should be present along Morses Road than at the borehole, however, the overall depth to the Torlesse should be similar along the strike of the units.

A thickness of 80-90 m for the gravels/Tertiary succession was obtained from the modelling (Figure 4.18), in agreement with the borehole information. Varying the density of the upper layer between 1800-2200kg/m^3 had very little effect on the model. The Morses Road profile helped constrain a density for the gravels of 2000kg/m^3 as was used for the other models. As expected the depth to the basement increases from NW to SE as you move down the flank of the Amuri Range.

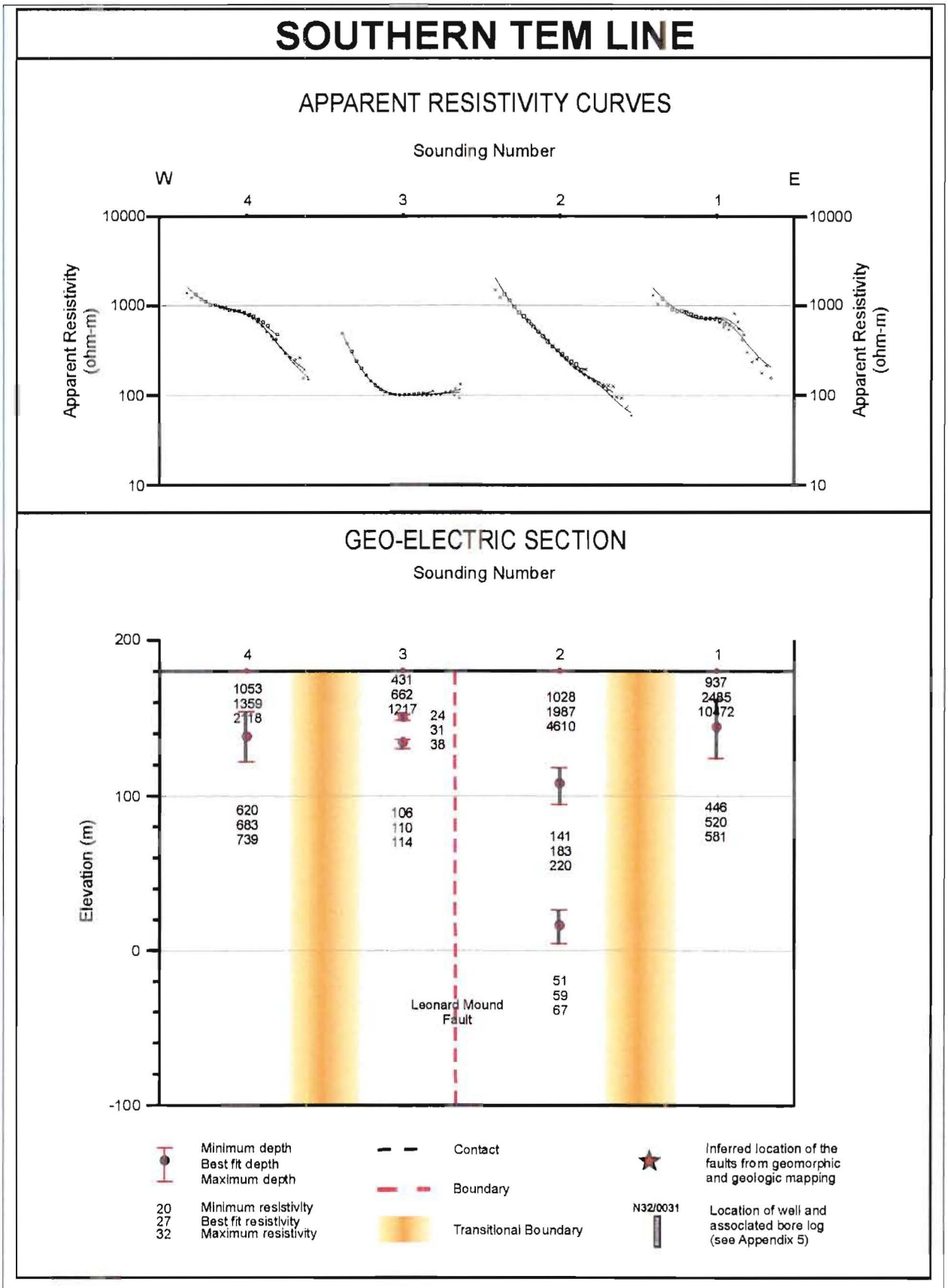

FIGURE 4.17. Southern Leonard Mound TEM soundings.

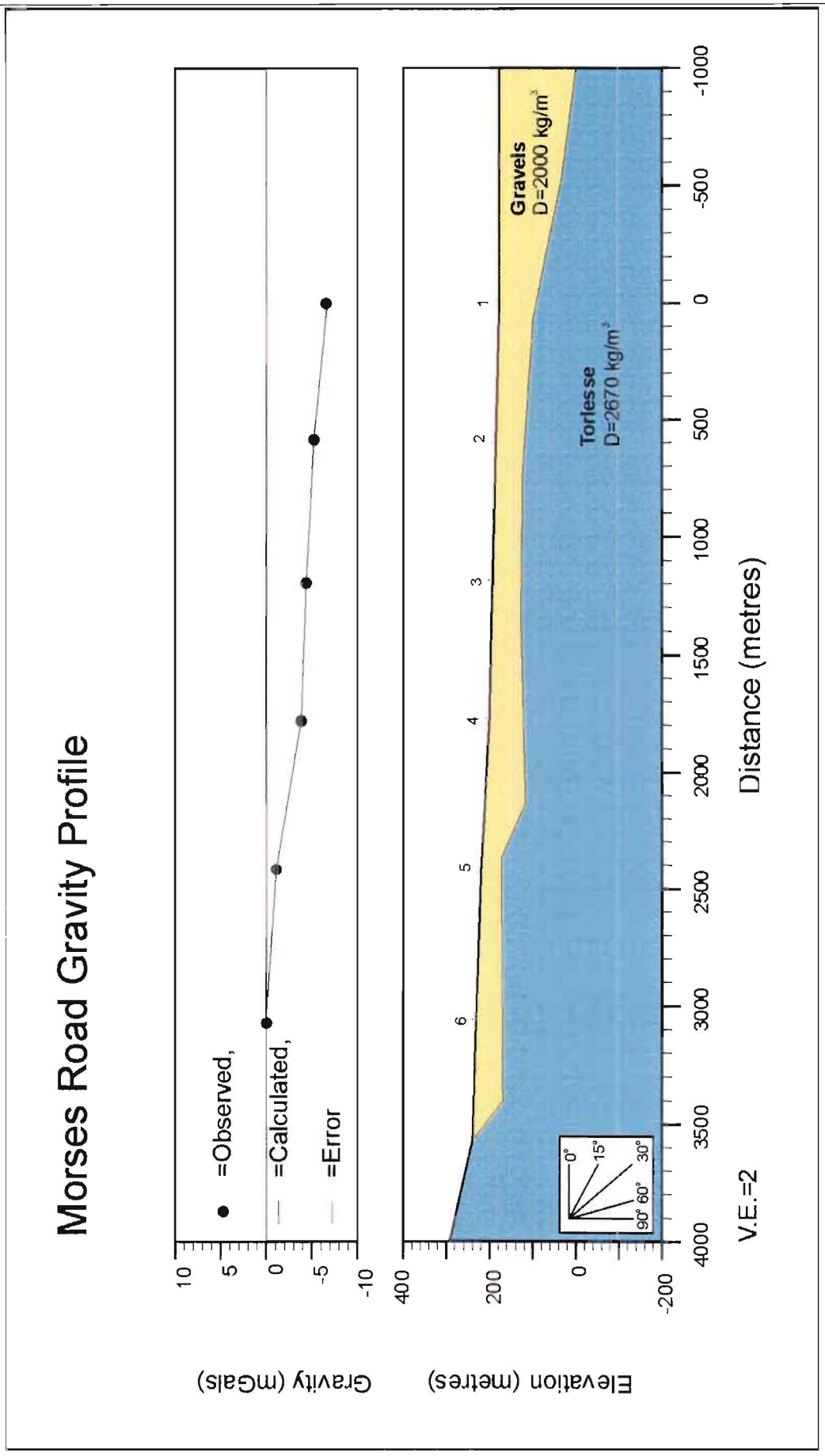

FIGURE 4.18. Morses Road gravity profile.

4.3.2 Mount Palm Road Gravity Profile

The Isolated Hill Fault dominates the Mount Palm Road gravity profile (Figure 4.19). A decrease of approximately 10 mgals is observed from SE to NW across the fault, which corresponds to a modelled uplift of approximately 1000 m of the SE side of the fault relative to the NW side. The relative size and location of the anomaly corresponds to Dibble's (1973) anomaly. The geological mapping of Isolated Hill Fault to the north, shows that the Isolated Hill Fault has juxtaposed the Torlesse basement against the younger Kowai Formation. On the upthrown side of the fault, the Mount Brown Formation and Kowai Formation have been eroded from the crest of the hill leaving a cap of Isolated Hill Limestone. In contrast, on the downthrown block, the Mount Brown and Kowai formations have been preserved substantially increasing the thickness of the cover sequence compared to the hanging wall sequence.

The syncline expected to have developed on the downthrown block of the fault is not well expressed in the model. It was evident from the mapping that there are several faults to the west of the Isolated Hill Fault, believed to be footwall imbricates of the main fault. It is inferred that these imbricate faults have partially faulted out the eastern limb of the syncline. The same faults may have produced a thrust stack, over-thickening the sequence. The modelled depth to basement of 1500 m is greater than the more usual 500-1000 m observed in adjacent areas (Mould, 1992; Litchfield, 1995; Kellahan, 1998). The faults are not resolved in the gravity modelling.

To the east of the Isolated Hill Fault two other faults are found. The transects start to the west of the fault with no stations run on the Lowry Peaks Range, as the steep terrain would have strongly affected the data. On the downthrown side of the Lowry Peaks Fault, a large syncline is not seen. Whilst there is no doubt that the syncline would have formed in response to the faulting, it has been destroyed by the smaller faults, such as the Leonard Mound Fault and Boundary Fault. Both of these faults have a surface expression, with the Leonard Mound Fault seemingly the more significant of the two. However, the gravity data suggests otherwise. At the location of the Boundary Fault there is a distinct gravity anomaly, whereas the Leonard Mound Fault does not show up in the data. The location of the Boundary Fault was also confirmed by the TEM models, which indicated a displacement of approximately 100 m of the Mount Brown Formation across the fault.

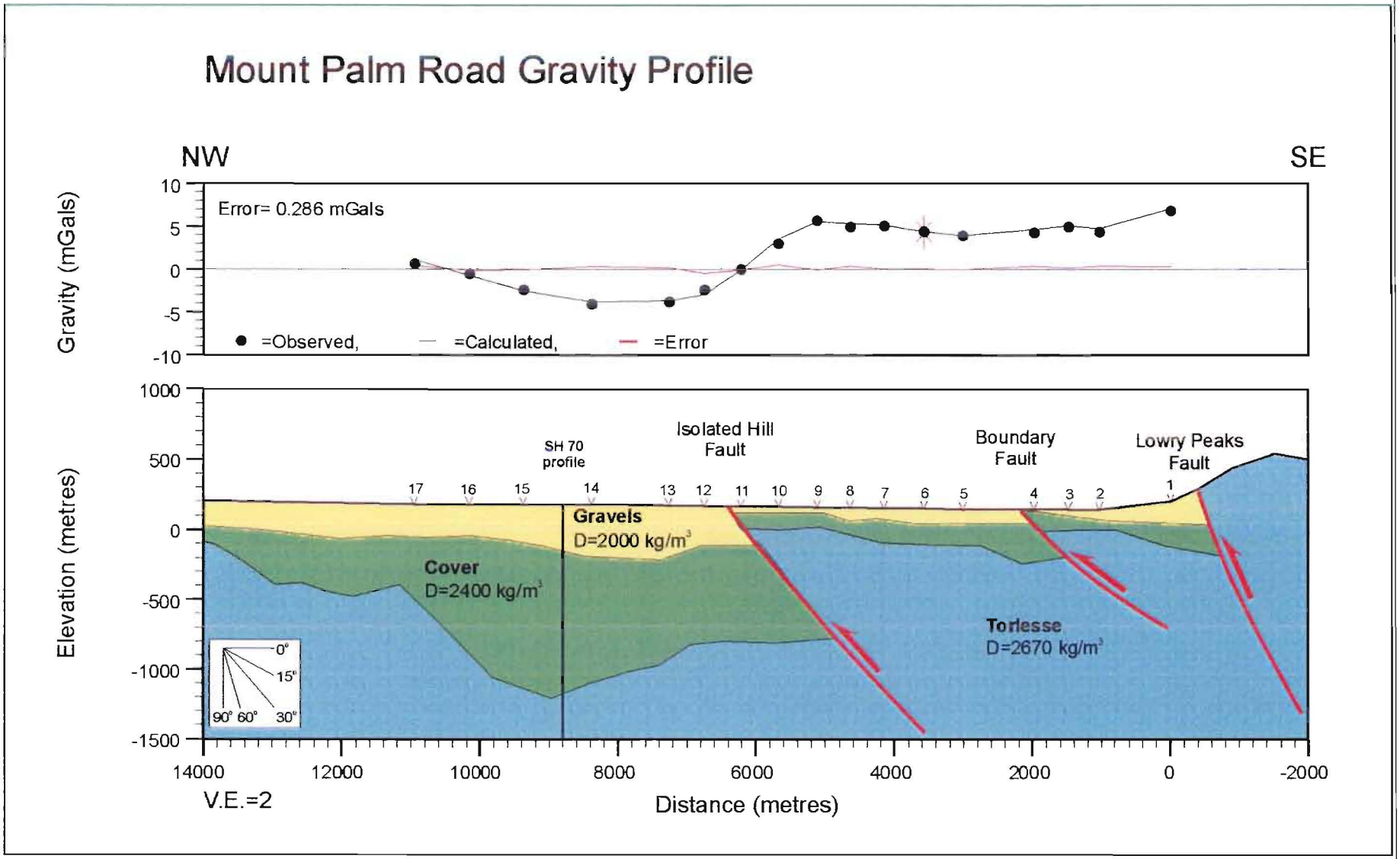

Figure 4.19: Mount Palm Road gravity profile.

4.3.3 Palmside Road and Flintoft Road Gravity Profiles

Although these two profiles were surveyed independently, they will be discussed together as they form a profile that extends from the Lowry Peaks Range across the basin to the eastern flank of the Amuri Range. Three faults have been modelled on the Palmside Road profile (Figure 4.20). The eastern-most of the three is the Lowry Peaks Fault. A syncline has clearly developed on the downthrown block of the fault, with a basement depth in excess of 1000 m.

To the west, the continuation of the Isolated Hill Fault is observed at approximately 8500 m along the profile. It has a slightly lower gravity anomaly than on Mount Palm Road (8 mgal versus 10 mgal), but displays similar characteristics. The cover sequence is very thin and at a shallow depth over the crest of the fold, as was also shown by the TEM modelling, due to erosion of the upper portion of the sequence. There is of the order of 1000 m of throw (or vertical displacement) on the fault. Adjacent to the fault on the downthrown side, the thickness of the gravels is similar to those seen in the Mount Palm Road profile, but the cover layer is significantly greater. It is inferred that the imbricate faults observed on Isolated Hill and inferred in the Mount Palm Road profile are not present to the same extent, thus the syncline has not been faulted out.

The third fault occurs between the two major faults and does not have a surface expression. It is comparable in position and size to the Boundary Fault to the north. From the geomorphic mapping, the Boundary Fault starts well to the north of Palmside Road, making this new fault a separate structure, but possibly one of a series of faults which have accommodated a significant portion of the deformation along the margin. As with the Mount Palm Road profile, the Leonard Mound Fault does not stand out clearly in the data. A small rise in the cover/gravels contact is observed at station 7. Whether or not this rise is associated with Leonard Mound is uncertain. The Flintoft Road gravity profile (Figure 4.21) is the extension of the Palmside Road profile and runs along Flintoft Road and State Highway 7. The model depicts the basement rising and the cover thinning quickly from station 8 westwards. The basement is exposed at river level adjacent to the final three stations, which are only several metres above the riverbed. The calculated response to the model does not fit well with the observed gravity for the last four stations. These stations are located adjacent to a high scarp running alongside State Highway 7 and at the entrance to the Waiau River gorge.

Consequently, the terrain effects will be substantially greater and have produced a larger error in the corrections.

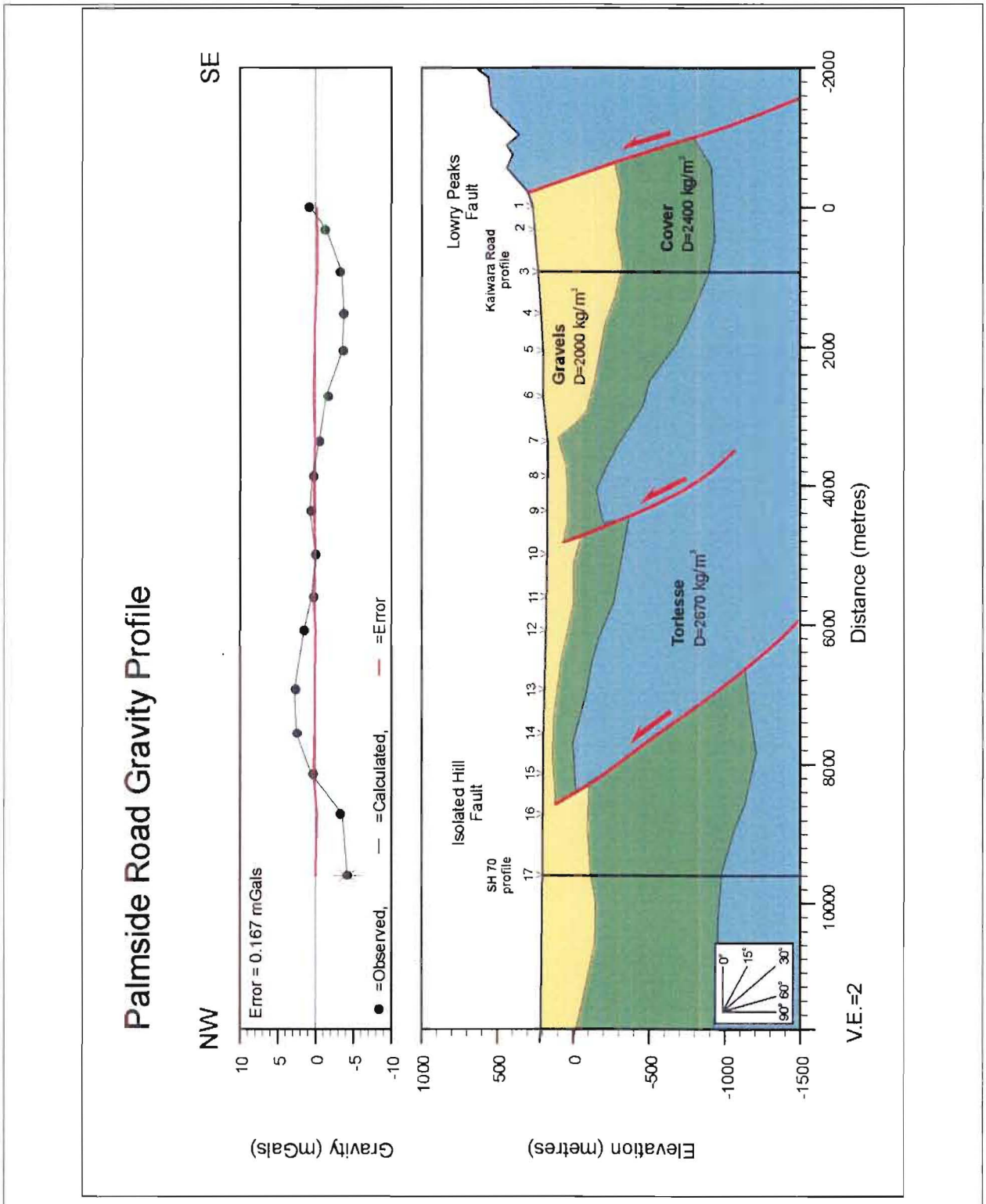

Figure 4.20: Palmside Road gravity profile

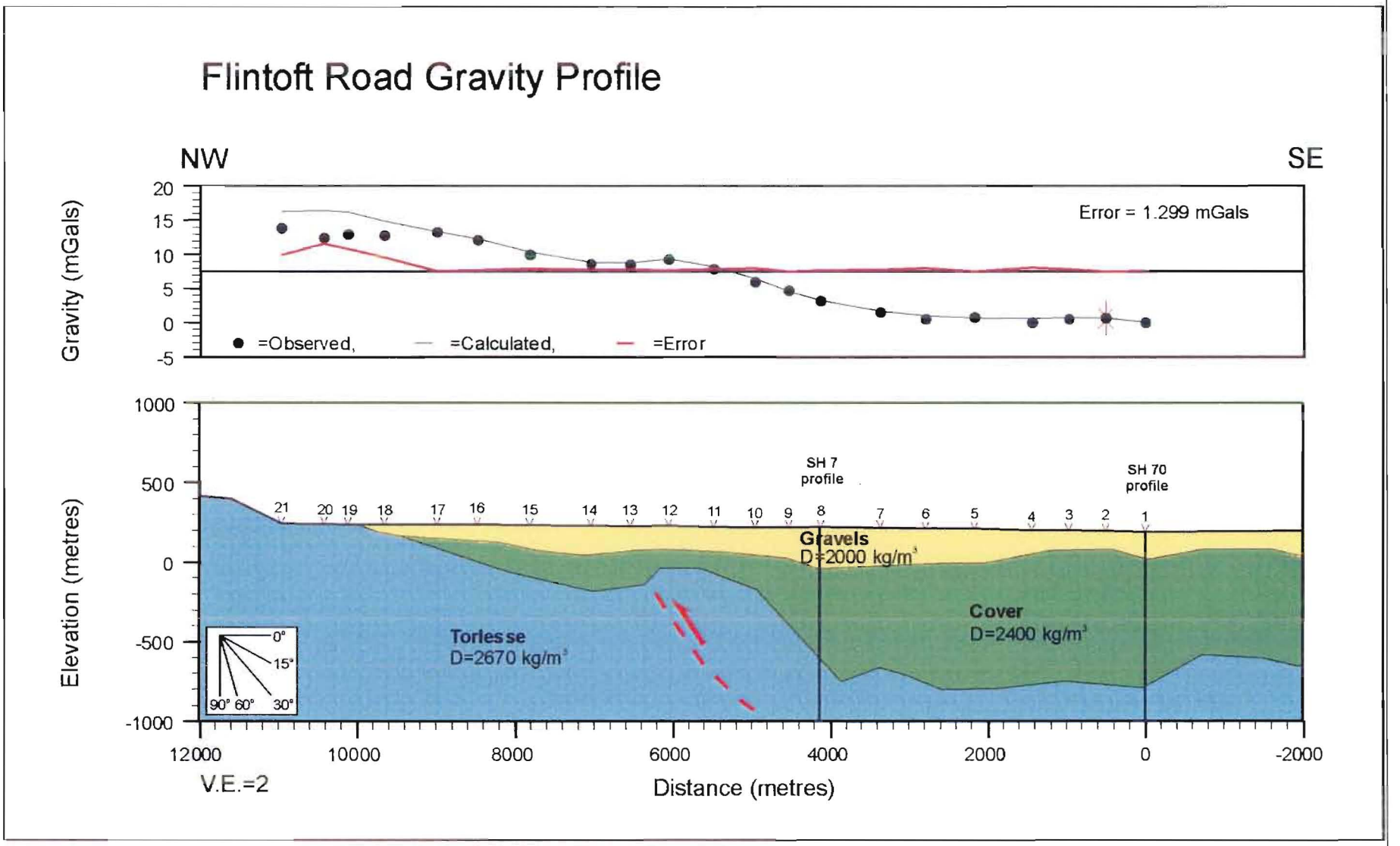

FIGURE 4.21. Flintoft Road-SH7 gravity profile.

Prior to running the survey, it was expected that an anomaly similar to that seen for the Isolated Hill Fault, would be observed for the Mount Culverden Fault. Hence, it came as a surprise that in the profiles that crossed the inferred location of the fault, there was no anomaly associated with the fault. The modelling indicates that there is a basement high located at 6000 m along the profile. It is believed that the high is another NE striking ridge that parallels and lies between Isolated Hill and the Amuri Range.

4.3.4 Lowry Peaks Road Gravity Profile

The quality of the data collected along the portion of the Lowry Peaks Road to the south of Leonard Mound is not as good as that along the other profiles. On the day the readings were taken there was a strong wind, making the gravity meter unstable. Consequently, only the general trend of the data was modelled rather than attempting to model some of the smaller fluctuations in the data.

From station 1 through to station 18 (Figure 4.22), the structure of the basin is as expected: deepest along the eastern margin and shallowing to the northwest. The basement reaches a high at 9 km, that is believed to be a continuation of the Isolated Hill structure seen in the Mount Palm Road and Palmside Road profiles. As with those two profiles to the north, the Leonard Mound Fault has no influence on the gravity data. Neither does the fault a short distance to the west, which was detected further north. That fault is still believed to exist based on the noisy TEM data and two boreholes (N33/0011 and N33/0045, Appendix 1) which show the Kowai Formation at a higher elevation than further west.

The fault observed at 10 km is the Isolated Hill Fault. In contrast to the profiles to the north, the size of the anomaly associated with the fault is considerably less indicating less displacement. To the west of the fault the basement slowly rises onto the southern flank of Mount Culverden.

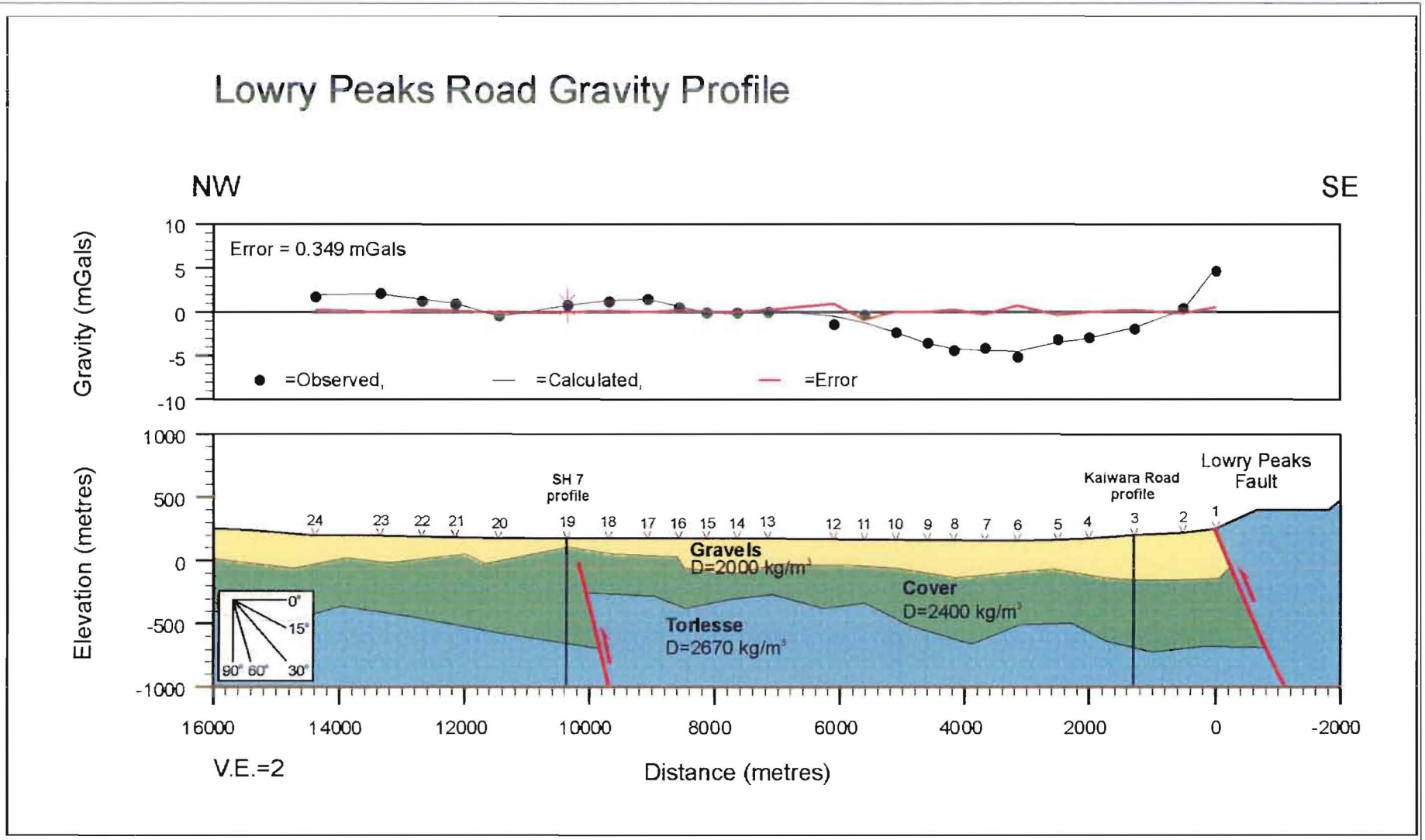

Figure 4.22. Lowry Peaks Road gravity profile.

4.3.5 Kaiwara Road Gravity Profile

The Kaiwara Road gravity profile (Figure 4.23) was a short SW-NE oriented profile to tie together the eastern ends of the Palmside and Lowry Peaks Road profiles. The most surprising aspect of the profile is the shallowing of the basement at the southern end of the profile. This shallowing may well relate to the Hemmingford Fault crossing the profile between stations 3 and 4. If this is the case, then it suggests that the Hemmingford Fault may be a significant fault that is accommodating the majority of the deformation along this section of the range.

4.3.6 Pahau Reserve Road Gravity Profile

The Pahau Reserve Road profile (Figure 4.24) starts several kilometres to the west of the Lowry Peaks Fault. It is interesting to note that the basin is very shallow adjacent to the range. Whilst this finding would be questionable based on this profile alone, the similarity with the Kaiwara Road profile indicates that there may be another major fault 1-2 km to the west of the range-front fault. The faulting has produced a structural high that was subsequently eroded producing a broad flat terrace that was buried by the Late Pleistocene gravels which floor the basin.

A broad high is located at 6 km along the profile, and from there westward the basin deepens. The location of the Balmoral Fault is constrained by the mapping of Mould (1992), as are the thicknesses and dips of the units on the hanging wall of the fault.

4.3.7 State Highways 7 & 70 Gravity Profiles

The State Highways 7 & 70 profiles (Figures 4.25 and 4.26) both run along State Highway 7 from the Hurunui River northwards to Red Post Corner. North of Red Post Corner, the profiles split and follow the State Highways after which they are named. From the Hurunui River (Station 1) to Culverden (Station 11), the profiles show very little structure. The basin very gradually shallows until reaching a high at stations 10-11. From Culverden to Red Post Corner (Station 15) a rapid decrease in the gravity indicates a rapid drop in the basement, resulting from the Isolated Hill Fault obliquely crossing the profile.

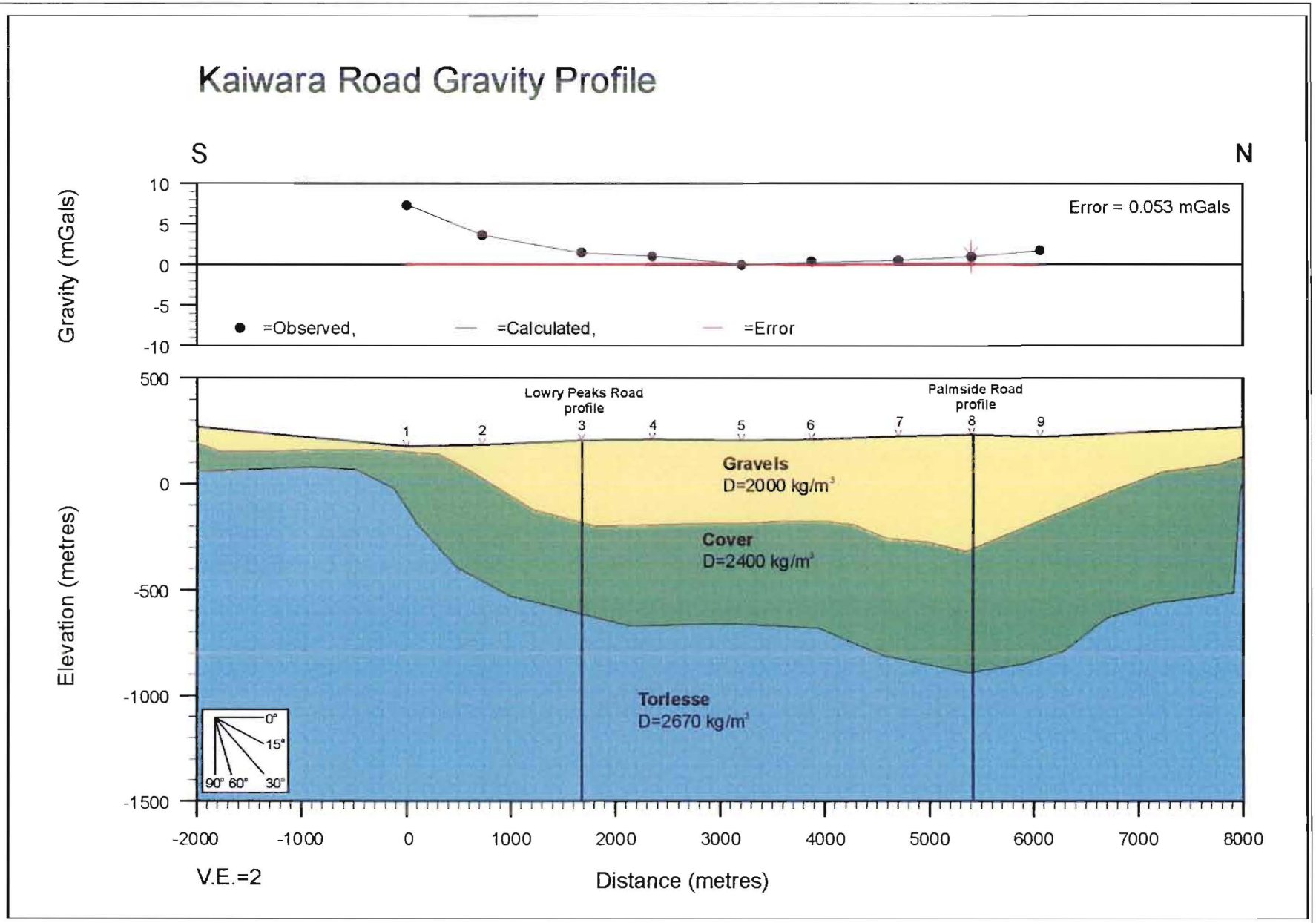

FIGURE 4.23. Kaiwara Road gravity profile.

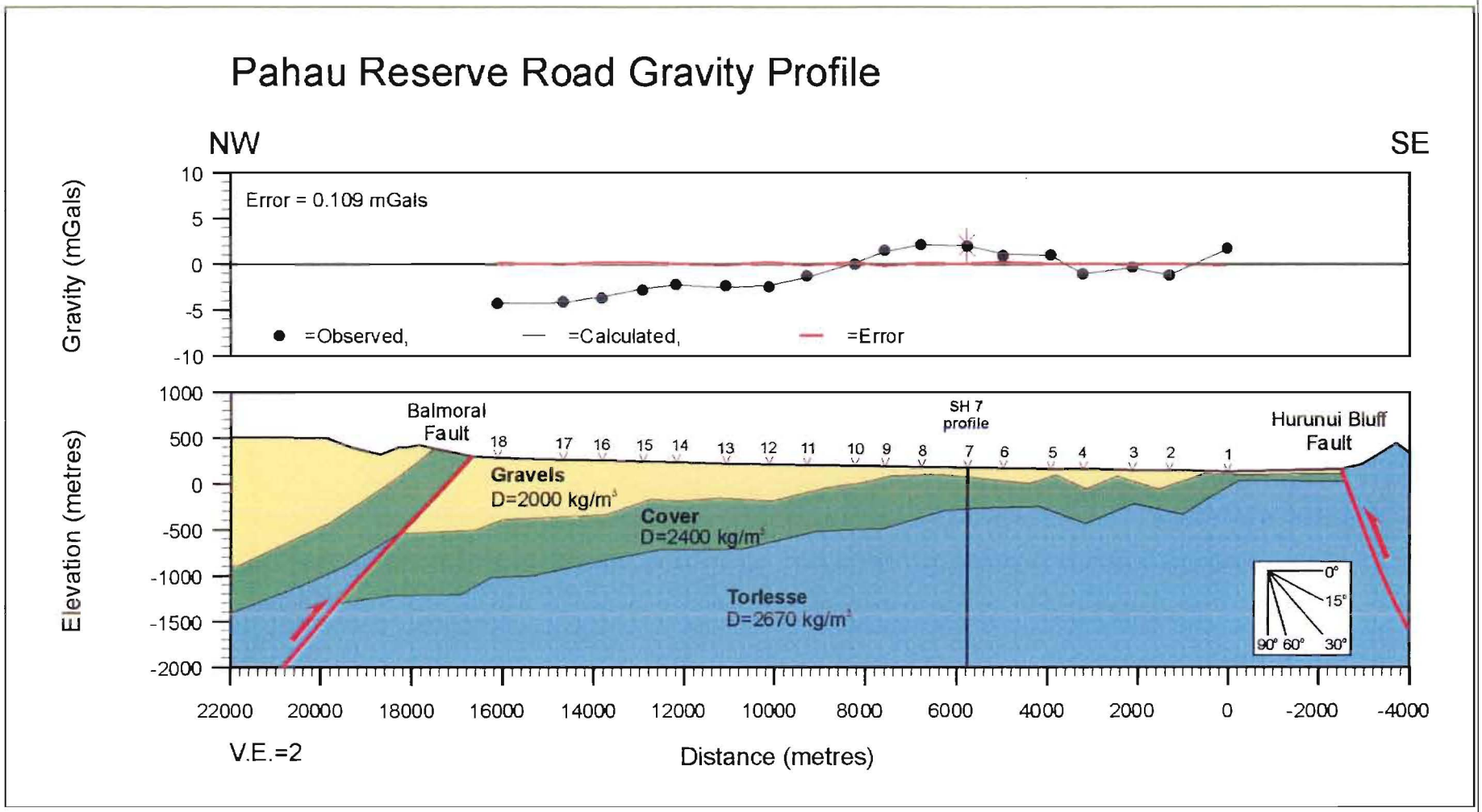

FIGURE 4.24. Pahau Road gravity profile

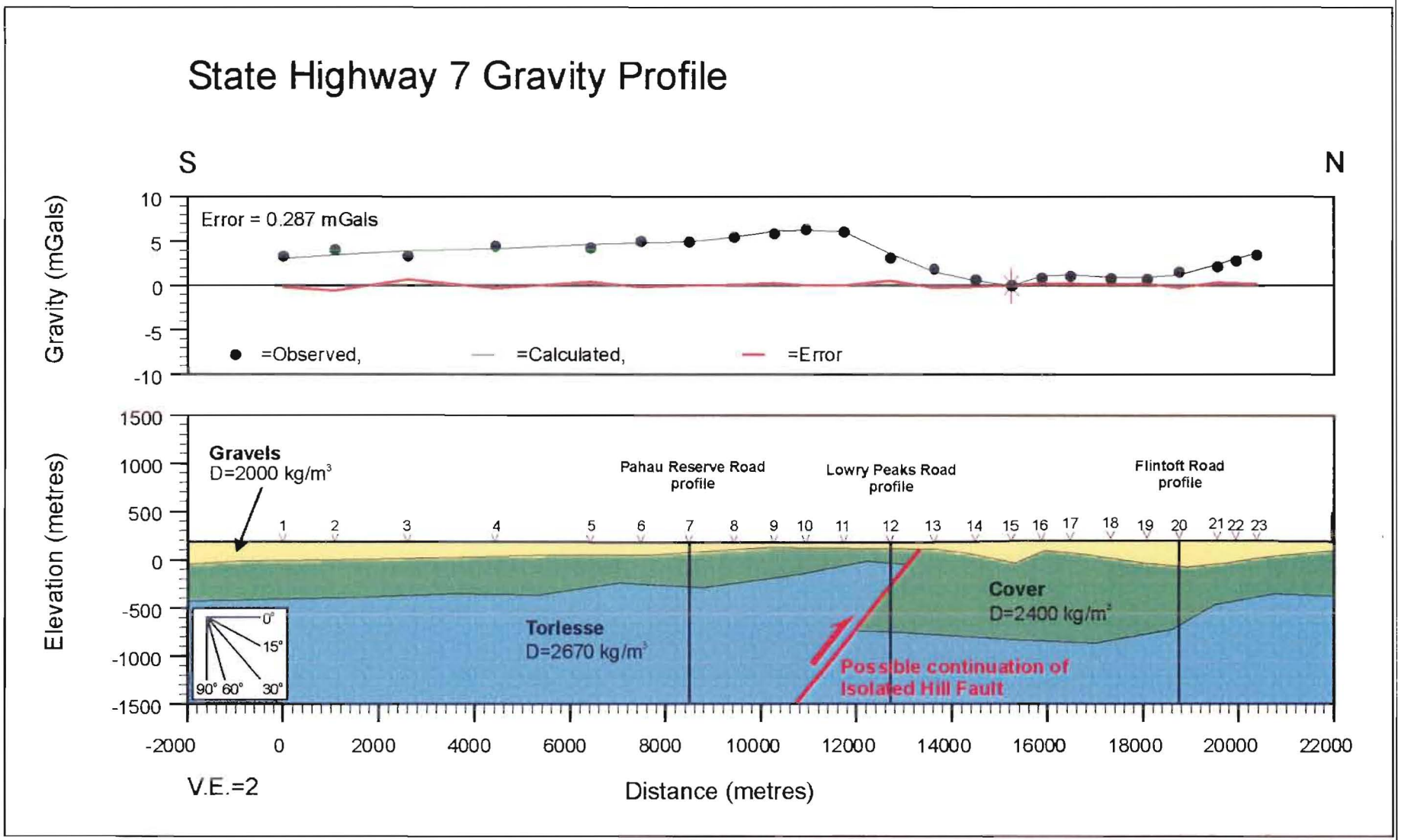

FIGURE 4.25. State Highway 7 gravity profile.

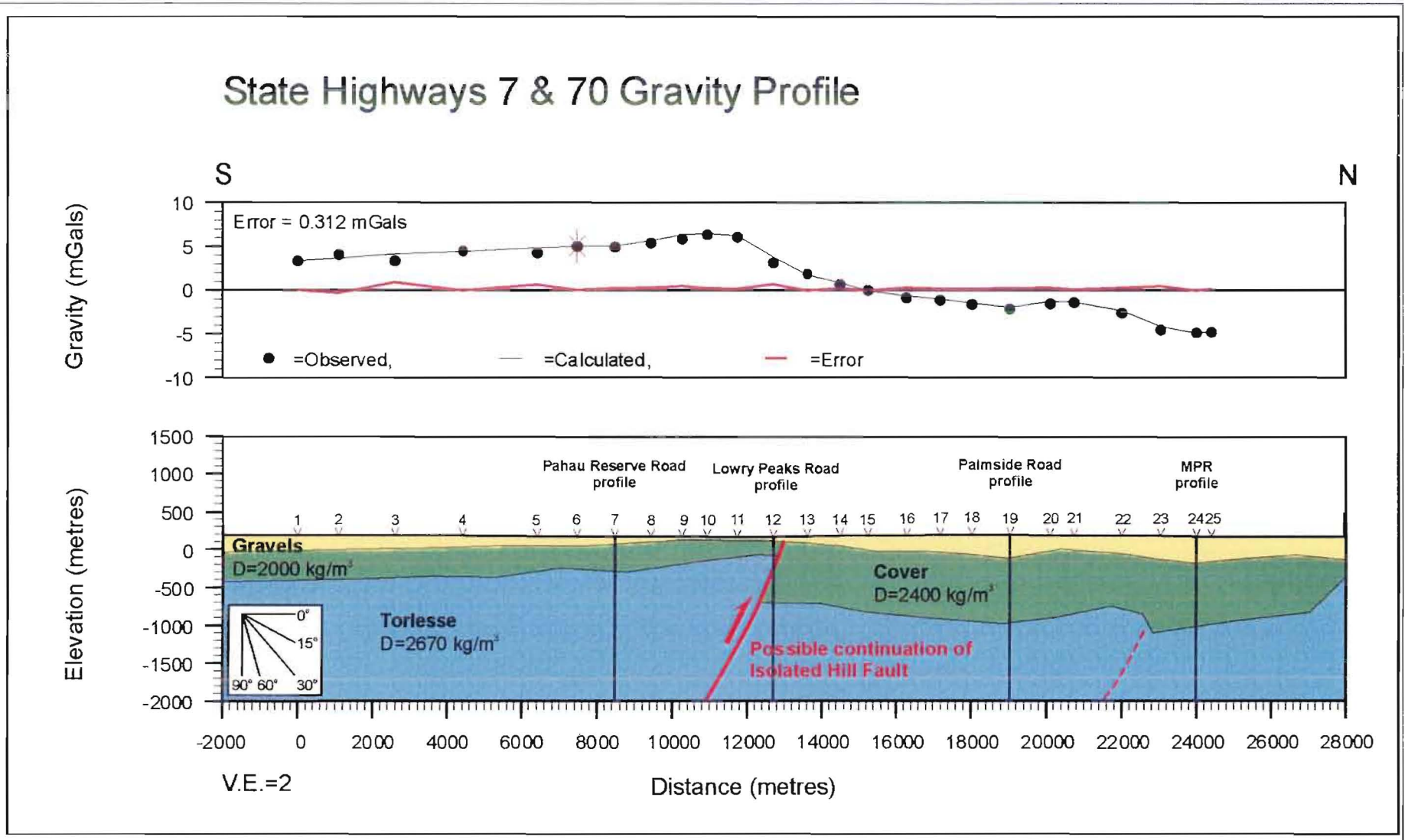

Figure 4.26: State Highway 7-State Highway 70 Gravity Profile.

North of Red Post Corner the profiles diverge along State Highway 7 and State Highway 70 respectively. Not only do the profiles diverge geographically at Red Post Corner, so do the gravity anomalies (Figure 4.27). The State Highway 7 gravity starts to rise, whereas the State Highway 70 gravity continues to drop. This is reflecting the orientation of the profiles relative to the strike of the structures and geological units observed on the eastern end of Mount Culverden. State Highway 70 continues along the strike, whereas in contrast State Highway 7 is oblique to the strike and is moving up-dip, hence the increasing gravity.

The Mount Culverden Fault does not show up in either profile. The State Highway 7 profile indicates that the basement is rising up onto a high located just off the end of the profile. The high would correspond to the high suggested in the Flintoft Road profile, which is parallel to the other major structures and lies between Isolated Hill and the Amuri Range.

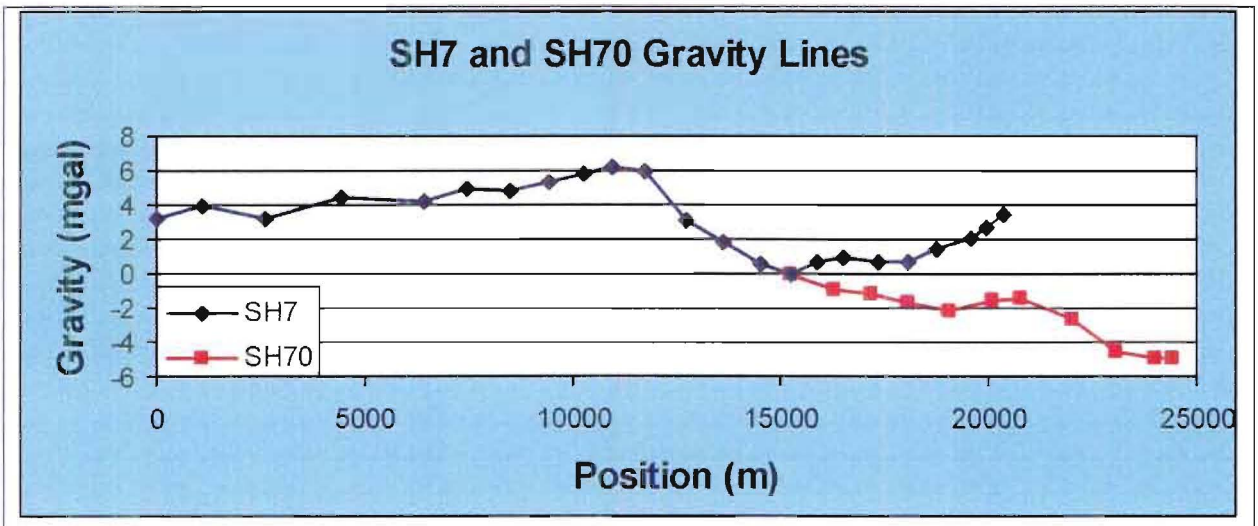

FIGURE 4.27. Graph of the State Highway 7 & 70 gravity surveys.

4.3.8 Summary

The gravity data provided valuable insights into the structure of the Culverden Basin that was otherwise unobtainable. Although there was no borehole information to help constrain the thicknesses and densities of the cover sequence units, the models were constrained, in part, by Dibble's (1973) data, the TEM results, checking for internal consistency and the geological mapping. The anomalies modelled from the data collected for this thesis were in good agreement with Dibble's (1973) gravity anomaly map. The anomalies indicate that the basin is

not a relatively simple asymmetric basin as first envisioned. Rather, the northern end of the basin appears to be divided into three sub-basins, as will be further examined in Chapter 5, by the major faults mapped around the eastern and northern basin margins.

4.4 GROUND PENETRATING RADAR PROFILES

The GPR did not prove to be as useful as was first hoped. As a consequence the GPR was only used at a few sites along Leonard Mound. Generally the depth of investigation was limited to the upper 150-200 ns or approximately 7-10 m. The GPR was used in the investigation of the active structures to investigate the active structures and to confirm the geomorphic interpretations. Data quality varied greatly with some profiles possibly showing the deformation whilst other profiles provided very little subsurface information.

The GPR profiles primarily concentrated on the Leonard Mound Fault System. A profile was also run along Lowry Peaks Road across the basin, however due to interference from surface objects the data were not used and have not been presented. Dairy farming in the basin has meant that the originally large paddocks have been divided making long continuous profiles even more difficult to run. As a result, the GPR lines were generally short and over the observed structures. In all approximately 10 km of profiling was run consisting of 4.5 km of short lines (GPR Profiles 1-6, Volume 2) and the 5.5 km long Lowry Peaks Road profile.

4.4.1 Southern Profiles (GPR Profiles 1: Volume 2)

The southern profiles proved to be some of the best obtained. Located immediately to the north of the pond off the southern end of Leonard Mound and by Lowry Peaks Road, the southern 1 and 2 profiles were run across the fold inferred to be the continuation of the Leonard Mound structure. The southern 1 profile was run using 50 MHz antenna initially to look at the broader scale features and to determine the location of structures followed by a 100 MHz survey to examine the deformation in more detail. Only the 100 MHz antenna were used on the southern 2 profile after examination of the southern 1 profiles.

The most apparent feature of the profiles is the complete lack of reflectors below 150 ns or 7-8 m depth. The cause of the attenuation of the signal is unclear and as will become apparent it

is a common feature in a significant proportion of the GPR profiles. There are no boreholes with logs in the near vicinity, and those a short distance away (N33/0045 and N33/0218, Appendix 1) do not show a change in the stratigraphy to account for the loss of signal. This issue will be addressed further in the discussion at the end of the chapter.

On the ground the deformation is expressed as warping of the gravels with no evidence of faulting having ruptured the surface. In the profiles there are zones where the stratigraphy has been clearly disrupted. The stratigraphy of braided river deposits can be rather chaotic and disrupted looking due to the environment in which they have been deposited. Despite the inherent problems, reflectors are still continuous even over short distances in the undeformed areas. In the deformed zones there is little or no continuity of the reflectors. The disrupted zones dip to the SE as would be expected of the thrusts controlling the formation of these folds. For the major zone at 100 m along the profile, folding of the gravels can be seen representative of the SE side of the fault being uplifted. It also appears as if the broad scale fold may be the product of several thrust/fold relationships. In front of the main zone of disturbance, there are several more disturbed zones which have not produced any surface expression as of yet.

On the southern 1 profiles the water table stands out clearly as a horizontal reflector that cuts across the tectonic and sedimentary features on the upthrown side of the fold. The water table is located at the surface on the downthrown side of the fold as the ponding indicates. It is interesting to observe that the water table does not show up as clearly on the southern 2 profile. It is probably indicating that the water table is deeper rather than a lack of contrast between the dry versus saturated gravels.

4.4.2 The Willows Profiles (GPR Profiles 2 and 3: Volume 2)

Several GPR profiles were run on and either side of Leonard Mound at the Willows. On the western side the Willows 1 and Blakiston profiles concentrated on the small warps inferred to represent footwall imbrication of the Leonard Mound Fault (Chapter 2). On the eastern side and on Leonard Mound itself, the Willows 2, 3 and 4 profiles were run to look at deformation of the strata, thickness of the gravels capping the ridge and the relationship between the older gravels capping the ridge and the younger fan gravels to the east.

4.4.2.1 Western Profiles

Starting with the profiles run on the western side of Leonard Mound, the folding of the gravels is quite clearly seen in the Willows 1 profiles. The Willows 1 profile started in a slip on the Leonard Mound Fault scarp and proceeded for 170 m across the inferred imbricate folds to the west of Leonard Mound. The profile was first run using the 50 MHz antenna followed by the 100 MHz antenna.

From 0-30 m the profile is reflector free. A diffraction resulting from a fence is seen at approximately 35 m after which the character of the response changes. The Leonard Mound Fault is inferred, from geomorphology, to cross the profile at 30 m. The lack of reflectors seen at the start of the profile is either due to:

1. the dielectric properties of the gravels are such that the signal is being attenuated in the near surface, or
2. the gravels have been eroded away to leave the underlying Mount Brown Formation sandstone near the surface which can be massive and hence reflector free.

It is unclear as to why the first 30 m of the profile is reflector free. There is no indication of the Mount Brown Formation being present in this section of Leonard Mound. All outcrop, even that in a larger landslide to the south, is of highly weathered gravel. The very dry nature of the gravels, combined with the weathering of the gravels is believed to be strongly attenuating the signal, leading to the lack of reflectors.

The diffractions from the fence, even after migration, affect the quality of the data from 30-45 m making it impossible to see any of the stratigraphy or structure. At 50 m there is a thrust distinguished by terminations in the bedding on either side of the thrust. From 50 m through to 100 m there is no apparent disruption to the stratigraphy. On the steeper limb of the fold, from 100-150 m the beds are clearly folded and some thrusts are present at the base of the fold limb.

Two different gravel packages can be distinguished based on the folding. The first package is that which has been folded and the second set is that which is undeformed and is onlapping onto the deformed gravels at the NW end of the profile. The undeformed set is clearly younger and is the Burnham Formation that covers the floor of the basin.

To the north of the Willows profiles, the Blakiston profile started just out from the base of Leonard Mound and headed northwest across another of the smaller folds to the west of Leonard Mound. At the start of the profile a buried channel is visible but across the fold no useful information pertaining to the stratigraphy or structure could be obtained from the profile. It has become more apparent from the profiles in the other sections of Leonard Mound that this type of response is characteristic of the gravels which have been uplifted by the imbricate faulting and folding to the west of Leonard Mound. Why this type of response results from these gravels is uncertain, and has not been investigated, except that these gravels are very dry which is obviously adversely effecting their physical properties.

4.4.2.2 Eastern Profiles

Two profiles were run from the crest of Leonard Mound down and across the Holocene gravels infilling the area between the Lowry Peaks Range and Leonard Mound. Another profile was run from the centre of the saddle up to a high point along the crest to determine whether or not the saddle is tectonically or fluvially controlled or a combination of both.

The Willows 2 and 3 profiles start from the crest and run down the eastern limb. They clearly show the gravels capping the ridge ramping down and being overlain by the fan gravels as expected.

The final profile run at the Willows was across the saddle to try and determine its origin. As with many of the GPR profiles very little useful information could be extracted from the profile. The apparent horizontal strong reflector observed at approximately 675 ns is an airwave reflection originating from pine trees planted on the western side of Leonard Mound. The profile was migrated to remove the airwave diffractions. Unfortunately, as the airwave velocity is greater than the ground velocity, the migration process has over-processed the in-ground diffractions turning them into "smiles". The upper 100-120 ns shows many subsurface diffractions related to the gravels capping the ridge.

4.4.3 Pukeiti Profile

Only one profile was run in the Pukeiti section of Leonard Mound. The profile was located on the terrace on the northern side of Palmside Road. The terrace is believed to have thrusts on both its NW and SE sides. It was hoped that the GPR would show the deformation within the gravels associated with the thrusting. Unfortunately this did not prove to be the case. On the profile (Figure 4.28 A) there are two large airwave diffractions arising from a fence-line and overhead powerlines. The profile was migrated (Figure 4.28 B), using the velocity of air (0.3m/ns), to remove the diffractions. The stratigraphy that can be seen is flat lying from 0-160m with possibly a slight SE dip at the NW end of the profile. Approximately 100m to the north, the gravels composing the terrace are exposed. The gravels are well stratified and are flat lying to very gently dipping (1-2°SE).

4.4.4 Kilsyth Profiles (GPR Profiles 4: Volume 2)

A wide, flat stream valley dissects Leonard Mound at the border of the Nukiwai and Kilsyth properties. It was hoped that GPR profiles (Nukiwai 1 and 2) along the valley floor would show the structure of the Mount Brown that is visible in outcrop on the valley sides, and the Leonard Mound Fault at the valley mouth. Unfortunately, this did not prove to be the case. Very little information was obtained from the profiles. What appear to be dipping strata on the profiles are diffractions arising from trees and fences on either side of the profiles. Even after migration to remove these events, no information regarding the deeper structure could be gleaned from the profiles.

To the west of the Leonard Mound Fault, there are other smaller faults (Chapter 3) across which several more profiles were run. From the main Leonard Mound Fault out to these secondary faults, the terrace is flat lying. Across the scarp, associated with the fault, there is a distinct change in the response. On the downthrown side there is a 30m zone of disrupted gravels that have been warped in response to a thrust at 45m (Kilsyth 3 profile) and another at 75m. Across the terrace the response is the same as that seen in the Blakiston profile and seems to be characteristic of these dry uplifted gravels.

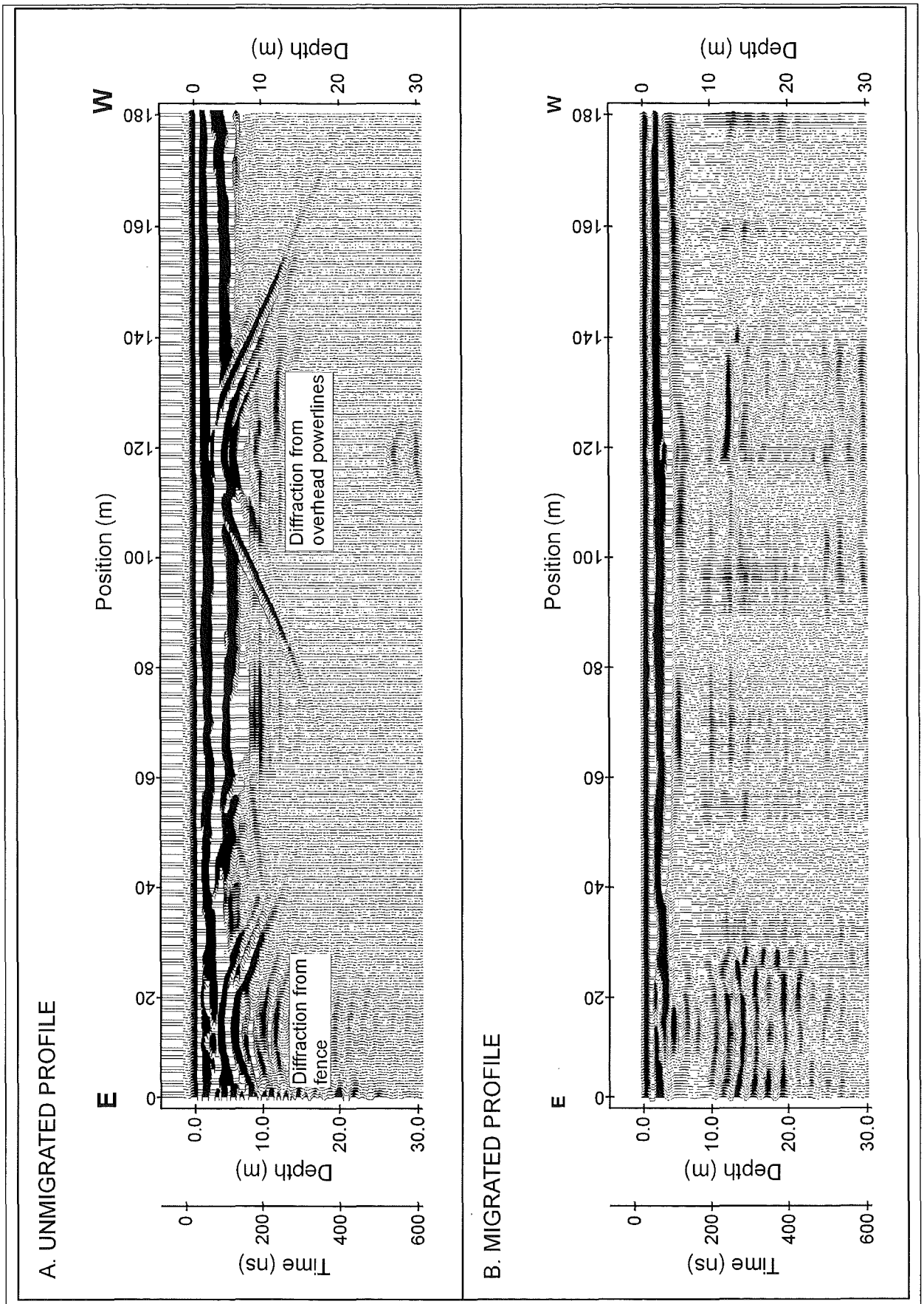

Figure 4.28. Pukeiti GPR profile: (A) unmigrated and (B) migrated.

4.4.5 Mount Palm Profiles (GPR Profiles 5: Volume 2)

Unfortunately, as with many of the profiles to the south, the Mount Palm GPR profiles did not provide much in the way of useful information. All the profiles ran across the inferred trace of the Leonard Mound Fault. No change is response was detected across the fault in any of the profiles. At the base of the scarp, a disruption is observed in the stratigraphy in each profile. Due to the lack of reflectors it is impossible to determine the nature of that deformation. Also, at various locations, generally to the west of the inferred fault trace, other changes in the character of the response occur. It is impossible to determine whether these changes are sedimentary or tectonic in origin.

Profile 2 is dominated by large airwave diffractions. When migrated, the diffractions disappear, however whether the remaining reflections are simply residues from the diffractions or real reflections is unclear.

4.4.6 Balmoral Fault Profiles (GPR Profiles 6: Volume 2)

The Balmoral Fault profiles were some of the earliest profiles run as the amount of movement on the fault had been well documented by Mould (1992) (Chapter 2). It was hoped to be able to compare the responses obtain for the Balmoral Fault with those from the Leonard Mound Fault System to help determine the nature of the deformation seen in the LMFS.

Five profiles were run across the fault on the northern side of Shortcut Road. All the profiles indicate folding towards the base of the scarp of the fault. However, the fault which has ruptured the surface and produced the scarp is not easily discernible. Compared with the southern profiles, there does not appear to be the wide zones of deformation. Instead, the deformation seems to be confined to a relatively narrow zone at the base of the scarp. It is impossible to determine from the GPR profiles the amount of vertical displacement across the fault.

4.4.7 Summary

The GPR results were disappointing given the success of GPR in aquifer and tectonic studies in other areas. As will be discussed at the end of the chapter, the reasons for the lack of reflectors are unknown and need to be the focus of further research.

Where reflections were obtained at the southern end of the Leonard Mound Fault System, the profiles showed the folding of the near-surface gravels by the small-scale footwall imbricate structures of the Leonard Mound Fault, confirming the geomorphic interpretations.

4.5 DISCUSSION AND SUMMARY

The purpose of the geophysical surveys was four-fold:

1. confirm the geomorphic interpretations along the LMFS,
2. determine the amount of displacement across the various tectonic structures mapped,
3. find any other tectonic structures with no surface expression, and
4. determine the thicknesses of the various stratigraphic units present and the depth of the basin.

4.5.1 Time-Domain Electromagnetics

There was concern initially after preliminary work by Bal (1999) in the Canterbury Plains which indicated that the gravels had very high resistivities that could not be measured by the TEM. Fortunately, this did not prove to be the case within the Culverden Basin. The quality of the data varied greatly from being exceptional to very noisy with no apparent cultural source for that noise. Initially it was hoped to be able to map the aquifer system and study the effect of the active deformation on the aquifers using both the TEM and GPR. Unfortunately, the TEM proved unsuccessful in this respect, due to the reasons discussed earlier in the chapter. Recent surveys in the Waipara Basin to the east (Loris, 2000) have also shown that TEM is not an effective method for mapping aquifers in North Canterbury.

It also became apparent that in tectonically deformed areas, modelling of the data is difficult due to rapid lateral variations in the stratigraphy. Not only did these variations affect the quality of the data, but in areas where the data quality was good modelling became difficult

without better constraints on the subsurface stratigraphy. Abrupt changes in the trend of the apparent resistivity curves proved to be the most effective way of locating buried structures.

4.5.2 Gravity Profiles

A gravity survey was not part of the original plan of the thesis. However, the gravity proved to be the most useful of the three methods for looking at the basin structure. The gravity profiles run across the basin proved useful indicators as to the location of the major structures present. Unfortunately, due to poor constraint on the density of the Late Cretaceous to Tertiary cover sequence and the Pleistocene to Holocene gravels, accurate modelling was difficult. However, despite those inaccuracies, reasonable thicknesses of the cover sequence were found that matched inferred thicknesses from geological mapping. From these thicknesses estimates of the amount of vertical displacements across various faults were constrained.

4.5.3 GPR Profiles

The main purpose of the GPR surveys was to confirm the geomorphic interpretations of the features seen along the Leonard Mound Fault System. The geomorphology suggested that these features were tectonically controlled rather than fluvial features. It was also hoped that the Leonard Mound Fault would be observed from which the attitude of the fault plane could be determined. This did not prove to be the case, as in the instance of the Nukiwai profiles, the recent stream gravels were too thick, and further to the north the strata were folded with no apparent displacement.

The quality of the GPR data varied from being very good and providing some useful information, to being of very little use. It is hard to understand the variation in the data quality as there appeared to be very little change in the nature of the near surface stratigraphy.

4.5.3.1 GPR Signal Attenuation

In all of the GPR profiles there is a distinct attenuation of the signal at approximately 150 ns. The reason for this abrupt cutoff is uncertain. It is well understood that zones of high conductivity attenuate the GPR signal so that reflections from below such a zone are

unobtainable. There are 2 main factors that contribute to high conductivities: clay and contaminated groundwater. In this case, groundwater contamination is not a contributing factor as shown by the chemistry of the groundwater in various wells within the basin (Close, 1987). For the 15 wells sampled, the conductivity of the groundwater varied from 11.6-25.1 mSm^{-1}, and the concentration of other indicators (e.g. Cl, SO_4, Na and K) were generally less than 10 gm^{-3}. That only leaves an increase in the clay content of the gravels. Boreholes in the vicinity of the GPR lines give no indication of a lithological change at 6-8 m depth in the gravels that was consistent throughout the entire area.

Other GPR surveys on the Canterbury Plains (Bal, 1999) have shown a similar response. However, Bal's profiles show a reflection at a much greater depth indicating that the gravels have become transparent to the GPR signal. Why this should be the case is uncertain and needs to be the focus of further research. It may be a function of a change in porosity, permeability and water content due to compaction of the gravels, or a chemical change, such as an increase in nitrates, from the long-term fertilization of the pastures. No deeper reflectors were seen in any of the profiles run in and around Culverden Basin leading the author to believe that the signal is being attenuated rather than the gravels becoming GPR transparent. It is interesting to observe that it makes no difference on which gravel package (i.e. glacial outwash deposits versus eastern margin alluvial fans) the profiles are situated, the attenuation still occurs at approximately the same time.

4.5.4 Summary

On the whole the geophysical results were of good quality and provided useful information that was otherwise unobtainable. Initially it was thought that GPR would be the most useful technique for investigating the nature of the deformation, with TEM aiding in the determination of displacement across the different features and in mapping the aquifers. As it turned out, the GPR did not prove particularly useful, even though it did confirm some of the geomorphic interpretations.

From the geophysical surveys, it is apparent that Culverden Basin can be divided into smaller sub-basins, separated by the structural highs associated with the major faults mapped around the margins of the basin. Within those basins there are thick sequences of the Kowai Gravels

and overlying Late Quaternary fluvio-glacial deposits. In Chapter 5 the geophysical results, along with the geological and geomorphic mapping, will be used to produce structure contour maps on the upper and lower surfaces of the aquifer-bearing units, from which isopach maps of those units will be produced.

CHAPTER 5

CONCEPTUAL HYDROGEOLOGICAL MODEL AND CONCLUSIONS

5.1 INTRODUCTION

The key objective of this study is to develop a hydrogeological model, based on the eastern margin of Culverden Basin, examining the effects of active earth deformation on the groundwater resource of tectonically active basins. The previous three chapters have described the different structural and sedimentary elements within the basin, all of which influence the groundwater regime. This chapter synthesises the geological, geomorphological and geophysical information into a hydrogeological model for the northeast portion of Culverden Basin, and also summarises the more general elements common to a hydrogeological resource evaluation in basins located in an active tectonic setting.

The hydrogeological model is conceptual. This study has not involved the quantification of the hydrological properties, such as hydraulic conductivity, transmissivity and storativity. Future investigations will need to address these properties, especially on the non-irrigated regions of the basin, if those regions wish to diversify away from the traditional sheep and cattle grazing.

5.2 TECTONIC DEFORMATION AND BASIN EVOLUTION

The tectonic deformation needs to be considered from three perspectives: (1) how did the pre-existing structurally controlled topography control the distribution of the Late Quaternary fluvial deposits, (2) how does ongoing tectonic deformation affect the facies relationships, and (3) how does the post-depositional deformation affect the aquifer architecture. The first part of this section examines the overall structure of the northern portion of Culverden Basin, based on the geological mapping of the basin margins (Chapter 2) and the subsequent geophysical surveys (Chapter 4). The actively evolving Leonard Mound imbricate fault system is the focus

of the second section, followed by a discussion of the sub-basins created by the structures outlined in the first two sections.

The structures represent the evolution of Culverden Basin and the subsequent partial inversion of the basin floor. As shown in figure 5.1A (Volume 2), three stages of evolution and inversion are documented. The first stage is the development of the primary thrust systems (East Culverden Fault Zone and western margin structures) along the basin margins. The second and third stages are the inversion of the basin floor by the imbrication of the primary thrust systems, initially by the Isolated Hill Fault, followed by the development of the Leonard Mound Fault System. The imbrication of the primary thrust systems has resulted in the development of the three sub-basins detected by the geophysical investigations. The development of the sub-basins has controlled the distribution and architecture of the aquifer-bearing deposits of Culverden Basin.

5.2.1 Northern Culverden Basin

The major faults mapped around the extremities of north Culverden Basin are considered to form thrust faults and belong to an imbricate thrust system. The faults generally have an associated major anticline on their upthrown (hanging wall) side and at least a partially developed syncline on their downthrown (footwall) side. The purpose of this discussion is to document the key findings of the geological mapping and geophysical investigations, with respect to the relationship between the tectonic deformation and the Late Quaternary sedimentation.

As will be shown in the final section of this chapter, the development of the structures discussed here have major implications on the groundwater resources of basins in active tectonic settings.

North Culverden Basin Imbricate Thrust System

The following common points can be drawn regarding tectonic structures of the north Culverden Basin imbricate thrust system.

- The thrust faults are generally considered to posses a listric form, locally steepening to reverse faults in the near surface. From the geological mapping and the gravity surveys,

the faults are observed to dip to the southeast at angles upto 60°. The faults have been drawn to flatten out into a mid-crustal detachment zone, at depths of 12-15 km. The detachment was first proposed for the North Canterbury region (Nicol, 1991; Cowan, 1992; Nicol and Wise, 1992; Reyners and Cowan, 1993) based on field evidence such as the limited lateral extent of the majority of the faults in North Canterbury, combined with their apparent imbricate thrust nature (e.g. Nicol, 1991; see also Mould, 1992; Litchfield, 1995); paleomagnetic evidence for crustal block rotation in the Marlborough Fault Zone Region (Lamb, 1988); and the apparent presence of an aseismic zone at depths of 12-17 km from a microseismic study of the North Canterbury Region (Cowan, 1992).

- It is well documented in Chapter 3 that the major thrust systems are not characterised by a single continuous thrust fault. As is best demonstrated by the range-front faults of the ECFZ, the thrust systems are comprised of a number of short, overlapping faults, characteristic of other large thrust belts, such as the Wyoming-Idaho Thrust Belt (e.g. Dahlstrom, 1970; Brown and Spang, 1978; O'Keefe and Stearns, 1982; Couzens and Dunne, 1994). The zones of displacement transfer are often complicated, and produce structural lows which the rivers have exploited on the eastern side of the basin.
- All of the folds observed in the study area have formed in response to movement on the major thrusts. Since the early 1980's, thrust fault-related folds have been categorised into three styles depending upon the geometry of their related fault planes: (i) fault-bend folds (Suppe, 1983); (ii) fault-propagation folds (Suppe and Medwedeff, 1984); and (iii) detachment folds (Jamison, 1987), and are shown in Figure 5.2. It is believed that the anticlines are fault-propagated folds, as they have been truncated through their inflection points, ruling out fault-bend folds, and the development of synclines beneath the faults dismisses detachment folding.

East Culverden Fault Zone

- The East Culverden Fault Zone (ECFZ) is the primary thrust system along the eastern margin of the basin (Figure 5.1A). The structurally propagated anticlines associated with the ECFZ (e.g. Lowry Peaks and Hurunui Bluff anticlines), have produced ranges which separate Culverden Basin from adjacent basins to the east (e.g. Waipara and Cheviot basins), and supply the Lowry Peaks Range alluvial fans which dominate the Quaternary stratigraphy along the eastern margin.

- As mentioned, the range-front fault system is complexly segmented and splayed, with the principal faults being the Hurunui Bluff, Hurunui Gorge, Lowry Peaks and Totika faults.

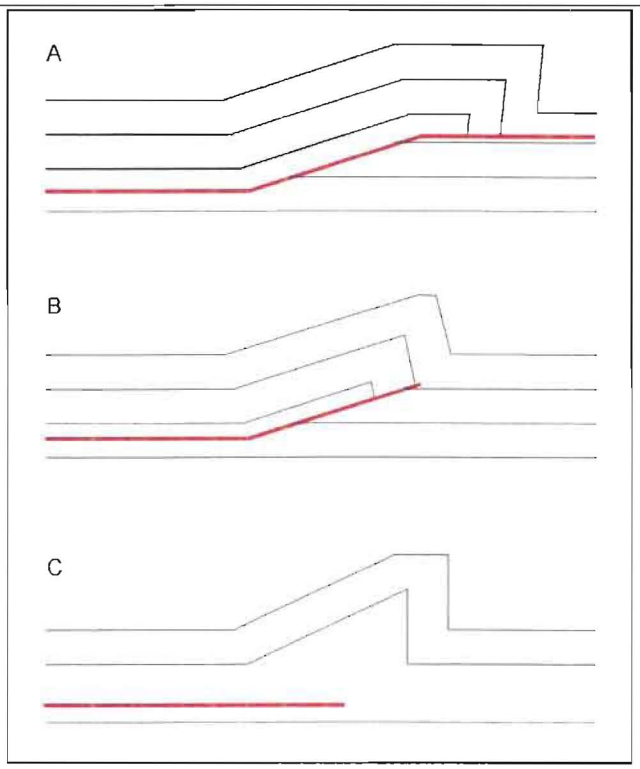

FIGURE 5.2. Diagrammatic illustration of the three end members of folds associated with thrust faults: **A**. fault-bend folding, **B**. fault-propagation folding and **C**. Detachment folding (from Jamison, 1992).

- The range-front faults have been responsible for the development of the Lowry Peaks Range, which is the product of three anticlines (Hurunui Bluff, Lowry Peaks and Ngawiro). The range is structurally mature and has supplied vast quantities of gravel to the basin, evident by the high degree of erosion of the Lowry Peaks Anticline. At either end of the range, from the elevation of the range, presence of the Cretaceous peneplain surface and the symmetrical nature of the folds compared to the asymmetric Lowry Peaks Anticline, it is inferred that the Hurunui Bluff and Ngawiro anticlines are structurally lower and possibly younger than the Lowry Peaks Anticline. There has not been the same amount of erosion of the Torlesse basement, resulting in a "smooth" topography.

- The Ben Lomond Syncline is the only surficial evidence of synclines having developed on the downthrown blocks of the faults. However, the gravity surveys show the syncline associated with the Lowry Peaks Fault to be present between the range and the southern end of Leonard Mound. In the Lowry Peaks Road and Palmside Road gravity profiles, it is estimated that along the axis of the syncline the Torlesse basement may be up to 1 km deep, and that there may be 500 m of gravels (Kowai Gravels and alluvial fans). To the north of Palmside Road, the faulting associated with Leonard Mound and Isolated Hill has overthrust the syncline, producing a relatively shallow basin.
- Propagating off the northern end of the Lowry Peaks Fault, the Leonard Mound Fault is presently accommodating the deformation along the eastern margin of the basin. The Leonard Mound Fault System is the focus of the next section as it has been, and is presently, the main structural influence on the aquifer architecture along the eastern margin of the basin.

Western Margin

- Two different sets of structures are observed along the western margin, separated by the Mount Culverden Fault. To the north, the Marble Point Fault and Amuri Range form the western extent of the north Culverden Basin imbricate thrust system. The Amuri Range is a fault-propagated asymmetric anticline that has a steep northwest limb and a shallower dipping southeast limb. The range is controlled by the Marble Point Fault along its northwest edge, which is another listric thrust, again inferred to extend down to the mid-crustal detachment zone.
- To the south of Mount Culverden, Mould's (1992) mapping of the western margin range-front, detailed eastward facing thrusts and associated folds, which he inferred to be back-thrusts off the Alpine Fault. As a result of this difference, the southern end of the basin is not structurally characterised by an imbricate thrust system. The southern end of Culverden Basin is deepest along the western margin, gradually shallowing to the east. Interestingly, there is not a syncline associated with the Hurunui Bluff Fault, as is observed for the Lowry Peaks Fault.
- Mount Culverden is structurally very interesting and needs to be the focus of further research. There were no gravity anomalies in the State Highway 7 and State Highway 70 gravity profiles, across the inferred location of the Mount Culverden Fault. It is believed that the cover sequence observed on the eastern end of Mount Culverden, is the eastern

flank of another NE-SW trending thrust-propagated anticline whose axis lies between the Rotherham Fault and the Amuri Range. The crest of the anticline is modelled at approximately 6 km along the Flintoft Road gravity profile, and it appears that the Torlesse basement is rising up onto that high in the State Highway 7 gravity profile.

- As with the ECFZ, the major faults (e.g. Marble Point and Waitohi faults) along the western margin are part of the western margin primary thrust system (Figure 5.1A). This system is actively propagating eastward, expressed by the Balmoral Fault, and progressively inverting the basin floor.

Isolated Hill

- Three faults have controlled the tectonic evolution of Isolated Hill. The largest of the three is the Isolated Hill Fault striking through the centre of Isolated Hill. To the east is the Cranford Downs Fault, and to the west is the Rotherham Fault. Both the Isolated Hill and Cranford Downs faults have juxtaposed Torlesse basement against the upper units of the cover sequence. On the crest of Isolated Hill, the Mount Brown Formation and Kowai Formation have been eroded off, leaving approximately 70 m of the cover sequence.
- To the south of Isolated Hill, the faults have been buried by the glacial outwash deposits. The gravity profiles (Mount Palm Road and Palmside Road) clearly locate the continuation of the Isolated Hill Fault, which can be traced as far south as Culverden, and may possibly be responsible for the development of the broad basement high observed in the Pahau Reserve Road gravity profile. A 10 mgal decrease from east to west across the fault is observed in the gravity data, corresponding to an elevation difference of approximately 1 km of the Torlesse basement/cover sequence unconformity. Dibble's (1973) gravity anomaly map indicated that the basin is deepest on the downthrown side of the Isolated Hill Fault. The gravity surveys performed for this study confirm this, with in excess of 1 km of cover sequence and 300 m of Quaternary gravels modelled to be present at the deepest point.
- To the east of the Isolated Hill Fault, the basin is relatively shallow with less than 300 m of cover sequence and less than 100 m of the Kowai Gravels and Late Quaternary glacial outwash deposits.
- The Isolated Hill and Mount Highfield structures reflect the onset of basin inversion at the north end of the basin, by the footwall imbrication of the eastern margin primary thrust

system (Figure 5.1A). The deep portion of the basin is possibly the old relic basin prior to basin inversion.

5.2.2 Leonard Mound Fault System

Splaying obliquely off the northern end of the Lowry Peaks Fault, Leonard Mound is an actively propagating, thrust driven anticlinal ridge, whose pristine preservation has allowed detailed geomorphological examination of the imbricate thrust system features. From analogies of other well studied thrust systems (e.g. King and Vita-Finza, 1981; Stein and King, 1984; Namson and Davis, 1988; Rockwell et. al., 1988; Avouac et. al., 1993; Hippolyte, 1994; Berbian, 1995; Namson, 1995; Barnes, 1996; Jackson et. al., 1996;) it is evident that Leonard Mound is underlain at shallow depths by a thrust. As was described in Chapter 3, the principal fault in the Leonard Mound Fault System is the Leonard Mound Fault, which has a traceable length of 15 km. The fault is clearly segmented into five sections (Southern, The Willows, Pukeiti, Kilsyth and Mount Palm, respectively from south to north), distinguished by the style of deformation mapped in the hanging wall and footwall of the fault. The southern three sections are characterised by the development of asymmetric, doubly plunging anticlines, on the upthrown side of the fault. The northern two sections do not display any sign of folding, rather, the uplifted Mount Brown Formation (Kilsyth section) and Lowry Peaks Range alluvial fan gravels (Mount Palm section) are tilted to the southeast.

The footwall of the Leonard Mound Fault is imbricated, evident from the array of smaller faults and folds mapped to the west of the Leonard Mound. These structures are active in the Holocene, clearly disrupting the range-bounding fans and Burnham Formation, and are often highlighted by water ponding on the relatively downthrown side of the faults/folds. In the southern three sections, these structures are accommodating only a relatively small portion of the deformation along the fault system, with the Leonard Mound Fault absorbing the majority. The geophysical data show no anomalies, associated with significant offsets of the Tertiary succession, across these structures. In contrast, splaying off the Kilsyth section of the Leonard Mound Fault, the Boundary Fault, from the geomorphology, appears to be another relatively small structure accommodating the Holocene deformation along the northern portion of the Leonard Mound Fault System. The TEM and gravity surveys both indicate that the Boundary Fault has a significant vertical displacement associated with it. From the TEM transects that

cross the fault, there appears to be 100-150 m of vertical displacement of the Mount Brown Formation/Kowai Gravels contact. In contrast, across the Leonard Mound Fault, to the east of the Boundary Fault, the deposits are folded with very little apparent displacement. It therefore appears, that in this section of the Leonard Mound Fault System, the Boundary Fault is the major fault.

To the south in the Southern, Willows and Pukeiti sections, the geophysical surveys all indicate that the Leonard Mound Fault is the dominant structure. Based on the depth to the Kowai Gravels in bore logs N33/0011 and N33/0045 (Appendix 1) of 28 m and 18 m respectively, and the elevation (70 m) of Kowai Gravels above the basin floor, there has been a minimum of 90 m of vertical displacement across the Leonard Mound Fault, in the Southern Section. On the Palmside Road TEM transect, a syncline has clearly developed to the west of the Leonard Mound Fault, in which there may be approximately 200 m of gravels.

The evolution of Leonard Mound represents the third stage of basin inversion, as shown in Figure 5.1A. The uplift of Leonard Mound has clearly created a smaller sub-basin (Wynyard sub-basin) between the southern end of Leonard Mound and the Lowry Peaks Range (Figure 5.1B, Volume 2). The sub-basin fill consists of Lowry Peaks Range alluvial fans and the Waiau River glacial deposits, complexly inter-related. As figure 5.1B schematically depicts, the development of Leonard Mound is characterised by fan deposition during the glacial periods, punctuated by erosion during the interglacial periods. The glacial deposits are restricted to the southern end of the sub-basin by Leonard Mound. Consequently, the glacial deposits are progressively forced southwards and confined to a smaller portion of the sub-basin as Leonard Mound continues to propagate southwards.

5.2.3 Sub-basins

The preceding discussion documented the development of fault-propagated NE trending, asymmetric anticlines and synclines associated with the inversion of north Culverden Basin by the major thrusts. The formation of these anticline/syncline pairs has lead to the basin becoming partitioned into three distinct sub-basins, clearly identified in the structure contour and isopach maps of the aquifer-bearing units (Figure 5.3, Volume 2). Nicol et. al., (1995) have shown that the formation of sedimentary basins in north Canterbury have an inherent

link to wavelength of the major folds. Nicol et. al. also made pertinent observations pertaining to the basin width and wavelength, and between basin length and fold length (or fault length) in North Canterbury, as shown in Figure 5.4. If the cores of the fault-related synclines are situated below the base level of sedimentation they will be filled with sediments according to the rate of sedimentation of the area. Clearly, the floor of Culverden Basin has been below the base level of sedimentation during the Late Quaternary, with the sub-basins acting as the depositional centres for the sedimentation.

Three sub-basins were identified, from the geological mapping and geophysical investigations, in the northern portion of Culverden Basin. Structure contouring on the upper and lower boundaries of the aquifer-bearing units (Figure 5.3) clearly shows the location and extents of the sub-basins. The sub-basin that is most easily recognised, due to its boundaries being observable at the surface, is the Wynyard sub-basin situated between the Lowry Peaks Fault and the southern end of Leonard Mound. To the west of Leonard Mound, the central and western sub-basins have been buried by the Burnham Formation, but were located by the gravity and TEM surveys. The central sub-basin occurs along the western edge of Leonard Mound and is separated from the western sub-basin by the inferred continuation of the Isolated Hill fold.

The sub-basins are approximately 3 km wide, with the widths controlled by the spacing of the thrusts. The basins have an asymmetric cross sectional shape, reflecting the asymmetric character of the fault-propagated folds of the thrust system. Therefore, the basins are deepest along their SE sides and progressively shallow to the west. The gravity and TEM surveys indicate that there may be up to 500 m of Early Pleistocene (Kowai Gravels) to Holocene gravels in the axes of the basins. The lengths of the basins are controlled by the lengths of the faults responsible for their developments, and consequently have finite lengths. The Kaiwara Road and State Highway 70 gravity profiles show the longitudinal cross sectional shapes and southern extents of the Wynyard and Western sub-basins respectively. It appears from the gravity that the Wynyard sub-basin extends only 2 km, approximately, to the south of Lowry Peaks Road, while the western sub-basin shallows and disappears onto a basement high under Culverden. Although a gravity line was not run down the axis of the central sub-basin, the southern limit of the basin occurs between the Palmside Road gravity profile, which shows the basin, and the Lowry Peaks Road that does not show the basin.

The development of the sub-basins has controlled the distribution of the aquifer-bearing units within Culverden Basin, which are the focus of the following discussion.

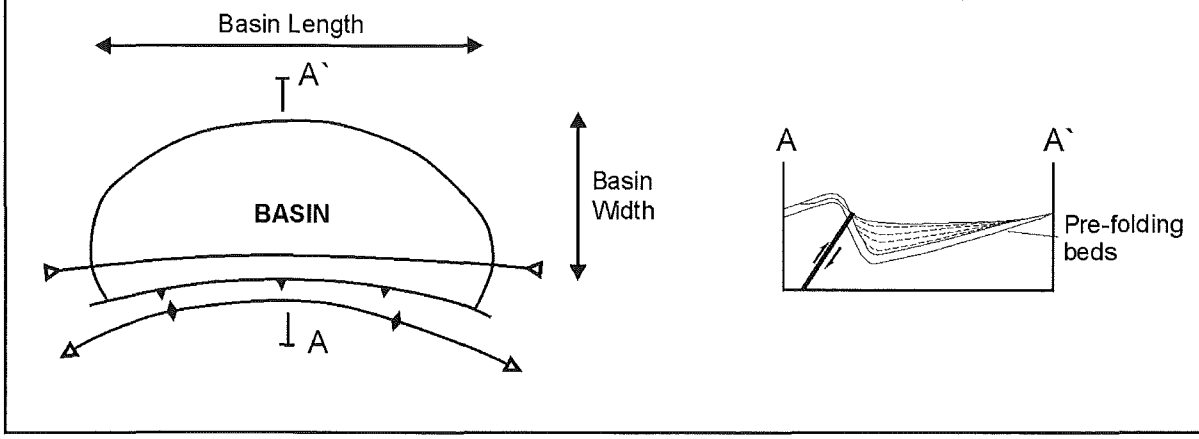

FIGURE 5.4. Schematic map and cross section showing the relationships between basin geometry, reverse (thrust) faulting and fault-related folding (from Nicol et. al., 1995).

5.3 HYDROSTRATIGRAPHY

Up until recent work (Loris, 2000) in the Waipara Basin, to the east of Culverden Basin, the Kowai Gravels were not considered an important source of groundwater. However, Loris's work showed the Kowai Gravels to have substantially higher yields than the overlying Late Quaternary fluvial gravels (2-20 l/s for the Kowai gravels versus 0.2-3 l/s for the fluvial gravels). Consequently, in the following discussions on the geological units that are important from a hydrological perspective, the Kowai Gravels will be included in the discussions. Consequently, the base of the Kowai Formation is considered the base of the groundwater resource.

The deposits that need to be considered in this discussion are the different gravel units found within the basin. The geological and geomorphological mapping, in conjunction with the TEM surveys, identified four gravel deposits: (i) the Kowai Gravels, (ii) the Burnham Formation, (iii) the eastern margin range-bounding alluvial fans, and (iv) the undifferentiated deposits modelled in the TEM transects.

5.3.1 Facies Distribution

The distribution of the different fluvial deposits has been strongly influenced by the tectonic structures described earlier. The development of the north Culverden Basin imbricate thrust system, including the Leonard Mound Fault System, has partitioned the basin into several smaller sub-basins (Figure 5.1 and 5.3). These sub-basins acted as the depositional centres for the Late Quaternary sedimentation, and have the greatest thickness of gravels, making them the obvious targets for groundwater exploration. For this discussion, the reader is referred to the structure contour and isopach maps of the aquifer-bearing units (Figure 5.3), which shows the distribution and thicknesses of those units.

5.3.1.1 Kowai Gravels

From the geophysical surveys, the Kowai Gravels appear to be the most extensive of the hydrostratigraphic units. In the TEM transects, the Kowai Gravels were only distinguishable from the Late Quaternary deposits to the west of Leonard Mound. To the east of Leonard Mound the alluvial fans and Kowai Formation apparently have a very similar electrical resistivity, making it impossible to distinguish the two. The TEM basin transects indicate that the Kowai Gravels underlie the Late Quaternary deposits and may be up to 150 m thick to the west of Leonard Mound. The thickness varies in response to the faulting and folding described earlier. The deepest occurrence of the Kowai Gravels is in the synclines associated with the faults. Although the TEM was unable to differentiate between the Kowai Gravels and the Lowry Peaks Range alluvial fan gravels, the Lowry Peaks Road and Palmside Road gravity profiles indicate that there may be 500 m of the deposits in the Wynyard sub-basin (Figure 5.3). In contrast, over the crest of the Isolated Hill Anticline, the Kowai Gravels are only 10-20 m thick, as shown in the Palmside Road TEM transect.

If the hydrologic properties of the Kowai Gravels are similar to those of Loris (2000), then the Kowai Gravels are potentially a large source of water. This is of particular interest along the eastern margin of the basin, away from the irrigation scheme, where the alluvial fans appear to be low yielding aquifers. However, as will be discussed shortly, groundwater recharge of the Kowai Gravels may be a severely limiting factor in their potential yields.

5.3.1.2 Burnham Formation

The Burnham Formation is readily identifiable geomorphologically by the presence of an extensive network of braid channels, visible on the aerial photographs. As is described in Chapter 3, the Burnham Formation occurs to the west of Leonard Mound, which clearly acted as a barrier to the Waiau River during the Late Pleistocene. The Waiau River was also hindered to the south by the Pahau River deposits, restricting the Waiau River derived Burnham Formation to the northern portion of the basin.

Electrically, the Burnham Formation was also readily identifiable in the TEM surveys, as it possessed a high electrical resistivity (>500 ohm-m) compared to the older gravels and the range-bounding alluvial fans. From the TEM surveys, the Burnham Formation forms a thin, extensive veneer of gravels, generally less than 50 m thick. The deposit is relatively uniform in thickness across the basin, suggesting that the Waiau River cut an extensive strath surface onto which the Burnham Formation was deposited. Even adjacent to the faults of the Leonard Mound Fault System, there is no appreciable thickening of the formation on the downthrown side of the faults, with the synclines having been infilled by older gravel deposits.

5.3.1.3 Range-bounding Fans

The structural maturity, combined with the highly eroded morphology of the central section of the Lowry Peaks Range, indicates that the range has been supplying gravel to the basin possibly for much of the Pleistocene through to the present. Four ages were recognised for the mapped fan surfaces. The oldest fans pre-date the Burnham Formation, have been displaced across the Leonard Mound Fault, are highly dissected, and are believed to form the composite surface to the west of Leonard Mound. They extend for a mappable distance of 4.5 km to the west of the Lowry Peaks Range. The uplift of the fans to the north of Palmside Road has preserved the fans, whereas to the south of Palmside Road, the streams draining the Lowry Peaks Range have eroded the majority of the fans. In contrast, the younger latest Pleistocene and Holocene fans are significantly smaller, and have been deposited onto the earlier fan deposits. The younger fans are restricted to the Wynyard sub-basin, and on the west side of Leonard Mound to the areas where the streams from the Lowry Peaks Range have managed to incise through the uplifting ridge.

5.3.1.4 Undifferentiated Deposits

The undifferentiated deposits were those in the Mount Palm Road and Palmside Road TEM transects that had an electrical resistivity of approximately 300 ohm-m. The undifferentiated deposits occur in the sub-basins (Figure 5.3) created on the downthrown side of the Leonard Mound and Isolated Hill faults, clearly reflecting the structural control on their distribution. A number of possibilities exist, outlined below, for the origin of the deposits.

1. Pre-Burnham Formation alluvial deposit

   During the Pleistocene the rivers flowing into the north end of the basin have been actively aggrading and degrading. As is described in Chapter 3, the aggradation and degradation cycles are controlled by the changing climatic conditions that characterise the Pleistocene. The geological mapping shows the presence of Windwhistle, Woodlands and Hororata deposits around the northern margin of the basin.

2. Lowry Peaks Range fans

   The Lowry Peaks Range has been supplying gravels into the basin for possibly much of the Pleistocene. The onset of each new glacial cycle, combined with periods of activity on the range-front faults, will produce a fresh injection of gravels into the system. At the southern end of Leonard Mound, the gravels have been deposited into the Wynyard sub-basin. To the north of Palmside Road, the streams draining the Lowry Peaks Range have been able to incise though the ridge, hence the fans have been deposited in the sub-basin that occurs on the downthrown block of the Leonard Mound Fault.

3. Colluvial gravels

   As with the Lowry Peaks Range, but on a smaller scale, periods of activity on the Leonard Mound and Isolated Hill faults, coupled with the degradation of the uplifted blocks by streams, will result in material being shed off the highs and deposited into the topographically low areas creating a wedge of localised fan gravels. There has clearly been significant erosion of the structural highs as shown on the geological mapping of Isolated Hill by the absence of the majority of the cover sequence, and the deeply eroded Torlesse basement.

4. Kowai Formation

   The deposits may represent a different facies within the Kowai Formation. The Kowai Formation is a diverse range of lithologies including gravels, sandstones and siltstones (Browne and Field, 1985). The higher resistivity measured for the undifferentiated deposits versus that measured for the Kowai Formation, indicates that the deposit may be a coarse grained facies of the Kowai Formation, with very few interbedded sandstones and siltstones.

5. Lake sediment

   The possibility exists that lakes formed in the tectonic depressions. Therefore, the undifferentiated deposit may well be an accumulation of fine lake sediment, with periodic slugs of coarse grained material during flood events.

Although it is unsubstantiated at the present time, it is the authors feeling that the undifferentiated deposits are a combination of possibilities 1, 2 and 3. Clearly, both the Lowry Peaks Range and the rivers have being depositing gravels into Culverden Basin during the Pleistocene. Leonard Mound and Isolated Hill have also been around long enough to be a source of the gravel, however, the volume of gravel will be substantially less than that from the Lowry Peaks Range. Whilst the other 2 options can not be ruled out, it is considered that the measured electrical resistivities of the undifferentiated deposits are too high to represent lake sediments.

5.3.2 Facies Relationships

The evolution of the hydrogeological model is a function of complex interfingering of distinct stratigraphic fluvial units. The coeval sedimentation and structural deformation has lead to a margin setting which is both complex and difficult to document in terms of subsurface geometries. Figure 5.1B (Volume 2) illustrates these complex spatial and temporal relationships with respect to the eastern margin of Culverden Basin, centred on Leonard Mound.

5.4 HYDROGEOLOGY

There are three components of the hydrologic system that should be considered in hydrogeological investigations:

Surface water - water found in rivers, streams, lakes, ponds and swamps,

Soil water - water found in the unsaturated (vadose) zone, and

Ground water - water located beneath the water table in an unconfined aquifer, or in a confined aquifer.

Whilst the groundwater is the main focus, the surface and soil waters are important as they will control the recharge to the groundwater, support the flora and fauna of the region, and surface water is a major pathway for contaminate transport. Each component has characteristics which need to be determined (Table 5.1), however, quantitative determination of the hydraulic properties of the three components (e.g. hydraulic conductivities, flow rates, transmissivity, storage capacities etc.) was not within the scope of this study. Work done prior to the irrigation scheme (Close, 1985 and 1987) looked at some of these properties and will be mentioned where appropriate. The properties that will be examined in detail are those that can be determined from the geological and geomorphic mapping of the area (e.g. recharge and discharge areas, drainage network, flow directions), focusing in particular on the eastern margin of the basin.

Table 5.1. List of the characteristics of each component of the hydrologic system.

Surface Water	**Soil Water**	**Groundwater**
Flowing water	Moisture content	Occurrence
Drainage area	Hydraulic conductivity of the soil	Recharge areas
Drainage pattern	Chemistry of the soil water	Flow direction and movement
Type of flow		Discharge zones
Discharge		Quality
Chemistry		
Standing water		
Origin of water		
Areal extent		
Depth		
Quality		

5.4.1 Surface Water

The Waiau River, flowing across the northern end of the Culverden Basin, is a very important source of water for the basin. Not only does it supply the majority of the natural recharge to the groundwater system of the northern portion of Culverden Basin, but it is also the source of water for the irrigation scheme, on which the dairy farming industry is so heavily reliant. The Waiau River is the largest of the rivers flowing into the basin, with an average flow of approximately 100 m^3/s. During storm events, such as those in August and October 2000, flow rates of 975 and 900 m^3/s, respectively, were recorded at the Marble Point recording station (Environment Canterbury), a few kilometres upstream of Culverden. By the time it reaches Culverden Basin has been joined by the Boyle, Hope and Lewis rivers, with the total catchment extending approximately 50 km to the west of Culverden to the crest of the Southern Alps, and is over 75 km wide at its widest point. The Hurunui River has an average flow rate of 25 m^3/s, and peaked at approximately 700 m^3/s during the August 2000 storm event.

The irrigation scheme, established in the late 1970's, is sourced from both the Waiau and Hurunui rivers, and forms the second largest volume of surface water in the basin. The intakes for both schemes are located where the rivers enter the basin (grid reference N32/937352 and M33/741234 for the Waiau River and Hurunui River respectively), and form an extensive network of canals. Excess irrigation, especially during the summer months, results in localised surface flooding, particularly along the western edge of Leonard Mound where the groundwater is very close to the surface.

Streams only form a minor component of the surface water of the area. As was shown in Chapter 3, the northern portion of the basin is noticeably devoid of streams. The streams that are present originate from the Lowry Peaks Range. Anecdotal evidence from the property owners along the range-front indicates that the streams are only active during storm events, such as those in August and October 2000. Throughout the course of the fieldwork as part of this study, it became apparent that during the months of October to March when the northwesterly winds prevail, rainfall is restricted to the foothills of the Southern Alps along the western margin of the basin. The Lowry Peaks Range and eastern margin of the basin received very little rainfall during that period. As a result of the warm dry northwesterly wind

and average daily temperatures during summer of 20°C, the water is rapidly lost from the system by evaporation and transpiration.

5.4.2 Groundwater

5.4.2.1 Aquifers

An aquifer is a geological unit that can both store and transmit water at rates fast enough to supply reasonable amounts of water (Fetter, 1980). Aquifers are classified as either confined or unconfined. An *unconfined*, or phreatic, aquifer (also termed a water table aquifer) is bounded by an upper phreatic surface (or water table), and is recharge by the downward percolation through the unsaturated zone. There may also be a component of recharge from lateral groundwater flow, or by upward leakage through a basal confining layer. A *perched aquifer* is a special case, where the groundwater is perched above an impervious layer, of limited lateral extent, in the zone of aeration. A *confined aquifer* is bounded from above and below by relatively impervious layers. Recharge for confined aquifers occurs either within the area of aquifer outcrop, or by slow leakage (upwards or downwards) through the confining layer(s).

At the start of this study, it was envisaged that the TEM and GPR would be used to map the aquifers and intervening aquitards, and examine the geometry of the aquifers. Unfortunately, as was shown in Chapter 4, the geophysical methods were not successful in this respect. Consequently, the only information pertaining to the aquifers comes from the bore logs of the wells throughout the basin, and the inferences made regarding the lithological facies relationships.

The aquifers occur in the glacial outwash deposits, range-bounding alluvial fans and the Kowai Formation. Historically, the upper unconfined aquifer of the Burnham Formation has been the main source of water for Culverden Basin. The major water-bearing units correspond to the old channels of the river and are typically composed of fresh, coarse, sandy gravels. Discontinuous layers of clay-bound gravels and clay are present and represent flood and overbank sediments deposited by a waning current. These fine grained layers will be acting as confining layers to the underlying aquifers. The upper aquifer is unconfined with the water

table located at the ground surface (adjacent to Leonard Mound) to a depth of 20 m near the Waiau River. A step drawn-down pump test of the unconfined aquifer (Close, 1985) determined transmissivity as 1960 m^2/day.

In the sub-basins, as is shown in Figure 5.1B, a very complex aquifer architecture is inferred to exist arising from the interaction between the sedimentation and the ongoing tectonic deformation. The eastern margin fans are thought to have low permeabilities, related to the higher fines content of the gravels. In conjunction, the low rainfall along the eastern margin of the basin, and high evapotranspiration rates during the summer, all point to the aquifers not yielding significant amounts of water. Consequently, as has been mentioned, the Kowai Gravels may well provide a source of water for the margin, if there is a thick enough sequence of the gravels. From Loris's (2000) work in the Waipara Basin, the Kowai Gravels were found to have transmissivities of 78 m^2/day and hydraulic conductivities of 6 m/day. The transmissivities were substantially higher than she recorded for the overlying Late Quaternary alluvial fans.

5.4.2.2 Recharge and Flow Direction

Recharge areas are those in which groundwater movement is downward, that is, away from the ground surface and toward the water table (Stone, 1999). Recharge areas are usually in topographic high places and there is often a deep unsaturated zone between the water table and land surface (Fetter, 1994). The recharge can be divided into two components: natural and artificial. Natural recharge is from sources such as precipitation, surface water inflow and groundwater inflow, whereas artificial recharge affects areas developed for agricultural, horticultural and domestic uses, with sources including irrigation, municipal water supplies, etc. The regional groundwater flow will generally mimic the regional topographic gradient, i.e. from topographic high areas to topographic low areas.

In Culverden Basin, there are three main sources of recharge (Figure 5.1C): precipitation, surface water inflow and irrigation. The Torlesse composed ranges bordering the basin, are considered to be major groundwater barriers, preventing the lateral migration of groundwater from adjacent basins. A piezometric contour map (Figure 5.5) by Close (1985), constructed prior to the irrigation scheme, indicates that the Waiau River was the main source of surface

water inflow, with a minor component from the streams. Close's piezometric shows that the groundwater flows from the Waiau River into the centre of the basin, at which point Leonard Mound splits the flow, with one branch flowing to the northeast to discharge into the Waiau River, and the other branch flowing southwards to discharge into the Hurunui River. The groundwater flow is mimicking the path the Waiau River took during the Late Pleistocene, as is evident from the Burnham Formation. Measurements made by Close indicate that the groundwater is flowing at a rate of 4 m/day.

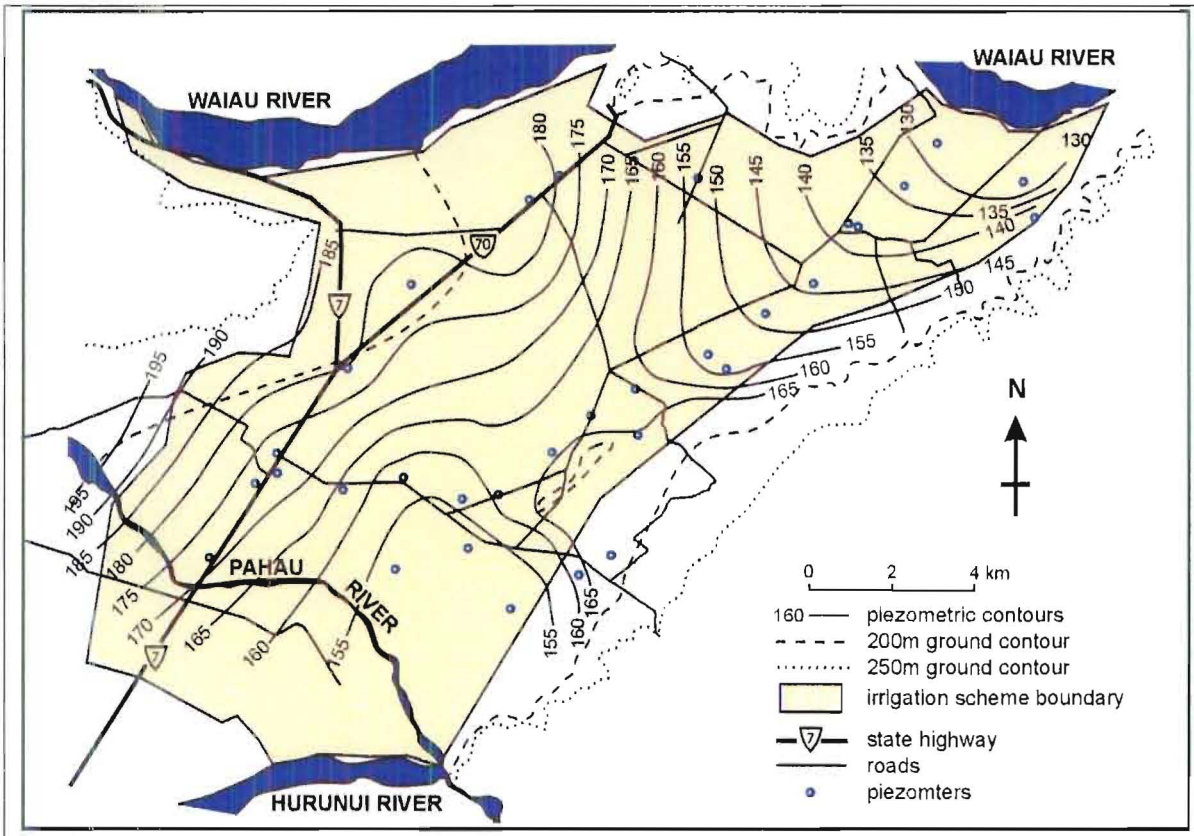

FIGURE 5.5. Piezometric contour diagram of north Culverden Basin (Close, 1985).

The main aim of Close's (1985 and 1987) studies, were to investigate the effects that the irrigation would have on the recharge and groundwater levels. Using a water balance model, Close calculated that for the years of 1976 to 1984 the recharge would have been on average 338 mm/yr without irrigation, and in excess of 700 mm/yr with the full implementation of the irrigation scheme. Close also showed that with the implementation of the irrigation scheme, the groundwater levels rise by on average 0.7 m/yr, and predicted that this would result in surface flooding of low lying areas. Close's models were based on an annual mean rainfall of

750 mm, that was an average of the Culverden, Lowry Hills and riverside meteorological stations. It is interesting to observe in Table 5.2, that for the Balmoral meteorological station, the mean monthly rainfall, for the years 1921-1975 (Southall and Rennie, 1975), varied very little. The controlling factor in the rate of recharge from percolation, is the rate of evapotranspiration, which varied greatly throughout the year. During the winter months when precipitation exceeds evapotranspiration, recharge from percolation occurs and in the summer months excess irrigation also results in percolating recharge to the groundwater.

Table 5.2. Monthly water balance, Balmoral Station, 1921-1975 (Southall and Rennie, 1977).

	J	F	M	A	M	J	J	A	S	O	N	D
Potential evapotranspiration (mm)	98	82	71	47	28	15	13	22	36	56	73	92
Rainfall (mm)	52	50	45	56	67	54	59	57	49	56	53	59
Run-off (mm)	2	2	4	5	19	23	40	36	21	15	5	7

Recharge to the sub-basins will be controlled by the aquifer connectivity between the sub-basins. Clearly, the Burnham Formation is providing a conduit for recharge into the central sub-basin (Figure 5.1C, Volume 2). In contrast, the blocking of the Waiau River during the Late Pleistocene by Leonard Mound, has removed that conduit to the Wynyard sub-basin. The amount of recharge into the Wynyard sub-basin will depend on the whether or not there are conduits through the uplifted ridge.

5.4.2.3 Discharge Zones

Discharge areas are places where groundwater flow is largely upward toward the water table or ground surface (Stone, 1999). Such areas will generally be associated with the lowest topographic point in an area, and there may be some physical manifestation of the discharging groundwater, which can take the form of a spring, seep, lake or stream. Changes in vegetation between the wet and dry areas will often highlight the discharge zones.

In the northern portion of Culverden Basin, the springs are found in the vicinity of Leonard Mound (Figure 5.1C). The main occurrence of the springs is along the western side of Leonard Mound, resulting from the interaction of the glacial outwash gravels and the Lowry Peaks Range fans, in conjunction with the disruption to the aquifers by the active tectonic

deformation. The springs were identified on the 1950's (pre-irrigation scheme) aerial photographs as the irrigation has resulted in surface flooding in the low-lying areas. Identification of the springs along the western side of Leonard Mound is further complicated as it is a topographic low zone, and is therefore the natural area for the surface water to accumulate, especially given the very low gradient of the surface.

Three types of springs have been recognised, and are shown on the hydrogeological model (Figure 5.1C). The first type of spring is the *depression spring*. In this case, the depression has been created by the footwall imbricate folds of the Leonard Mound Fault. The water table, which now sits very close to the surface as a consequence of the irrigation scheme, intersects the ground surface on the downthrown side of the folds. The ponding of the water highlights the deformation. The Southern 1 GPR profile, run across one of these low zones off the southern end of Leonard Mound, clearly shows the water table intersecting the surface. The springs occurring along the Boundary Fault are examples of the *fault springs*. The uplift of the impermeable Mount Brown Formation on the eastern side of the fault has acted as a barrier to the groundwater, forcing it to the surface. The third type of spring is the *contact spring*, which occur in two locations: (i) along the interface of the Burnham Formation and Lowry Peaks Range fans, and (ii) along the contact of the Lowry Peaks Range fans and the uplifted strata of the southern end of Leonard Mound. Seepages also occur at the interfaces of the fans in the Wynyard sub-basin, and are the source for some of the streams in the Wynyard sub-basin.

5.5 CONCLUSIONS

The hydrogeological model developed for north Culverden Basin has implications not only for the farmers of Culverden Basin, especially those along the eastern margin of the basin, but also for the evaluation of groundwater resources in other basins in active tectonic settings.

5.5.1 Implications of the Hydrogeological Model for Culverden Basin

With the development of the irrigation scheme, and the high recharge to the shallow unconfined aquifer within the Burnham Formation, the farmers to the west of Leonard Mound will probably never need to locate a deep source of groundwater. A stark contrast in land use occurs between the irrigated areas and the non-irrigated areas of the basin. Along the eastern

margin of the basin, land use is still restricted to the low water using sheep and cattle grazing. The region is also still subjected to frequent summer droughts, making it desirable to locate a good sustainable source of water for the region.

As mentioned earlier, Loris's (2000) work to the east in the Waipara Basin, documented relatively high water yields from the Kowai Gravels compared to the alluvial deposits, as well as showing the permeabilities of the alluvial deposits increases with depth. If this is also true for the Wynyard sub-basin, then the deeper aquifers may potentially be a viable source of water for the margin. However, the issue that needs to be resolved is whether or not there is sufficient recharge to those aquifers. As is seen in the model (Figure 5.1C), the recharge to the Wynyard sub-basin is going to be primarily controlled by the amount of water able to get into the sub-basin from the high yielding Burnham Formation. Clearly, this needs to be addressed further, and ideally a deep borehole needs to be drilled to test the aquifer properties.

Although the irrigation scheme has removed the need for the farmers to the west of Leonard Mound to locate a deep source of groundwater, two concerns are raised regarding the ongoing effects of the irrigation scheme. The first is the surface flooding caused by excessive irrigation. Along the low-lying boundary between the Burnham Formation and the Lowry Peaks fans, it is not uncommon to observe water ponding on the surface. The paddocks have been border dyked to reduce the flooded area as much as possible. The second concern is the effects of the irrigation on the nitrogen levels in the soil. High nitrate levels in groundwater have been recognised as a public health risk (WHO, 1971). Irrigation leads to the leaching of solutes from the soil to the groundwater system deteriorating the groundwater quality (Close, 1987). In this case, the leached nitrogen is derived mainly from the urine patches from grazing animals. Close's study showed that there was no significant change in the nitrogen levels during the first four years of the irrigation scheme. In the proceeding 16 years there has been no monitoring of the water quality to check the nitrogen levels.

5.5.2 Application of Selected Geophysical Techniques to Hydrogeological Investigations

The geophysical surveys had two primary goals:

1. to map the base of the gravel aquifer sequence and any faults or other structural features, and

2. to delineate the main aquifers.

These goals can, in essence, be redefined in terms of the targets: the geological structure and the hydrogeology. To a large extent the first goal was met, but the second was not, and the purpose of this section is to summarise the utility of geophysical surveying, specifically gravity, time-domain EM (TEM), and ground-penetrating radar (GPR), within the North Canterbury context.

All geophysical methods are sensitive to contrasts in the subsurface physical properties. In the case of gravity, the property is the density; for TEM, it is the electrical resistivity; and for GPR, it is the dielectric permittivity and, to a lesser extent, the electrical conductivity. Each of these physical properties, in turn, depend to varying degrees on the water content, water quality, and lithology. It is then the size of the target and the degree of physical property contrast that determines the success or failure of a geophysical survey technique.

1. Hydrogeology - Aquifers and Aquitards

Because geophysical methods respond best to large clear contrasts in the subsurface physical properties, and because of the inherent limitation on the resolution of subsurface features, the geophysical surveys were less successful in mapping the hydrogeological boundaries of the Culverden Basin. This is consistent with the results from other North Canterbury fluvial and alluvial gravels, in particular in the nearby Waipara region (Loris, 2000).

The GPR surveys should have yielded much greater depth of penetration than observed, given the relatively high electrical resistivities (of the order of 100's of ohm-m) and the nature of the material (gravels and sandy gravels). Significant depth of penetration has been observed in such sequences elsewhere in New Zealand, including the West Coast of New Zealand (Yetton and Nobes, 1999), and in worldwide (e.g. Smith and Jol, 1995; Liner and Liner, 1997; Gross et. al., 2000; Jol et. al., 2000; Madeira et. al., 2000; Liner and Liner, 2000). However, as discussed earlier, the depth of penetration in the gravel sequences of Culverden Basin has been poor, which is consistent with results obtained over the Canterbury Plains (Bal, pers. comm., 1999) and the nearby area of Omihi (Nobes, pers. comm., 1999). This is an issue that, as noted earlier, bears more examination.

In Culverden Basin, the aquifer sequences are composed of gravels and sandy gravels, whereas the aquitards are silts (not "clay" as many drillers' logs may indicate) and sandy silts. Thus, the density contrasts are not sufficient nor is there significant topographic variation on the aquifer boundaries to yield more than minor gravity variations. Gravity was useful, however, for determining the depth to the underlying Mt Brown formation, which acts as the local hydrogeological basement, and for mapping the locations of major fault boundaries, which can act either as conduits or barriers for flow in the basin.

Similarly, TEM was successful at delineating the depth to the base of the gravel formations (e.g. Burnham Formation, Kowai Gravels), but not in delineating individual gravel aquifers within each formation. The electrical properties of the units are a function of the clay content, water content and water quality. Each aquifer is too thin, or too lacking in electrical contrast with the layers above and below, to be resolved using TEM.

2. Delineation of Geological Boundaries

Geological boundaries tend to be larger-scale features, and the techniques that worked best in Culverden Basin - gravity and TEM - are governed by larger-scale variations in the physical properties. While GPR did show some near-surface structure, its lack of penetration is puzzling, and, as outlined in the summary of the geophysical surveying chapter, more work is needed to determine why GPR penetration is extremely limited in Culverden Basin, and indeed in much of the North Canterbury fluvial and alluvial gravel sequences.

The gravity surveys delineated the topography of the Tertiary Mt Brown sequence, in large part because of the density contrast between the gravels above and the limestone below. This is also the case for the faults that have been inferred from the gravity results, consistent with the TEM results, and confirmed in many cases by the geomorphology and geological mapping. The gravity modelling is restricted in its utility, to some extent, because of the inherent non-uniqueness of the method, and the lack of constraints on the densities and thicknesses of the subsurface units. Whilst the TEM was able to constrain the thicknesses of the gravels in some locations, there was no information pertaining to the Tertiary sequence or Torlesse basement, preventing the development of a more accurate picture of the basement depth and structure.

TEM was also successful in delineating the boundary between the gravels and the underlying Tertiary sequence, in this case because of the contrast in the electrical properties. The sandy/silty gravels, filled with fresh water, are more electrically resistive than the underlying Mt Brown limestones and mudstones. Poor data in TEM soundings result from either a very electrically resistive medium, so that the current dissipates before it can be measured, or from the lack of lateral continuity of the layers. Very high electrical resistivities generally occur in very dry, very course glacial deposits and not in water saturated sandy/silty gravels as are present in the North Canterbury environment. Consequently, a noisy TEM response, in the absence of a cultural source, appear to be correlative with the presence of subsurface structure. This is supported by the gravity surveys and the geomorphological mapping.

5.5.2.1 Recommendations

As can be seen in the above discussion, the TEM and gravity generally worked well for delineating the geological boundaries, but not for the identification and mapping of the aquifers. The GPR showed its potential to be useful in hydrogeological studies, but the poor depth of investigation severely restricted its use in this study. It is questionable as to whether other techniques, such as seismic reflection, would be able to adequately delineate the aquifers given the complex facies relationships. However, a seismic reflection survey would be very beneficial for (A) gaining a better understanding of the complex relationships between the tectonic deformation and the fluvial architecture, and (B) for determining the thicknesses of the aquifer bearing deposits, in particular the Kowai Gravels in the Wynyard sub-basin . The main drawbacks with seismic reflection surveying are the time taken to acquire and process the data, and the consequent expense involved. Consequently, it is recommended for future geophysical investigations of the hydrogeology of Culverden Basin, that seismic reflection surveys are performed in the areas highlighted by this study.

5.5.3 Broader Implications of Model to Groundwater Resources in Active Tectonic Settings

The geometry and evolution of the Culverden Basin and the stages which can be recognised in the inversion of the basin (Figure 5.1), together with the controls these processes exert on the distribution of sediments (Figure 5.3) and basin hydrology have wider implications for many

New Zealand basins and analagous active convergent regimes. Basin inversion has been widely described and documented, mainly driven by the petroleum industry where the focus is on basins where thick sediments are still preserved at the relatively early stages. Because the later stages of uplift, exhumation and erosion of the basin contents are no longer prospective, this is less well documented, but this is the stage where the interplay of climatically controlled cycles of sedimentation and the emergent structures on the margins and floor of the basin become critical in controlling both the surface hydrology and the architecture and character of subsurface aquifers. While there has been widespread recent research on the geomorphic response of rivers to ground deformation, the literature on the practical implications for water resources and in particular groundwater is minimal.

There are essential characteristics of the inversion process, illustrated by the Culverden model which are likely to be common to many basins at a similar stage of evolution. Each impacts on the tectonic controls on sedimentation in specific ways. These can be broadly categorised as follows.

1. *Uplift of the basin margins*

- Initially defines the transition from regional to basin controlled sedimentation
- Initiates the growth of alluvial fans along the margins which interfinger and transgress out from the margin with time.
- Controls the location of both inlet, and particularly outlet locations for river systems entering the basin, and because the margins are rarely defined by a single fault fold system, the switching of episodes of fold and fault growth the low points where the sysems overlap mean that the drainage pattern may be radically altered during the life of the basin. In turn the sediments and sedimentary facies associated with the rivers may be distributed in distinctive packets on the basin floor relating to the duration of a particular drainage pathway.
- Not withstanding these effects, the early stages of basin fill may be expected to consist of relatively thick bodies of fluvial gravels with widespread distribution of individual gravel facies and well constrained pathways for the flow of groundwater in relation to former channels.
- Importantly the nature of the sediments preserved below the true basin sediments, inherited perhaps from more widespread sheets of gravel reflecting the onset of regional

convergence (in this case the Kowai gravels) may also be important as possible aquifers, but clearly local conditions may determine whether equivalant sediments exist and the their potential as an aquifer target would need to be assessed. Their limitation may be in the potential for recharge, particularly when subsequent burial and disruption by growing structures breaks up the original continuity and connection to potential recharge sites.

2. *Uplift of the basin ends*

- potentially recycles basin contents down the axis of the basin into the remaining depocentres and develop longitudinal drainage into the ends of the basin.
- tends to divert rivers which once crossed the basin ends into the middle to find new outlets, particularly when flushes of aggradation allow lateral avulsion out of the existing channel.
- progressively confines sediments to the central part of the basin.

3. *Uplift of the basin floor*

- The fundamental mechanism of inversion is the imbrication of the primary thrust system, by footwall propagation of thrust splays associated with fault propagation anticlines.
- The stages of emergence and the fact that uplift does not occur uniformly along strike are reflected in the facies distribution and drainage systems both aerially and up through the sedimentary succession.
- The fundamental effect is of the evolution of sub basins within the larger basin, and increasingly complexity in the interrelationship of facies, the reduction in the volume and area occupied by any one lithology and time transgressive, onlap relationships of individual units, not only across the individual basins, but along strike where continuity between sub basins may be maintained around the tips of the structures.
- Crucial to the nature of the sub basin fills is the balance between regional base level (which will be gradually dropping because of the general uplift associate with crustal thickening and convergence) the short term, overwhelming base level adjustment associated with climatically controlled flushes of sedimentation, and the local effects of the sub floor deformation.
- Over the emergent basin in general and the uplifting folds and fault blocks, there will increasingly widespread removal of older gravels with each glacially driven increase in both stream power and sediment flux when the rivers spill over the channels cut during

interglacials. Only in the synclinal basins and on uplifted margins are the older Pleistocene gravels likely to be preserved.

- As interglacial conditions return there is a critical relationship between the rate of local relative subsidence in the sub basins and the overall drop in base level. If the two rates are similar, downcutting may not take place and streams will continue to occupy the aggradation surface, reworking and modifying the surface, introducing finer grained sediments and possibly forming local swamp filled depressions and channels. Particularly if slow aggradation continues, the hydraulic characteristics of the glacial aggradation gravels may become highly modified and limited in their aquifer potential, as has been the case in the Omihi basin. Deposits of this type will be difficult to characterise using geophysical methods.
- The irregularities evolving under the gravel cover, may cause not only very thin, or lensoid aquifers to develop, but also to control the flow of groundwater by forming barriers. A major problem with this environment is the potential to isolate gravel bodies which may intially appear to provide a good water supply, but are cut off from a source of recharge.

The implications of this study are based on Culverden Basin, but show the effects of basin inversion and climatically controlled cycles of deposition on the fluvial architecture, and consequently the hydrogeology, of basins located within active tectonic settings.

REFERENCES

Annan, A.P., and S.W. Cosway. Ground penetrating radar survey design, presented at the *Symposium on the Application of Geophysics to Engineering an Environmental Problems (SAGEEP)*, Chicago, Illinois, 1992.

Andrewa,P.B., 1960. Sedimentary history of the Lower most Otaian horizon in North Canterbury, New Zealand. Unpubl. MSc. Thesis, University of Canterbury Library 129 pp.

Andrews, P. B., 1962, Stratigraphic nomenclature of the Omihi and Waikari Formations, North Canterbury: *New Zealand Journal of Geology and Geophysics, v. 6, p. 228-256.*

---, 1963, Stratigraphic nomenclature of the Omihi and Waikari Formations, North Canterbury: *New Zealand Journal of Geology and Geophysics, v. 6, p. 228-256.*

---, 1968. Patterns sedimentation during Early Otaian (Early Miocene) time. N. Z. J. Geol. *Geophys. 11: 711-752.*

Andrews, P. B., Speden, I. G., and Bradshaw, J. D., 1976, Lithological and paleontological content of the Carboniferous-Jurassic Canterbury suite, South Island, New Zealand: *New Zealand Journal of Geology and Geophysics, v. 19, no. 6, p. 791-819.*

Andrews, P. B., 1967, Patterns of sedimentation during early Otaian (Early Miocene) time in North Canterbury, New Zealand: *New Zealand Journal of Geology and Geophysics, v. 11, no. 3, p. 711-752.*

Arabasz, W. J., and Robinson, R., 1976, Microseismicity and geologic structure in the northern South Island, New Zealand: *New Zealand Journal of Geology and Geophysics, v. 19, no. 5, p. 569-601.*

Armstrong, M. J., 1993, Geophysical mapping of the leachate plumes emanating from the Burwood and Kaiapoi landfills: B.Sc. Honours Thesis, University of Canterbury, Christchurch, New Zealand.

Avouac, J. P., 1993, Analysis of scarp profiles: Evaluation of errors in morphological dating: *Journal of Geophysical Research, v. 98, no. B4, p. 6745-6754.*

Bal, A. A., 1994. To TEM or not to TEM: That is the question: Geological Society of New Zealand Annual Conference, v. Programme and Abstracts, p. 25.

Barnes, P. M., 1993. Structural Styles and sedimentation at the southern termination of the Hikurangi Subduction Zone, offshore North Canterbury, New Zealand. Unpub. Ph.D. Thesis, University of Canterbury Library, Christchurch, New Zealand 211 pp.

Barnes, P., 1996, Active folding of Pleistocene unconformities on the edge of the Australian-Pacific plate boundary zone, offshore North Canterbury, New Zealand: *Tectonics, v. 15, no. 2, p. 623-640.*

Berberian, M., 1995, Master "blind" thrust hidden under the Zagros folds: active basement tectonics and surface morphotectonics: *Tectonophysics, v. 241, p. 193-224.*

Berger, Z., and Aghassy, J., 1982, Near-surface groundwater and evolution of structurally controlled streams in soft sediments, in LaFleur, ed., Groundwater as a geomorphic agent: Boston, Allen and Unwin, p. 390.

Berry, M. E., 1990, Soil catena development on fault scarps of different ages, eastern escarpment of the Sierra Nevada, California: *Geomorphology, v. 3, p. 333-350.*

Berthe, D., and Brun, J. P., 1980, Evolution of folds during progressive shear in the South Armorican Shear Zone, France: *Journal of Structural Geology, v. 2, no. 1/2, p. 127-133.*

Bibby, H. M., 1976, Crustal strain across the Marlborough faults, New Zealand: New Zealand *Journal of Geology and Geophysics, v. 19, no. 4, p. 407-425.*

Bibby, H.M. 1981. Geodetically determined strain across the southern end of the Tonga-Kermadec
Hikurngi Subduction Zone. *Geophys.J.R .Astr. Soc. 66: 513-533.*

Birkeland, P. W., 1990, Soil-geomorphology research-a selective overview: *Geomorphology, v. 3, p. 207-224.*

Bishop, D. G., J.D. Bradshaw and C.A. Landis, 1985. Provisional Terrain map of the South Island, New Zealand. In; Tectonostratigraphic Terrains in the Circum-Pacific Region p 515-521 D. G. Howell (ed) Circum-Pacific Council for Minerals and Energy, Houston, Texas.

Bishop, D. G., 1968, The geometric relationships of major structural features associated with major strike-slip faults in New Zealand: *New Zealand Journal of Geology and Geophysics, v. 11, no. 2, p. 405-417.*

Blick, G. H., Read, S. A. L., and Hall, P. T., 1989, Deformation monitoring of the Ostler Fault Zone, South Island, New Zealand: *Tectonophysics, v. 167, p. 329-339.*

Boggs, S., 1984, Principles of sedimentology and stratigraphy: Columbus, Ohio, Merrill Publishing Company.

Boggs, S. J., 1987, Principles of sedimentology and stratigraphy [2nd ed.]: New Jersey, Prentice Hall, 691 + appendices p.

Boyer, S. E., and Elliot, D., 1982, Thrust systems: The American Association of Petroleum *Geologists Bulletin, v. 66, no. 9, p. 1196-1230.*

Bradshaw, J. D., 1971, Stratigraphy and structure of the Torlesse Supergroup (Triassic-Jurassic) in the foothills of the Southern Alps near Hawarden (S60-61), Canterbury: *New Zealand Journal of Geology and Geophysics, v. 15, no. 1, p. 71-87.*

---, 1975, The folds at Castle Hill (Canterbury) and their bearing on Kaikouran deformation style in the Canterbury Basin: *Journal of the Royal Society of New Zealand, v. 5, no. 2, p. 209-217.*

Bradshaw, J. D., and Newman, J., 1979, Low-angle thrusts in Cenozoic rocks in Canterbury, New Zealand: New Zealand Journal of Geology and Geophysics, v. 22, no. 4, p. 435-442.

Bradshaw, J.D., 1989: Cretaceous Geotectonics Patterns in the New Zealand Regions. *Tectonics, 803-820.*

Brown, S.P. and J.H. Spang, 1978. Geometry and mechanical relationships of folds to thrust propagation using a minor thrust in the Front Ranges of the Canadian Rocky Mountains. *Bull.Can.Petr.Geol. 26:551-571*

Brown, L. J., and Wilson, D. D., 1988, Stratigraphy of the Quaternary deposits of the northern Canterbury Plains, New Zealand: *New Zealand Journal of Geology and Geophysics, v. 31, p. 305-335.*

Browne, G. H., 1984a: The Balmoral Forests Inlier, North Canterbury. Immediate Report, New Zealand Geological Survey.

Browne, G.H., 1984b: Geological features related to the excavation in early 1984 of the Balmoral Irrigation Scheme Race, Green Hill, North Canterbury. Immediate Report, New Zealand Geological Survey.

Browne, G. H., 1992, The northeastern portion of the Clarence Fault: tectonic implications for the late Neogene evolution of Marlborough, New Zealand: *New Zealand Journal of Geology and Geophysics, v. 35, p. 437-445.*

Browne, G. H., and Field, B. D., 1985, The lithostratigraphy of late Cretaceous to early Pleistocene rocks of Northern Canterbury, New Zealand: New Zealand Geological Survey Record 6.

---, 1988. A review of Cretaceous-Cenozoic sedimentation and Tectonics, East Coast, South Island, New Zealand. In : Sequences, Stratigraphy, Sedimentology; surface and sub-surface. D.P. James.D.A. Leckie (eds). *Can. Soc. Petrol. Geol. Mem. 15: 37-48.*

Bull, W. B., 1990, Stream-terrace genesis: implications for soil development: *Geomorphology, v. 3, p. 351-367.*

---, 1991, Geomorphic response to climatic change: Oxford, New York, Oxford University Press.

Bull, W. L., and Knuepfer, P. L. K., 1987, Adjustments by the Charwell River, New Zealand, to uplift and climatic changes*: Geomorphology, v. 1, p. 15-32.*

Bull, W. B., 1984, Tectonic geomorphology: *Journal of Geological Education, v. 32, p. 310-324.*

Bull, W. B., and Cooper, A. F., 1986, Uplifted marine terraces along the Alpine Fault, *New Zealand: Science, v. 234.*

Bull, W.B., 1977b. Tectonic geomorphology of the Mojave Desert: US. Geological Survey Contract Report 14-08-001-G-394; Office of Earthquakes , Volcanoes and Engineering, Menlo Park, California. 188 pp.

Bunting, B. T., 1961, The role of seepage moisture in soil formation, slope development, and stream initiation: *American Journal of Science, v. 259, p. 503-518.*

Burnett, A. W. S. A. Schumm, 1983. Alluvial –River respone to Neotectonic deformation in Louisianna and Mississippi. *Science 222: 49-50*

Busby, J. P., and Merrit, J. W., 1999, Quaternary deformation mapping with ground penetrating radar: *Journal of Applied Geophysics, v. 41, p. 75-91.*

Butler, R. W. H., 1982, The terminology of structures in thrust belts: *Journal of Structural Geology, v. 4, no. 3, p. 239-245.*

Butler, R. W. H., and Grasso, M., 1993, Tectonic controls on base-level variations and depositional sequences within thrust-top and foredeep basins: examples from the Neogene thrust belt of central Sicily: *Basin Research, v. 5, p. 137-151.*

Campbell, J. K. and H. S. Yousif, 1985. Tectonic geomorphology of the Lower Waipara Gorge, North Canterbury. *Geol. Soc. Misc. Publ. 32b: 53-65.*

Cant, D.J., 1982, Fluvial facies models and their applications, in P.A. Scholle and D. Spearing (eds.), Sandstone depositional environments: Am.Assoc. Petroleum Geologists Mem. 31, p 115-138

Cai, J., McMechan, G. A., and Fisher, M. A., 1996, Application of ground-penetrating radar to investigation of near surface fault properties in the San Francisco Bay region: *Bulletin of the Seismological Society of America, v. 86, p. 1459-1470.*

Campbell, M. R., 1896. Drainage modifications and their interpretation. *J. Geol. 4: 567-581*

Carter, R. M., and Carter, L., 1982, The Motanau Fault and other structures at the southern edge of the Australian-Pacific Plate boundary, offshore Marlborough, New Zealand: *Tectonophysics, v. 88, p. 133-159.*

Chorley, R. J., 1957, Climate and morphometry: *Journal of Geology, v. 65, p. 628-638.*

Clark, G. M., 1989, Central and Southern Appalachian water and wind gap origins: review and new data: *Geomorphology, v. 2, p. 209-232.*

Clayton, L., 1968, Late Pleistocene glaciations of the Waiau Valleys, North Canterbury: *New Zealand Journal of Geology and Geophysics, v. 11, no. 3, p. 753-767.*

Clayton, L. S., 1965, Late Pleistocene geology of the Waiau Valleys, North Canterbury, New Zealand: Ph.D. Thesis, University of Illinois, 93 p.

Clayton, L., 1966, Tectonic depressions along the Hope Fault, a transcurrent fault in North Canterbury, New Zealand: *New Zealand Journal of Geology and Geophysics, v. 9, p. 95-104.*

Close, M. E., 1985, Simulating the effects of the Waiau irrigation scheme on recharge and groundwater levels: *Journal of Hydrology, v. 24, p. 49-63.*

---, 1987, Effects of irrigation of water quality of a shallow unconfined aquifer: *Water Resources Bulletin, v. 23, no. 5, p. 793-802.*

Cobbald, P. R., and Quinquis, H., 1980, Development of sheath folds in shear regimes: *Journal of Structural Geology, v. 2, no. 1/2, p. 119-126.*

Cook, F. A., 1988, Proterozoic thin-skinned thrust and fold belt beneath the Interior Platform in northwest Canada*: Geological Society of America Bulletin, v. 100, p. 877-890.*

---, 1995, Proterozoic thin-skinned thrust and fold belt beneath the interior Platform in northwest Canada: *Geological Society of America Bulletin, v. 100, p. 877-890.*

Coote, A., 1987; Cenozoic volcanism in the Waiau area, North Canterbury. Unpubl. MSc. Thesis, University of Canterbury, Christchurch, New Zealand

Cotton, C, C. A., 1913. The physiography of the Middle Clarence Valley, New Zealand. *Geography Journal. 42: 225-245.*

---1938. Some penepanations in Otago, Canterbury and the North Island of New Zealand. *N.Z. Sci. Tech. 20b: 1-8*

Couzens, B. A., and Dunne, W. M., 1994, Displacement transfer at thrust terminations: the Saltville thrust and Sinking Creek anticline, Virginia, USA: *Journal of Structural Geology, v. 16, no. 6, p. 781-793.*

Cowan, H. A., 1989. An evaluation of the Late Quaternary Displacements and seismic hazard associated with the Hope and Kakapo Faults, Amuri District, North Canterbury, New Zealand. Unpubl. MSc. Thesis, University of Canterbury Library, Christchurch, New Zealand 213-pp.

Cowan, H. A., 1990, Late Quaternary displacements on the Hope Fault at Glynn Wye, North Canterbury: *New Zealand Journal of Geology and Geophysics, v. 33, p. 285-293.*

Cowan, H.A., 1992, Structure, seismicity and tectonics of the Porters Pass-Amberley Fault Zone, North Canterbury. Unpubl. Ph.D. Thesis, University of Canterbury Library, Christchurch, New Zealand 181 pp.

Dahlstrom, C. D. A., 1990, Geometric constraints derived from the law of conservation of volume and applied to evolutionary models for detachment folding: *The American Association of Petroleum Geologists Bulletin, v. 74, no. 3, p. 336-344.*

Davey, F. J., Hampton, M., Lewis, K., and Pettinga, J. R., 1986, Structure of a growing accretionary prism, Hikurangi margin, New Zealand: *Geology, v. 14, p. 663-666.*

Davis, J. L., and Annan, A. P., 1989, Ground penetrating radar for high resolution mapping of soil and rock stratigraphy*: Geophysical Prospecting, v. 27, p. 531-551.*

Davis, T. L., Namson, J., and Yerkes, R. F., 1989, A cross section of the Los Angeles area: seimically active fold and thrust belt, the 1987 Whittier Narrows earthquake, and earthquake hazard*: Journal of Geophysical Research, v. 94, no. B7, p. 9644-9664.*

De Mets, C., R. G. Gordon, D. F. Argus and S. Stein, 1990. Current plate motions. Geophys. *J. Int. 101: 425-428*

Deffontaines, B., P. Chotin, L. Ait Brahim and M. Rozanov, 1992. Investigation of active faults in Morrocco using morphometric methods and drainage pattern analysis. *Geologishe Rundschau 81: 199-210.*

Dibble, R.R. 1973. Unpublished: Gravity Data, with Map and cross sections from the Culverden Basin Area, North Canterbury

Dittmar, D., Meyer, W., Oncken, O., Schievenbusch, T., Walter, R., and von Winterfeld, C., 1994, Strain partitioning across a fold and thrust belt: the Rhenish Massif, Mid-European Variscides: *Journal of Structural Geology, v. 16, no. 10, p. 1335-1352.*

Dunne, T., 1980, Formation and controls of channel networks: Progress in Physical Geography, v. 4, p. 211-239.

Elliot, D., 1976. The Energy Balance and Deformation mechanisms of thrust sheets. Phil. Tranz. Roy. Soc. Lond. A 283: 289-312.

Endharto, M. A., 1987, Upper Cretaceous-Tertiary geology of the Wandle river-Whales Back area, northern Waiau, North Canterbury: Unpublished M.Sc. Thesis, University of Canterbury, Christchurch, New Zealand.

Erickson, S. G., 1996, Influence of mechanical stratigraphy on folding vs faulting: *Journal of Structural Geology, v. 18, no. 4, p. 443-450.*

Falloon, A.S., 1954. Geology of the Culverden Basin, North Canterbury, North Canterbury, New Zealand. Unpubl. MSc Thesis , University of Canterbury Library, Christchurch, New Zealand.

Fetter, C. W., 1994, Applied hydrogeology [third ed.]: London, Prentice-Hall, Inc.

Field, G. M., 1999, Test of a buried seacliff model using geophysical survey methods, Canterbury Plains, New Zealand: B.Sc (Honours) Unpublished Thesis, Department of Geological Sciences, University of Canterbury, Christchurch, New Zealand.

Field, B. D. and G.H. Browne, 1989. Cretaceous and Cenozoic sedimentary basins and geological evolution of the Canterbury Region, South Island, New Zealand. N.Z. Geol. Surv. Basin Studies
2. New Zealand. Geological Survey, Lower Hutt. 94 pp.

Fillipone, J. A., and Yin, A., 1994, Age and regional tectonic implications of Late Cretaceous thrusting and Eocene extension, Cabinet Mountains, northwest Montana and northern Idaho: The American Association of Petroleum Geologists Bulletin, v. 106, p. 1017-1032.

Fischer, M. P., Woodward, N. B., and Mitchell, M. M., 1992, The kinematics of break-thrust folds: *Journal of Structural Geology, v. 14, no. 4, p. 451-460.*

Fitterman, D. V., 1989, Detectability levels for central induction transient soundings: *Geophysics, v. 54, no. 1, p. 127-129.*

Fitterman, D. V., and Stewart, M. T., 1986, Transient electromagnetic sounding for groundwater: *Geophysics, v. 51, no. 4, p. 995-1005.*

Fitzgerald, M. G., Mitchum, R. M., Uliana, M. A., and Biddle, K. T., 1990, Evolution of the San Jorge Basin, Argentina: The American Association of Petroleum Geologists Bulletin, v. 74, no. 6, p. 879-920.

Fyfe, H.E., 1934: Amuri Subdivision. *New Zealand Geological Survey annual report 28*: 4-5

Gamond, J. F., 1994, Normal faulting and tectonic inversion driven by gravity in a thrusting regime: *Journal of Structural Geology, v. 16, no. 1, p. 1-9.*

Gardner, T. W., 1989, Neotectonism along the Atlantic passive continental margin: a review: *Geomorphology, v. 2, p. 71-97.*

Garlick, R. D., 1992, Lees Valley Fault, North Canterbury: Unpublished BSc (Hons) project, University of Canterbury, Christchurch, New Zealand. 86 p.

Ge, S., and Garven, G., 1989, Tectonically induced transient groundwater flow in foreland basin, in Origin and evolution of sedimentary basins and their energy and mineral resources.

Gillespie, P. A., Walsh, J. J., and Watterson, J., 1992, Limitations of dimension and displacement data from single faults and the consequences for data analysis and interpretation: *Journal of Structural Geology, v. 14, no. 10, p. 1157-1172.*

Gomez, F., Barazangi, M., and Bensaid, M., 1996, Active tectonism in the intracontinental Middle Atlas Mountains of Morocco: synchronous crustal shortening and extension: *Journal of the Geological Society, London, v. 153, p. 389-402.*

Gregg, D. R., 1964, Sheet 18 Hurunui. Geological Map of New Zealand 1:250,000: Department of Scientific and Industrial Research, Wellington, New Zealand.

---, 1978, North Canterbury, in Suggate, R. P., Stevens, G. R., and Te Punga, M. T., eds., The Geology of New Zealand: Wellington, Government Printer, v. 2, p. 503-510.

Gregg, R. C., 1965, The pre-Quaternary geology of an area around Waiau, North Canterbury: Unpublished M.Sc. Thesis, University of Canterbury, Christchurch, New Zealand.

Gross, R., Holliger, K., Greem, A., and Begg, J., 2000, 3D ground penetrating radar applied to paleoseismology: examples from the Wellington Fault, New Zealand, in Noon, D. A., Glen, F., and Stickley, D. L., eds., Eighth International Conference on Ground Penetrating Radar: SPIE Vol. 4084, p. 478-481.

Haast, J. von, 1871a. On the Geology of the Amuri District, in the Provinces of Nelson and Malborough. Report on Geological Explorations 1870-1871 6: 5-19.

Hamilton, D., 1950. The Geology of the Waikari Valley and its Northern Ridges, North Canerbury, New Zealand. Unpubl. MSc. Thesis, University of Canterbury Library, Christchurch, New Zealand 202 pp.

Harvey, A. M. and S. G. Wells, 1987. Response of Quaternary fluvial systems to differential epeirogenic uplift: Aguas and Feos river systems, south east Spain. *Geology 15: 689-693.*

Hazell, J. R. T., Cratchley, C. R., and Preston, A. M., 1988, The location of aquifers in crystalline rocks and alluvium in Northern Nigeria using combined electromagnetic and resistivity techniques: Quarterly Journal of Engineering *Geology, v. 21, p. 159-175.*

Healy, J. 1939: Amuri subdivision. New Zealand Geological Survey annual report, 33; 2-4.

Hempton, M. R., and Dunne, L. A., 1984, Sedimentation in pull-apart basins: Active examples in Eastern Turkey: *Journal of Geology, v. 92, p. 513-530.*

Herzer, R. H., and Bradshaw, J. D., 1985, The Motanau Fault and other structures at the southern edge of the Australian-Pacific Plate boundary, offshore Marlborough, New Zealand-Discussion: *Tectonophysics, v. 115, p. 161-166.*

Hicks, S. R., 1989, Structure of the Canterbury Plains, New Zealand, from gravity modelling: Research Report, v. 222, p. Geophysics Division. D.S.I.R. Wellington, New Zealand.

Higgins, C. G., and Coates, D. R., 1990, Groundwater geomorphology; the role of subsurface water in Earth-surface processes and landforms*: Geol Soc Am, Special Paper 252.*

Hippolyte, J. C., Angelier, J., Roure, F., and Casero, P., 1994, Piggyback basin development and thrust belt evolution: structural and paleostress analyses of Plio-Quaternary basins in the Southern Apennines: *Journal of Structural Geology, v. 16, no. 2, p. 159-173.*

Hobbs, W. H., 1901. The river system of Connecticut. *J. Geol. 9: 469-485*

Horton, R. E., 1945, Erosional development of streams and their drainage basins; hydrophysical approach to quantitative geomorphology: *Geological Society of America Bulletin, v. 56, p. 275-376.*

Hull, A. G., and Berryman, K. R., 1986, Holocene tectonism in the region of the Alpine Fault at Lake McKerrow, Fiordland, New Zealand: Royal Society of New Zealand Bulletin, v. 24, p. 317-331.

Hutton, F. W., 1885, On the geological position of the "Weka-Pass Stone" of New Zealand: *Quarterly Journal of the Geological Society, p. 266-278.*

Hutton, F.W., 1874. Report on the geology of the North-East Portion of the South Island, from Cook Straits to the Rakaia. *Report on Geological Explorations 1873-1874 8b: 27-58.*

--- 1888. On some railway cuttings in the Weka Pass. Trans N.Z Inst. 20: 257-263.

Jackson, P.D., Smith, D.T. and Stanford, P.N., 1978, Resistivity-porosity-particle shape relationships for marine sands: *Geophysics, 4, no.6, 1250-1276*

Jackson, J., Norris, R., and Youngson, J., 1996, The structural evolution of active fault and fold systems in central Otago, New Zealand: evidence revealed by drainage patterns: *Journal of Structural Geology, v. 18, no. 2/3, p. 217-234.*

Jamison, W. R., 1987, Geometric analysis of fold development in overthrust terranes: *Journal of Structural Geology, v. 9, no. 2, p. 207-219.*

Jol, H. M., Junck, M. B., and Kaminsky, G. M., 2000, High resolution ground penetrating radar imaging (225-900 MHz) of geomorphic and geologic settings: examples from Utah, Wahington and Wisconsin, in Noon, D. A., Glen, F., and Stickley, D. L., eds., Eigth International Conference on Ground Penetrating Radar: SPIE Vol. 4084, p. 69-74.

Jones, D. L., Graymer, R., Wang, C., McEvilly, T. V., and Lomax, A., 1994, Neogene transpressive evolution of the California Coast Ranges: *Tectonics, v. 13, no. 2, p. 561-574.*

Jordan, T. E., and Allmendinger, R. W., 1986, The Sierras Pampeanas of Argentina: A modern analogue of Rocky Mountain foreland deformation*: American Journal of Science, v. 286, p. 737-764.*

Junck, M. B., and Jol, H. M., 2000, Three-dimensional investigation of geomorphic environments using ground penetrating radar, in Noon, D. A., Glen, F., and Stickley, D. L., eds., Eighth International Conference on Ground Penetrating Radar: SPIE Vol. 4084, p. 314-318.

Kamp, P., JJ, 1988, Tectonic geomorphology of the Hikurangi Margin: surface manifestations of different modes of subduction: *Zeitschrift fur Geomorphologie N.F. Suppl.-Bd., v. 69, p. 55-67.*

Kellahan, H. J. R., 1998, Structure and Stratigraphy on the Cheviot Basin margin, northeast Canterbury: Unpublished M.Sc. Thesis, University of Canterbury, Christchurch, New Zealand.

King, G. C. P., and Vita-Finzi, C., 1981, Active folding in the Algerian earthquake of 10 October 1980: *Nature, v. 292, p. 22-26.*

Kirkby, M. J., and Chorley, R. J., 1967, Throughflow, overland flow and erosion: Bulletin of the International Association of Scientific Hydrology, v. 12, p. 5-21.

Knuepsfer, P. L. K., (1984). Tectonic Geomorphology and Present day Tectonics of the Alpine Shear System, South Island, New Zealand. Unpublished Ph.D Thesis, The University of Arizona. United States. 489 p.

LaFleur, R.G., (ed) 1984, Groundwater as a Geomorphic Agent: Allen and Unwin Inc: USA

LaFleur, R. G., 1999, Geomorphic aspects of groundwater flow: *Hydrogeology Journal, v. 7, p. 78-93.*

Lamb, S. H., 1988, Tectonic rotations about vertical axes during the last 4 Ma in part of the New Zealand plate-boundary zone: *Journal of Structural Geology, v. 10, No. 8, p. 875-893.*

Lamb, S. H., and Bibby, H. M., 1989, The last 25 Ma of rotational deformation in part of the New Zealand plate-boundary zone: *Journal of Structural Geology, v. 11, No. 4, p. 473-492.*

Lammerink, W. L., 1976, The structure and some sedimentological aspects of the Mount Highfield area, North Canterbury: B.Sc. (Honours) Thesis, University of Canterbury, Christchurch, New Zealand, 77 p.

Lecce, S. A., 1990, The alluvial fan problem, in Rachocki, A. H., and Church, M., eds., Alluvial fans: a field approach: New York, John Wiley & Sons, p. 3-24.

Leckie, D. A., 1994, Canterbury Plains, New Zealand-Implications for sequence stratigraphic models: *The American Association of Petroleum Geologists Bulletin, v. 78, no. 8, p. 1240-1256.*

Le Gall, B., 1992, The deep structure of the Ardennes Variscan thrust belt from structural and ECORS seismic data: *Journal of Structural Geology, v. 14, no. 5, p. 531-546.*

Lewis L, D.W.: Smale, D. : van der Lingen, G. J. 1979a: A sandstone diapir cutting the Amuri Limestone, North Canterbury, New Zealand. *New Zealand Journal of Geology and Geophysics 22: 295-305.*

Lewis, L, D. W, 1992. Anatomy of an unconformity on Mid-Oligocene Amuri Limestone, Canterbury, New Zealand. *N.Z. J. Geol. Geophys. 35:463-475.*

Lewis, D. W., and McConchie, D., 1994, Practical sedimentology [2nd ed.]: New York, Chapman and Hall.

Lin, J., and Stein, R. S., 1989, Coseismic folding, earthquake recurrence, and the 1987 source mechanism at Whittier Narrows, Los Angeles Basin, California: *Journal of Geophysical Research, v. 94, no. B7, p. 9614-9632.*

Liner, C. L., and Liner, J. L., 1997, Application of GPR to a site investigation involving shallow faults*: The Leading Edge, v. 16, p. 1649-1651.*

Litchfield, N.J., 1995, Structure and Tectonic Geomorphology of the Lowry Peaks Range-Waikari Valley District, North Canterbury. Unpublished MSc. Thesis, University of Canterbury. Christchurch, New Zealand.

Little, T. A., 1996, Faulting-related displacement gradients and strain adjacent to the Awatere strike-slip fault fault in New Zealand: *Journal of Structural Geology, v. 18, no. 2/3, p. 321-340.*

Loris, P., 2000, Hydrogeology of the Waipara Alluvial Basin: M.Sc thesis summary. Environment Canterbury Unpublished Report U00/59.

Loris, P., 2000, Hydrology of the Waipara Alluvial Basin: Unpublished MSc Thesis, University of Canterbury Library, Christchurch, New Zealand.

MacKinnon, T. C., (1983). Origin of the Torlesse terrain and coeval rocks, South Island, New Zealand. Geological Society of America Bulletin, v. 94, p. 967-985.

Madeira, C., Mello, C., Pilon, J., and Moura, J., 1998, Paleorelief reconstruction and 3D geometry of Quaternary sedimentary deposits of southeastern brazil:

Madeira, C. V., Mello, C. L., and da Silva de Moura, J. R., 2000, Mapping neotectonic featires using ground penetrating radar in southeastern Brazil, in Noon, D. A., Glen, F., and Stickley, D. L., eds., Eigth International Conference on Ground Penetrating Radar: SPIE Vol. 4084, p. 635-641.

Mancktelow, N. S., and Pavlis, T. L., 1994, Fold-fault relationships in low-angle detachment systems: *Tectonics, v. 13, no. 2, p. 668-685.*

Markewich, H. W., 1985, Geomorphic evidence for Pliocene-pleistocene uplift in the area of the Cape Fear Arch, North Carolina, in Morisawa, M., and Hack, J. T., eds., Tectonic Geomorphology: Boston, Massachusetts, Allen and Unwin, p. 279-297.

Masson, D. G., Cartwright, J. A., Pinheiro, L. M., Whitmarsh, R. B., Beslier, M. O., and Roeser, H., 1994, Compressional deformation at the ocean-continent transition in the NE Atlantic*: Journal of the Geological Society, London, v. 151, p. 607-613.*

Mawell, P. A. 1964: Structural Geology and pre-quaternary stratigraphy of the Kaiwara District, North Canterbury, New Zealand. Unpublished MSc. Thesis, University of Canterbury Library.

Mayer, L., 1984, Dating Quaternary fault scarps formed in alluvium using morphological parameters*: Quaternary Research, v. 22, p. 300-313.*

---, 1986, Tectonic geomorphology of escarpments and mountain fronts, in R.E. Wallce (panel chairman), ed., Active Tectonics: studies in geophysics: Washington, National Academy Press, p. 125-324.

McKay, A., (1890). On the Earthquakes of September 1888, in the Amuri and Malborough districts of the South Island. *New Zealand Geological Survey Report of Geological Explorations, v. 20, p. 1-16.*

McKay, A., 1892, On the geology of the Middle Waipara and Weka Pass districts, North Canterbury: *New Zealand Geological Survey of Geological Explorations, v. 1890-1891 21, p. 97-103.*

McNeill, J.D. 1990. Use of electromagnetic methods for groundwater studies: in Ward, S.H (ed). *Geotechnical and Environmental Geophysics*, vol. 1 – *Review and Tutorial,* Society of Exploration Geophysicists *191-218*

Meghraoui, M., Jaegy, R., Lammali, K., and Albarede, F., 1988, Late Holocene earthquake sequences on the El Asnam (Algeria) thrust fault: *Earth and Planetary Science Letters, v. 90, p. 187-203.*

Miall, A. D., 1977, A review of the braided-river depositional environment: *Earth Science Reviews, v. 13, p. 1-62.*

Mills, H. H., and Allison, J. B., 1995, Weathering and soil development on fan surfaces as a function of height above modern drainageways, Roan Mountain, North Carolina: *Geomorphology, v. 14, p. 1-17.*

Milson, J., 1989, Field Geophysics, Great Britain: , Butler and Tanner Ltd.

Mitra, S., 1990, Fault-propagation folds: Geometry, kinematic evolution, and hydrocarbon traps: *The American Association of Petroleum Geologists Bulletin, v. 74, no. 6, p. 921-945.*

Morley, C. K., 1986, A classification of thrust fronts*: The American Association of Petroleum Geologists Bulletin, v. 70, p. 12-25.*

Mould, R. J., 1992, Structure and kinematics of Late Cenozoic deformation along the western margin of the Culverden Basin, North Canterbury, New Zealand: Unpublished M.Sc. thesis, University of Canterbury, Christchurch, New Zealand, 174 p.

Nabighian, M. N. and Macnae, J. C., 1991. Time domain electromagnetic prospecting methods: in Nabighian, M. N. (ed). *Electromagnetic Methods in Applied Geophysics, Applications Part A and Part B,* Society of Exploration Geophysicists *427-520.*

Namson, J. S., and Davis, T. L., 1988, Seismically active fold and thrust belt in the San Joaquin Valley, central California: *Geological Society of America Bulletin, v. 100, p. 257-273.*

---, 1995, Seismically active fold and thrust belt in the San Joaquin Valley, central California: *Geological Society of America Bulletin, v. 100, p. 257-273.*

New Zealand Soil Bureau, 1968, Soils of New Zealand. Part 1 [N.Z. Soil Bur. Bull. 26 (1) ed.].

Nicol, A., 1991, Structural styles and kinematics of deformation on the edge of the New Zealand plate boundary zone, mid Waipara region, north Canterbury: Ph.D. thesis, lodged in the library, University of Canterbury, Christchurch, New Zealand.

---, 1993, Haumurian (c. 66-80 Ma) half-graben development and deformation, mid Waipara, North Canterbury, New Zealand: *New Zealand Journal of Geology and Geophysics, v. 36, p. 127-130.*

Nicol, A., and Campbell, J. K., 1990, Late Cenozoic thrust tectonics, Picton, New Zealand: *New Zealand Journal of Geology and Geophysics, v. 33, p. 485-494.*

Nicol, A., Cowan, H., Campbell, J., and Pettinga, J., 1995, Folding and the development of small sedimentary basins along the New Zealand plate boundary: *Tectonophysics, v. 241, p. 47-54.*

Nicol, A., Watterson, J., Walsh, J. J., and Childs, C., 1996, The shapes, major axis orientations and displacement patterns of fault surfaces: *Journal of Structural Geology, v. 18, no. 2/3, p. 235-248.*

Nicol, A., 1992, Tectonic structures developed in Oligocene limestones: implications for New Zealand plate boundary deformation in North Canterbury: *New Zealand Journal of Geology and Geophysics, v. 35, p. 353-362.*

Nicol, A., and Wise, D. U., 1992, Paleostress adjacent to the Alpine Fault of New Zealand: Fault, vein, and styolite data from the Doctors Dome area: *Journal of Geophysical Research, v. 97, no. B12, p. 17,685-17,692.*

Nicol, A.,B, Alloway and P. Tonkin, 1994. Rates of Deformation, uplift and landscape development with active folding in the Waipara area of North Canterbury, New Zealand. *Tectonics 13: 1327-1344*

Nino, F., Philip, H., and Chery, J., 1998, The role of bed parallel slip in the formation of blind thrust faults: *Journal of Structural Geology, v. 20, no. 5, p. 503-516.*

Nobes, D.C. 1996, Troubled Waters: Environmental Applications of electrical and electromagnetic methods. *Surveys in Geophysics , 17: 393-454*

Nobes, D. C., Armstrong, M. J., and Close, M. E., 2000, Delineation of a landfill leachate plume and flow channels in coastal sands near Christchurch, New Zealand, using a shallow electromagnetic survey: *Hydrogeology Journal, v. 8, p. 328-336.*

O'Keefe, F.Z. and D.W. Stearns, 1982. Characteristics of displacement transfer zones associated with thrust faults in: Geologic Studies of the Cordilleran Thrust Belt 1: 219-233. Rocky Mountains Association of Geologists, Denver, Colorado.

Ouchi, S., 1985, Response of alluvial rivers to slow active tectonic movement: *Geological Society of America Bulletin, v. 96, p. 504-515.*

Parasnis, D.S., 1986. Principles of Applied Geophysics. Fourth edition. London: Chapman and Hall

Patton, T. L., and Fletcher, R. C., 1995, Mathematical block-motion model for deformation of a layer above a buried fault of arbitary dip and sense of slip: *Journal of Structural Geology, v. 17, no. 10, p. 1455-1472.*

Pettinga, J. R., 1997, Aspects of North Canterbury active tectonics and landscape evolution, in Bradshaw, J. D., ed., Terrane Dynamics, 1997: Guidebook for Field Excursions A, B & C: p. C1-C32.

Pettinga, J. R., Campbell, K. J., Nicol, A., Cowan, H. A., and Barnes, P. M., 1995, From oblique subduction to continental collision: tectonics and structure of the plate boundary transfer zone, central New Zealand. Programme and Abstracts, New Zealand Geophysical Society Symposium August 1995, keynote address. .

Pettinga, J. R., and Wise, D. U., 1994, Paleostress adjacent to the Alpine Fault: Broader implications from fault analysis near Nelson, South Island, New Zealand: *Journal of Geophysical Research, v. 99, no. B2, p. 2727-2736.*

Pettinga, J. R, C.G. Chamberlain, M.D. Yetton, R.J., Van Dissen, G. Downes., 1998, Earthquake Source Identification and Characterisation. A report prepared for Canterbury Regional Council. *Rivers and Coastal Resoures and Hazards Section.*

Powers, W. E., 1962, Terraces of the Hurunui River, New Zealand: *New Zealand Journal of Geology and Geophysics, v. 5, p. 114-129.*

Prothero, D. R., and Schwab, F., 1996, Sedimentary geology: An introduction to sedimentary rocks and stratigraphy: New York, W.H. Freeman, 575 p.

Read, J. R. L., 1964, The geology of the Hurunui River valley between Lake Sumner and the Mandamus River, North Canterbury: Unpublished M.Sc. Thesis, Department of Geological Sciences, University of Canterbury, Christchurch.

Read, S. A. L., and Blick, G. H., 1991, Late Quaternary deformation and geodectic monitoring in the area of 'The Knot' on the Ostler Fault Zone, South Island, New Zealand: *New Zealand Geological Survey Record, v. 43, p. 85-91.*

Reyners, M and H. Cowan, 1993. The transition from subduction to continental collision: crystal structure in the North Canterbury Region, New Zealand. *Geophys. J.Int. 115: 1124-1136.*

Reynolds, C.J., 1997. An introduction to applied and environmental geophysics. John Wiley and Sons. 796pp.

Rhea, S., 1993. Geomorphic observations of Rivers in the Oregon Coast Range from a Regional Reconnaissance Perspective. *Geomorphology 6: 135-150.*

Rhue, R.V., 1956, Geomorphic surfaces and the nature of soils: Soil Science, v 82, pp 441-455

---, 1995, Neotectonics of the San Cayetano fault, Transverse Ranges, California: Geological Society of America Bulletin, v. 100, p. 500-513.

---, 1995, Quaternary rate of folding of the Ventura Avenue anticline, western Transverse Ranges, southern California: *Geological Society of America Bulletin, v. 100, p. 850-858.*

Rockwell, T. K., Keller, E. A., and Johnson, D. L., 1985, Tectonic geomorphology of alluvial fans and mountain fronts near Ventura, California, in Morisawa, M., and Hack, J. T., eds., Tectonic geomorphology: Boston, Massachusetts, Allen and Unwin, p. 183-207.

Roy, M., Royden, L. H., Burchfiel, B. C., Tzankov, T., and Nakov, R., 1996, Flexural uplift of the Stara Planina range, central Bulgaria: *Basin Research, v. 8, p. 143-156.*

Rynn, J.M.W and C.H. Scholz, 1978. Seismotectonics of the Arthurs Pass Region, South Island, New Zealand. *Geol.Soc.Am.Bull. 89:1373-1388.*

Schofield, J. C., 1949. The Geology of the McDonald Downs and Waikari Districts North Canterbury. Unpublished. MSc. Thesis, University of Canterbury Library, Christchurch, New Zealand

Schofield, J.C., 1951: Distribution of Lower Oligocene volcanics in New Zealand. *New Zealand Journal of Science and Technology 33(8): 201-217.*

Sevon, W. D., 1968, Stratigraphy and sedimentology of the tertiary rocks of the Mandamus-Dove RIver area, North Canterbury, New Zealand: *New Zealand Journal of Geology and Geophysics, v. 12, p. 283-309.*

Sharma, P. V., 1997, Environmental and Engineering Geophysics: Cambridge, Cambridge University Press, 475 p.

Shaw, J. H., and Suppe, J., 1994, Active faulting and growth folding in the eastern Santa Barbara Channel, California: Geological Society of America Bulletin, v. 106, p. 607-626.

Sherriff, R. E., 1984, Encyclopedic dictionary of exploration geophysics [2nd edition ed.]: Tulsa, Oklahoma, Society of Exploration Geophysics.

Smith, D. G., and Jol, H. M., 1995, Wasatch Fault (Utah), detected and displacement characterized by ground penetrating radar: *Environmental and Engineering Geoscience, v. 1, no. 4, p. 489-496.*

Smith, D. G., and Jol, H. M., 1995, Ground penetrating radar: antenna frequencies and maximum probable depths of penetration in Quaternary sediments: *Journal of Applied Geophysics, v. 33, p. 93-100.*

Song, T., and Wang, X., 1990, Structural styles and stratigraphic patterns of syndepositional faults in a contractional setting: examples from Quaidam Basin, northwestern China: *The American Association of Petroleum Geologists Bulletin, v. 77, no. 1, p. 102-117.*

Soons, J. M., 1979, Late Quaternary environments in the central South Island of New Zealand: *New Zealand Geographer, v. 35, p. 16-23.*

Southall, P. G., and Rennie, W. F., 1977, Interim report on the soils of part Waiau Plains, North Canterbury, and their suitablility for irrigation-Waiau Plains irrigation scheme, stage 1. N.Z. Soil Bureau Record 53. .

Speight, R., 1915, The intermontane basins of Canterbury (Part 1): *Transactions of the New Zealand Institute, v. 47, p. 336-353.*

---, 1918, Structural and Glacial features of the Hurunui Valley: *Transactions of the New Zealand Institute, v. 50, p. 93-105.*

---, 1926, Intermontane basins of Canterbury (Part 2): *Transactions of the New Zealand Institute, v. 56, p. 355-360.*

Spies, B. R. and Frischknecht, F. C., 1991. Electromagnetic sounding: in Nabighian, M. N. (ed). *Electromagnetic Methods in Applied Geophysics, Applications Part A and Part B,* Society of Exploration Geophysicists *285-411*

Srivastava, P., Parkash, B., Sehgal, J. L., and Kumar, S., 1994, Role of neotectonics and climate in development of the Holocene geomorphology and soils of the Gangetic Plains between the Ramganga and Rapti rivers*: Sedimentary Geology, v. 94, p. 129-151.*

Stearns, D. W., 1999, Faulting and forced folding in the Rocky Mountains foreland: *Geological Society of America Memoir 151, p. 1-37.*

Stein, R., and King, G. C. P., 1984, Seismic potential revealed by surface folding: 1983 Coalinga, California, Earthquake*: Science, v. 224, p. 869-872.*

Stone, W.J. 1999, Hydrology in Practice, A guide to characterizing ground-water systems. Prentice-Hall Inc- London.

Strahler, A. N., 1957, Quantitative analysis of watershed geomorphology. *Am. Geophys. Un. Trans. 38: 913-920.*

Strahler, A. N., 1958, Dimensional analysis applied to fluvial eroded landforms*: Geological Society of America Bulletin, v. 69, p. 279-300.*

Suppe, J., 1983. Geometry and kinematics of fault-bend faulting. *Am.J.Sci. 283: 684-721*

Suppe,J., and D.A. Medwedeff, 1984. Fault-propagation folding. *Geol.Soc.Am.Abstr Progr. p 60*

Sylvester, A. G., 1988, Strike-slip faults: Geological Society of America Bulletin, v. 100, p. 1666-1703.

Syme, A. R., 1991, Structural analysis of the deformation of the Marble Point outlier, Waiau River, North Canterbury: Unpublished BSc (Hons) project, University of Canterbury, Christchurch, New Zealand, 95 p.

Talling P.J., S.S., Stewart, C.P., Stark, S. Gupta and S.J. Vincent, 1997. Regular Spacing of drainage outlets from linear fault blocks. *Basin Research 9: 275-302*

Theimer, B.D., D.C. Nobes, and B.G. Warner. A study of the geoelectrical properties of peatlands and their influence on ground penetrating radar surveys, *Geophysical Prospecting,* 42: 179-209, 1994.

Telford, W.M., L.P. Geldart, R.E. Sheriff and D.A. Keys, 1976. Applied Geophysics. Great Britain; Cambridge University Press.

Thompson, J.A., 1920. The Notocene Geology of the Middle Waipara and Weka Pass District, North Canterbury, New Zealand. Tranz. Proc. NZ. Inst. 52: 322-415.

Tobin, H. J., Moore, J. C., MacKay, M. E., Orange, D. L., and Kulm, L. D., 1993, Fluid flow along a strike-slip fault at the toe of the Oregon accretionary prism: Implications for the geometry of frontal accretion: *Geological Society of America Bulletin, v. 105, p. 569-582.*

Trabant, P. K., 1984, Applied high-resolution geophysical methods: Boston, International Human Resources Development Corp.

Van Dissen, R. J., 1991, An evaluation of seismic hazard in the Kaikoura Region, southeastern Marlborough: New Zealand Geological Survey Record 6, v. 43, p. 93-99.

Van Dissen, R. J., Hull, A. G., and Read, S. A. L., 1993, Timing of some large Holocene earthquakes on the Ostler Fault, New Zealand: *Proceedings of the CRCM '93, Kobe, December 6-11, p. 381-386.*

Van Dissen, R., and Yeats, R. S., 1991, Hope Fault, Jordon Thrust, and uplift of the Seaward Kaikoura Range, New Zealand: *Geology, v. 19, p. 393-396.*

van Lissa, R. V., van Maanen, H. R. J., and Odera, F. W., 1987, The use of remote sensing and geophysics for groundwater exploration in Nyanza province-Kenya. African Water technology Conference, Nairobi. .

Warren, G. 1967: Sheet 17 Hokitika. Geological Map of New Zealand. 1: 250 000. Wellington New Zealand Department of Scientific and Industrial Research.

Walcott, R.I., 1978. Present tectonics and Late Cenozoic evolution of New Zealand. *J. Geophys. Res. 52: 137-164.*

Wallace, R.E., 1978: Geometry and rates of change of fault generated range fronts, north-central Nevada. United States Geological Survey Journal of Research, 637-650

Wasson, R.J., 1974. Intersection Point deposition on alluvial fans: An Australian example. *Geografiska Annaler, 56, 83-92*

Wells, S. G., Bullard, T. F., Menges, C. M., Drake, P. G., Karas, P. A., Kelson, K. I., Ritter, J. B., and Wesling, J. R., 1988, Regional variations in tectonic geomorphology along a segmented convergent plate boundary, Pacific coast of Costa Rica: *Geomorphology, v. 1, p. 239-265.*

Wells, S. G., Bullard, T. F., Menges, C. M., Drake, P. G., Kelson, P. A., Ritter, J. B., and Wesling, J. R., 1988, Regional variations in tectonic geomorphology along a segmented convergent plate boundary, Pacific Coast of Costa Rica*: Geomorphology, v. 1, p. 239-265.*

West, G. F., and Macnae, J. C., 1991, Physics of the electromagnetic exploration method, in Nabighian, M. N., ed., Electromagnetic Methods in Applied Geophysics, Volume 2, Part A: *Society of Exploration Geophysicists, p. 5-45.*

Whiteford, C. M., and Lumb, J. T., 1975, A catalogue of physical properties of rocks volume 3: Listing by rock type [Report No. 107 ed.]: Wellington, New Zealand, Geophysics Division, Department of Scientific and Industrial Research.

Whitehouse, I. E., 1992, Tectonic geomorphology: recent studies of faulting and tectonic landforms: *Progress in Physical Geography, v. 16, no. 3, p. 361-369.*

WHO, 1971. International Standards for Drinking Water (3rd Edition). 70 pp.

Wilkerson, M. S., 1992. Differential transport and continuity of thrust sheets. *J. Struct. Geol. 14: 749-751.*

Wood, P. R., 1984, Guidebook to the South Island scientific excurions international symposium on recent crustal movements of the Pacific region, Wellington, New Zealand: Wellington, Royal Society of New Zealand, v. Royal Society Miscellaneous Series: 9 Part Two (Greymouth-Christchurch), 149 p.

Wood, P. R., and Blick, G. H., 1986, Some results of geodetic fault monitoring in South Island, New Zealand: *Royal Society of New Zealand Bulletin, v. 24, p. 39-45.*

Wood, R., Pettinga, J. R., Bannister, S., Lamarche, G., and McMorran, T., 1994, Structure of the Hanmer strike-slip basin, Hope Fault, New Zealand: *Geological Society of America Bulletin, v. 106, p. 1459-1473.*

Woodward, D.J., and A.F Carmen, 1982. Precise gravity measurements between Lyttelton and Westport, SouthIsland, New Zealand. Geophysics Division Report No. 163

Yeats, R. S., 1986, Faults related to folding with examples from New Zealand*: Royal Society of New Zealand Bulletin, v. 24, p. 273-293.*

Yetton, M.D. and D.C. Nobes., 1998. Recent vertical offset and near-surface structure of the Alpine Fault in Westland, New Zealand , from ground penetrating radar profiling. *New Zealand Journal of Geology and Geophysics Vol 41: 485-492*

Yielding, G., Needham, T., and Jones, H., 1996, Sampling of fault populations using sub-surface data: a review: *Journal of Structural Geology, v. 18, no. 2/3, p. 135-146.*

Young, M. E., de Bruijn, R. G. M., and bin Salim Al-Ismaily, A., 1998, Exploration of an alluvial aquifer in Oman by time-domain electromagnetic sounding: *Hydrogeology Journal, v. 6, p. 383-393.*

Yousif, H. S., 1987, The application of remote sensing to geomorphological neotectonic mapping in North Canterbury, New Zealand: Ph.D. Thesis, University of Canterbury Library, Christchurch, New Zealand.

Zeng, H., Zhang, Q., and Liu, J., 1994, Location of secondary faults from cross-correlation of the second vertical derivative of gravity anomalies: *Geophysical Prospecting, v. 42, p. 841-854.*

Zernitz, E. R., 1932, Drainage patterns and their significance*:* *Journal of Geology, v. 40, p. 498-521.*

APPENDIX 1

BORE LOGS

This appendix contains the logs for the 62 wells which are deeper than 10 m within Culverden Basin. Whilst there are many more wells that only go down a few metres, they show very little information that was useful for this study, and have hence been left out. Table A1.1 lists all the wells shown on the map (Figure A1.1), followed by the logs, courtesy of Environment Canterbury (formerly the Canterbury Regional Council).

Table A1.1. List of the wells deeper than 10 m in Culverden Basin

WELL NUMBER	GRID REFERENCE	OWNER	DEPTH (M)	DATE DRILLED
M33/0144	M33:848-274	MURGATROYD, G.F.	19.20	07/03/63
M33/0208	M33:874-276	FROST, E.M.	36.00	02/25/93
N32/0010	N32:078-336		22.90	00000000
N32/0030	N32:129-391		13.70	00000000
N32/0031	N32:126-391		11.60	00000000
N32/0033	N32:128-391		18.20	00000000
N32/0034	N32:124-391		18.20	00000000
N32/0035	N32:116-395		10.00	00000000
N32/0036	N32:120-394		10.00	00000000
N32/0037	N32:079-352		17.70	00000000
N32/0038	N32:084-352		23.70	00000000
N32/0062	N32:116-328	DIST.COMM.WORKS.CHCH	30.00	00000000
N32/0069	N32:1330-3953	AMURI COUNTY COUNCIL	12.30	00000000
N32/0086	N32:077-309	TASMAN AGRICULTURE	23.00	02/26/93
N32/0111	N32:9943-3242	APPLEFIELDS DAIRY	12.60	07/15/89
N32/0112	N32:0138-3010	AMAPEX HOLDINGS	35.50	07/10/89
N32/0113	N32:994-328	APPLEFIELDS DAIRY	36.00	07/14/89
N32/0144	N32:997-315	RIDDINGTON, K.A.	41.00	04/04/95
N32/0147	N32:0660-3680	AMURI SALMON LTD	15.00	10/26/95
N32/0171	N32:1220-3220	EGDEN, A.F	12.00	11/29/95
N32/0203	N32:0546-3433	ALLNUT, R.G	11.25	06/22/96
N32/0210	N32:0133-3338	ROBERTS, T. M.	25.00	08/01/96
N32/0211	N32:0122-3101	KAIROMA TRUST	35.50	12/14/96
N32/0212	N32:0662-3683	AMURI SALMON LTD	15.00	01/30/97
N32/0216	N32:0292-3192	SMITH, B.J& L.A	36.00	04/29/97
N32/0217	N32:0120-3313	ROBERTS, T.M.	35.00	10/28/97
N32/0232	N32:1358-3946	STRATFORD, GG	15.00	07/14/98
N32/0233	N32:0584-3502	WALKER, MJD & WM	10.00	07/22/98
N32/0236	N32:0278-3988	FLORANCE, RA & PM	66.00	01/14/99
N33/0001	N33:995-288		20.10	00000000
N33/0011	N33:011-261		81.00	07/01/53
N33/0013	N33:980-264		22.50	00000000
N33/0019	N33:963-239		17.60	00000000
N33/0020	N33:976-263	MICHARD, HAROLD.	18.80	05/26/60
N33/0044	N33:9788-2600	TOPIA, JULIE.(STATE HOUSE)	21.60	07/20/49
N33/0045	N33:022-257		30.00	00000000
N33/0061	N33:987-216		14.30	00000000
N33/0076	N33:961-233		11.50	00000000
N33/0077	N33:961-233		12.10	00000000
N33/0113	N33:9945-2587	DIST.COMM.WORKS.CHCH	30.00	00000000
N33/0186	N33:9703-2382	MILLAR EJ & NP	15.20	02/12/90
N33/0187	N33:0273-2755	DELANY JR & IR	30.00	03/11/90
N33/0193	N33:993-282	DOBSONS FOODS NZ LTD	46.50	07/01/90
N33/0194	N33:943-230	KYENTON FARM LTD	18.00	06/30/92
N33/0196	N33:9805-2200	HEDLEY HOLDINGS	36.00	02/22/93
N33/0197	N33:9462-2495	TASMAN AGRICULTURE	12.00	02/23/93
N33/0203	N33:9410-2600	TASMAN AGRICULTURE LTD	63.10	08/02/93
N33/0204	N33:0435-2529	DELANY, J.R.& I.R.	54.00	04/22/94
N33/0205	N33:0091-2691	TASMAN AGTURE,SCHAT FMS	27.50	04/20/94
N33/0208	N33:0000-2868	STEELE, G.C.	41.50	09/17/94
N33/0209	N33:9677-2210	WILLIAMSON, A.N.	36.00	06/14/94
N33/0210	N33:999-300	THOMSON, R.M.	35.00	01/24/95
N33/0215	N33:9290-2700	MILNE, MK & CLARKE, NR	12.00	04/01/95
N33/0218	N33:040-264	DELANY, J.R. & I.R.	27.50	07/12/95
N33/0219	N33:9116-2637	BACKHOUSE, K. & J. V	18.20	07/31/95
N33/0220	N33:922-249	SUTTON, G.J.	15.50	00000000
N33/0221	N33:925-264	SUTTON, G.J.	18.00	00000000
N33/0242	N33:9069-2524	BACKHOUSE, K AND J.V	16.00	05/22/96
N33/0243	N33:9975-2652	MOSSMAN, P.R	30.00	11/05/96
N33/0244	N33:9545-2587	NEILL, S.W	17.80	00000000
N33/0246	N33:9586-2592	AMURI PASTORAL LIMITED	44.20	12/16/96
N33/0254	N33:0469-2358	RA KANOHI AMURI LTD	36.10	04/30/97

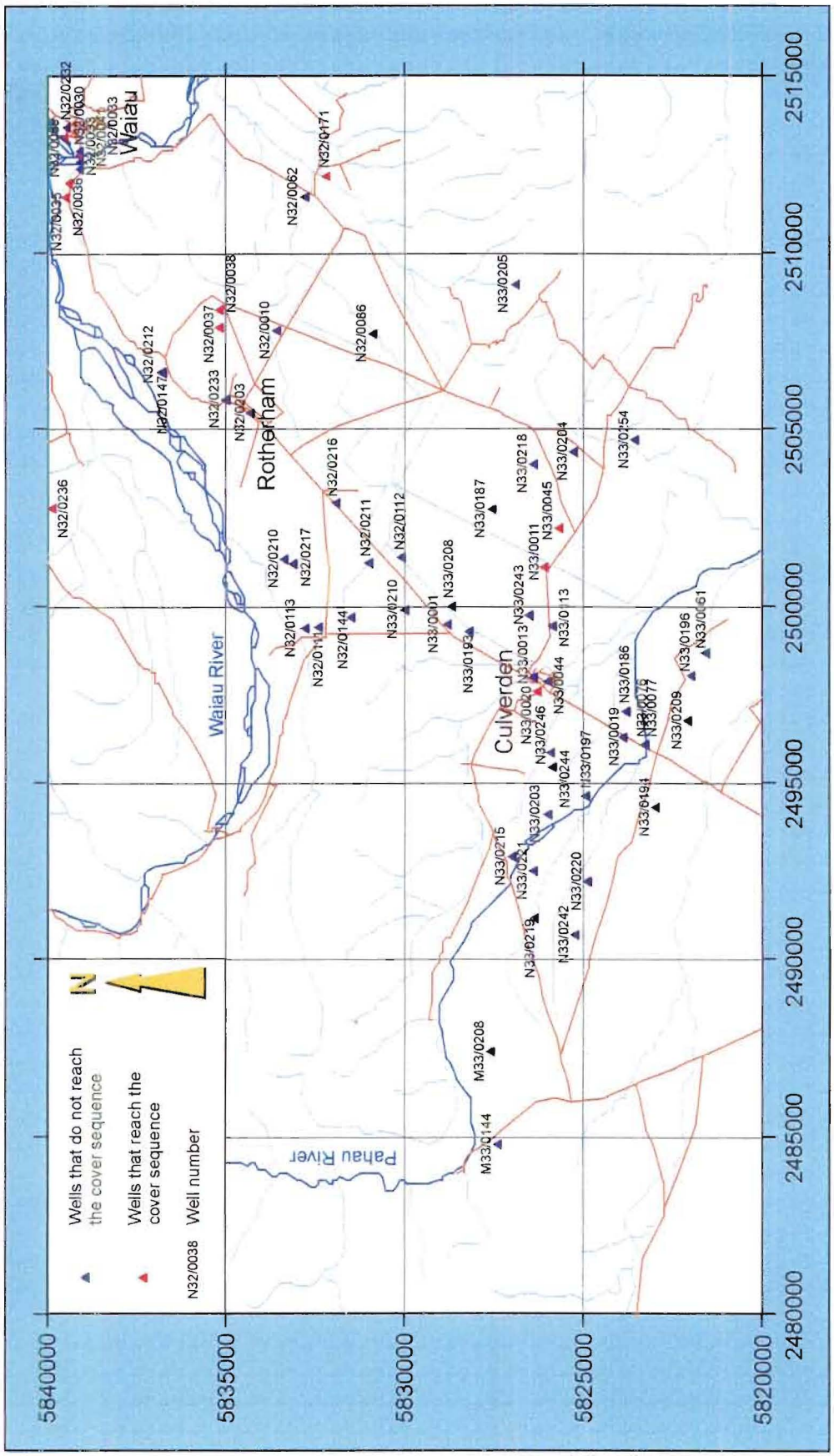

FIGURE A1.1. Map of the wells that extend deeper than 10 m within Culverden Basin

Borelog for well M33/0144

Gridref: M33:848-274

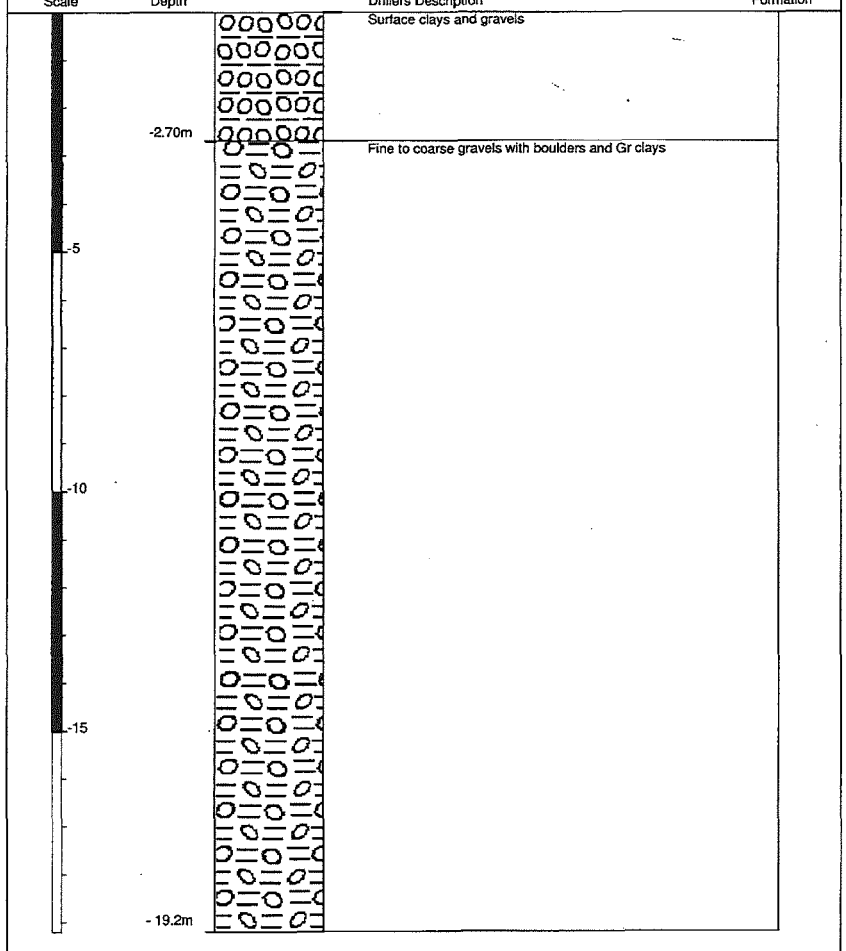

Borelog for well M33/0208

Gridref: M33:874-276

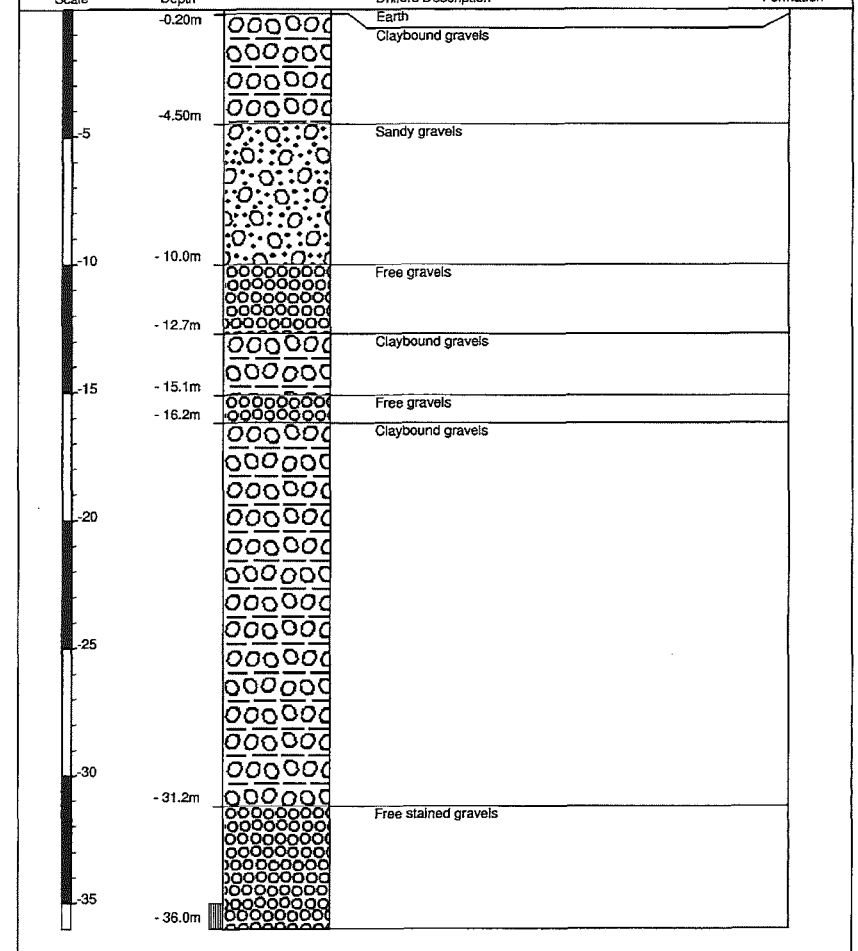

Borelog for well N32/0010

Gridref: N32:078-336

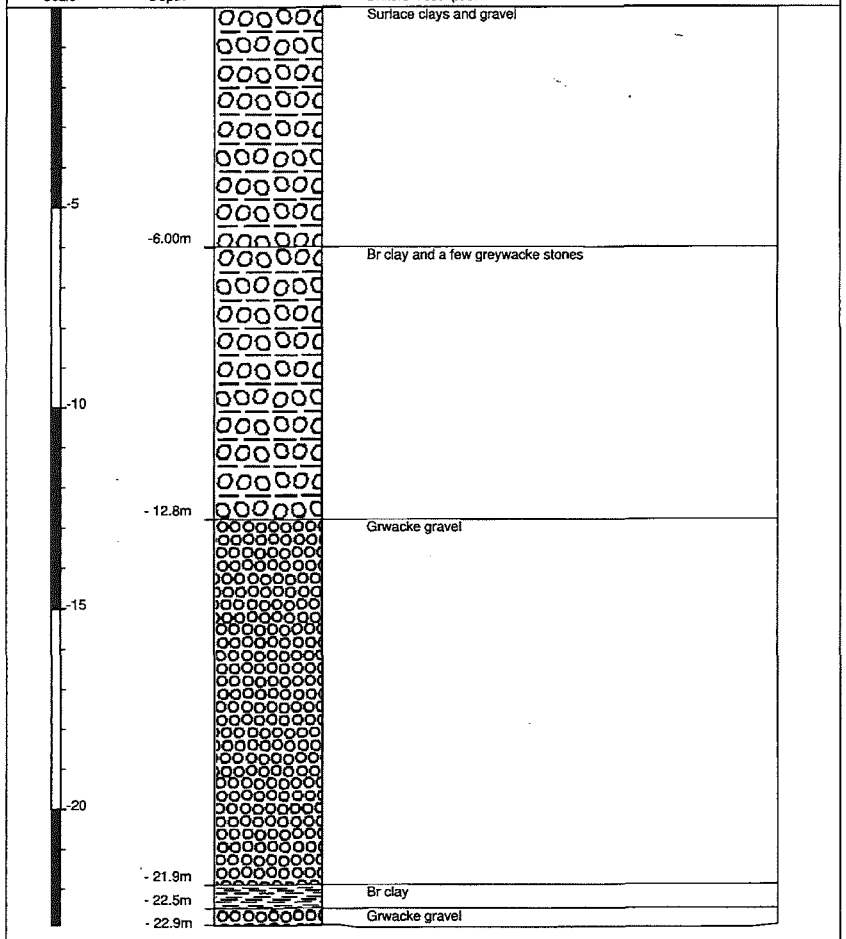

Borelog for well N32/0030

Gridref: N32:129-391

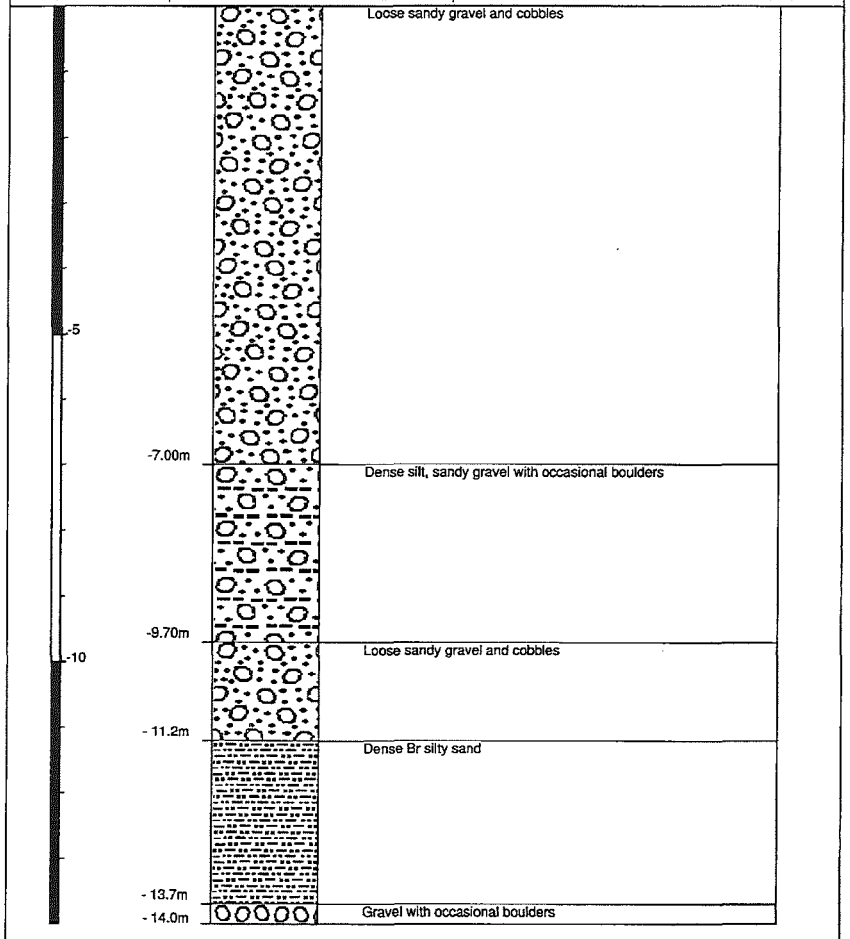

Borelog for well N32/0031

Gridref: N32:126-391

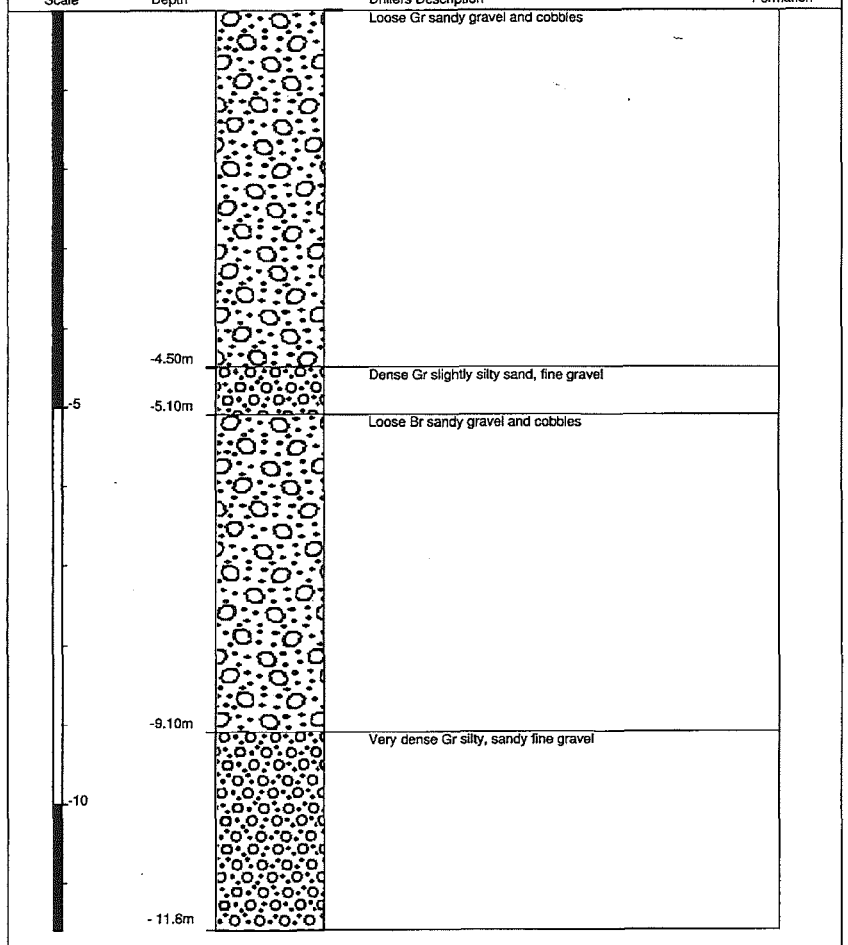

Borelog for well N32/0033

Gridref: N32:128-391

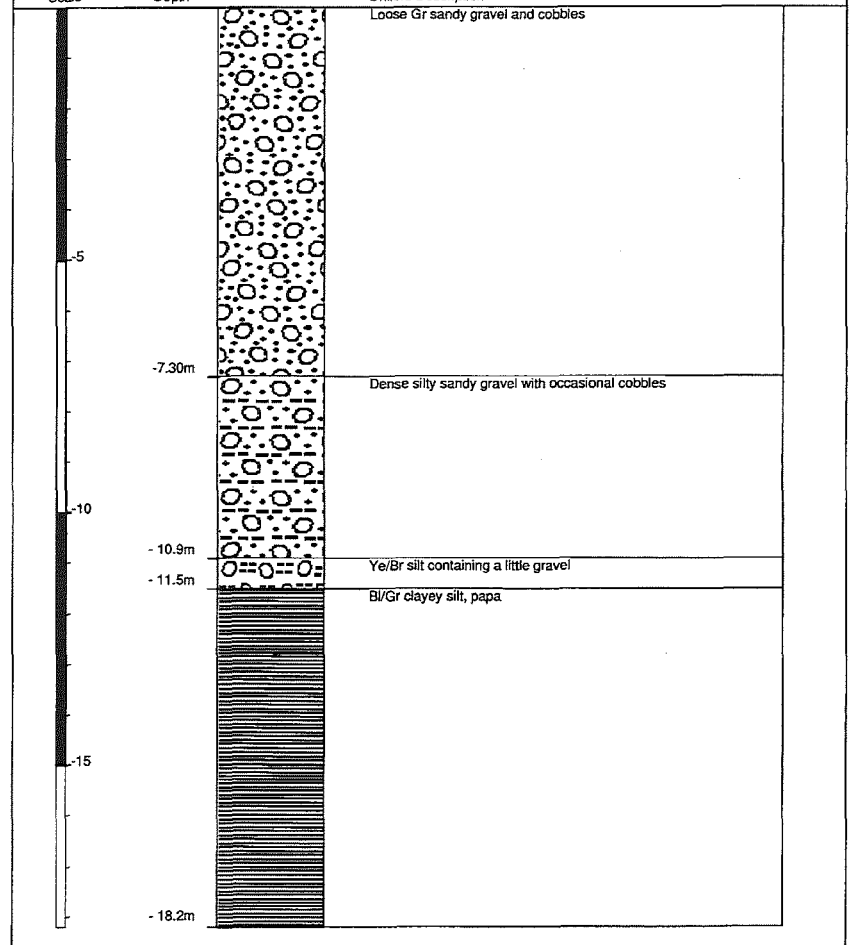

Borelog for well N32/0034

Gridref: N32:124-391

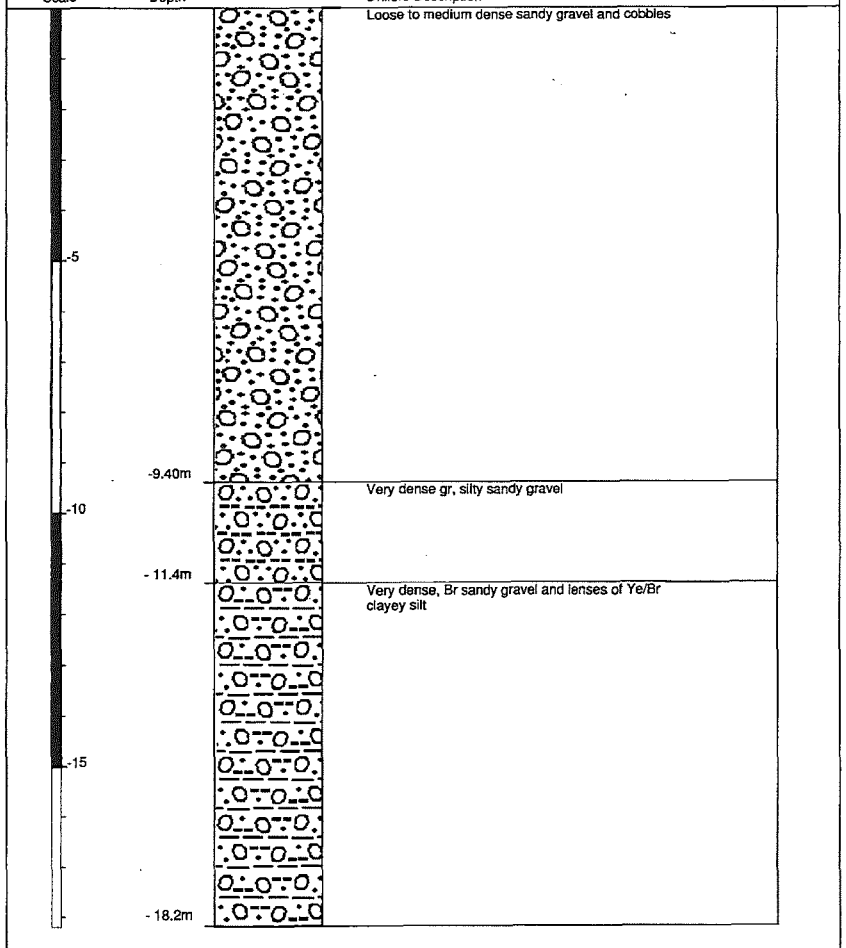

Borelog for well N32/0035

Gridref: N32:116-395

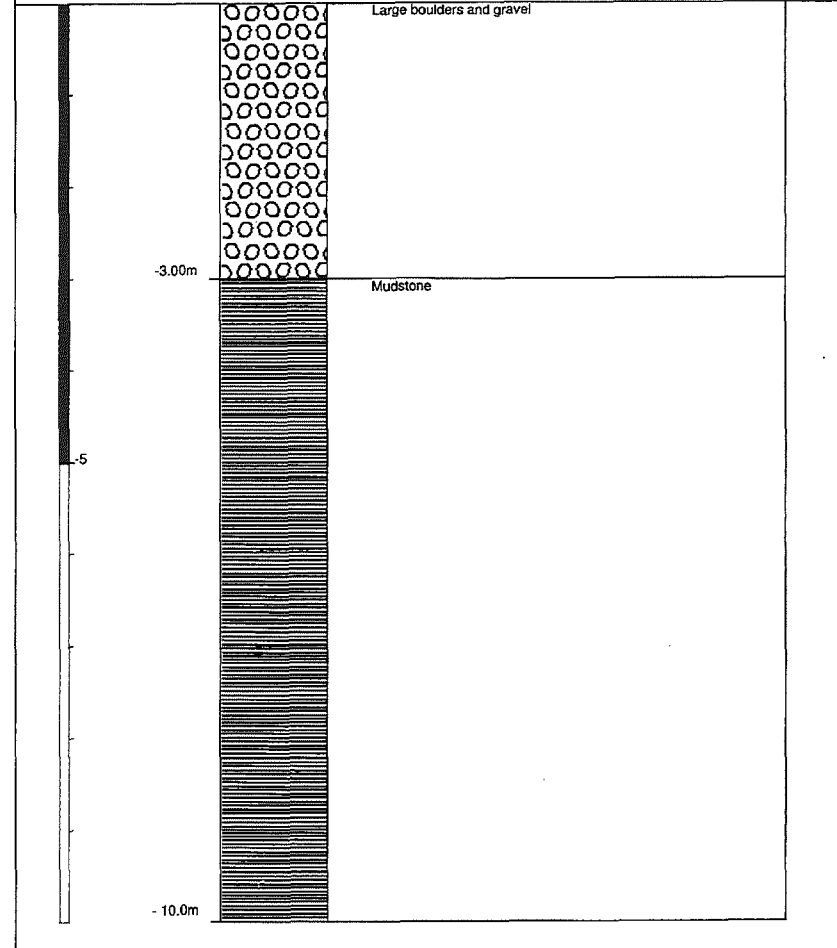

Borelog for well N32/0036

Gridref: N32:120-394

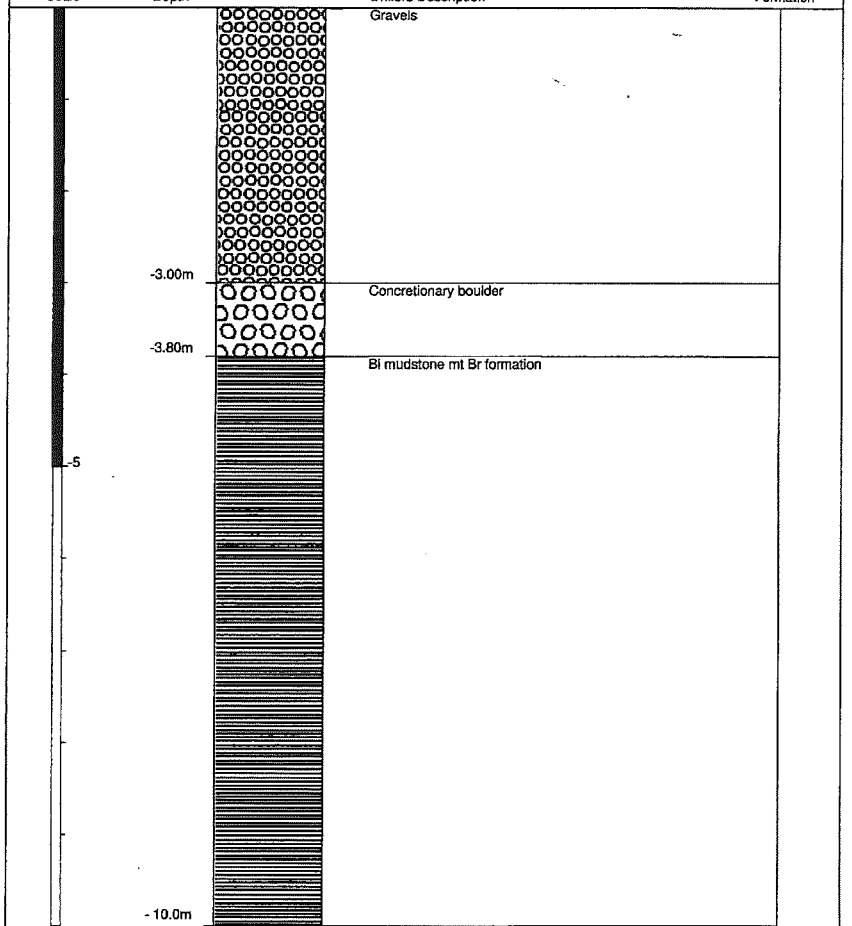

Borelog for well N32/0037

Gridref: N32:079-352

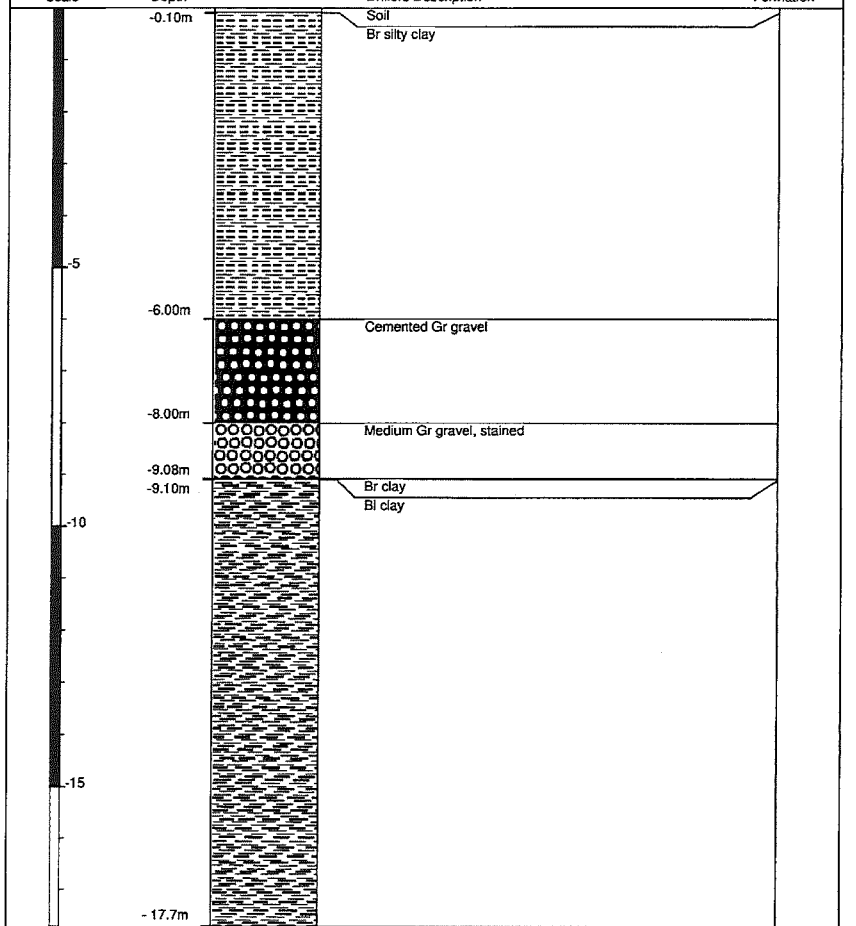

Borelog for well N32/0038

Gridref: N32:084-352

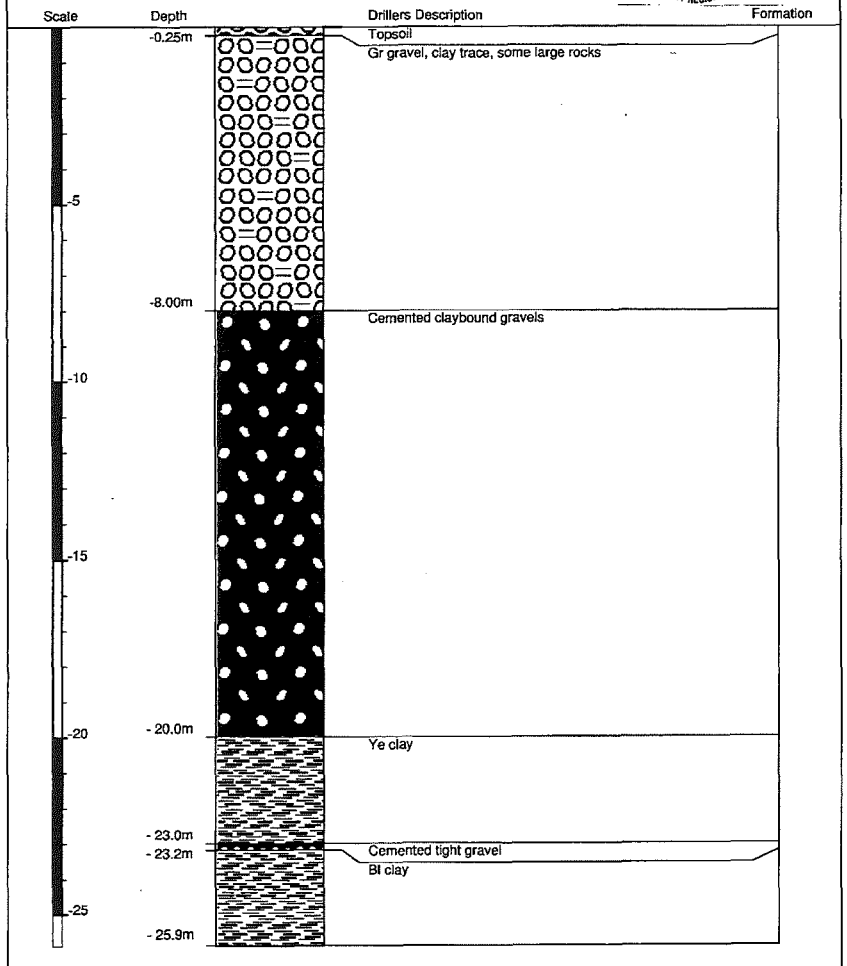

Borelog for well N32/0062

Gridref: N32:116-328

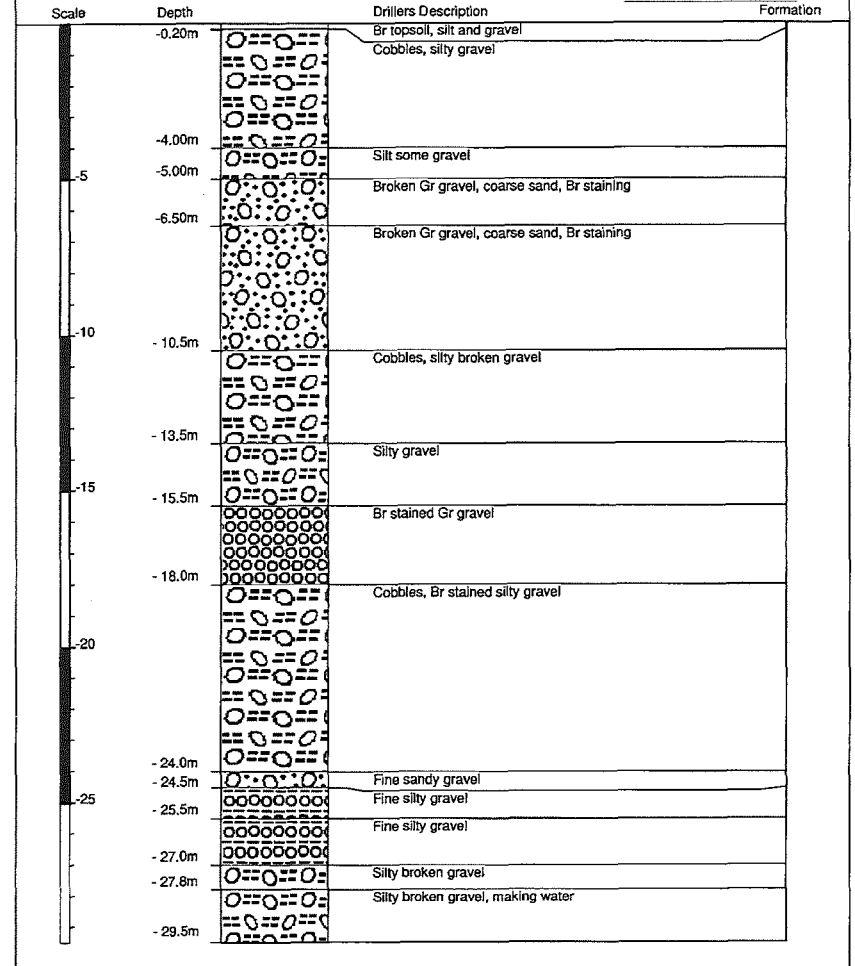

Borelog for well N32/0069

Gridref: N32:1330-3953

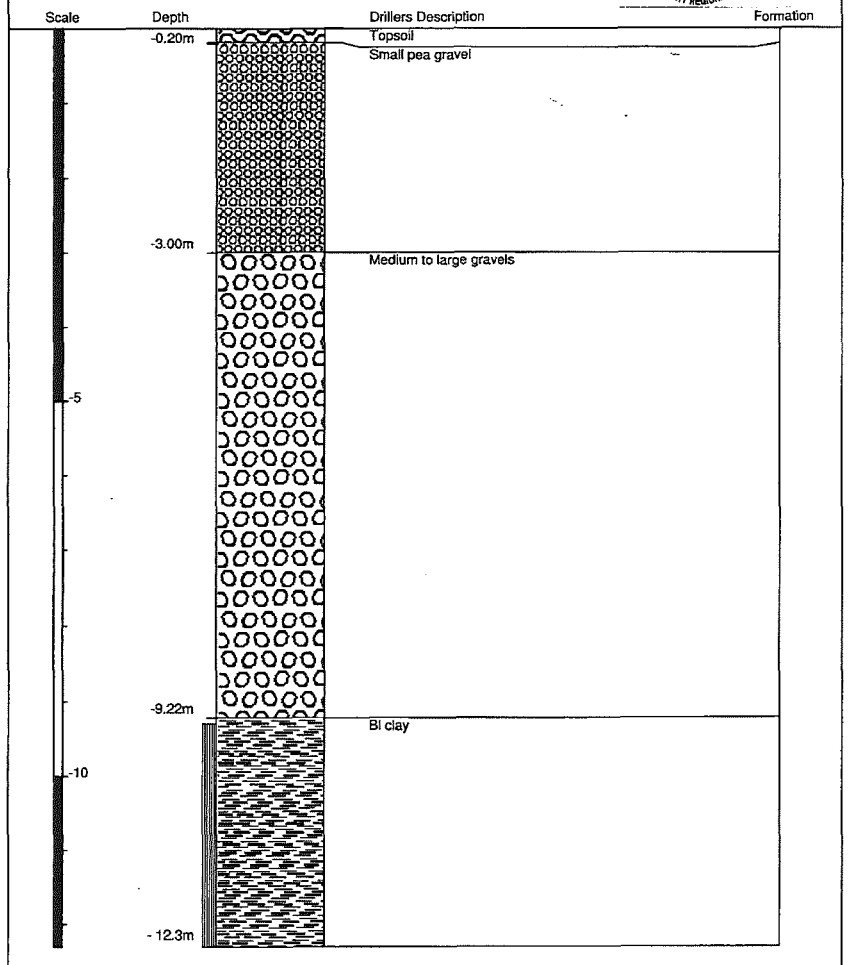

Borelog for well N32/0086

Gridref: N32:077-309

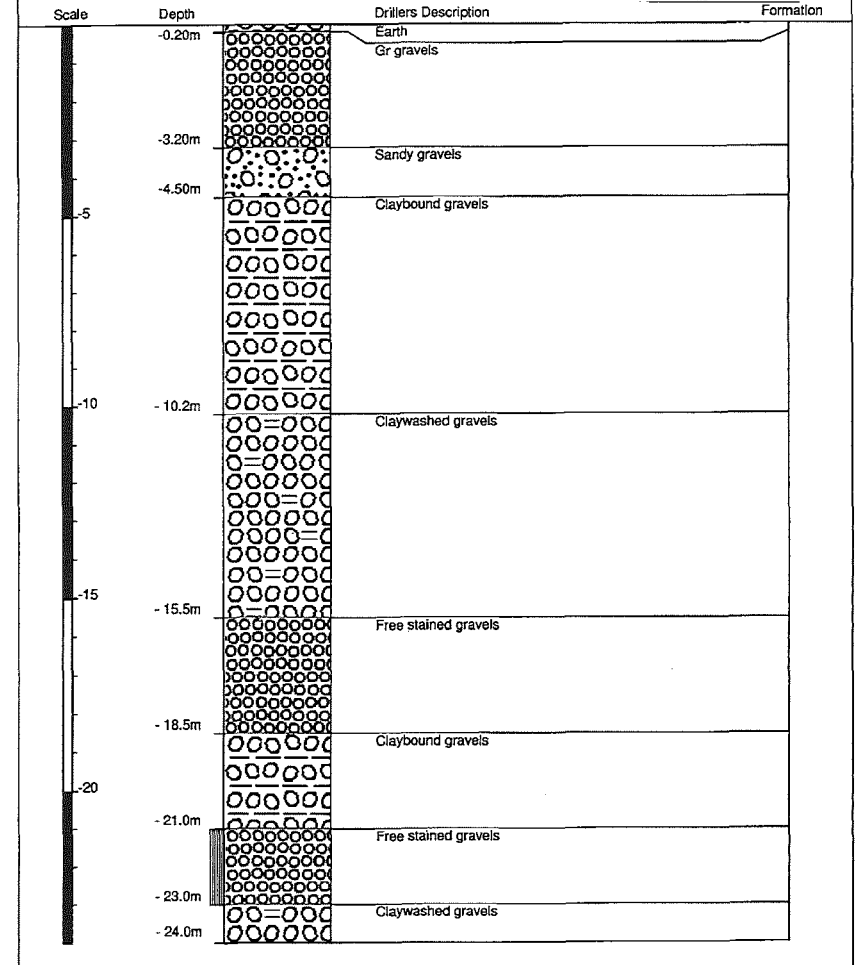

Borelog for well N32/0111

Gridref: N32:9943-3242

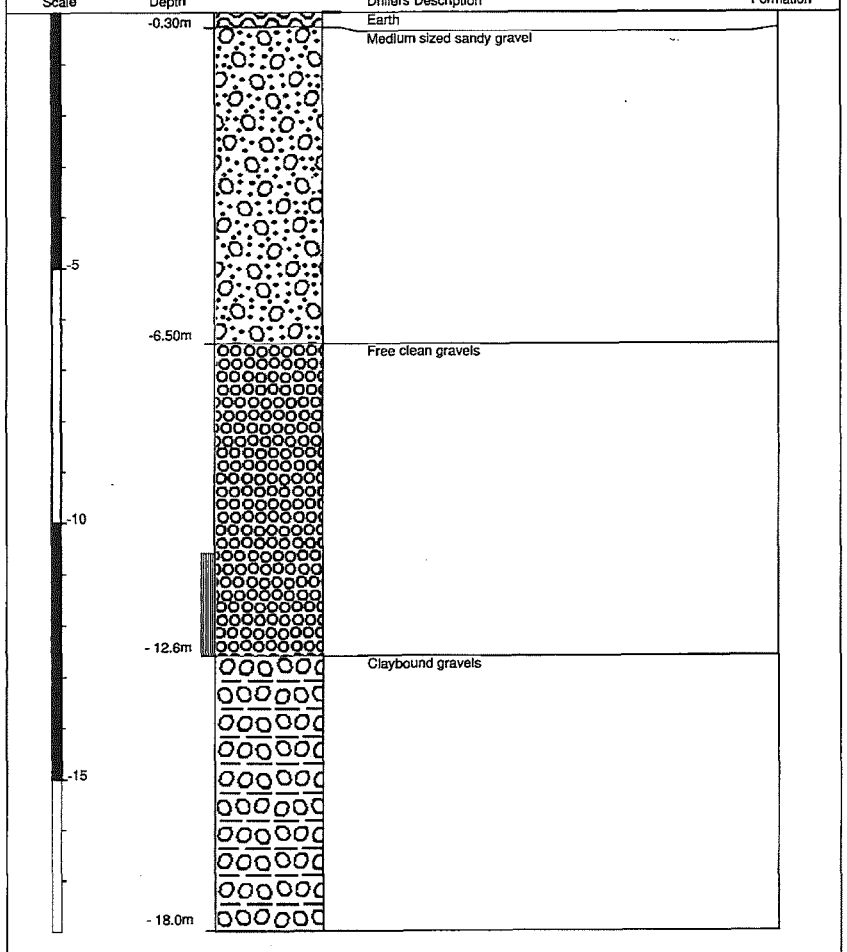

Borelog for well N32/0112

Gridref: N32:0138-3010

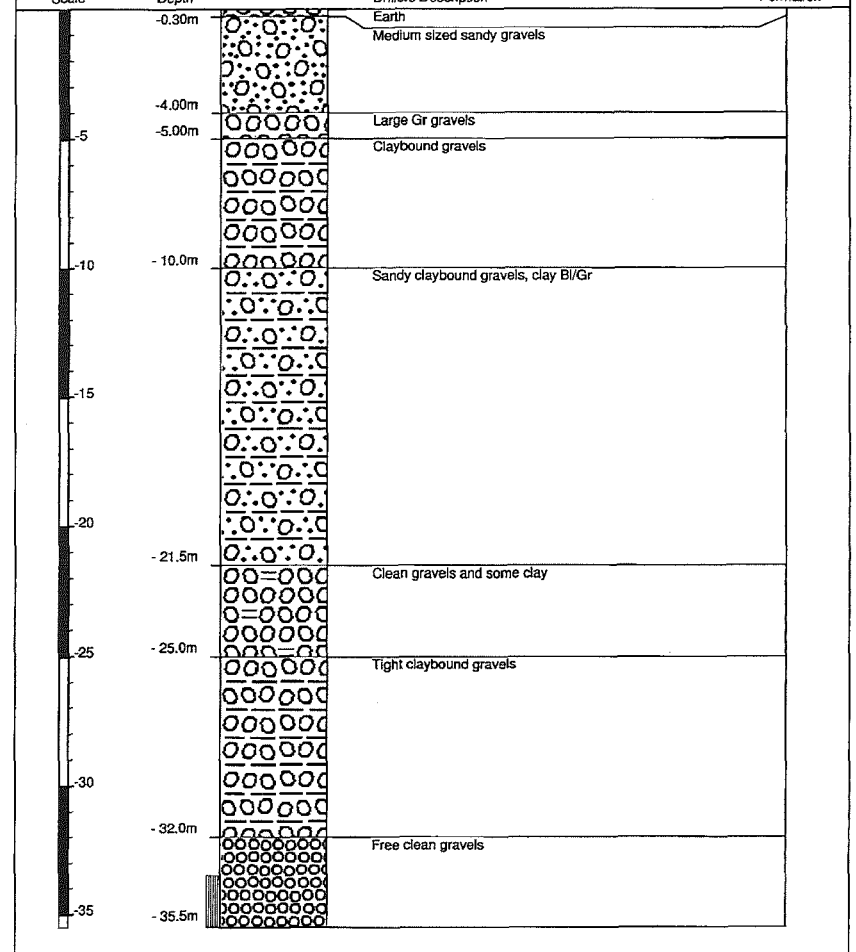

Borelog for well N32/0113

Gridref: N32:994-328

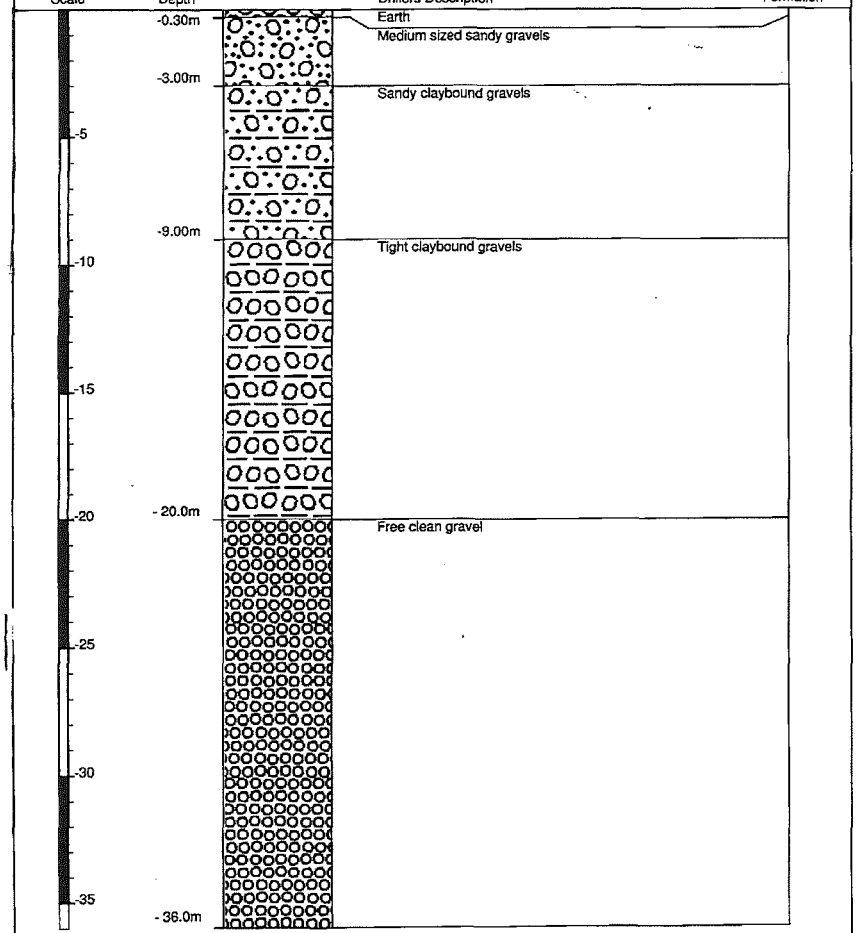

Borelog for well N32/0144

Gridref: N32:997-315

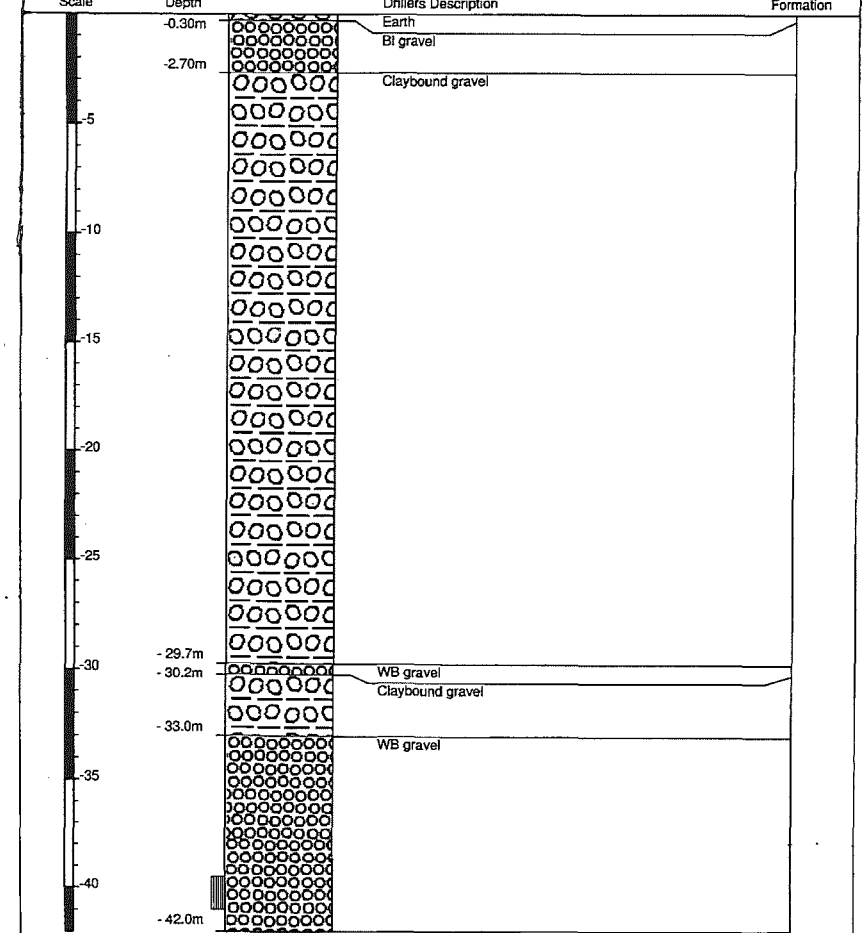

Borelog for well N32/0147

Gridref: N32:0660-3680

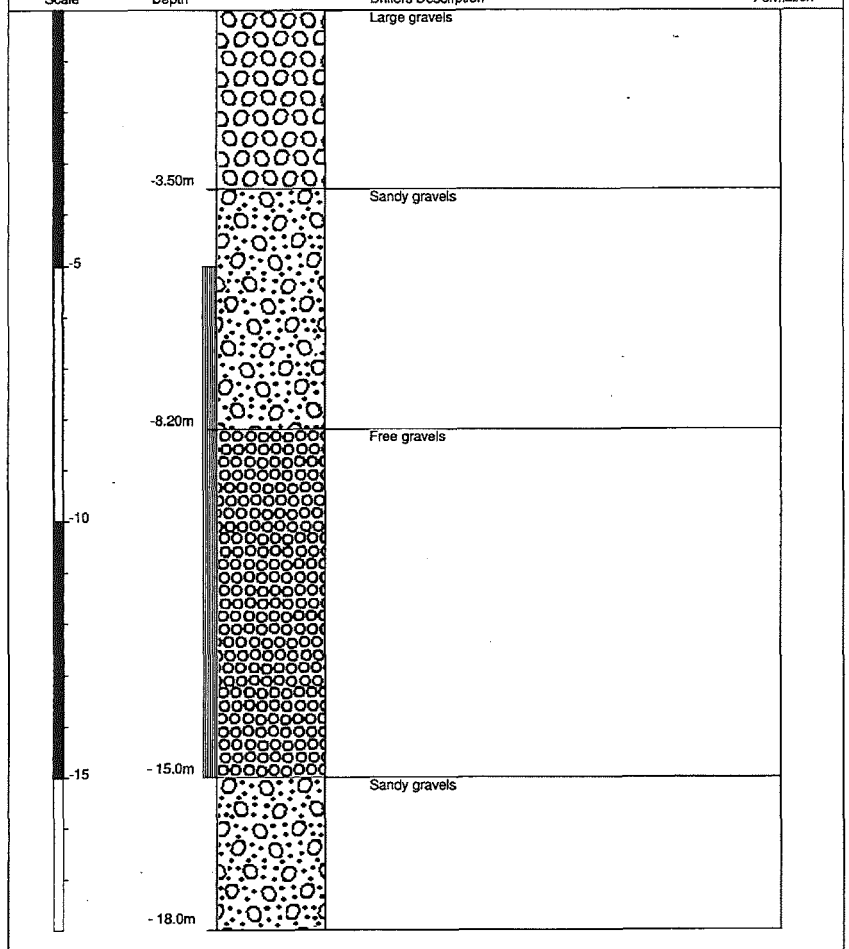

Borelog for well N32/0171

Gridref: N32:1220-3220

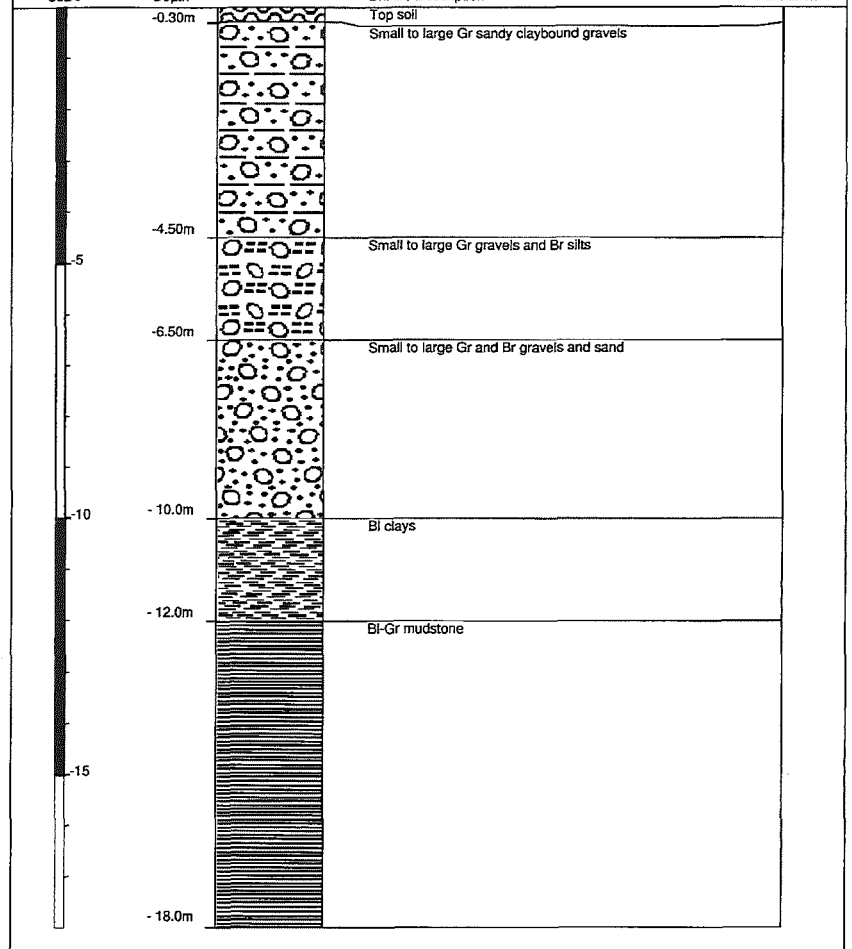

Borelog for well N32/0203

Gridref: N32:0546-3433

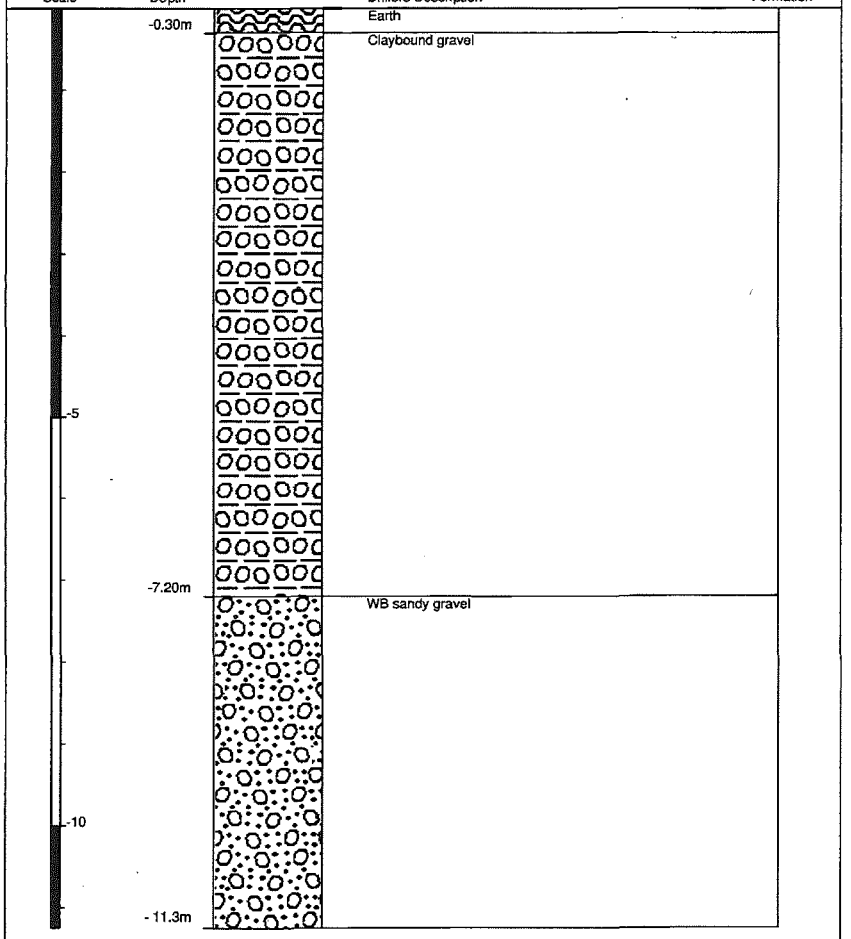

Borelog for well N32/0210

Gridref: N32:0133-3338

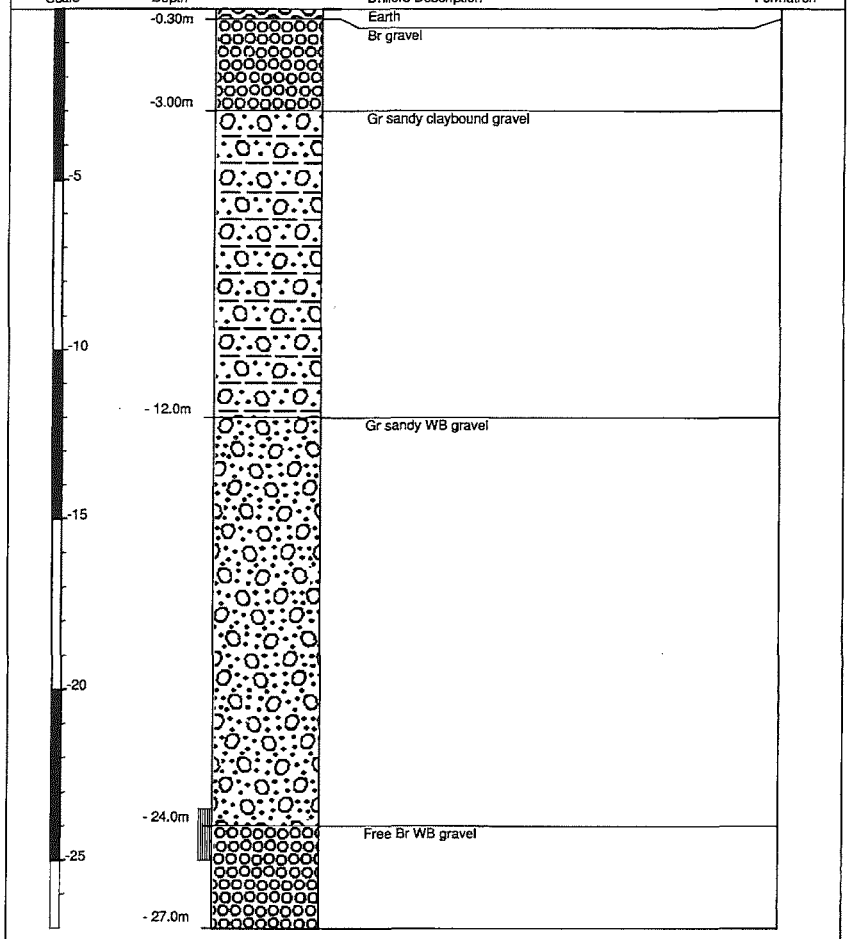

Borelog for well N32/0211

Gridref: N32:0122-3101

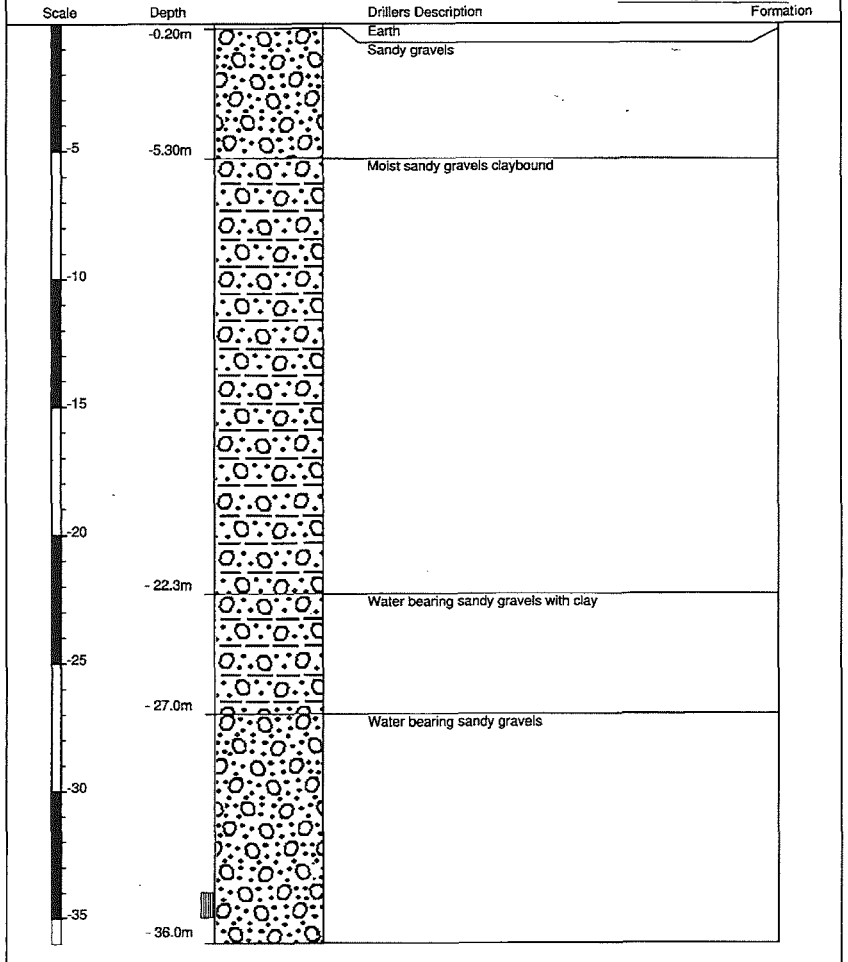

Borelog for well N32/0212

Gridref: N32:0662-3683

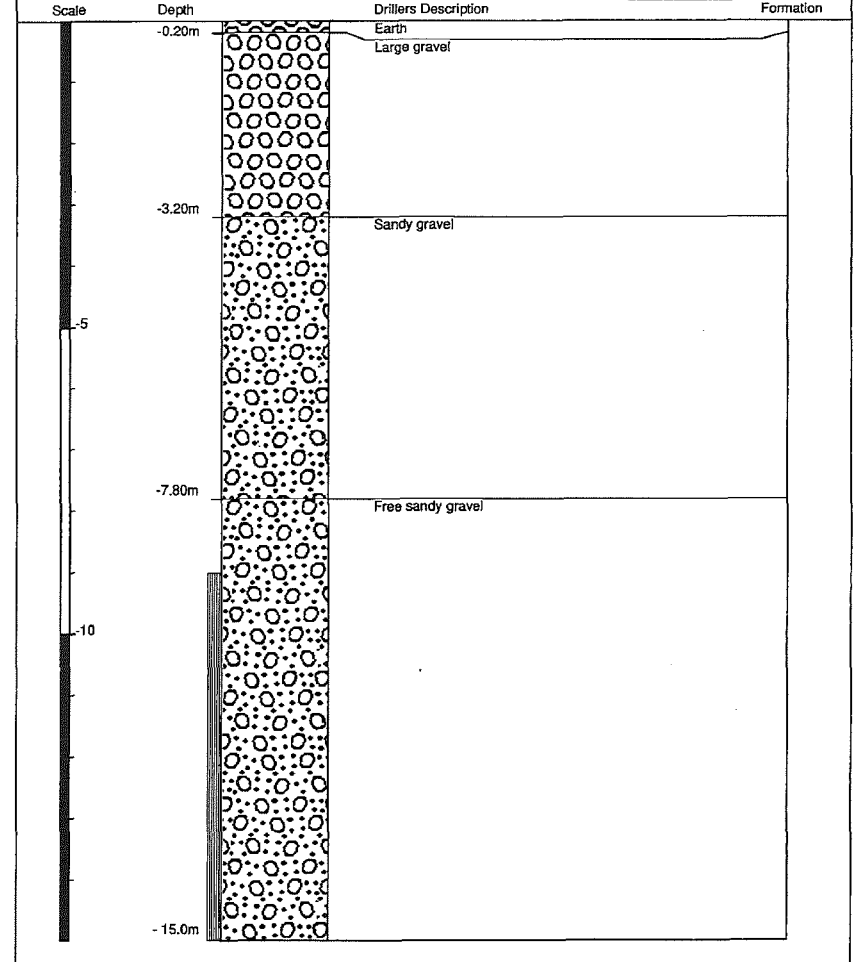

Borelog for well N32/0216

Gridref: N32:0292-3192

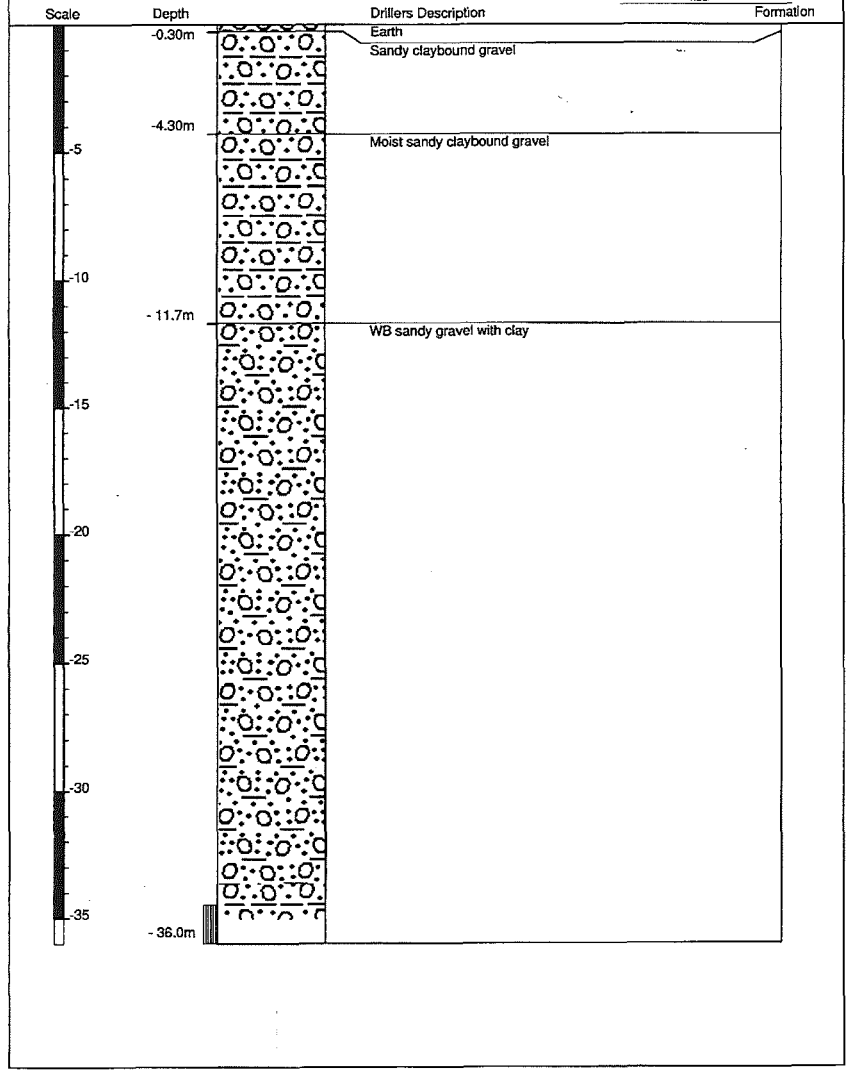

Borelog for well N32/0217

Gridref: N32:0120-3313

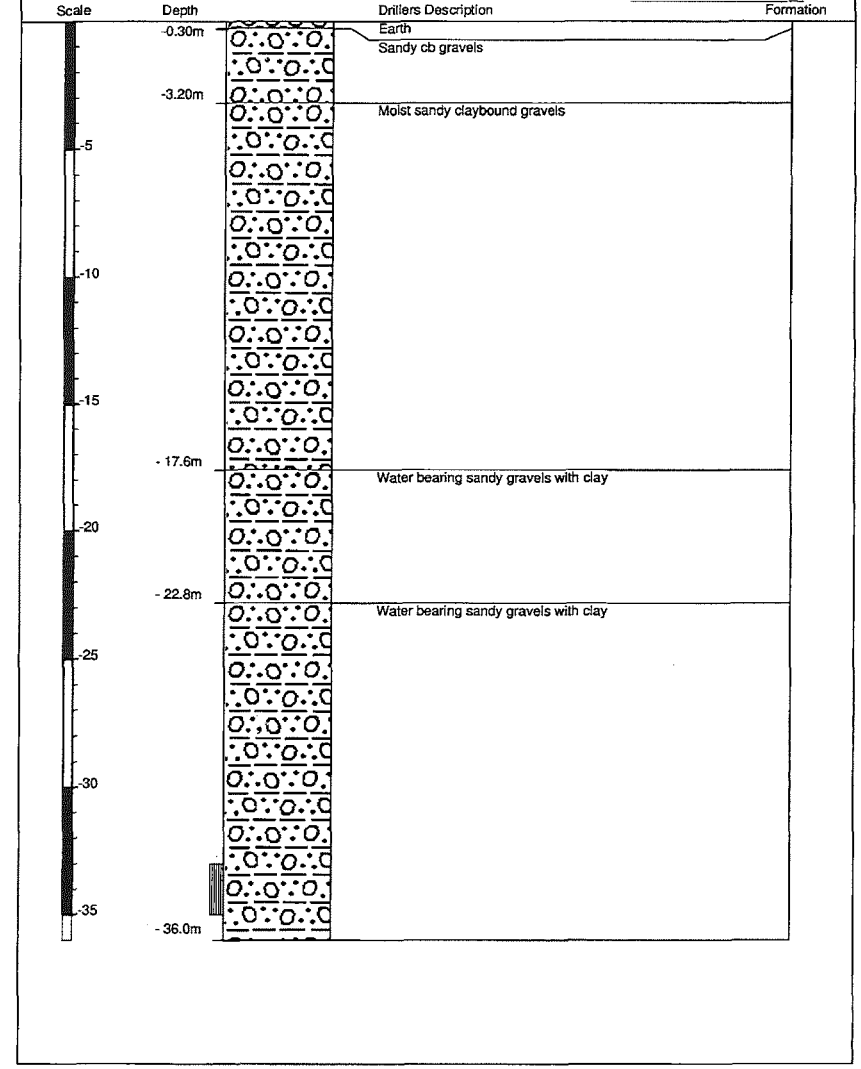

Borelog for well N32/0232

Gridref: N32:1358-3946

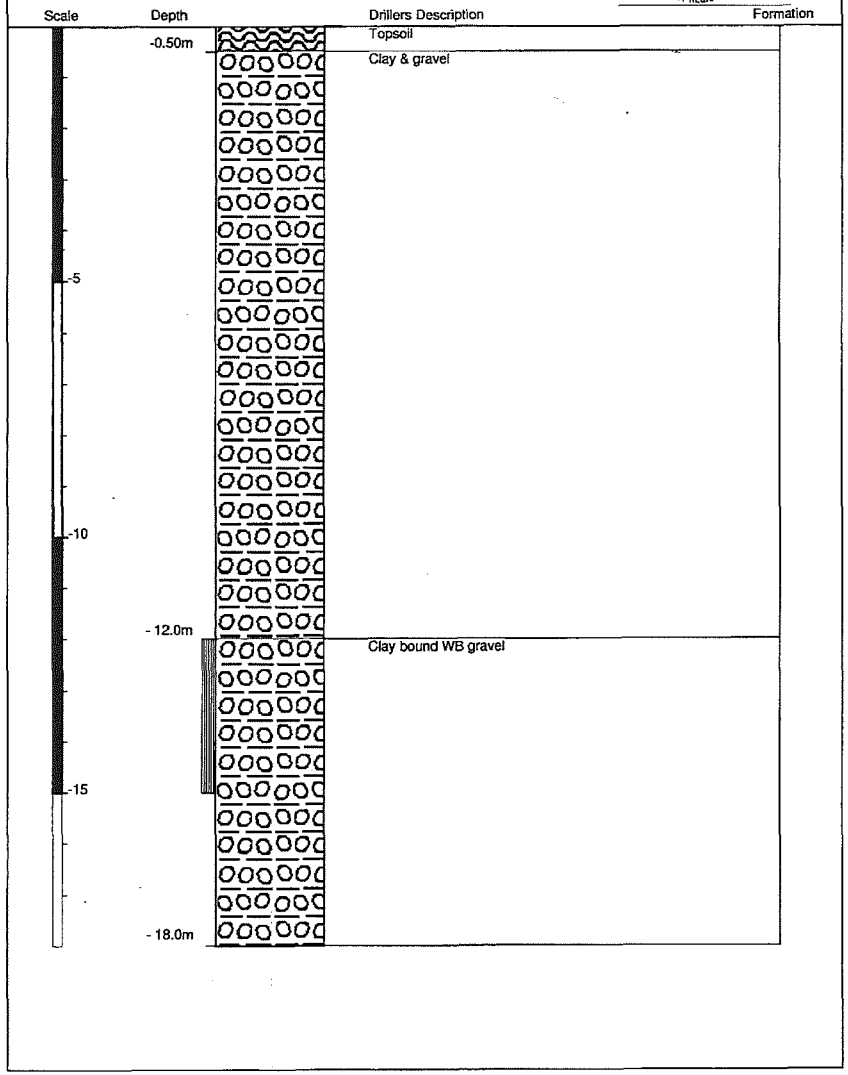

Borelog for well N32/0233

Gridref: N32:0584-3502

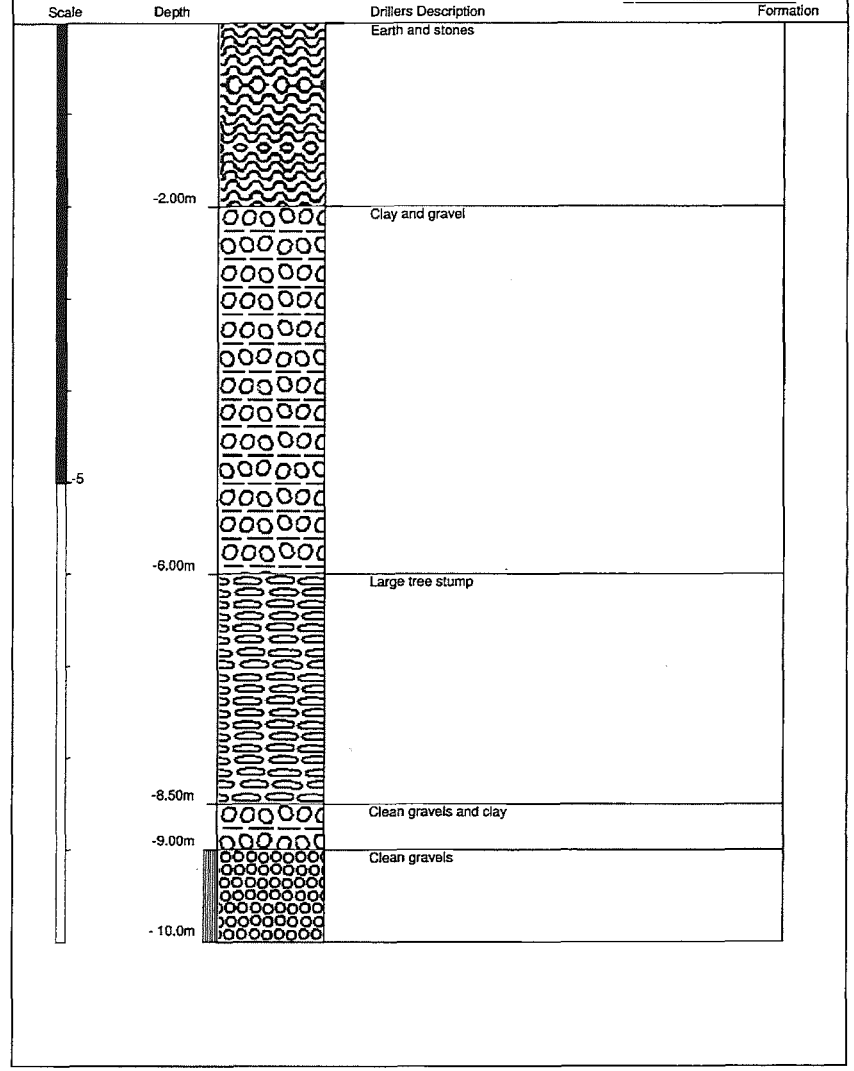

Borelog for well N32/0236 page 1 of 2
Gridref: N32:0278-3988

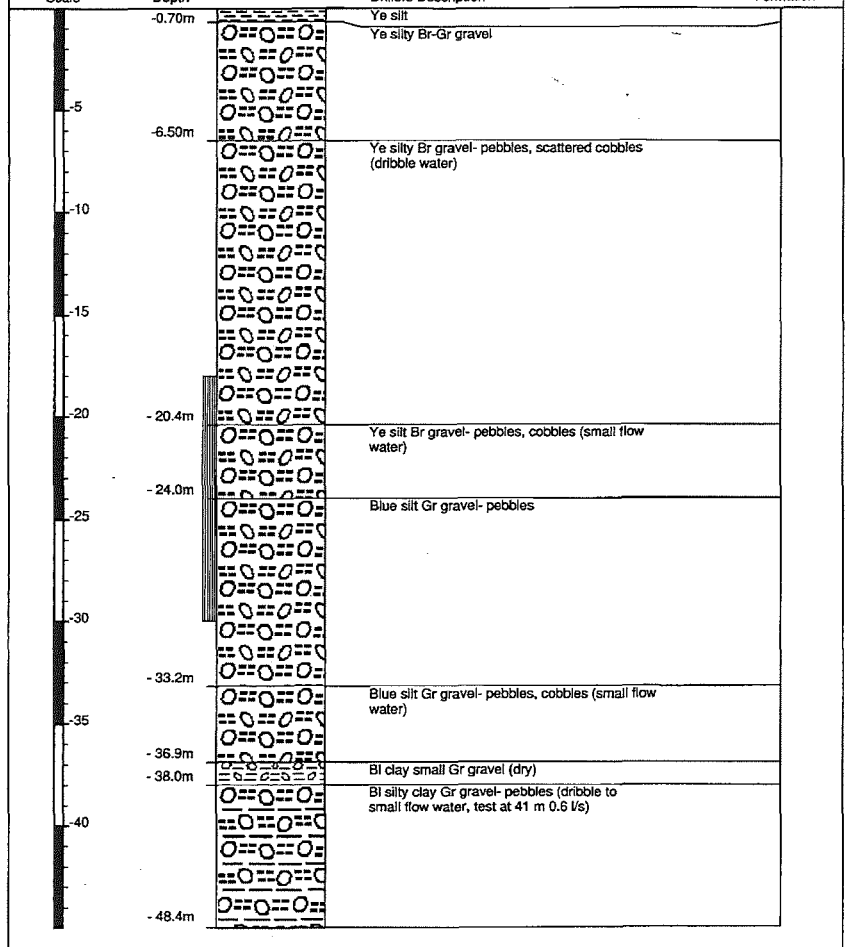

Borelog for well N32/0236 page 2 of 2
Gridref: N32:0278-3988

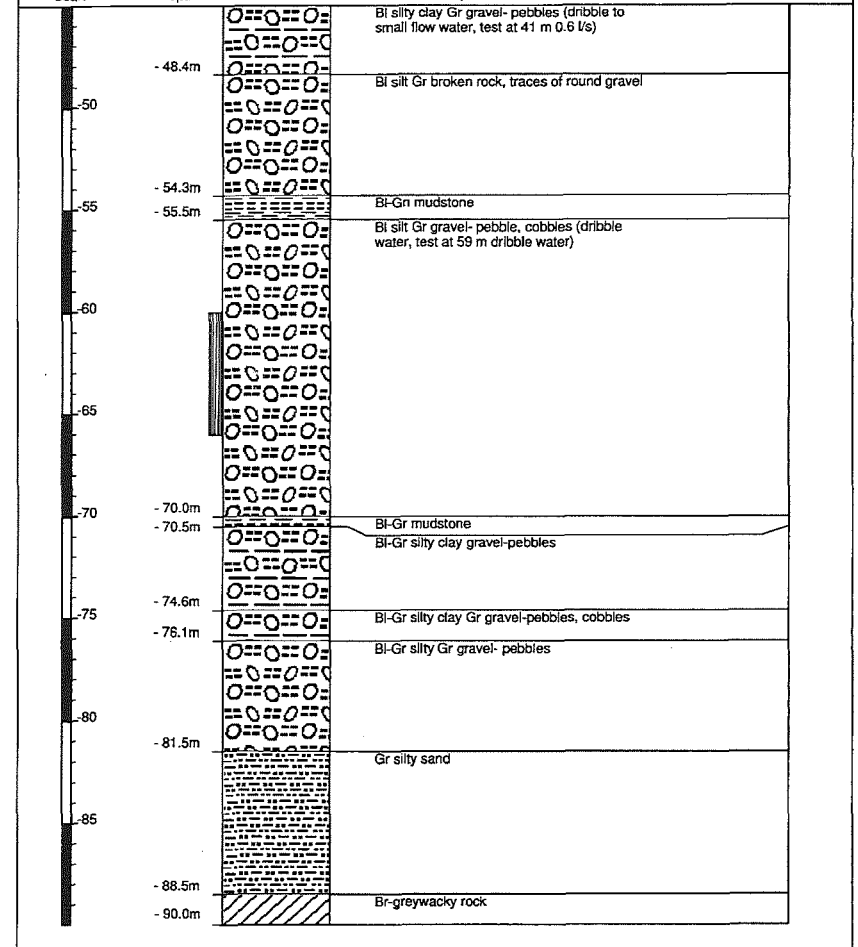

Borelog for well N33/0001

Gridref: N33:995-288

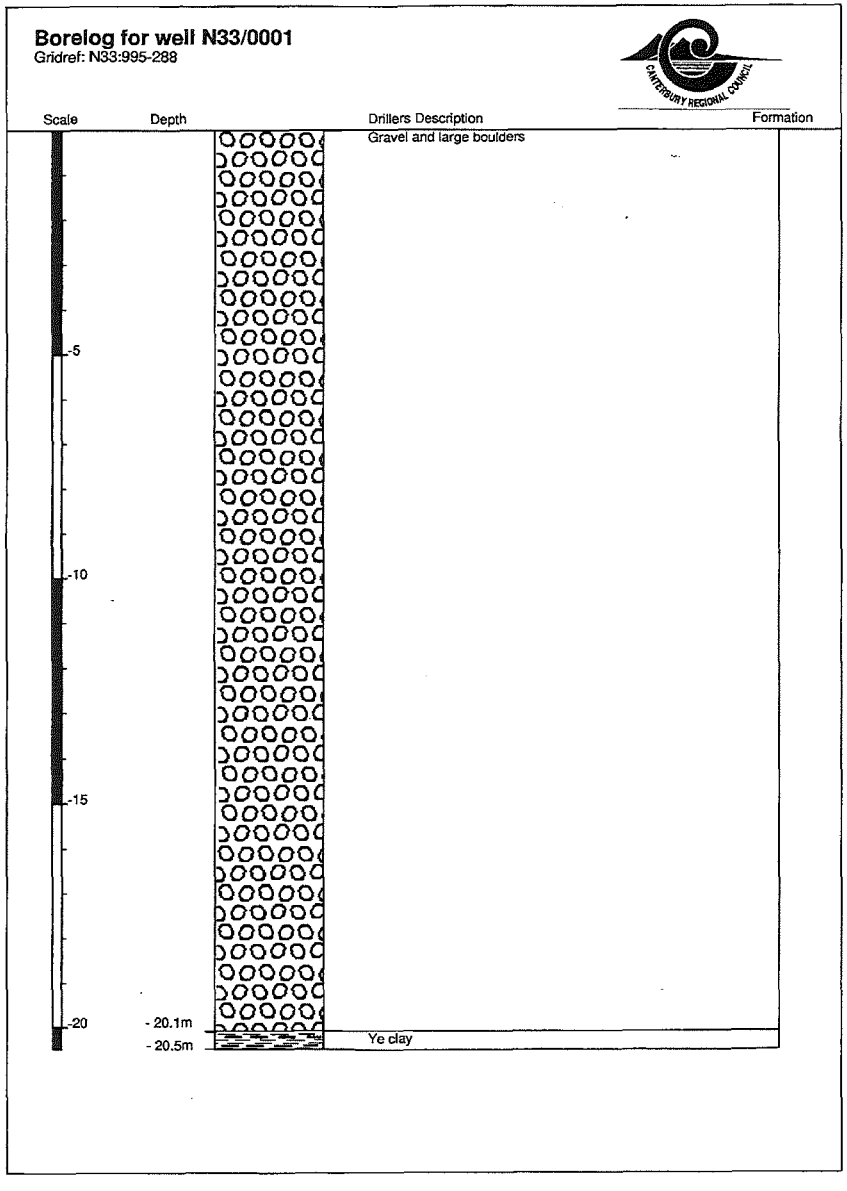

Borelog for well N33/0011

Gridref: N33:011-261

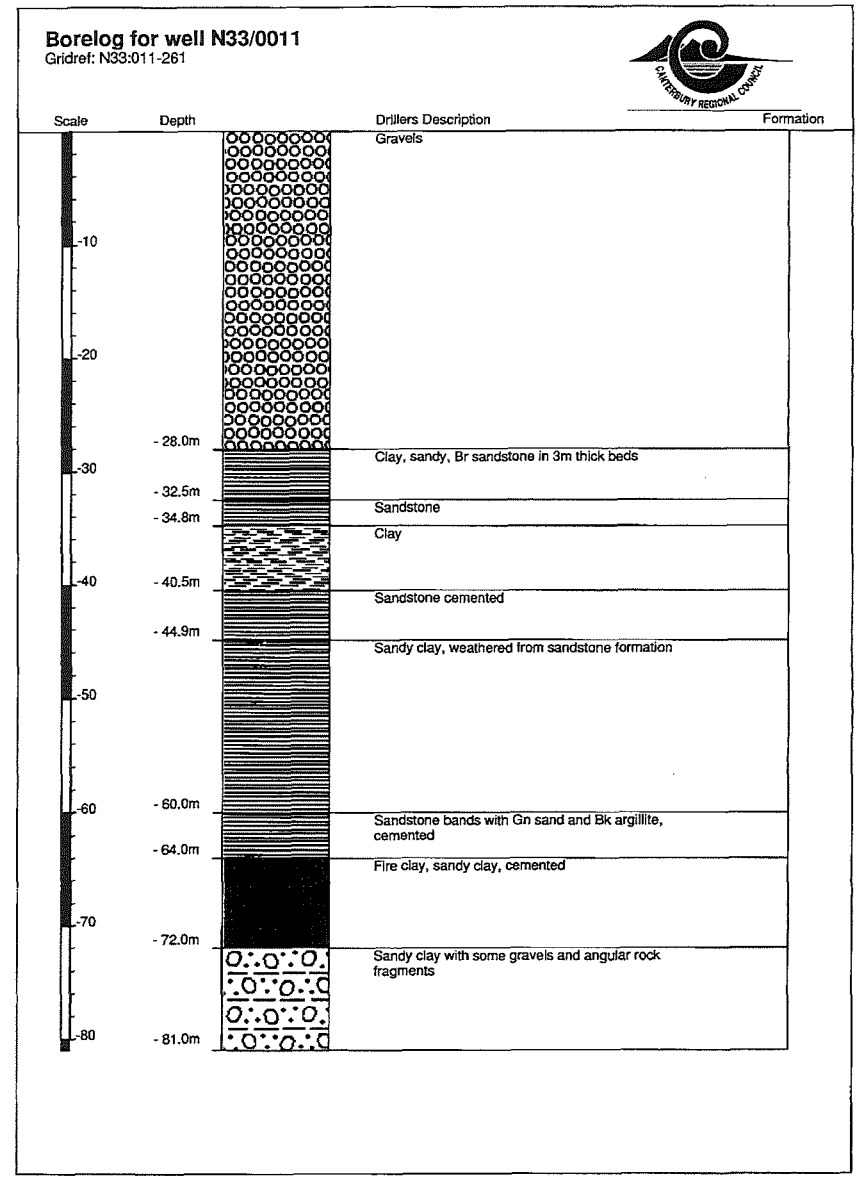

Borelog for well N33/0013

Gridref: N33:980-264

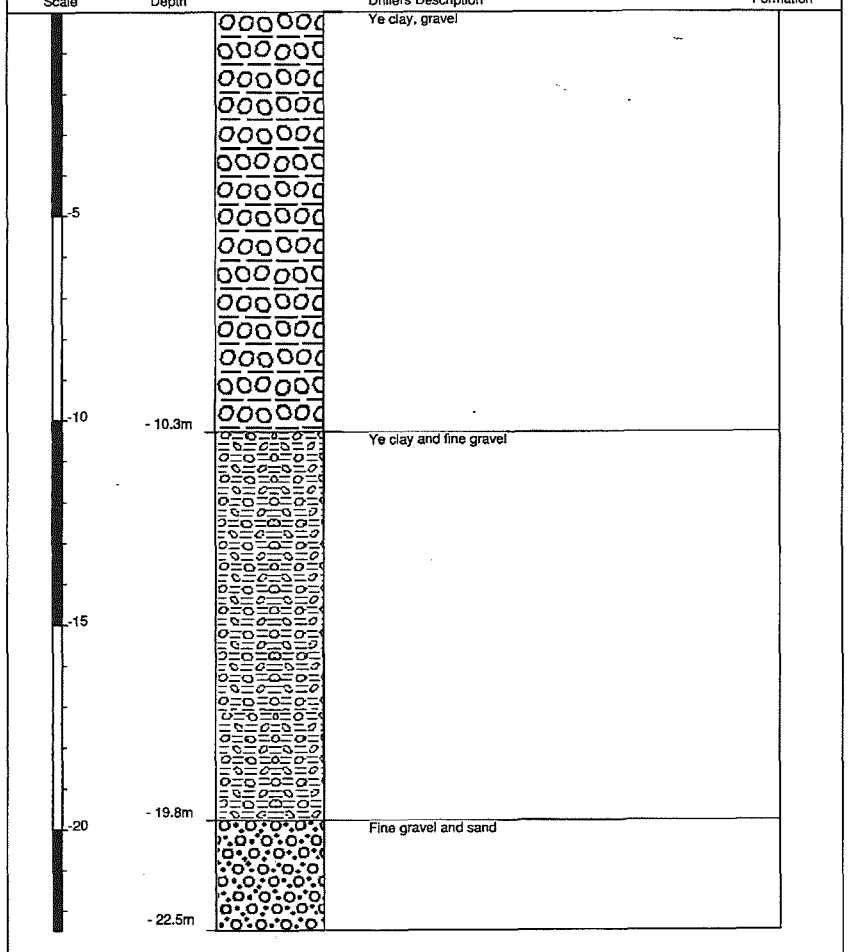

Borelog for well N33/0019

Gridref: N33:963-239

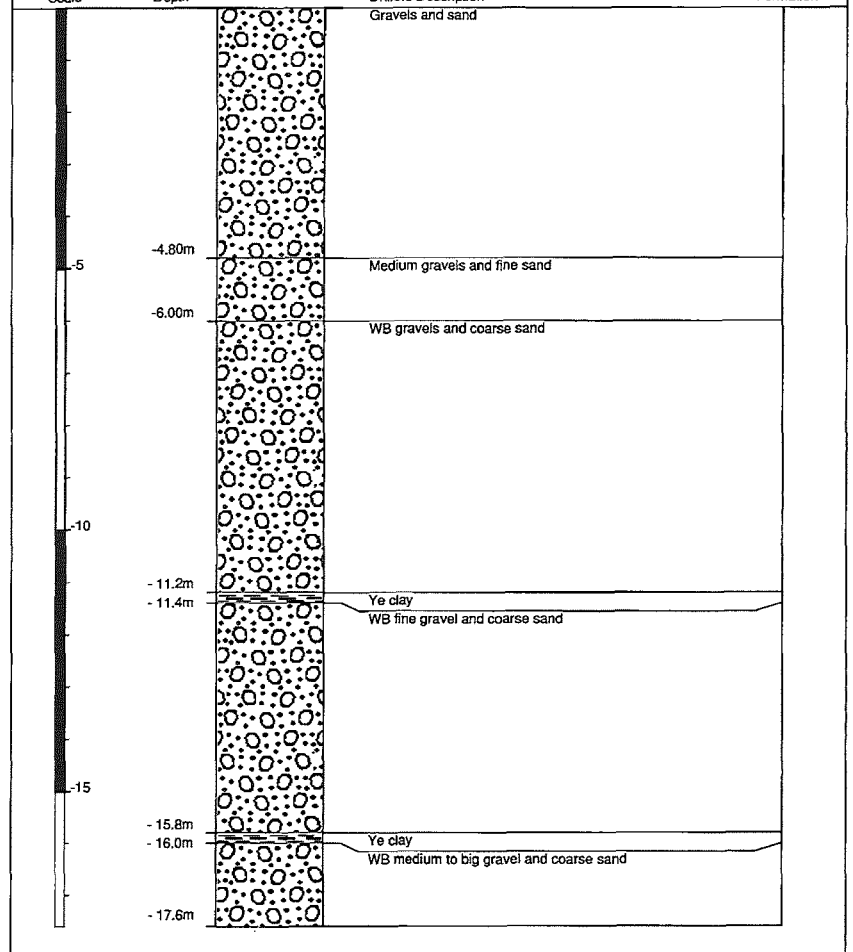

Borelog for well N33/0020

Gridref: N33:976-263

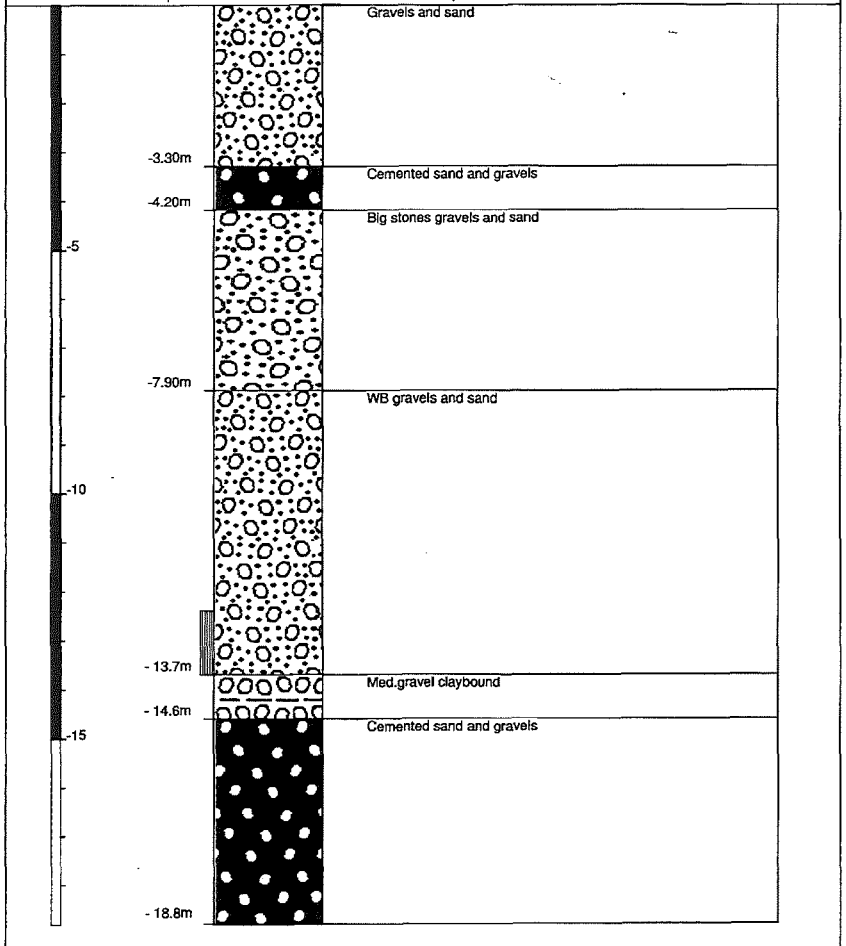

Borelog for well N33/0044

Gridref: N33:9788-2600

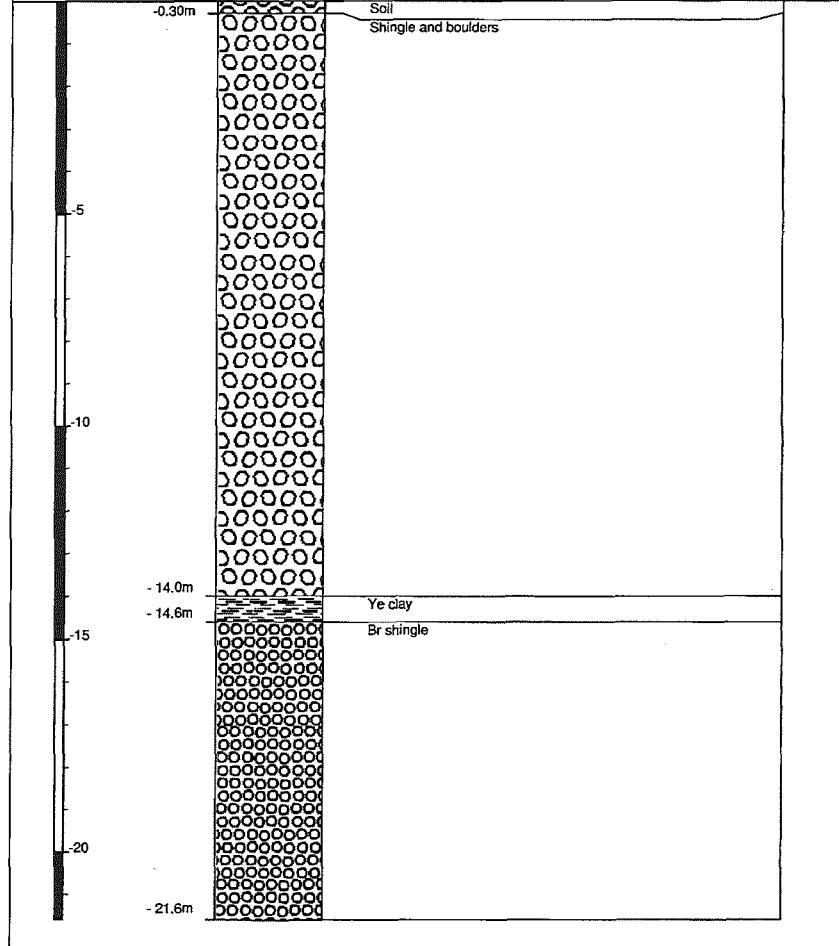

Borelog for well N33/0045

Gridref: N33:022-257

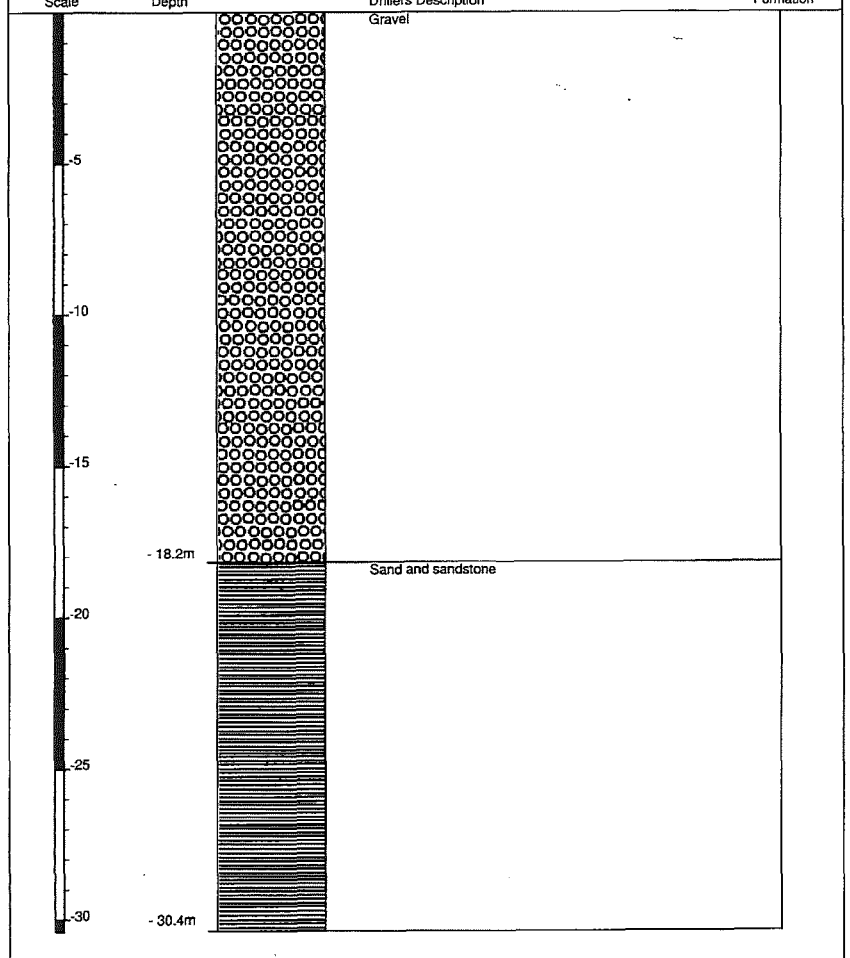

Borelog for well N33/0061

Gridref: N33:987-216

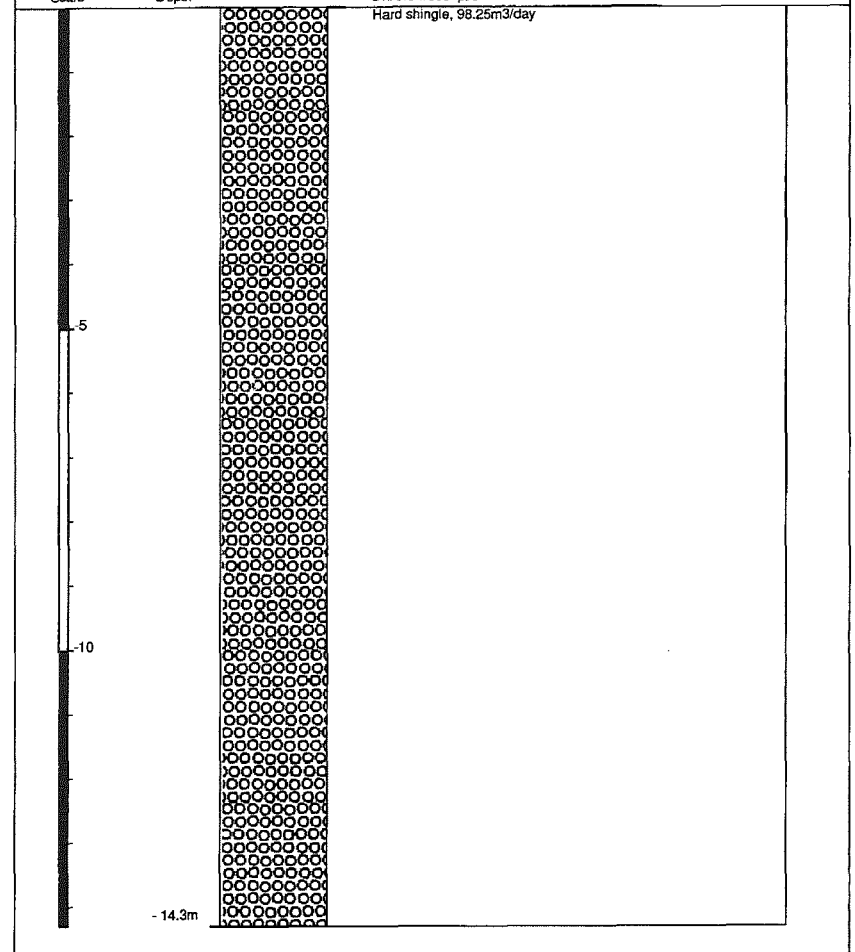

Borelog for well N33/0076

Gridref: N33:961-233

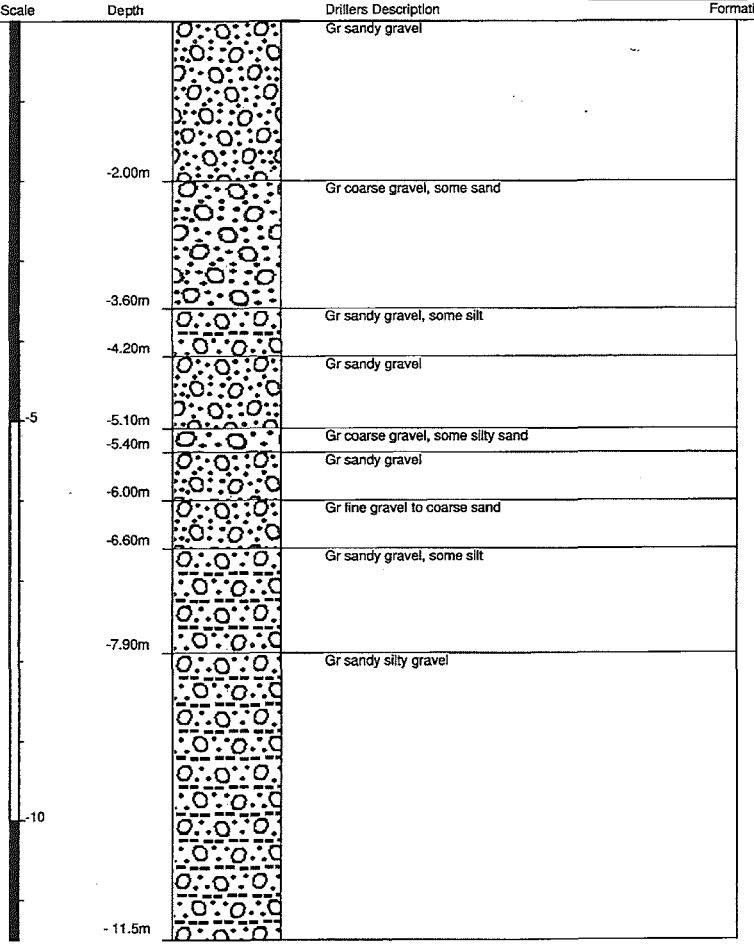

Borelog for well N33/0077

Gridref: N33:961-233

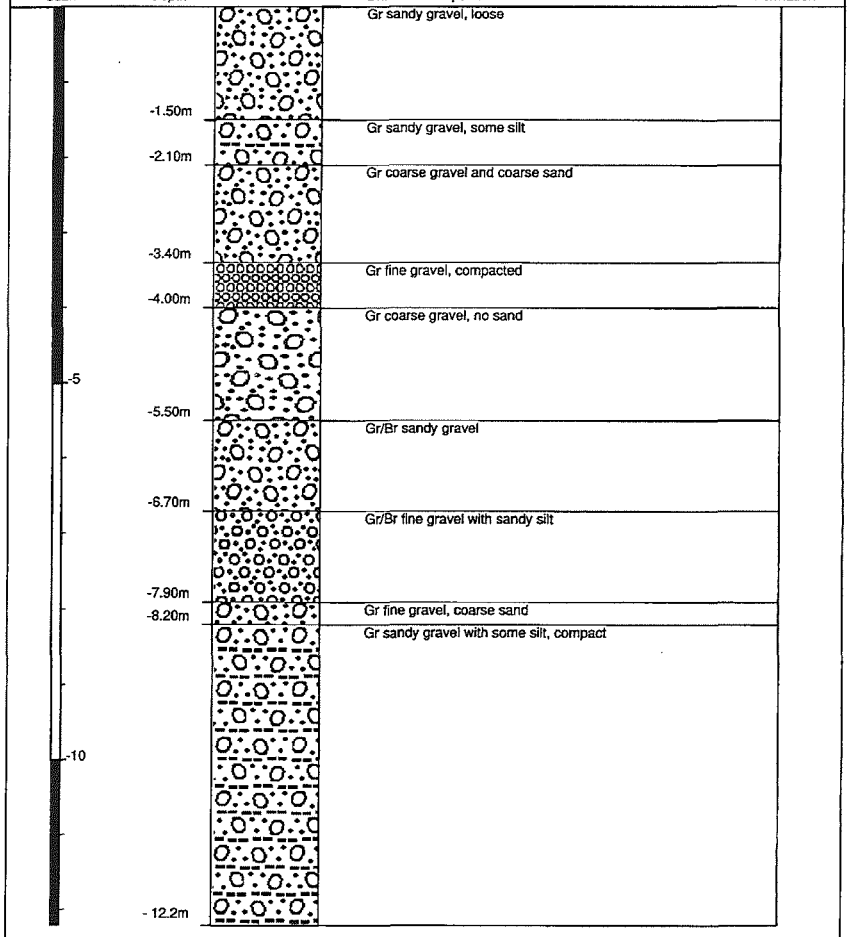

Borelog for well N33/0113

Gridref: N33:9945-2587

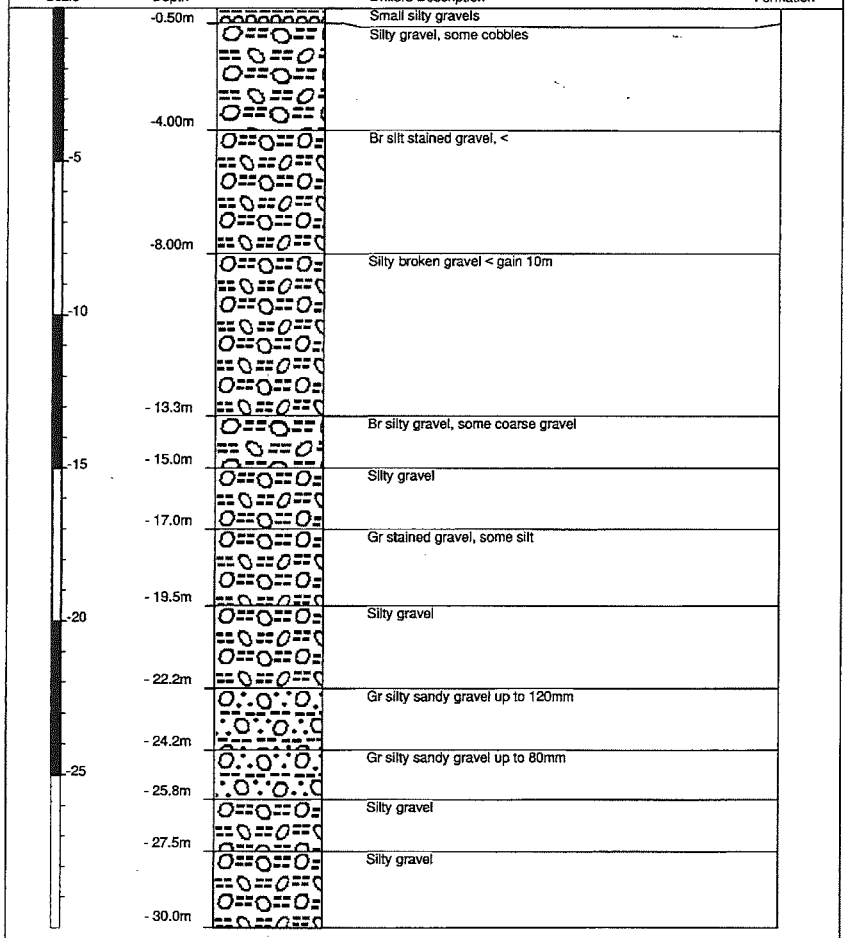

Borelog for well N33/0186

Gridref: N33:9703-2382

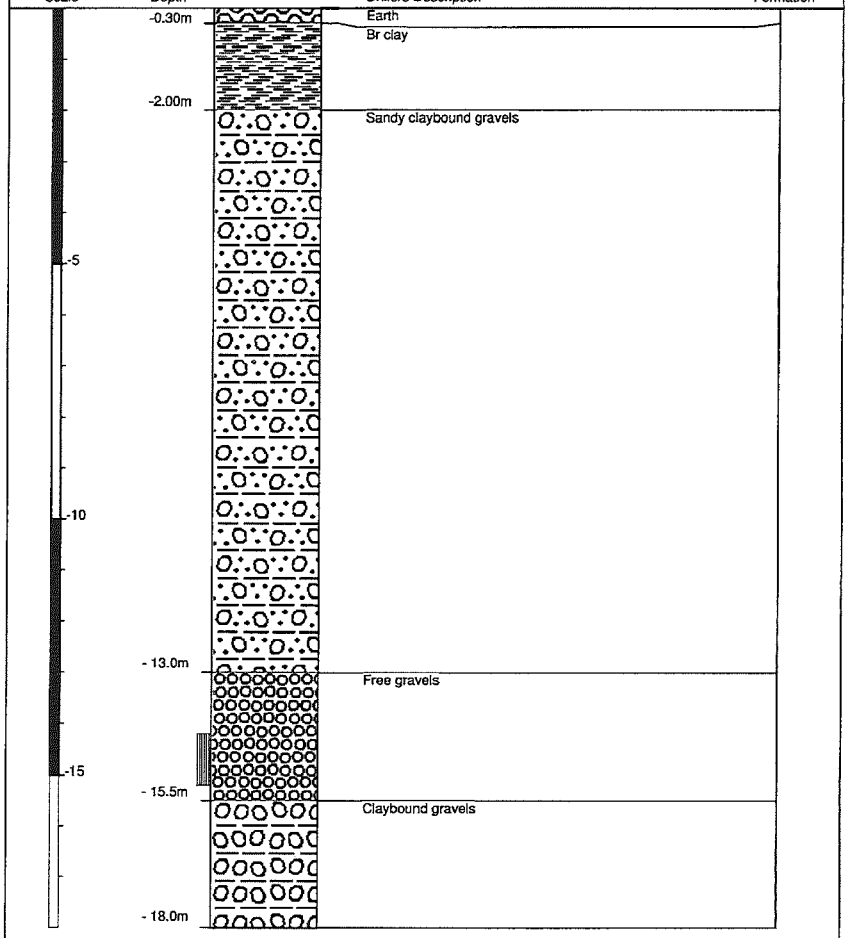

Borelog for well N33/0187

Gridref: N33:0273-2755

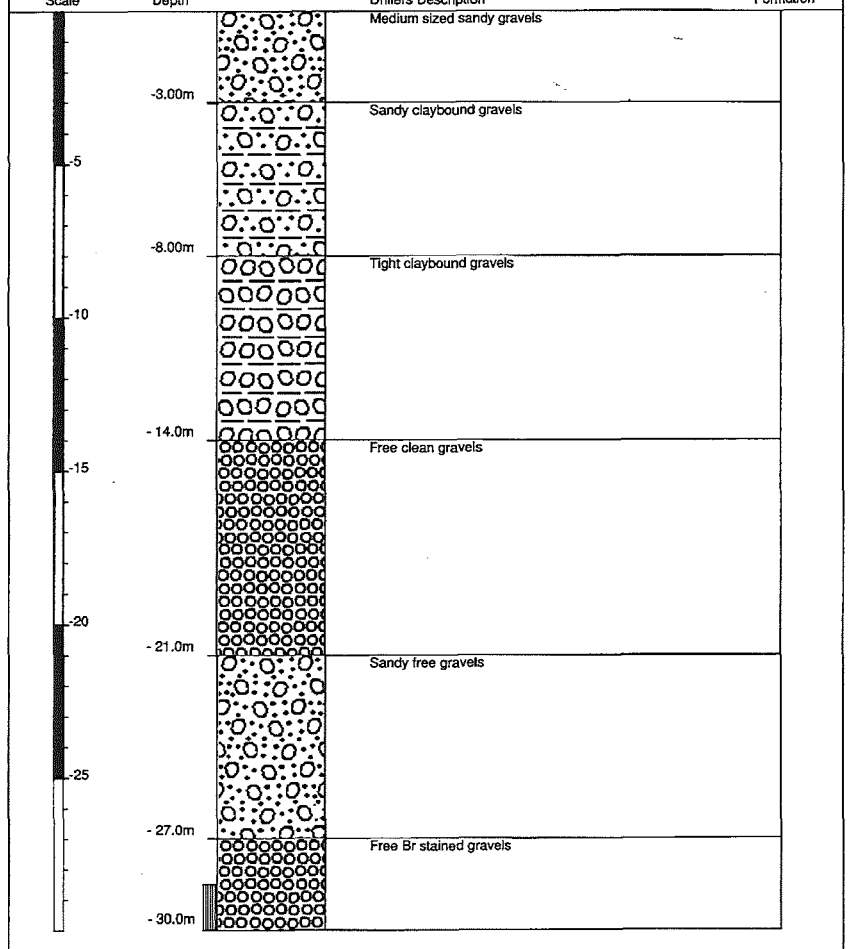

Borelog for well N33/0193

Gridref: N33:993-282

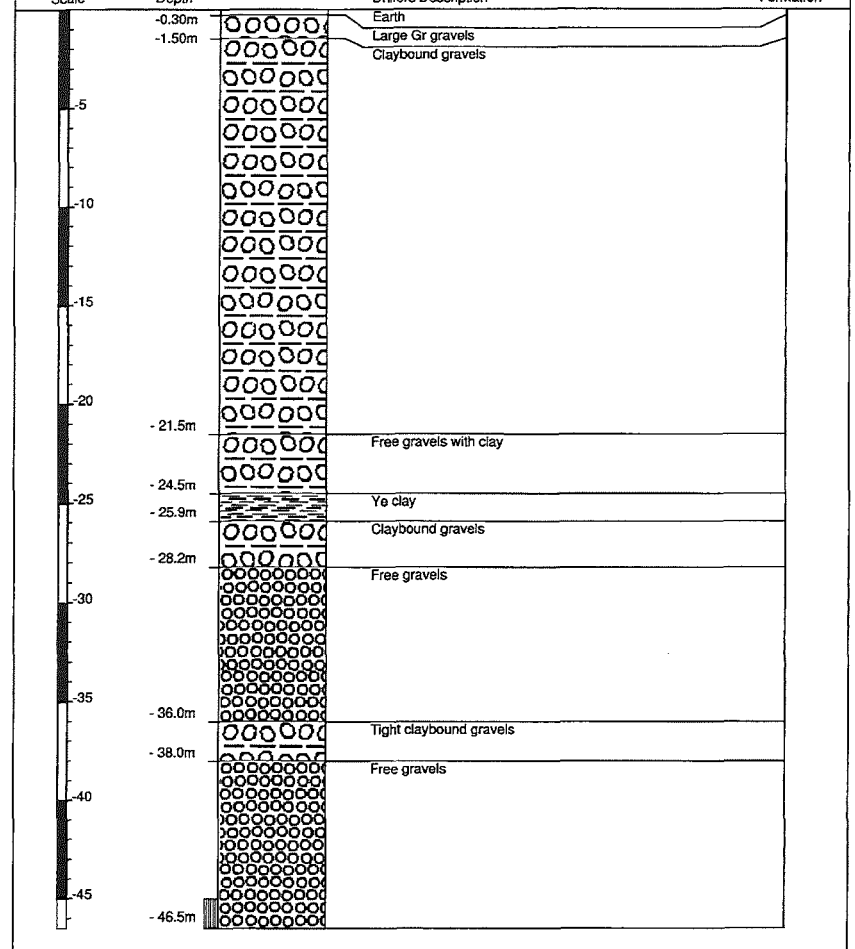

Borelog for well N33/0194

Gridref: N33:943-230

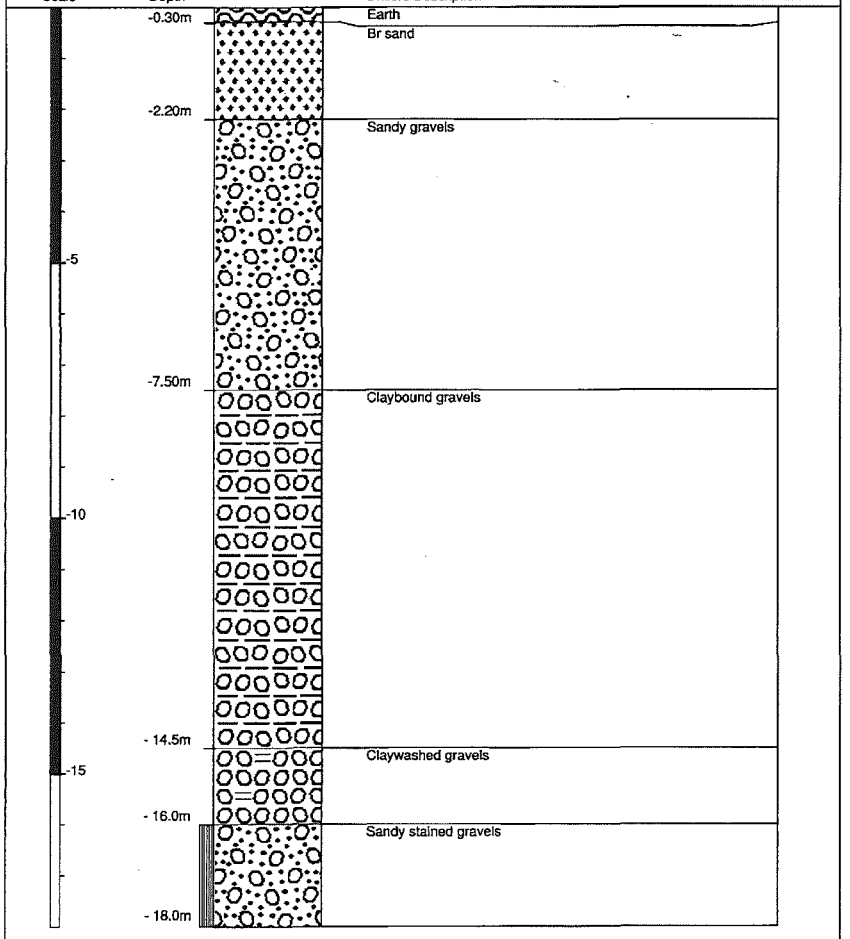

Borelog for well N33/0196

Gridref: N33:9805-2200

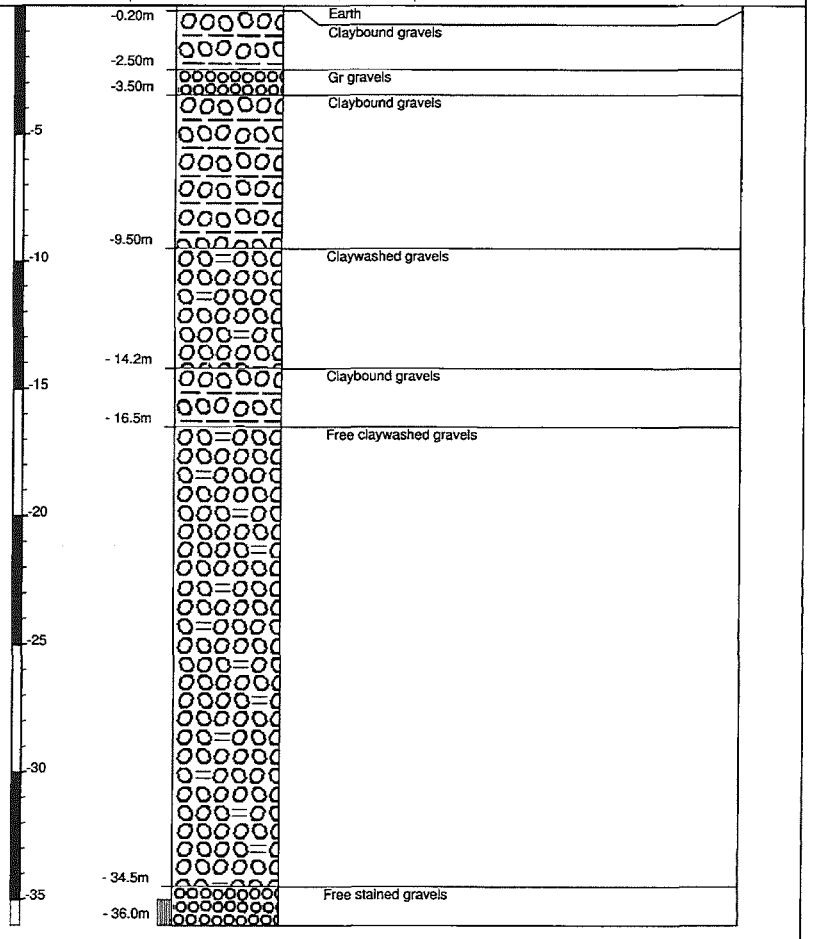

Borelog for well N33/0197

Gridref: N33:9462-2495

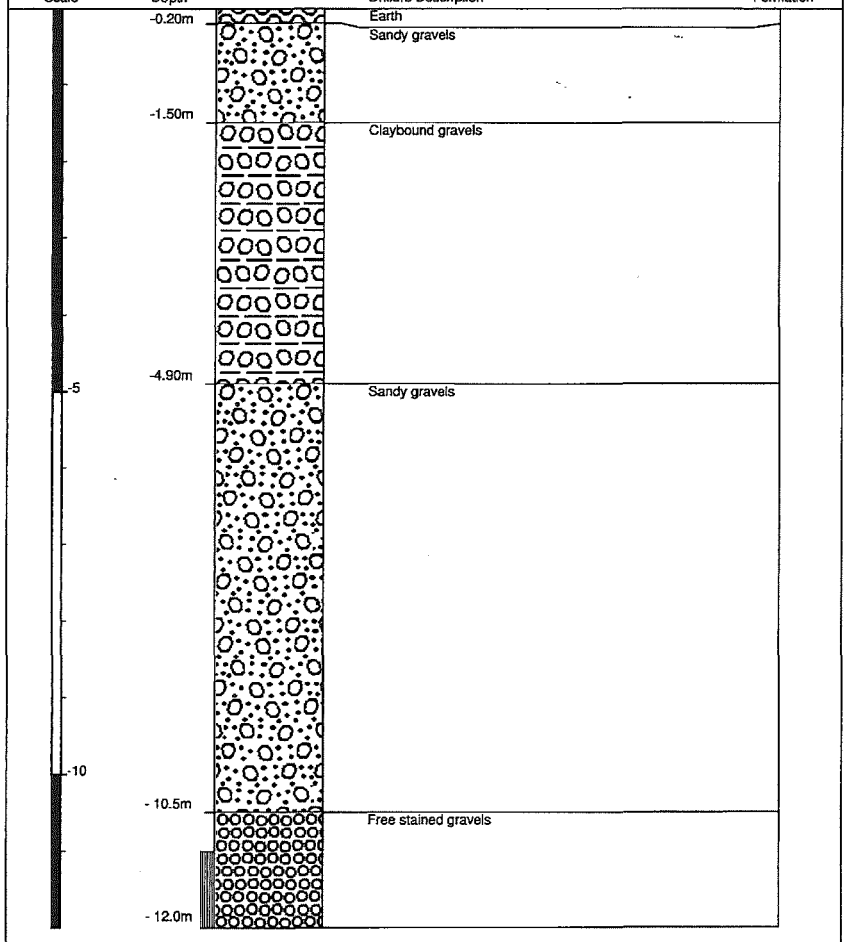

Borelog for well N33/0203

Gridref: N33:9410-2600

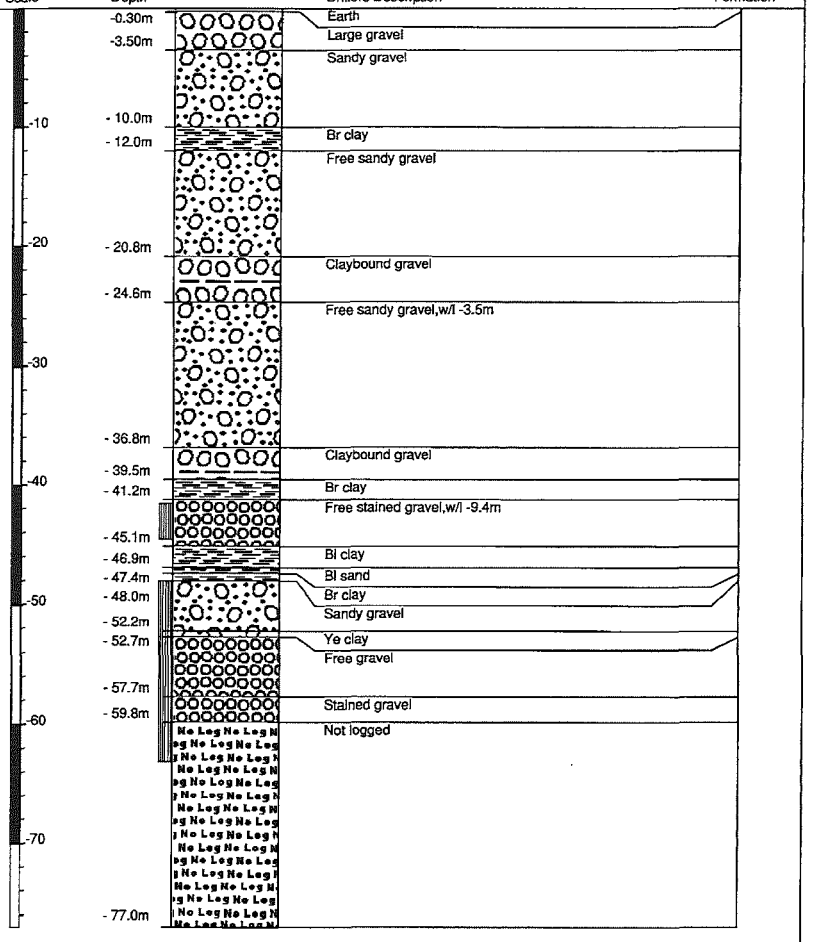

Borelog for well N33/0204

Gridref: N33:0435-2529

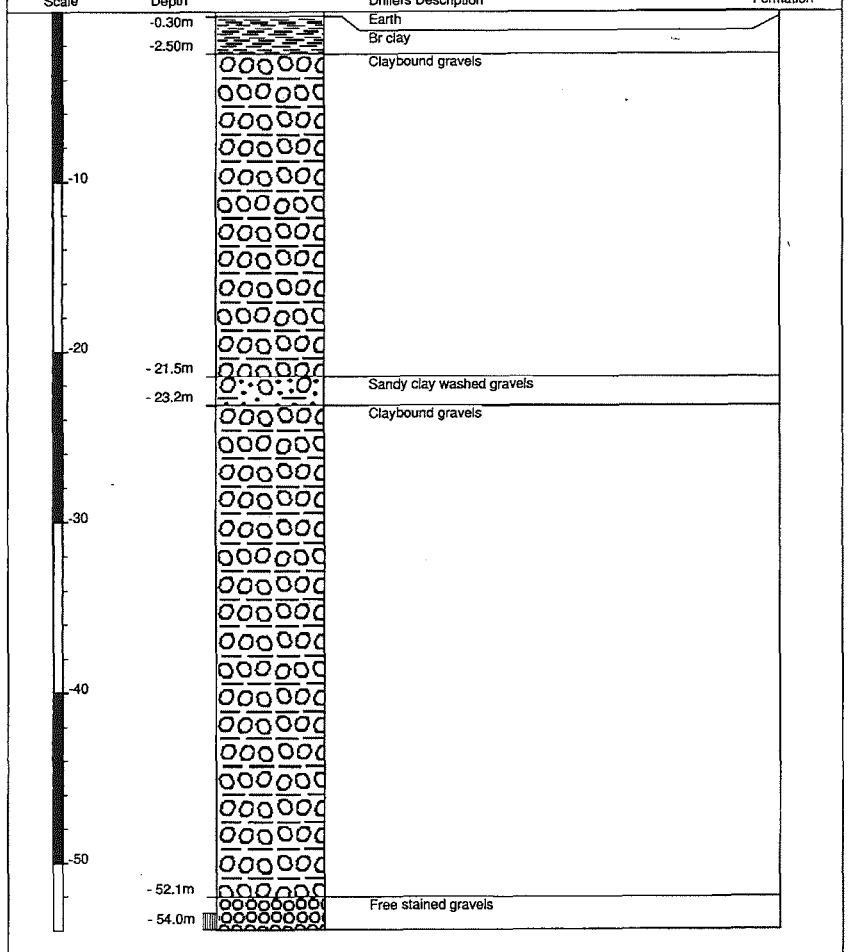

Borelog for well N33/0205

Gridref: N33:0091-2691

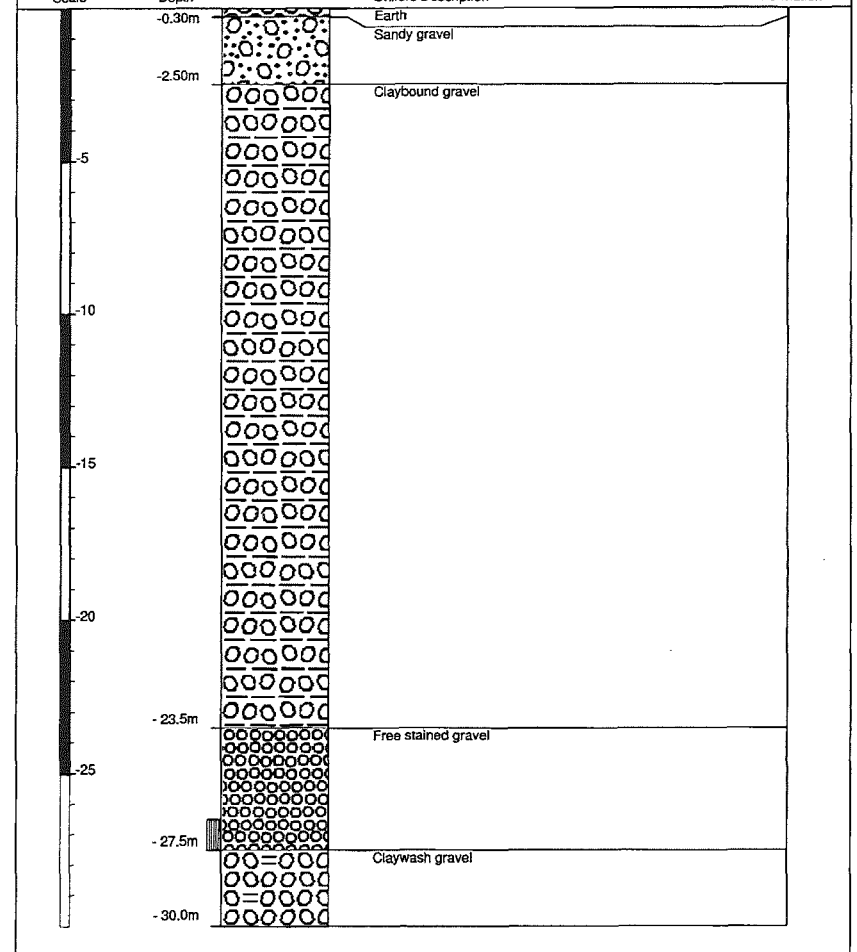

Borelog for well N33/0208

Gridref: N33:0000-2868

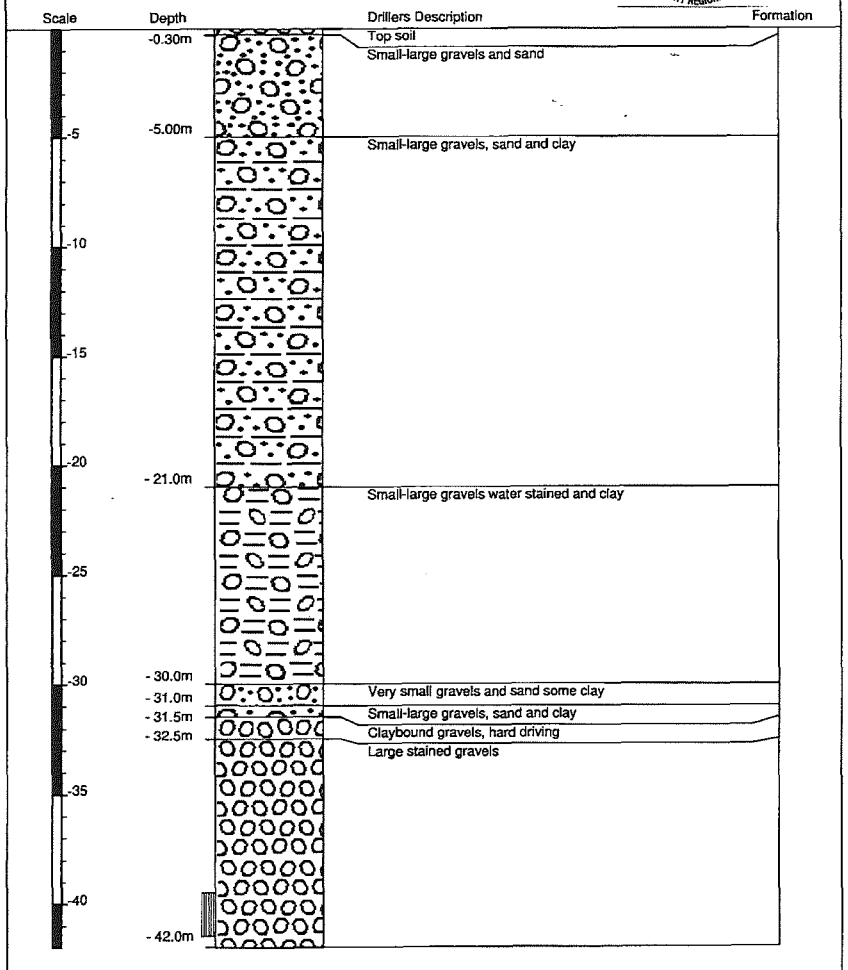

Borelog for well N33/0209

Gridref: N33:9677-2210

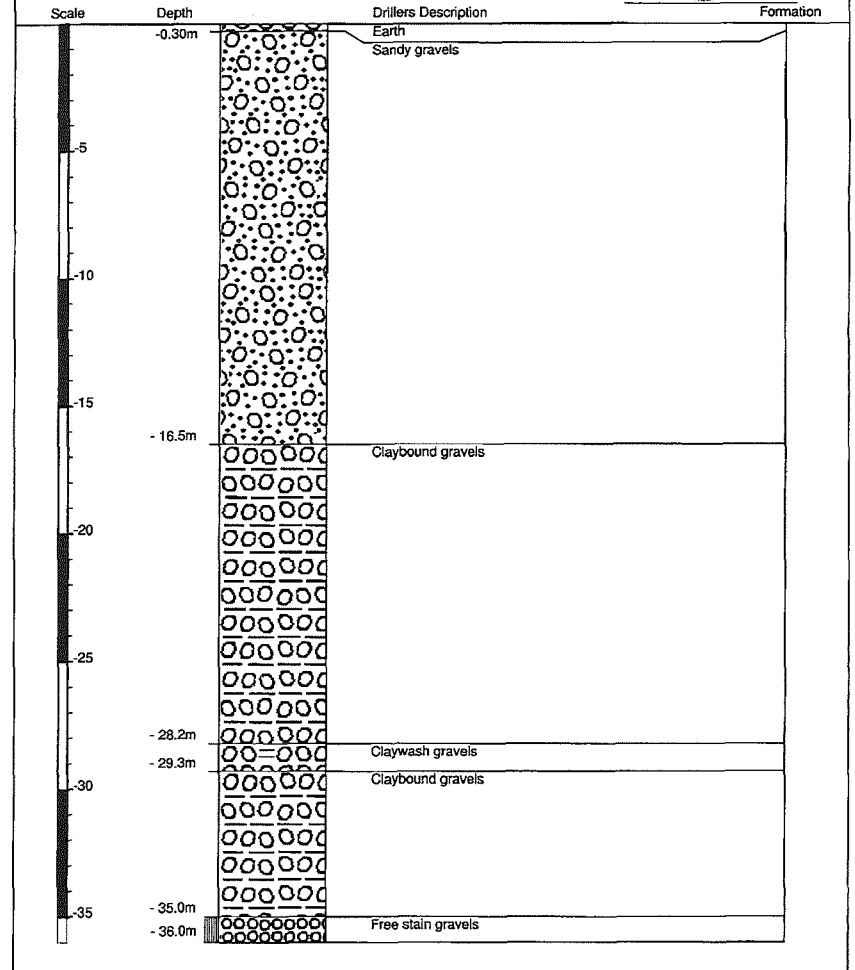

Borelog for well N33/0210

Gridref: N33:999-300

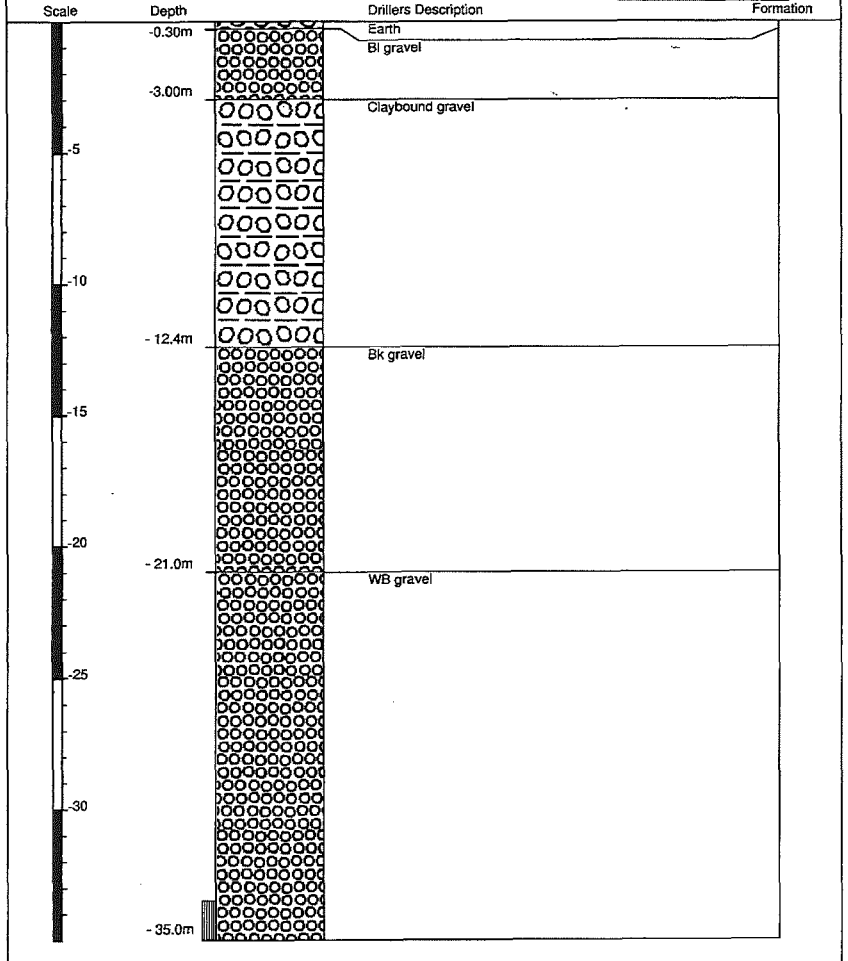

Borelog for well N33/0215

Gridref: N33:9290-2700

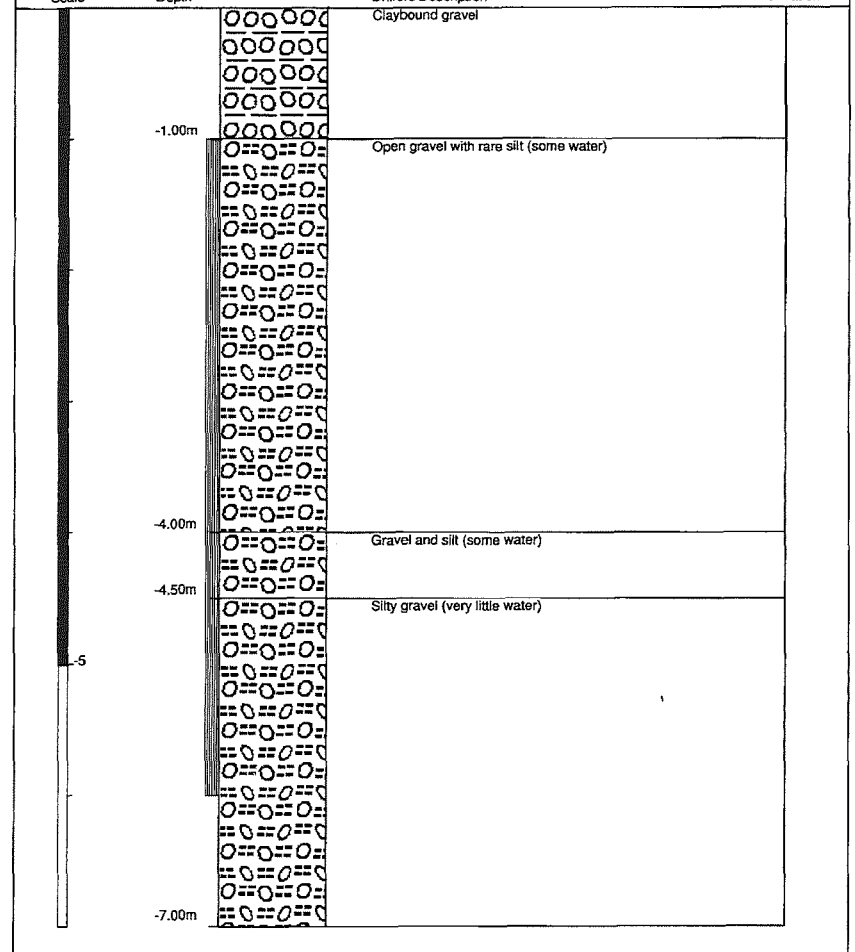

Borelog for well N33/0218

Gridref: N33:040-264

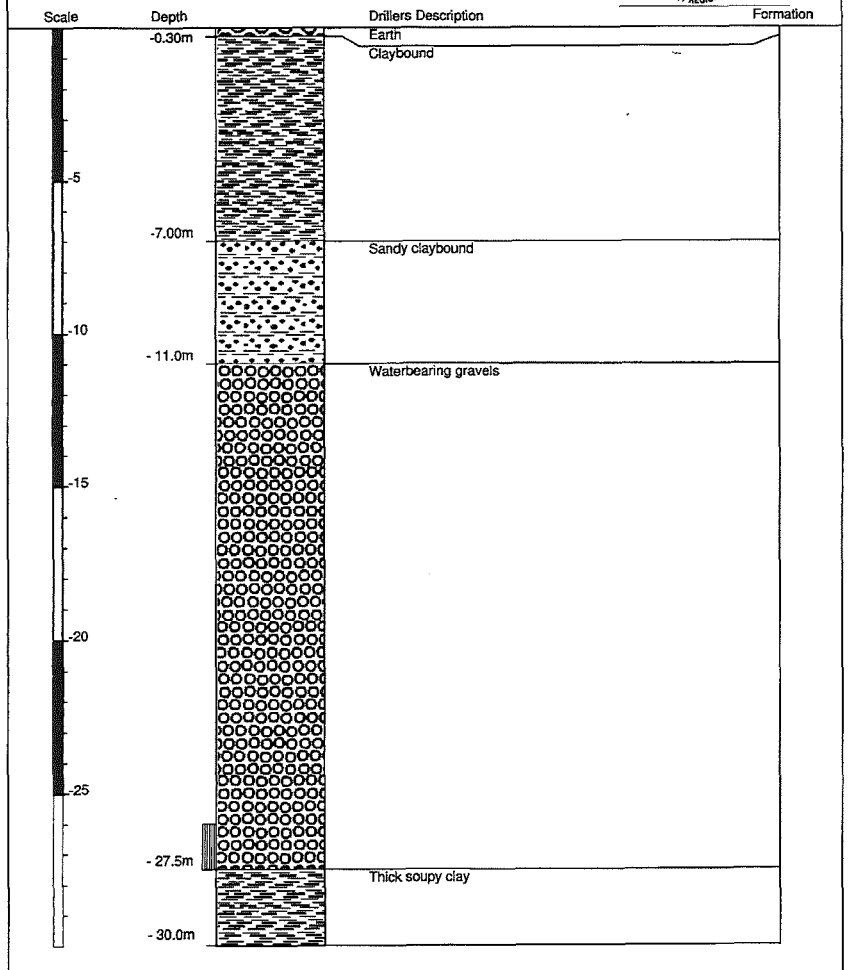

Borelog for well N33/0219

Gridref: N33:9116-2637

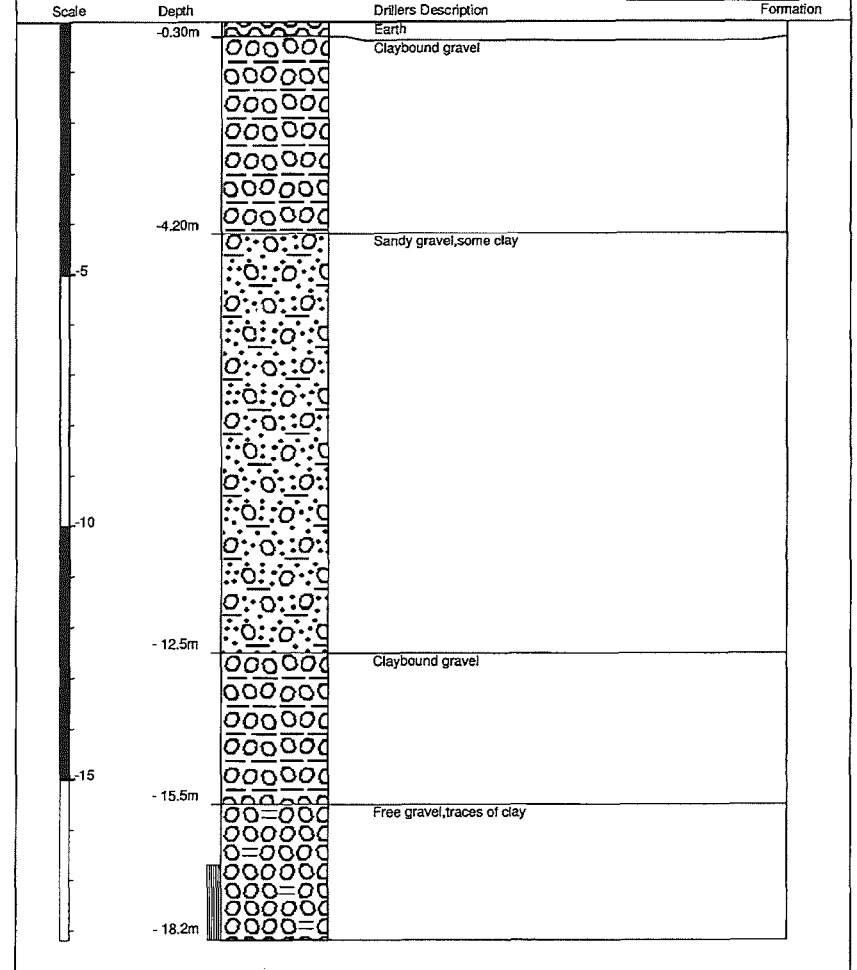

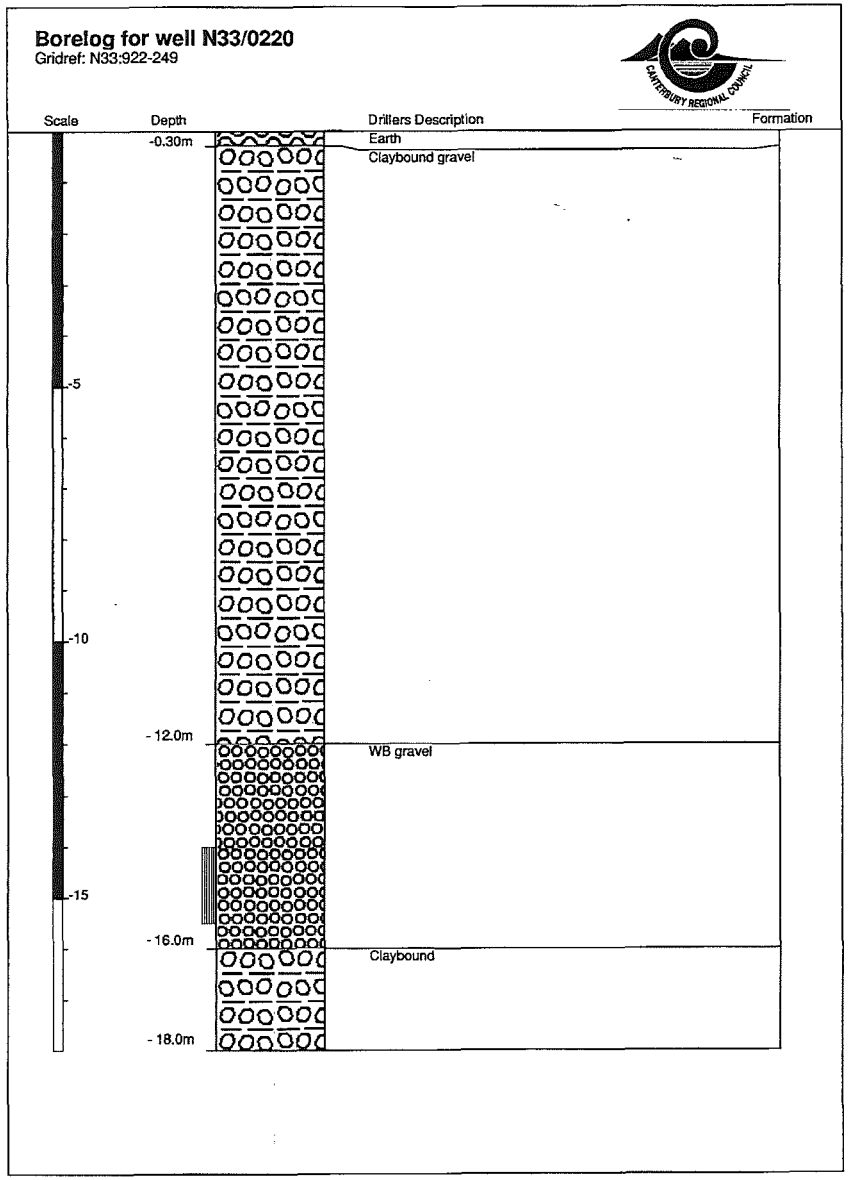
Borelog for well N33/0220
Gridref: N33:922-249
Scale
Depth
Drillers Description
Formation
-0.30m
Earth
Claybound gravel
-5
-10
- 12.0m
WB gravel
-15
- 16.0m
Claybound
- 18.0m

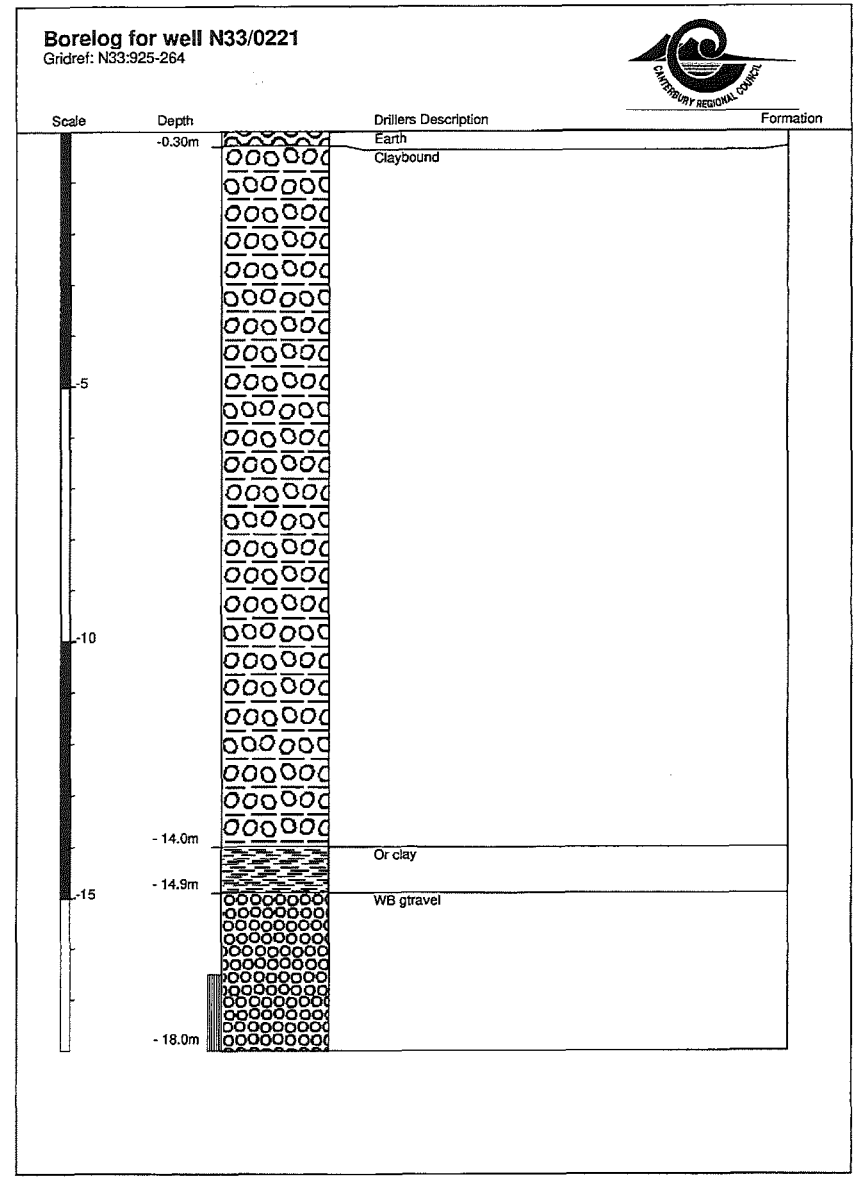
Borelog for well N33/0221
Gridref: N33:925-264
Scale
Depth
Drillers Description
Formation
-0.30m
Earth
Claybound
-5
-10
- 14.0m
Or clay
- 14.9m
-15
WB gtravel
- 18.0m

Borelog for well N33/0242

Gridref: N33:9069-2524

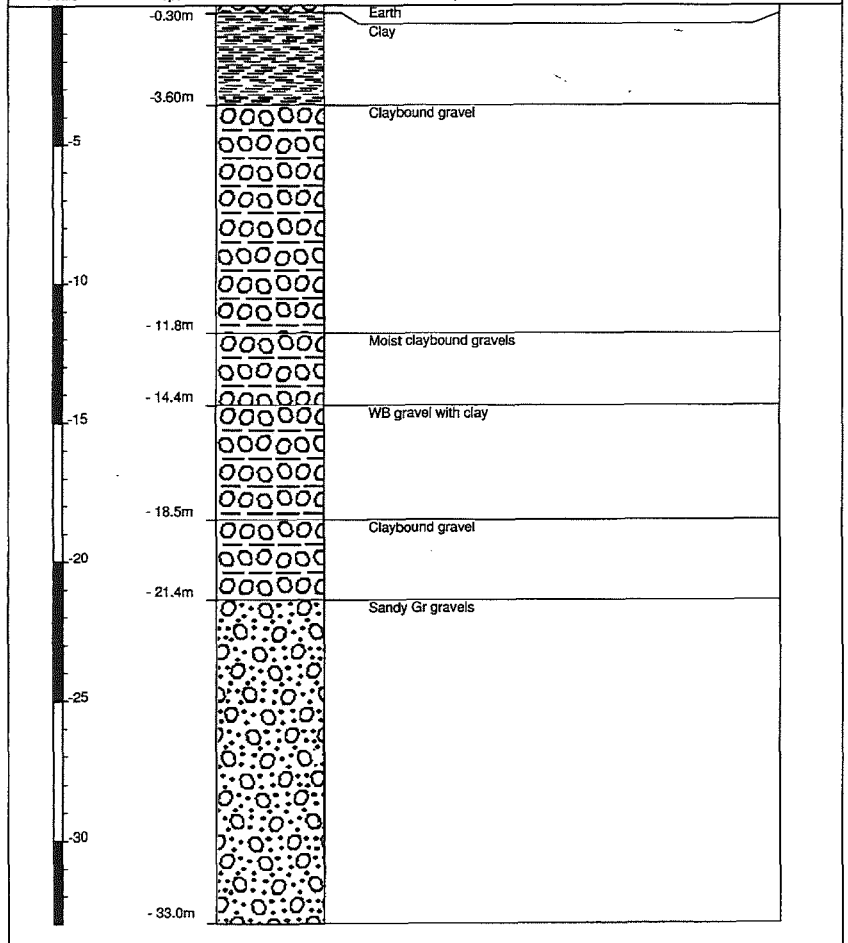

Borelog for well N33/0243

Gridref: N33:9975-2652

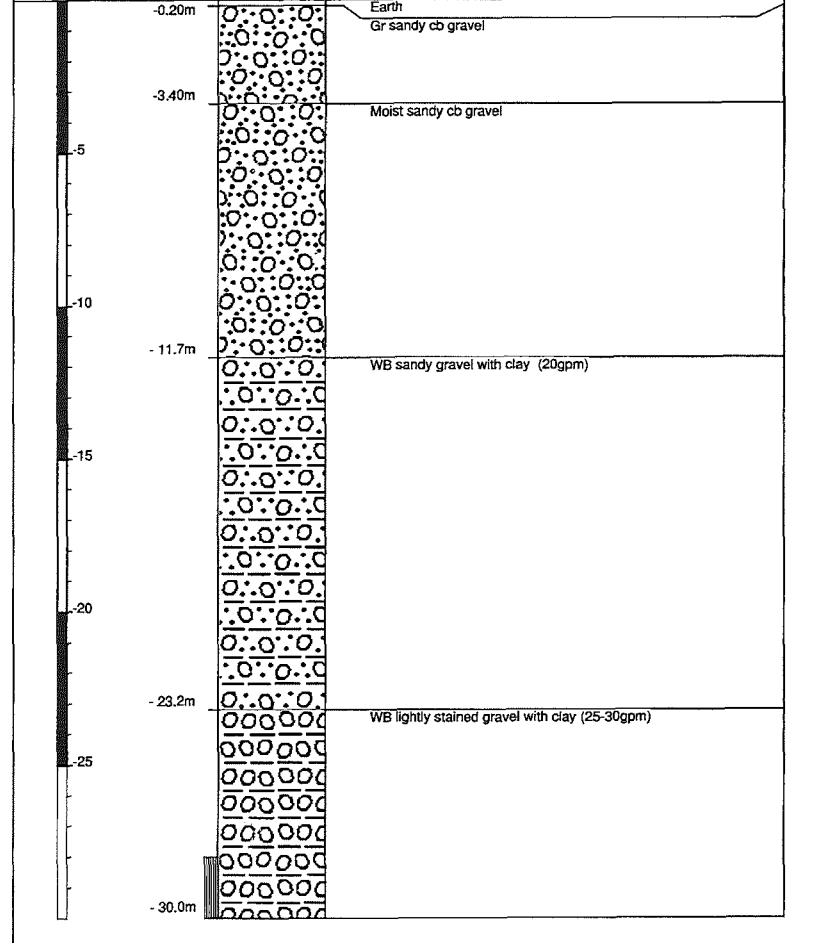

Borelog for well N33/0244

Gridref: N33:9545-2587

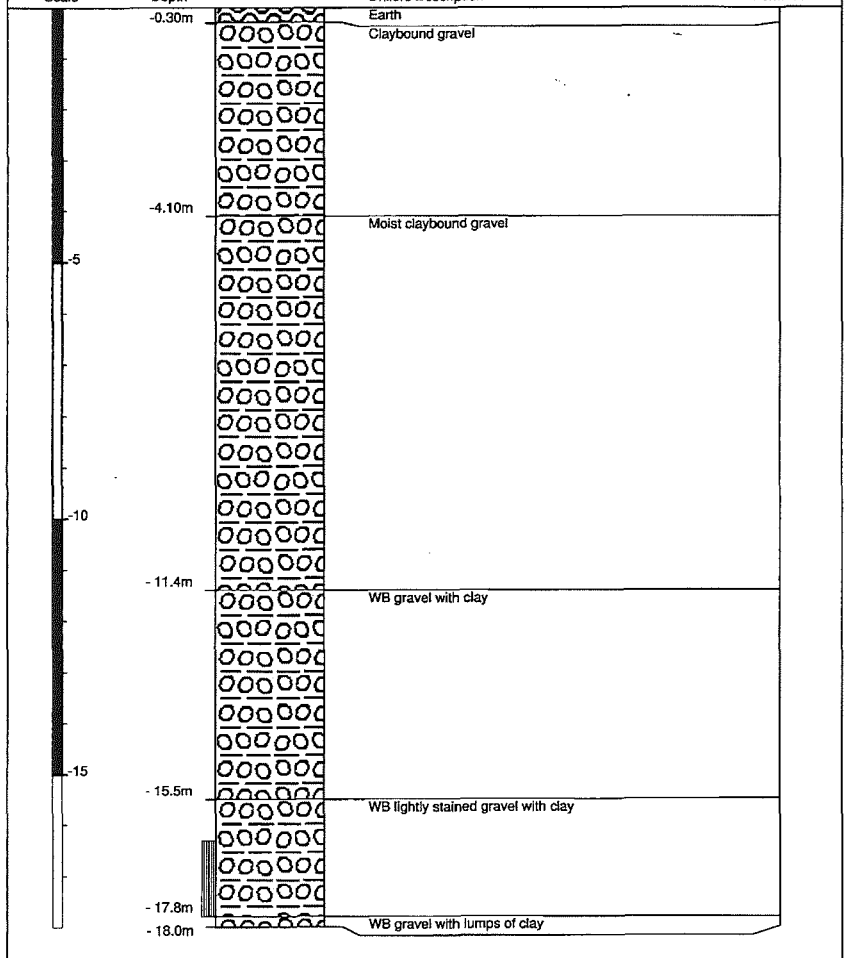

Borelog for well N33/0246

Gridref: N33:9586-2592

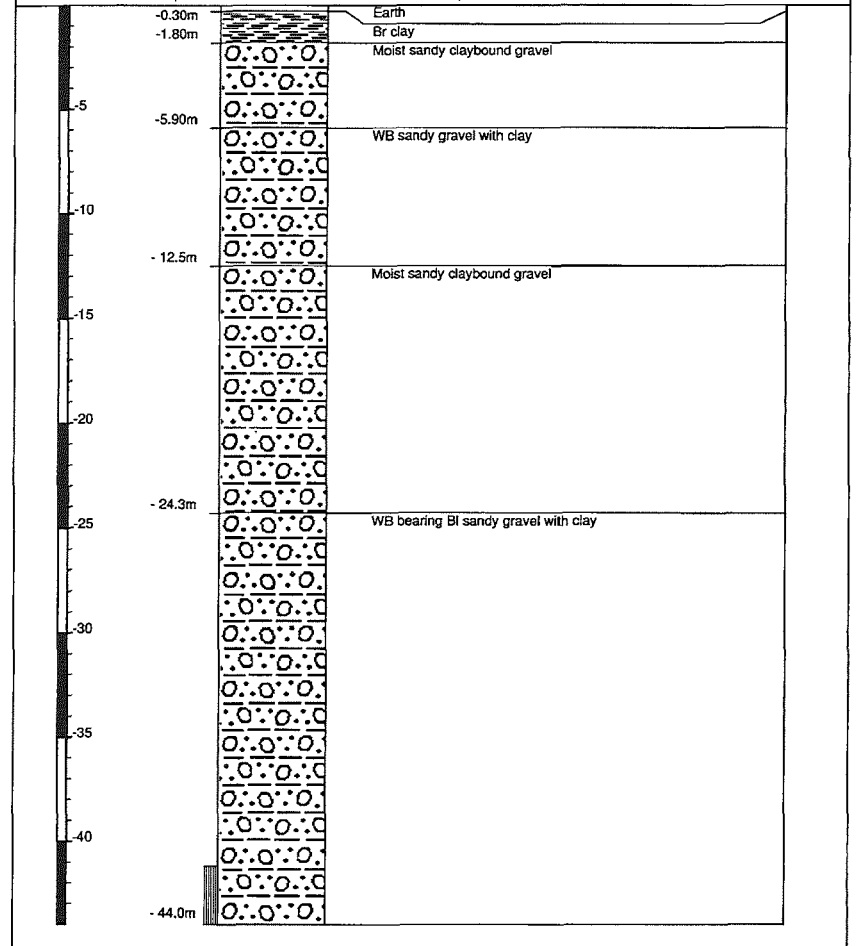

APPENDIX 2

GEOPHYSICAL THEORY AND SURVEY PROCEDURES

This appendix outlines the different geophysical methods employed during this thesis, and gives a brief description of the theory, survey procedures and data processing and modelling operations. The reader is referred to the vast quantity of literature on EM, GPR and gravity methods for a more detailed discussion. The results and interpretation of the geophysical surveys are presented in Chapter 4.

A2.1 TIME-DOMAIN ELECTROMAGNETICS

The time-domain, or transient, electromagnetic method has been used to measure the electrical structure of the earth for a number of years. Prior to TEM resistivity methods involving grounded electrodes (Werner, Schlumberger, etc.) were used to obtain resistivity soundings or profiles. There were several problems associated with the resistivity method: i) in areas of very high surface resistivity, it can be difficult to obtain a sufficient current level in the ground to achieve the desired depth of penetration, ii) generally depth of penetration is half of the electrode spacing, hence to obtain information from a depth of 100m then the total length of the array will have to be over 600m, and iii) it is very time consuming per sounding.

TEM, unlike resistivity, does not pump current straight into the ground. For TEM, a loop of wire, the transmitter loop, is commonly laid out in the form of a square on the ground. The size of the transmitter loop is dictated by the electrical properties of the ground, the depth of investigation and the size of the site under investigation (Nabighian and Macnae, 1991). A current is passed through the transmitter loop which establishes a static magnetic field in the earth. When the current, and thus the primary magnetic field, is switched off rapidly an electromotive force (emf) is induced in the ground causing eddy currents to flow (Figure A2.1). These eddy currents decay with time, moving downwards and outwards away from the transmitter loop (Figure A2.2), creating a decaying secondary magnetic field which induces a decaying voltage in the receiver loop at the surface. Since the secondary magnetic field is generated when the primary magnetic field is off, it is relatively easily measured by measuring the voltage in the receiver loop. the rate of decay of the eddy currents is dependent on the electrical properties of the subsurface. Thus by measuring the change in the signal with time, we can determine the electrical structure of the subsurface.

The time taken for the current in the transmitter loop to decrease to zero after it is switched off is known as the *ramp time.* The secondary magnetic field is measured, during the "off time" (Figure A2.2), in a series of time slices called channels, 20 in all for the PROTEM. As the eddy currents decrease exponentially with time the channels increase in size with time to compensate. At the end of the off-time the current is switched back on again with the current flowing in the opposite direction and the resulting secondary magnetic fields are recorded in the subsequent off-time. The results are stacked to improve the signal strength. The number of times this process is repeated is known as the *transmitter recycling rate*, or the *repetition*

rate, and is dependent on the transmitter off-time. For shallower information a shorter transmitter off-time is used. However, since all of the signal may not have decayed during that particular transmitter off-time, the transmitter off-time can be increased by selecting a different transmitter repetition rate. the PROTEM has four transmitter frequencies ranging from 237.5 Hz (cycles per second) for the shallowest information, down to 6.25 Hz for deeper information.

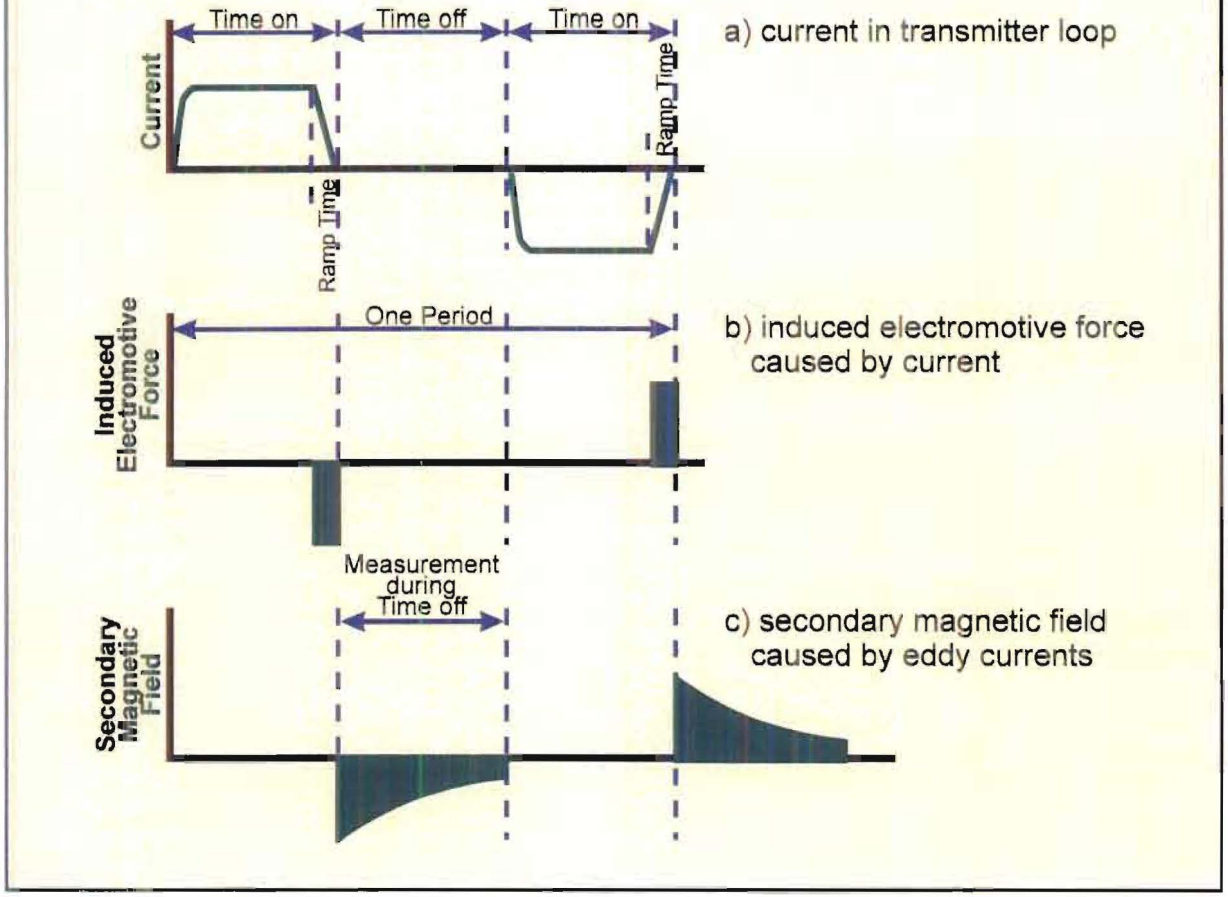

FIGURE A2.1. Time-domain electromagnetic waveforms (McNeill, 1990).

There are two configurations commonly employed for TEM surroundings (Spies and Frischknecht, 1991). The first is the "offset-loop" or "loop-loop", configuration where the receiver loop; is outside and offset some distance from the transmitter loop. The second configuration is the "central loop" or "in loop" configuration where the receiver loop is placed at the centre of the transmitter loop. Generally the offset-loop configuration is used for

smaller transmitter loops otherwise there may be some induced polarization (IP) effects that may affect the data.

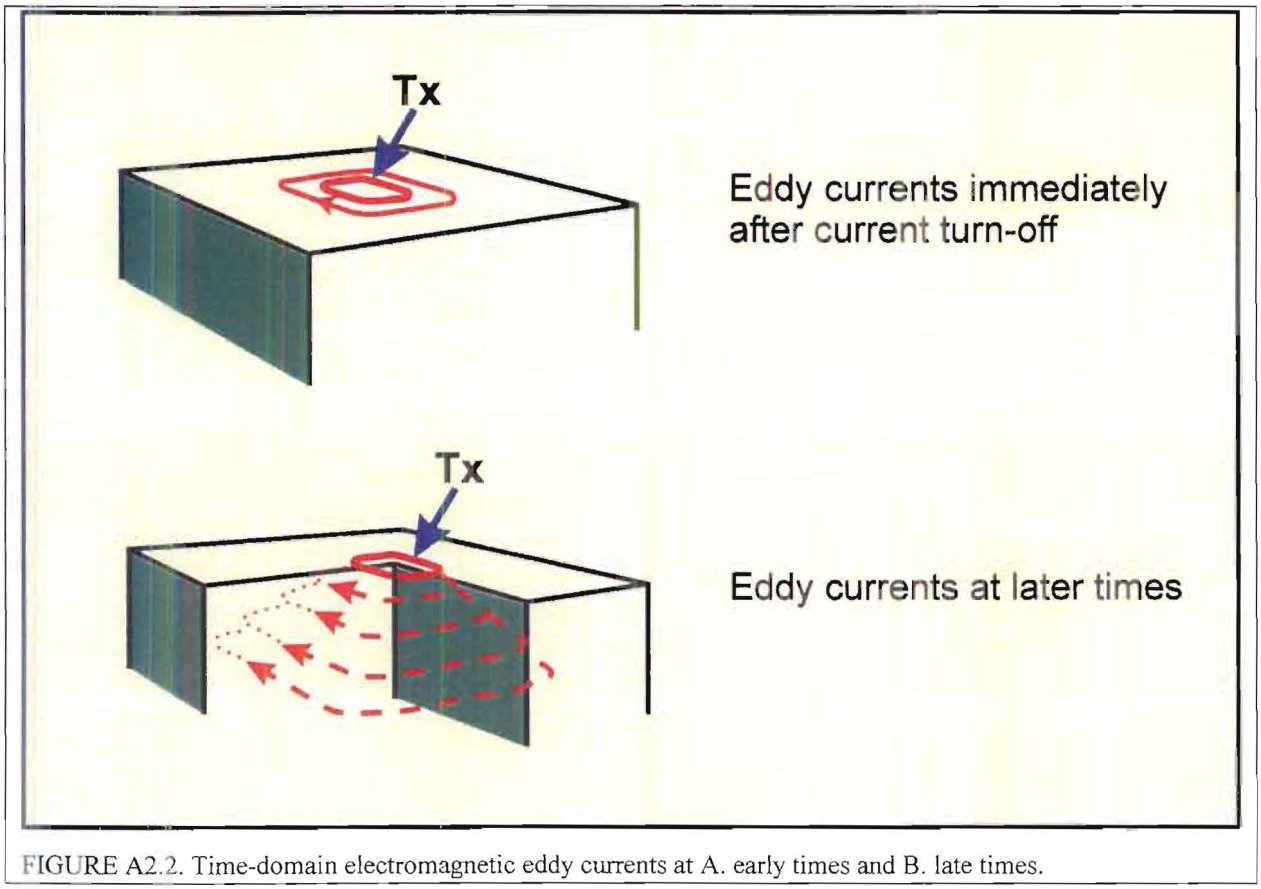

FIGURE A2.2. Time-domain electromagnetic eddy currents at A. early times and B. late times.

A2.1.1 Survey Design

As mentioned earlier the purpose of the TEM investigations was primarily to determine the thickness of the gravel deposits throughout Culverden Basin especially in conjunction with the active faulting along the eastern margin. The majority of the TEM investigations have focused on the eastern margin of the basin as it is currently the most active part of Culverden Basin.

Four transects were run perpendicular (northwest-southeast) to the basis axis to determine: i) how the gravel thickness varied across the basin, ii) how much uplift there has been across the active faults especially along the eastern margin, and iii) whether or not there are faults with no surface expression. The four transects were run alongside major roads with station spacings initially of 1000m. Where the traces of known faults cut the line, or thee appeared to

be a change in the response between two stations, the station spacing was reduced down to 200-500m, depending on paddock size and fence location. The location of the loops was largely influenced by fence-lines. As seems to be typical of any geophysical investigation, there is always a fence located on the feature that you wish to study making data acquisition impossible. Where possible the electric fences were turned off in the immediate vicinity of the survey site, however, occasionally this was not possible which has affected some of the readings.

Along with the four basin transects, shorter lines and individual soundings were located in areas of interest based on the geomorphic mapping or earlier geophysical results. These secondary soundings primarily focused on the Leonard Mound Fault System and also the region between Mount Culverden and isolated hill to determine if the faults associated with their developments are connected.

For all of the TEM loops, except MPR 19, an 80m by 80m loop was employed with the sides of the loop trending NE-SW and NW-SE, i.e. the sides are parallel and perpendicular to the basin axis and the major structures present. An 80m by 80m loop was chosen as the depth to the gravel/Tertiary interface was not known hence the greatest depth of penetration possible was desired. The parameters used for the soundings are shown in Table A2.1.

TABLE A2.1. TEM setup parameters

Parameter	**Setting**	**Description**
Transmitter loop size	80m x 80m	
Transmitter loop turn-off time	4.5μs	Time taken to shut off the current in the transmitter loop
Transmitter current	2 amperes	Amount of current passed through the transmitter loop
Receiver coil area	$31.4m^2$	
Integration time	30 seconds	
Repetition rate	237.5/62.5/25/12.5 Hz	See section 3.2.1
Gain	Varied depending on the repetition rate. 1 / 3 / 5 / 7 respectively for the repetition rates above.	

A2.1.2 Data Quality

As with any geophysical surveying the interpretation of the data is only as good as the data quality. There are two aspects of data quality the need to be considered: i) do the data appear to be repeatable and unaffected by noise in the field, and ii) the modelling of the data after field work.

For the TEM survey it is desirable to run several soundings at each site to check for consistency in the results. The quality of TEM data can be monitored in the field by examining the time decay of the signal as it is acquired. The time decay is displayed in real time as the measurements are made. If the decay appears to be smooth and the late time measurements are stable down to the noise level of the receiver, then the data are likely to be of high quality. The time decay is expressed as the voltage measured in the receiver loop normalized by the size of the receiver loop and the transmitter field strength ($nV/(A\text{-}m^2)$).

The other measure of data quality is obtained when trying to model the electrical structure with depth. For a given model, the TEM response is calculated and compared to the measured response. The deviation between the calculated and measured responses is determined. The model is varied until a minimum deviation, usually expressed as a percentage, is found. The deviation is smallest when the data are of high quality.

Noisy TEM data can arise from both cultural and geological sources. In terms of cultural noise, power lines, electric fences, machinery, etc. all have a significant effect on the data quality. Geological conditions also play a significant role in the quality of the data. In areas of high resistivity, the signal dissipates so rapidly that there is insufficient time to measure it during the off-time. In highly conductive layers, the signal gets trapped in the near-surface and masks the underlying strata. In areas where there is significant lateral variation in the resistivities over the area of the transmitter loop, the data will also display significantly higher noise levels.

On the whole the TEM data collected were of good quality. As already mentioned electric fences were turned off in the immediate vicinity for most soundings. There were a few soundings where that was not possible which has affected the results. It is interesting that some stations are very noisy which could not be attributed to cultural influences. As

discussed in chapter 6, it is believed that the erratic results are a function of significant lateral variations in the resistivities of the subsurface. These rapid lateral variations are believed to be due to faulting which can be observed on the surface.

A2.1.3 Data processing and Modelling

TEM data are stored in the PROTEM receiver in the field, and are transferred to a computer in the laboratory or office. The data are then loaded into the Interpex TEMIX-GL^{TM} modelling package during which time the data are checked. Measured voltages which are obviously below the noise level or are affected by external influences are "masked" and are not used in the subsequent modelling. As TEM averages over a volume of the subsurface, the voltage should decay smoothly over time. Any sudden change from the smooth voltage decay indicates that the noise level of the instrumentation has been reached or that there is cultural interference.

At the modelling stage the voltage response is converted to a normalized value called *apparent resistivity*. This gives a general view of the trend of the electrical properties of the subsurface. Only by modelling of the response can we determine the electrical structure as a function of depth. At this stage a few additional points may be masked but only if they fall well of the trend set by the other points. Sharp and sudden changes are physically impossible, except in presence of external influences, as the TEM method averages a given volume of the subsurface. The masked points are represented by the crosses on the plots of apparent resistivity versus time.

The modelling of the data is relatively straightforward. The first step in the modelling of the data was to let the computer fit a "smooth model" (Figure A2.3) to the data. For the smooth model the computer is allowed to adjust the thicknesses and resistivities of 19 layers until the modelled response matches the measured response. From this model the general electrical structure can be deduced which is then used in the layered model. From the smooth model an initial model is constructed and the calculated response is shown. The initial model is generally a simple one or two layered model and layers are added as required until the major features of the data are produced, and the calculated response is as close as possible to the measured response. The resulting model was then used as the starting point for a more

detailed inversion, which yielded the "best-fitting" model. The best-fitting model was then used for equivalence analysis; that is, each model was perturbed to establish how robust the layer thicknesses and resistivities were, and how well the data constrained the models (Figure A2.4). The equivalent models that fit within a prescribed error bound are shown as dashed lines in the plots of resistivity versus depth.

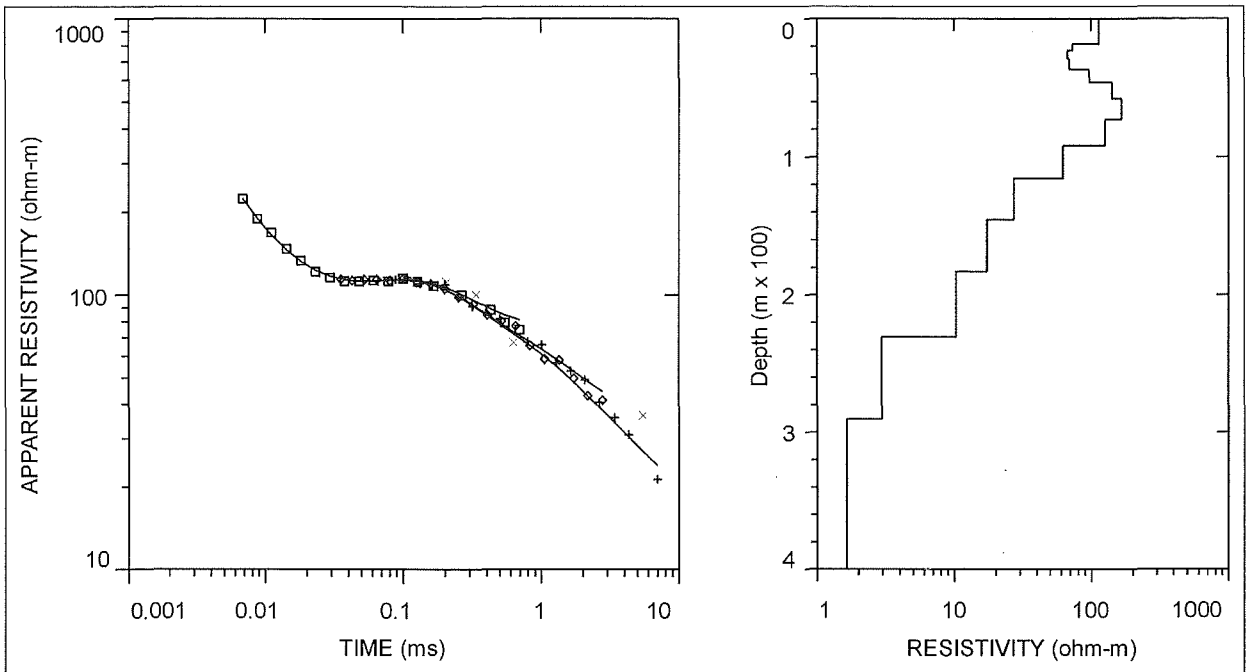

FIGURE A2.3. Example of a smooth model.

Where possible it is desirable to constrain the TEM modelling. Without constrains the general electrical structure can be determined, however a large degree of uncertainty in the models will result. Due to the lack of deep boreholes within Culverden Basin it was difficult to constrain the modelling. However, there were several shallower boreholes that reached the top of the Tertiary succession particularly around Isolated Hill which aided in the modelling.

A2.2 GROUND PENETRATING RADAR

The introduction of GPR in the mid 1970's gave geophysicists a technique to study shallow subsurface stratigraphy quickly, efficiently and non-destructively. Unlike EM, radar is a "contrast" method; readings are only obtained if there is a contrast in physical properties at a subsurface boundary resulting in the reflection oft he radar signal. The resultant profile is a

series of wiggle traces, commonly with positive signal returns shaded and negative signal returns unshaded, and looks somewhat similar to a geological cross-section.

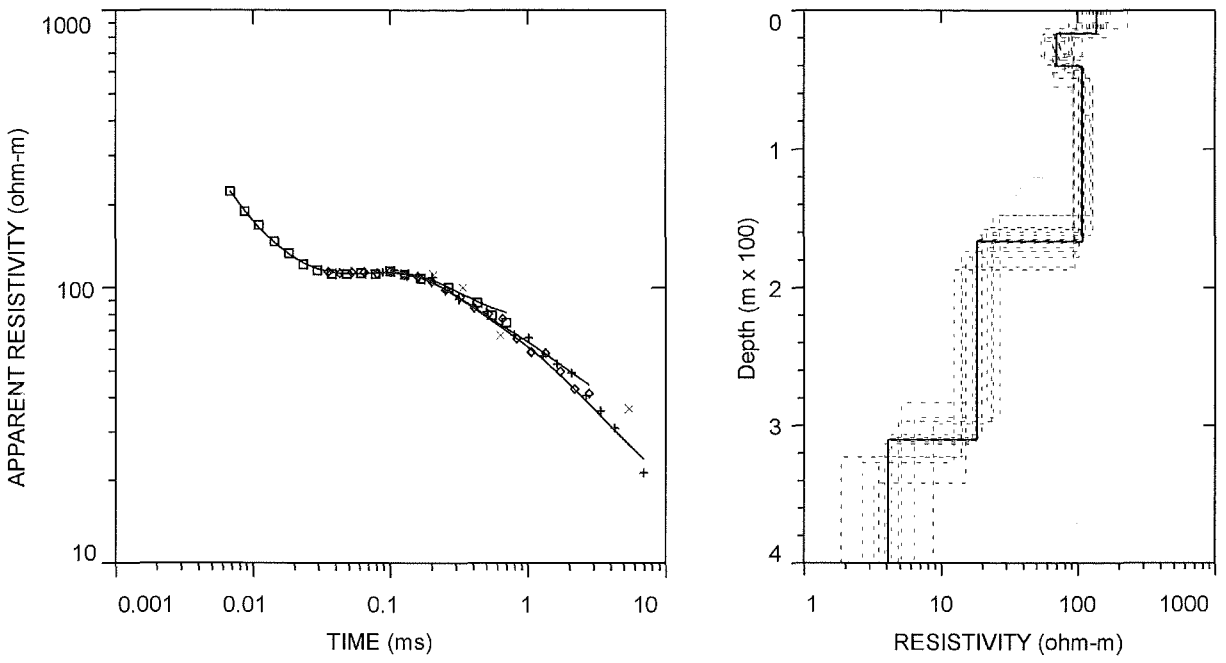

FIGURE A2.4. Example of equivalence analysis.

A short pulse of electromagnetic energy is emitted from the transmitter antenna, reflected from electrical boundaries and detected by the receiver antenna (Figure A2.5). The time taken for the pulse to get from the transmitter to the receiver via the reflector is known as the two-way travel time (TWT). The propagation of the electromagnetic waves through the ground is described by the velocity and the attenuation of the waves, and are dependent on the dielectric and electrical properties of the ground.

When an electrical field is applied to a material, displacement of charge in the material gives rise to an intrinsic dipole moment distribution. The charge separation is described in terms of a dipole moment which, in simple materials, is proportional to the applied electric field and the proportionality constant, or dielectric permittivity. Simply, the dielectric permittivity is the extent to which the material is polarisable over high frequencies (Nobes, 1994). More commonly the ratio of the material permittivity to the free space permittivity (8.854×10^{-12}F/m) is used and is known as the relative permittivity or dielectric coefficient (K).

The dielectric coefficient is given by:

$$K - K' + iK'''$$

where K = the dielectric coefficient,

K' = the real part of the dielectric coefficient, and

K''' = the imaginary or loss part of the dielectric coefficient.

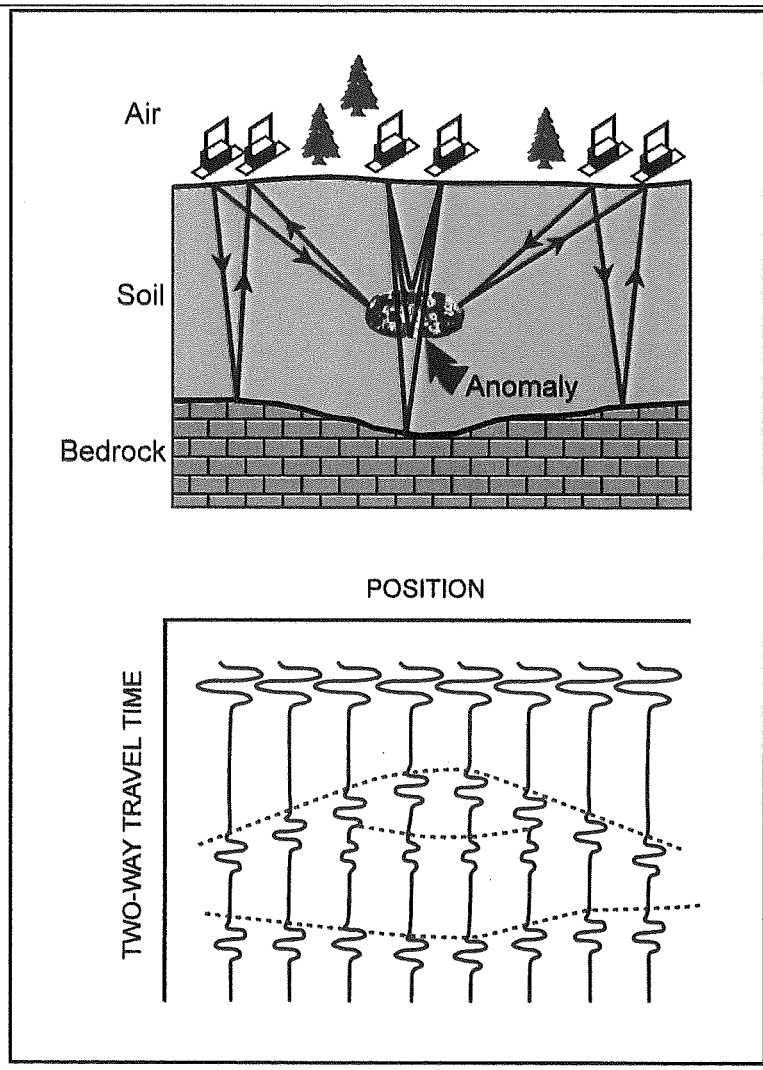

FIGURE A2.5. Schematic illustration of common-offset GPR reflection profiling (Annan and Cosway, 1992).

It is often useful to separate K''' into high frequency and dc conductivity components of the loss form of:

$$K = K' + i\left[K'' + \frac{\sigma_{dc}}{\omega\varepsilon_0}\right]$$

where σ_{dc} = the dc (low frequency) conductivity (S/m),

ω = angular frequency,

ε = the free space permittivity, and

K" = frequency dependent loss from relaxation of the water molecule.

The velocity of the electromagnetic waves through the ground is a function of the dielectric coefficient as described by:

$$V = \frac{C}{\sqrt{K'}}$$

where V = velocity

C = 3×10^8 m/s and is the propagation velocity of electromagnetic waves in free space, i.e. the speed of light.

As Figure A2.6 shows, the velocity remains constant for materials with conductivities less than 100 mS/m over the 1-2000 MHz frequency range. It is important to note that the graphs shown are for a given material and that changes in the composition, water content and magnetic properties of that material will affect the velocity. As a result most GPR systems have been designed to operate in this frequency range.

Table A2.2 shows the dielectric coefficient for different materials, at a given temperature, and shows that the water is the most easily polarisable with a dielectric coefficient of 80. In contrast most rock types have dielectric coefficients in the range of 2 to 8. Hence water is going to be the major contributor to variations of the dielectric coefficient, and hence the velocity of subsurface materials.

TABLE A2.2. Typical dielectric coefficient, electrical conductivity, velocity and attenuation observed in common geological materials at 100 MHz (after Davis and Annan, 1989).

Dielectric Coefficient	Material	Conductivity (ms/n)	Velocity (ms/n)	Attenuation (ms/n)
1	Air	0	0.30	0
80	Fresh Water	0.5	0.033	0.1
80	Sea Water	$3x10^4$	0.01	10^3
3-5	Dry Sand	0.01	0.15	0.01
20-30	Saturated Sand	0.1	0.06	0.03-0.3
5-30	Silts	1-100	0.07	1-100

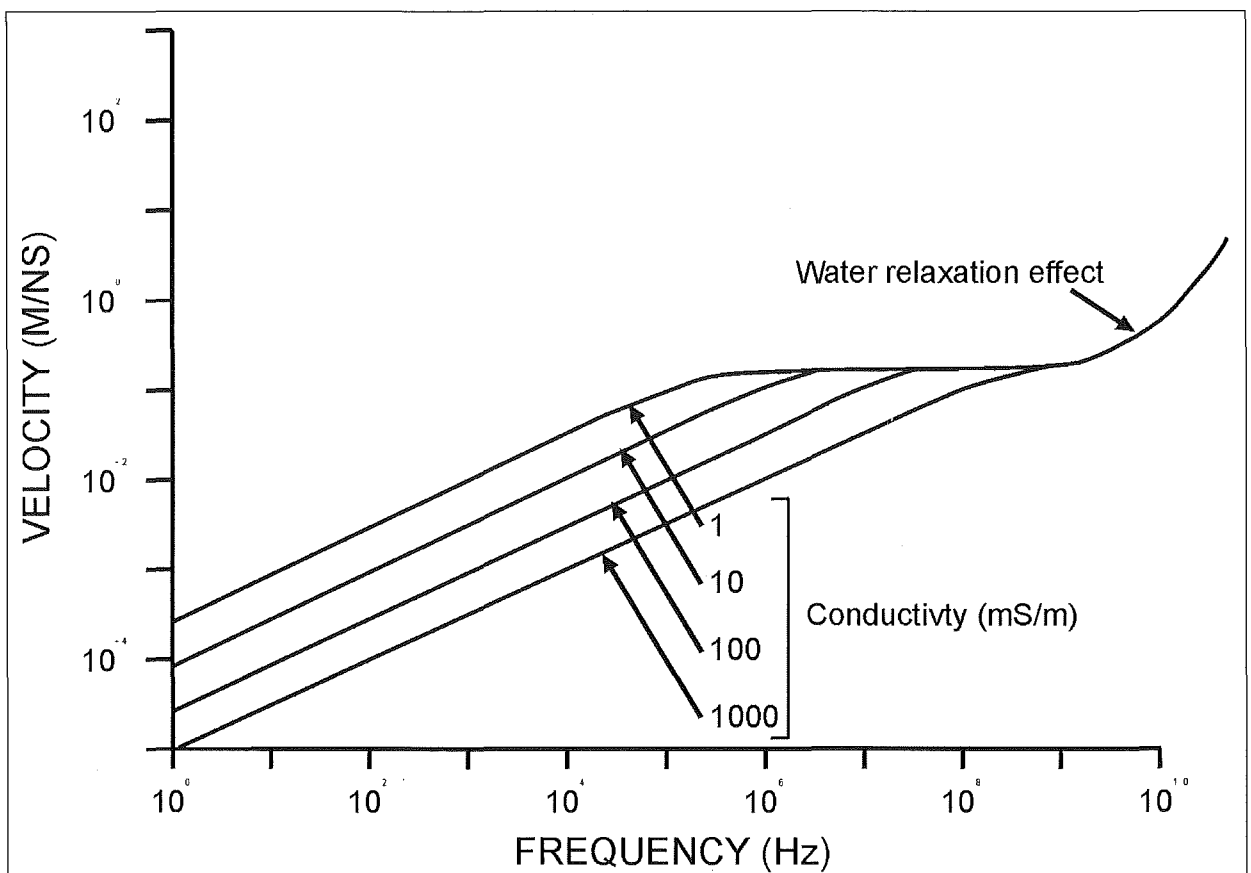

FIGURE A2.6. Graphs showing the effects of conductivity on the velocity of the GPR signal (after Annan and Davis, 1989).

So far the dielectric properties have been mentioned as they have the most significant effect on the velocity of wave propagation at these frequencies. The conductivity of the materials has very little effect on the velocity of the electromagnetic waves, but plays a significant role in the attenuation of the signal, as governed by the equation:

$$\alpha = 1.69 \frac{\sigma}{\sqrt{K}} \text{ dB/m}$$

where α = the attenuation, and

σ = the conductivity (mS/m)

Figure A2.7 shows a graph of frequency versus attenuation over a range of conductivities and shows that as the conductivity increases so does the attenuation. It is difficult to determine the electrical conductivity of a soil as it is very dependent on the pore water conductivity filling the pore spaces, and the surface conduction mechanisms present in the soil matrix. The conductivity of the pore water is proportional to the total dissolved solids (TDS) in the water, i.e. the higher the TDS the higher the conductivity (Theimer et al., 1994). The surface conduction mechanisms, which is how the charge is transported on the mineral grains, is very small for coarse grained material such as sands. Clays, due to their very fine particle size, have a significant effect on the conductivity of a soil as the surface conductivity is high, thus raising the conductivity of the soil. Archie's Law (Jackson et al., 1978; McNeill, 1990) relates the bulk conductivity of the soil to the pore water conductivity and porosity as given by:

$$\sigma_a = \sigma_w \phi^m$$

where σ_a = bulk conductivity of soil (S/m)

σ_w = pore water conductivity (S/m)

ϕ = soil porosity

m = factor which varies with particle shape (1.2 for spheres to 2.5 platey fragments)

An additional component to the electrical conductivity is added tot he equation when clays are present (Keller and Frischknecht, 1970) which s a function of clay content and type. Thus, the bulk conductivity of the soil becomes:

$$\sigma_a = \sigma_w \phi^m + \sigma_{clay}$$

As mentioned earlier, radar is a contrast method. Reflections from subsurface boundaries are the result of the electrical impedance in the ground, which in turn is dominated by the changes in relative permittivities of the different subsurface materials. The reflection coefficient (R) is defined by the following equation:

$$R = \frac{\sqrt{K_1} - \sqrt{K_2}}{\sqrt{K_1} + \sqrt{K_2}}$$

where K_1 = dielectric coefficient of unit 1, and

K_2 = dielectric coefficient of unit 2.

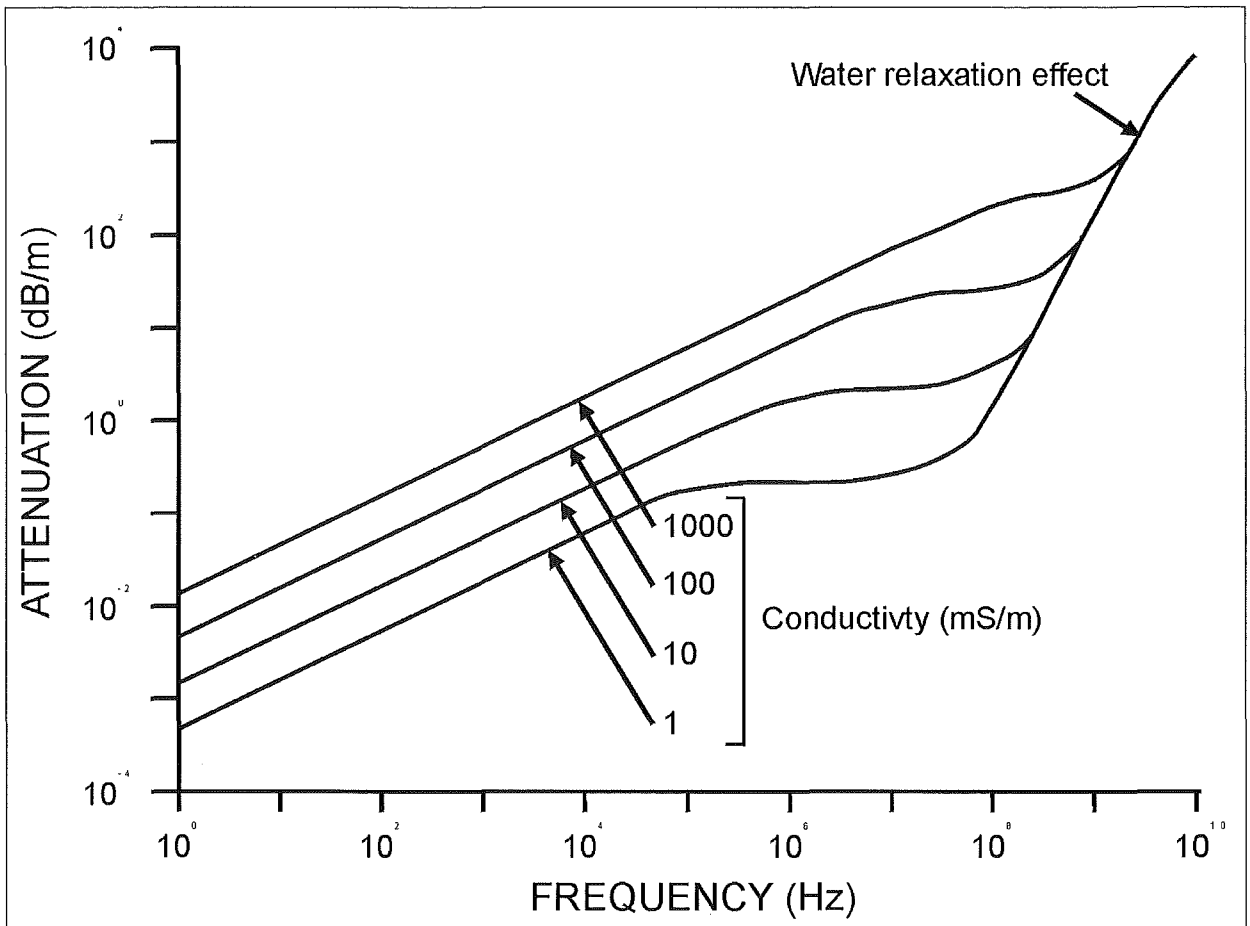

FIGURE A2.7. Graphs showing the effects of conductivity on the attenuation of the GPR signal (after Annan and Davis, 1989).

If there is insufficient contrast in the physical properties of the two layers then a reflection will not be seen from the interface. The above equation assumes that the boundary between the layers is horizontal, the layers are thicker than the wavelength of the signal and that the incident, reflected and transmitted waves are normal to the boundary. The presence of thin layers, or dipping boundaries, will affect the strength of the reflections. Since the reflection is dependent on the dielectric coefficients of the materials, variation in the magnetic properties will also affect the reflection strength. This is not an issue in this situation as the gravels are

non-magnetic. Reflections will also not occur if the physical change occurs over a short distance relative to the resolution.

A2.2.1 Velocity Analysis

An accurate determination of the velocity of the subsurface stratigraphy is essential to convert the two-way travel time to depth. The traditional way is to perform a common mid point (CMP) survey where the antennas are stepped out either side of a central position (Figure A2.8). From the profile obtained (Figure A2.9) the velocities of the different units at depth can be determined. CMPs were performed at several locations, however, for the majority of the GPR profiles the diffractions arising from subsurface objects were used to determine the velocity.

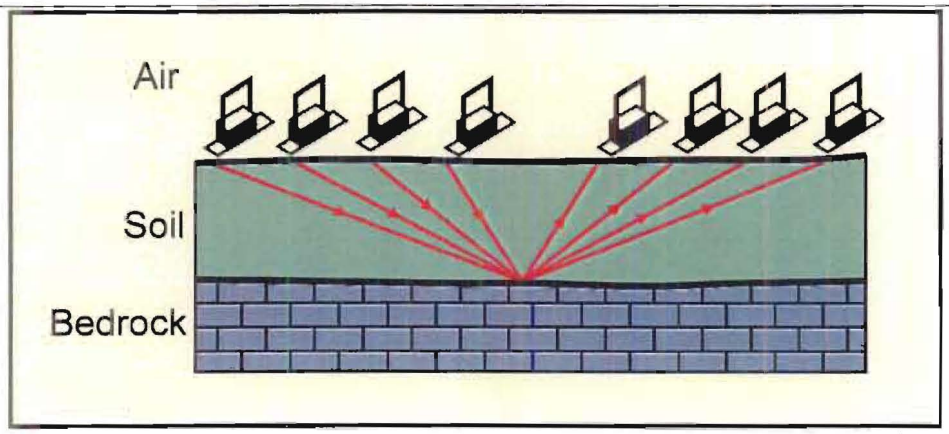

FIGURE A2.8. Schematic illustration of a CMP survey (Annan and Cosway, 1992).

Diffractions arise from objects whose lateral dimensions are smaller than the resolution of the antenna being used. As the antenna pass over the object, the TWT increases away from the position vertically above the object as the distance between the object and the antenna is increasing. The slope of the diffraction tails is the velocity of the material in which the object is located. To use the diffractions for the velocity determination, the profiles were imported into Interpex GRADIX^{TM} in which velocity hyperbolas were fitted to the diffractions to find the velocity.

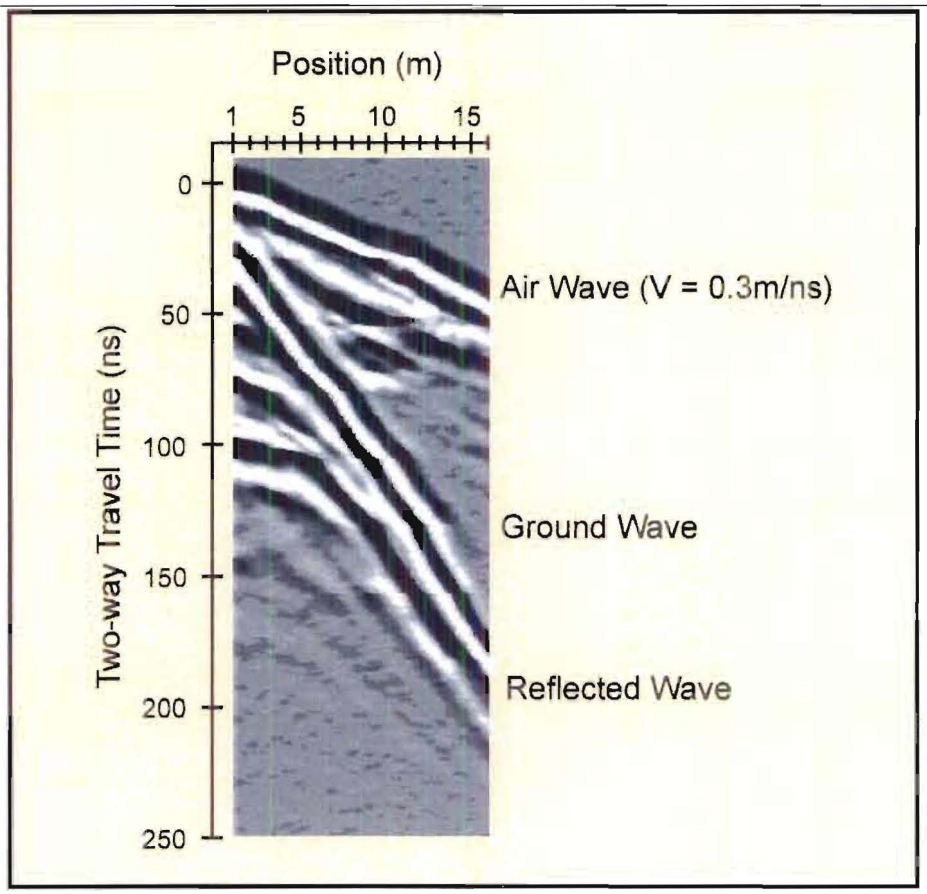

FIGURE A2.9. Example of a CMP profile.

A2.2.2 Survey Procedures

In the design of a GPR survey several key factors need to be considered to optimise the survey, namely:

- line location,
- antenna frequency, separation and orientation,
- station spacing,
- time window, and
- time sampling interval

Al the GPR lines were run over the inferred locations of faults to study the effects of the deformation on the near surface gravels. The lines were run perpendicular to the trace of the faults and away from the near surface objects such as fences, buildings, overhead powerlines etc., which all give rise to airwave diffractions in the profile. The airwave diffractions clutter the profile masking the subsurface features.

The most crucial selection of the survey design is the antenna frequency. There is a trade-off between depth of penetration and resolution. As stated by Annan (1997) there is no use having great resolution if the desired target cannot be detected. However, for stratigraphic studies greater resolution is often required to observe the stratigraphic relationships in the deposits. For this study two operating frequencies were primarily used: 50 MHz to look at the deeper stratigraphy and broader scale features and 100 MHz to study the detailed deformation in the upper layers. In most cases the 50 MHz antenna wer3 used first to pin-point areas of interest along the profile, followed by the 100 MHz to look at those areas in greater detail.

In terms of selecting the antenna separation and station spacing the following equations sere used:

$$\text{Antenna separation } (S) = \frac{2\,Depth}{\sqrt{(\mathrm{K}-1)}}$$

$$\text{Nyquist sampling interval } (NSI) = \frac{1}{4}\lambda$$

$$\text{Station spacing } (n_x) = \frac{c}{4f\sqrt{\mathrm{K}}} = \frac{75}{f\sqrt{\mathrm{K}}} \text{ (in m)}$$

for f in MHz.

It is critical that for the station spacing the Nyquist sampling interval is not exceeded to ensure that the ground response is not aliased. It was found that the recommended values (Table A2.3) given by Sensors and Software were suitable for the surveys.

TABLE A2.3. Station spacings and antenna separations used during the surveys.

Centre Frequency (MHz)	Station Spacing (m)	Antenna Separation (m)
200	0:1	0.5
100	0.2	1.0
50	0.5	2.0
25	1.0	4.0

The sampling interval, which is the time interval between points on a recoded wavelet, dictates how well the wavelet will be resolved. Too few points and the wavelet will not be adequately characterised, and too many points will unnecessarily over-sample the wavelet adding time to the survey. The minimum number of points needed to characterise the wavelet is six, therefore the sampling interval is:

$$\text{Sampling interval } (t) = \frac{1000}{6f}$$

where is the centre frequency of the antenna. Based on the equation, the sampling intervals used for the different antenna are shown in Table A2.4

TABLE A2.4. Sampling intervals for the different antenna frequencies

Centre Frequency (MHz)	Station Spacing (m)
200	0.83
100	1.67
50	3.30
25	16.68

A2.2.3 Data Processing

The GPR data are recorded and stored in a laptop computer in the field. The pulseEKKO software package is used for both the data collection and the data processing. Dewow or signal saturation correction is applied to the data set before any other processing. Depending on the proximity of the transmitter and receiver as well as the electrical properties of the ground, the transmitter signal may induce a slowly decaying low frequency "wow" on the trace which is superimposed on the high frequency reflections.

The "first break" or "time-zero" point on a trace is the point at which the transmitted pulse first arrives at the receiver. The traces usually line up horizontally on this time-zero datum. However this is not always the case and there may be a small shift in the data from trace to trace. The shift is most commonly caused by temperature changes in the equipment along

with dropping battery voltage. A correction is applied to realign the first breaks of the traces in the profile.

If the data are good, these two corrections may be sufficient. However further filtering of certain frequencies may be required if there is a lot of noise in the data set. For the majority of profiles it was considered unnecessary to apply filters to the data.

When viewing the data, a gain is applied which amplifies the signal. There are five gain types of which only two are commonly used: 1. AGC (automatic gain control), and 2. SEC (spreading and exponential compensation). AGC attempts to equalize all signals by applying a gain which is inversely proportional to the signal strength. This gain helps to define the continuity of reflecting events. SEC has the objective of compensating for the spherical spreading losses and the exponential ohmic dissipation of energy. The SEC gain preserves the relative reflector strengths. For the two profiles AGC was used as it enhanced the desired features.

As mentioned earlier, diffractions are recorded which clutter the profile and may mask the desired features. These diffractions can be removed by migrating the profile. Migration tries to remove the distorting effects of diffractions and interference by attempting to focus all scattered energy to its true spatial position, and returns dipping reflectors to their true dip. As long as the dips are small and the layering sub-horizontal, the profile will portray the geologic structure well. GPR assumes normal-incidence, i.e. the energy is perpendicular to the reflector boundary. When the dips are substantial the horizontal position of the reflector will not be plotted in its true horizontal position, as the energy is not normal to the reflector boundary. The reflectors will be steeper dipping than they appeared in the raw data. The profiles were migrated using the velocity determined for the subsurface.

A2.3 GRAVITY

Gravitation is the force of attraction between two bodies. The strength of the attraction between the two bodies depends on the mass of the bodies and the distance between them as defined by Newton's law which is given by the equation

$$F = G\left(\frac{m_1 m_2}{r^2}\right)$$

where F is the force of attraction between two masses, m_1 and m_2, separated by distance, r. G is the universal gravitational constant which has a measured value of 6.672×10^{-11} N m^2/kg^2.

A mass falls to the ground with increasing velocity, and the rate of increase is called gravitational acceleration, g, or gravity. The acceleration of m_2 due to the presence of m_1 can be found by dividing F by m_2. In particular, if m_1 is the mass of the Earth, M_2, the acceleration of the mass m_2 at the surface of the earth is

$$g = \frac{F}{m_2} = G\left(\frac{M_E}{R_E^2}\right)$$

where R_E is the radius of the Earth. In honour of Galileo who first measured the acceleration of gravity, the unit of the acceleration of gravity, 1cm/sec^2, is called the *gal*.

For the gravity readings a Worden 'Pioneer' gravity meter was used. All gravity meters are essentially extremely sensitive mechanical balances in which a mass is supported by a spring. The meter is read by measuring the force required to restore the beam back to the horizontal position (Figure A2.10).

Gravity surveys exploit the very small changes in gravity from place to place that are caused by changes in the subsurface rock density. So what controls the density of rocks? Generally sediments have the lowest density (Table A2.5) because they have in general a greater porosity than both igneous and metamorphic rocks. The density of sediments and sedimentary rocks is dominantly dependent on the porosity, however, fluid content, age, previous history and depth below surface also influence the density. As the fluid content, age and depth below surface increase so does the density. Porosity plays an insignificant role in the density of igneous and metamorphic rocks unless they are highly fractured. Basic igneous rocks generally have larger densities than acidic types, and the degree of metamorphism controls the density in metamorphic rocks as the metamorphic process tends to fill pore spaces and recrystallise the rock in a denser form.

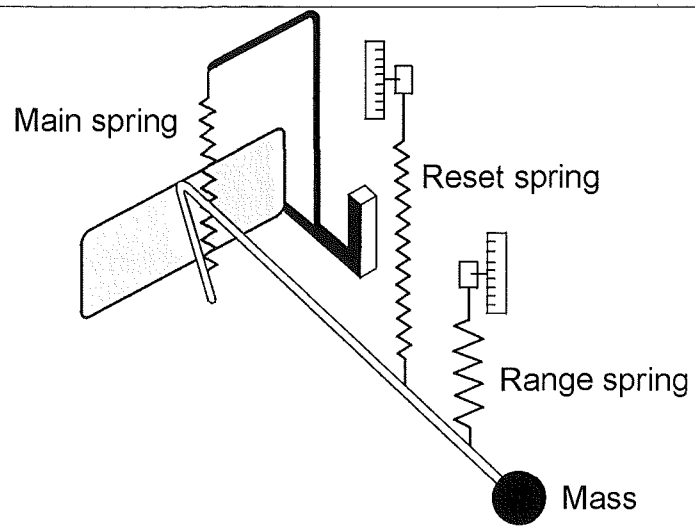

FIGURE A2.10. Schematic diagram of the Worden gravimeter (from Parasnis, 1986).

The density of a particular rock type can vary greatly making accurate modelling of the gravity results difficult. Part of the problem arises because most density measurements are made on rocks exposed at the surface rather than at depth. By exposing the rocks at the surface, the density will be lowered as a result of weathering.

TABLE A2.5. Densities of selected rocks

Rock Type	**Density Range (kg/m^3)**	
	Wet	**Dry**
Alluvium	1960-2000	1.5-1.6
Gravels	1700-2400	1.4-2.2
Sandstones	1600-2760	1.6-2.68
Limestones	1930-2900	1.74-2.78
Greywacke	2600-2700	
Basalt	2700-3300	

A2.3.1 Survey Procedures

Borrowed from Otago University for a month, a Worden 'Pioneer' gravity meter (model 115, number 679) was used to obtain approximately 150 gravity stations. Due to time constraints, the gravity surveys were performed along the roads throughout the basin. In total nine transects (Table A2.6) were run: four across the basin, four transects running parallel to the

Lowry Peaks Range, and the final transect was run along Flintoft Road extending along State Highway 7 Towards Lewis Pass.

TABLE A2.6. Table showing the number of stations and station spacing for each of the six gravity lines

Transect	Transect Length	Number of Stations	Station Spacing (m)
Mount Palm Road (MPR)	10.8	17	400-700]500
Palmside Road (PR)	9.6	24	500
Lowry Peaks Road 1 (LPR1)	43.8	25	500-1000
Lowry Peaks Road 2 (LPR2)	6	9	
Pahau Reserve Road (PRR)			1000
Isolated Hill Road (IHR)	16.7	18	1000
Sandersons Road (SR)	6.3	10	
Flintoft Road (FR)	10.7	26	500-700
State Highway 7 (SH)	4.5	10	1000

For each line a base station was established which was revisited every hour during the survey so that the effects of instrument drift and tidal fluctuations could be corrected. At each station measurements were taken until 2 readings were within 0.5 of the dial reading with equated to 0.044 mgal. Up to 6 readings were required at some stations until the gravity meter became stable.

The elevation for each station was determined to within 30 cm from a topographic survey conducted as part of the Waiau Plains irrigation scheme. The irrigation scheme maps covered the majority of the area surveyed. Only those stations to the east of Leonard Mound were not covered. The elevation was then converted to metres for the purpose of the data reduction. For the portions of the basin which were not covered by the irrigation scheme topographic map the standard topographic maps were used. It was found that there was no more than 1m difference between the irrigation scheme maps and that estimated using the standard topographic maps. This difference equates to less than 0.5 mgal difference to the final corrected data. This error was deemed acceptable given the lack of good density information on the subsurface strata making accurate modelling difficulty.

A2.3.2 Data Reduction

Unlike TEM and GPR, gravity readings are influenced by topography and geographical position, hence they must be corrected for variations in latitude, elevation and topography to reduce them to the values they would have on some datum equipotential surface such as sealevel. This section describes the data reductions applied to the gravity data prior to the modelling of the results.

A2.3.2.1 Drift Correction

The drift correction is applied to remove the effect of instrument drift and tides. Instrument drift is caused by the stretching of the springs within the gravimeter. Base station readings were taken every hour during a survey (Figure A2.11) from which the rate of change in the readings could be calculated. A correction value was then added or subtracted to the data based on the time since the first reading and the rate of change.

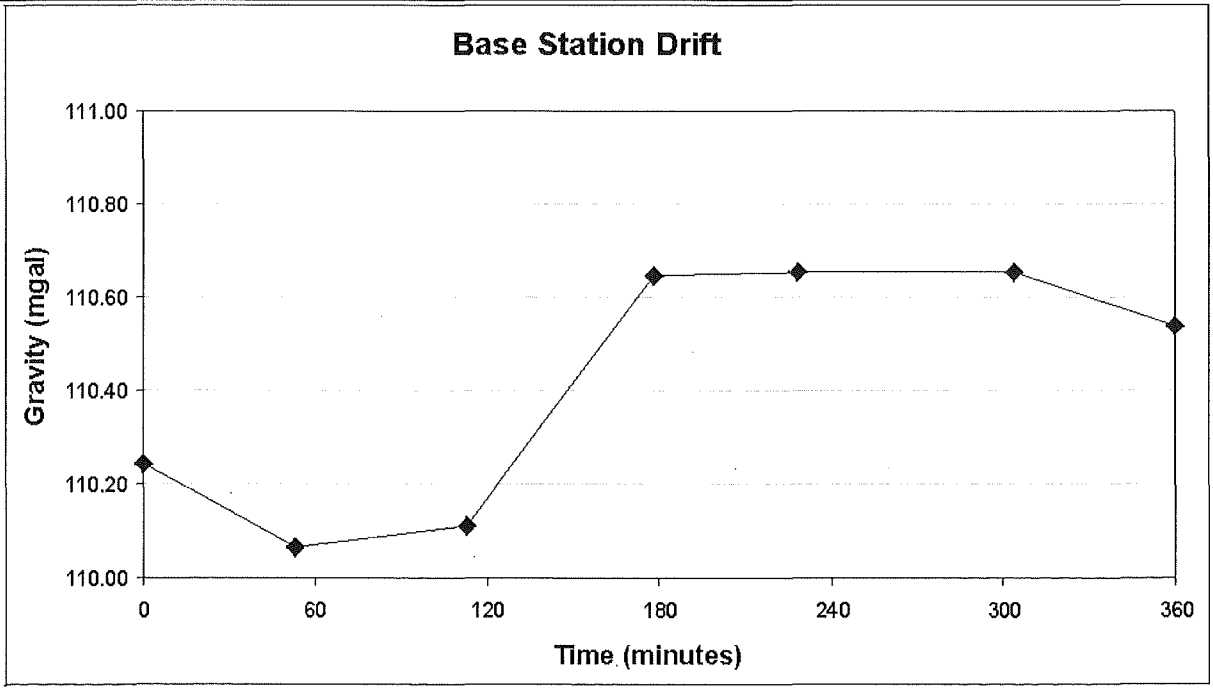

FIGURE A2.11. Graph showing the effects of instrument drift and tides on the base station readings during a gravity survey.

A2.3.2.2 Latitude Correction

As the value of gravity increases with the geographical latitude, the data must be corrected for latitude. For each survey line an arbitrary station was selected from which the changes in the north-south position of successive stations was calculated. From that information the latitude correction was calculated as:

$$\Delta g_{latitude} = \Delta g_{measured} + 0.811 \sin 2L \quad mgal/km$$

where L = latitude (Parasnis, 1986)

A2.3.2.3 Free Air Correction

The observed gravity will be due in part to the height of the gravity station above the sea level datum. It is necessary to correct for changes in elevation between stations to reduce field readings to the sea level datum using:

$$\Delta g_{FA} = \Delta g_{latitude} + 0.3086h \quad mgal/km$$

where h is the elevation above sea level (Parasnis, 1986). The quantity obtained after applying the latitude and free air corrections is called the *free-air anomaly* (FAA).

A2.3.2.4 Bouguer Correction

The Bouguer correction accounts for the mass that exists between the stations and sea level that was ignored in the free-air correction.

$$\Delta g_{bouguer} = \Delta g_{FA} - 0.04192 \rho h \quad mgal/m$$

where ρ is the slab density (kgm^{-3}) (Milsom, 1989). If we assume an average crustal density of 2670 kgm^{-3} the equation becomes:

$$\Delta g_{bouguer} = \Delta g_{FA} - 0.112h \quad mgal/km$$

A2.3.2.5 Terrain Correction

The terrain correction uses a much more complete representation of the local topography than the Bouguer correction, and is essential in mountainous areas. The normal procedure for calculating the terrain correction is to use a Hammer chart. A transparent chart is centered on each gravity station, and the difference in elevation for each segment of the chart relative to the station is found from which the corresponding terrain correction is calculated. The terrain correction for each segment is then added to the Bouguer anomaly.

For this survey, the terrain corrections calculated by Dibble (1973) were used. Dibble's terrain corrections were used where stations were recorded at the same location and were inferred for the other stations. Checks of several stations were performed using a hammer chart and were found to be consistent with Dibble's results. The inner correction is out to zone E on the Hammer chart and the outer goes out to zone J. From the data (Appendix 3), it is noticeable that for nearly all of the stations the inner terrain correction was zero whilst the outer terrain correction was generally less than 1 mgal.

A2.3.2.6 Removal of Regional

The anomalies of interest along a gravity profile are often masked by deep-seated structures. The deep-seated structures give rise to the regional gradient, which was removed to leave the residual anomalies. The residual anomalies were used in the modelling of the data. As for the terrain corrections, Dibble's data were used to remove the regional gradient. Dibble calculated the regional gradient, which was used to remove the effects of the Torlesse basement. The regional gradient has a slow change of Δg compared to the relatively rapidly varying local gradient. Across the basin there was up to a 30 mgal decrease from east to west.

A2.3.2.7 Errors

Gravity data tend to have greater errors than GPR and TEM due to the nature of the data collection and data processing. The gravity mater is very sensitive in the field to vibrations, whether that be from the wind or passing vehicles. Consequently the readings may be unstable. This problem was greatly reduced by taking up to six readings per site until the readings were within 0.5 units on the meter dial, which equated to less than 0.1 mgal. If the

APPENDIX 3

GRAVITY DATA

This appendix contains the Microsoft Excel spreadsheets of the gravity lines run throughout the Culverden Basin. Map 4 (Volume 2) shows the location of the lines. The lines are in the order they are discussed in Chapter 4.

MORSES ROAD GRAVITY DATA

Date	Field Stations	Stations	Time	Position (m)	Elevation (m)	Northing	Easting	Latitude	Dial Readings							Measured g (mgal)	Terrain Correction		Data Corrections				Corrected g (mgal)	Regional g (mgal)	Residual g (mgal)	Anomalies (mgal)
									Reading 1	Reading 2	Reading 3	Reading 4	Reading 5	Reading 6	Av. Reading		Inner	Outer	Drift	Latitude	Free-air	Bouguer				
111/6/97	*1 (Base)*	1	12:10	0	179.0	5839465	2504770	42.6538	1148.8	1148.6					1148.7	102.29	0	0.32	102.29	0.00	0.00	0.00	102.61	-42.5	145.11	-6.58
	2	2	12:17	587	186.3	5840000	2504529		1134.3	1134.6					1134.5	101.03	0	0.48	101.02	0.43	2.24	-0.81	103.36	-43.1	146.46	-5.23
	3	3	12:22	1196	193.8	5840585	2504359		1114.2	1112.7	1113				1112.9	99.10	0	0.65	99.09	0.91	4.56	-1.65	103.55	-43.8	147.35	-4.34
	4	4	12:29	1780	201.0	5841103	2504090		1088	1089.4	1089.2				1089.3	97.00	0	0.81	96.98	1.32	6.79	-2.46	103.44	-44.4	147.84	-3.85
	5	5	12:37	2416	220.0	5841692	2503849		1065.1	1062.6	1066.8	1063.4	1062.5		1062.6	94.62	0	1.05	94.59	1.80	12.65	-4.59	105.51	-45.1	150.61	-1.08
	6	6	12:46	3071	232.0	5842316	2503649	42.6281	1028.7	1029.7	1026.6	1029.8			1029.8	91.70	0	1.3	91.66	2.30	16.36	-5.93	105.69	-46.0	151.69	0.00
	Base Station Readings		*12:10*		*179.0*	*5839465*	*2504770*		*1148.8*	*1148.6*					*1148.7*	*102.29*										
			12:56						*1147.1*	*1149.2*	*1149.3*				*1149.3*	*102.35*										

MOUNT PALM ROAD GRAVITY DATA

Date	Field Stations	Stations	Time	Position (m)	Elevation (m)	Northing	Easting	Latitude	Dial Readings						Av. Reading	Measured g (mgal)	Terrain Correction		Drift	Data Corrections			Corrected g (mgal)	Regional g (mgal)	Residual g (mgal)	Anomalies (mgal)
									Reading 1	Reading 2	Reading 3	Reading 4	Reading 5	Reading 6			Inner	Outer		Latitude	Free-air	Bouguer				
26/5/97	11	1	10:45	0	200.0	5829971	2513123	42.7393	1340.4	1337.5	1339.8				1340.1	119.34	0.0	0.9	119.28	-2.62	10.80	-3.92	124.45	-26.5	150.95	6.79
	10	2	10:30	1023	145.0	5830538	2512271	42.7342	1410.2	1409	1407.5	1406.1	1408.6		1408.8	125.45	0.0	0.7	125.45	-2.16	-6.17	2.24	120.05	-28.4	148.45	4.29
	9	3	10:10	1475	145.0	5830813	2511913	42.7317	1414.4	1411	1415.1				1414.8	125.99	0.0	0.6	126.04	-1.94	-6.17	2.24	120.77	-28.3	149.07	4.91
	8	4	9:55	1978	146.0	5831066	2511478	42.7294	1392.2	1395.7	1395.3				1395.5	124.27	0.0	0.3	124.37	-1.73	-5.86	2.13	119.22	-29.2	148.42	4.26
	7	5	9:40	3010	144.8	5831617	2510605	42.7245	1377.9	1375.3	1377.1				1377.5	122.67	0.0	0.3	122.81	-1.29	-6.23	2.26	117.85	-30.2	148.05	3.89
	6	6	9:18	3579	150.0	5831931	2510131	42.7216	1358.7	1357.5	1355.3	1361	1361.8	1361.5	1361.6	121.25	0.0	0.3	121.40	-1.03	-4.62	1.68	117.71	-30.8	148.51	4.35
	5	7	9:08	4148	155.2	5832209	2509634	42.7191	1348	1348.2	1347.9				1348	120.04	0.0	0.3	120.17	-0.81	-3.01	1.09	117.71	-31.5	149.21	5.04
	4	8	8:55	4640	159.0	5832409	2509186	42.7173	1330.5	1328.7	1329.6				1329.6	118.40	0.0	0.3	118.50	-0.65	-1.85	0.67	116.93	-32.1	149.03	4.87
	3	9	8:42	5117	161.0	5832697	2508805	42.7147	1319.9	1325	1324.2				1324.6	117.96	0.0	0.3	118.02	-0.41	-1.23	0.45	117.07	-32.7	149.77	5.61
	2	10	8:27	5679	163.0	5832993	2508328	42.7121	1280	1279.2	1281.7				1280.3	114.01	0.0	0.2	114.04	-0.17	-0.62	0.22	113.71	-33.4	147.11	2.95
	1 (Base)	11	8:15	6216	165.0	5833209	2507836	42.7101	1239	1235.9	1234.6	1234.3			1234.5	109.93	0.0	0.2	109.93	0.00	0.00	0.00	110.16	-34.0	144.16	0.00
	12	12	11:07	6749	167.0	5833477	2507375	42.7077	1191.7	1191.2	1191.1				1191.4	106.09	0.0	0.2	105.97	0.22	0.62	-0.22	106.80	-34.9	141.70	-2.46
	13	13	11:15	7270	174.0	5833750	2506932	42.7053	1148.1	1148.3	1149.3				1148.2	102.25	0.0	0.2	102.10	0.44	2.78	-1.01	104.51	-35.8	140.31	-3.85
	14	14	12:12	8386	182.0	5834330	2505980	42.7	1114.5	1114.8	1116.6				1114.6	99.26	0.0	0.2	98.96	0.91	5.25	-1.90	103.40	-36.7	140.10	-4.07
	15	15	12:30	9375	181.0	5834722	2505072	42.6965	1124.5	1123.6	1123.9				1123.8	100.07	0.0	0.0	99.81	1.22	4.94	-1.79	104.21	-37.5	141.71	-2.45
	16	16	12:50	10166	181.0	5835141	2504401	42.6927	1131.8	1130	1132				1131.9	100.80	0.0	0.0	100.57	1.56	4.94	-1.79	105.31	-38.3	143.61	-0.55
	17	17	1:00	10963	181.0	5835365	2503636	42.6907	1133.7	1135.5	1135.5				1135.5	101.12	0.0	0.0	100.91	1.74	4.94	-1.79	105.82	-39.0	144.82	0.66
Base Station Readings			*8:15*		*165.0*	*5833209*	*2507836*	*42.7101*	*1239*	*1235.9*	*1234.6*	*1234.3*			*1234.5*	*109.93*										
			9:30						*1235.4*	*1232.7*	*1232.3*				*1232.5*	*109.75*										
			11:00						*1235.7*	*1236.6*	*1235.6*				*1235.6*	*110.03*										
			12:05						*1238*	*1234.5*	*1238*				*1238*	*110.24*										
			1:22						*1236.4*	*1235.8*	*1234.7*				*1236.3*	*110.09*										

PALMSIDE ROAD GRAVITY DATA

Date	Field Stations	Stations	Time	Position (m)	Elevation (m)	Northing	Easting	Latitude	Dial Readings						Av. Reading	Measured g (mgal)	Terrain Correction		Data Corrections				Corrected g (mgal)	Regional g (mgal)	Residual g (mgal)	Anomalies (mgal)
									Reading 1	Reading 2	Reading 3	Reading 4	Reading 5	Reading 6			Inner	Outer	Drift	Latitude	Free-air	Bouguer				
29/5/97	14	1	11:30	0	273.0	5825475	2509250	42.7798	1232.8	1234.9	1233.5	1232.1			1232.8	109.78	0.0	0.8	109.34	-2.74	30.86	-11.19	127.07	-24.0	151.07	0.84
	13	2	11:12	324	255.0	5825695	2509012		1245.8	1243.5	1243.5				1243.5	110.73	0.0	0.8	110.31	-2.56	25.31	-9.18	124.65	-24.3	148.95	-1.28
	8	3	10:00	927	231.0	5826184	2508660		1265.5	1265.8	1266				1265.8	112.72	0.0	0.8	112.26	-2.17	17.90	-6.49	122.26	-24.7	146.96	-3.28
	7	4	9:55	1524	215.0	5826588	2508220		1282.8	1282.9	1283.1				1282.9	114.25	0.0	0.8	113.78	-1.84	12.96	-4.70	120.95	-25.5	146.45	-3.79
	6	5	9:47	2050	200.0	5826976	2507865		1305.7	1304.5	1304.7				1304.6	116.17	0.0	0.7	115.70	-1.53	8.33	-3.02	120.22	-26.3	146.52	-3.71
	5	6	9:00	2709	198.0	5827393	2507354		1319.6	1318	1317.7				1317.9	117.36	0.0	0.7	117.08	-1.19	7.72	-2.80	121.53	-27.0	148.53	-1.70
	4	7	8:43	3358	168.0	5828042	2507350		1379	1378.6	1379.6				1379.1	122.81	0.0	0.7	122.63	-0.66	-1.54	0.56	121.68	-28.0	149.68	-0.55
	3	8	8:34	3863	170.0	5828293	2506912		1374.1	1375	1375.5				1375.3	122.47	0.0	0.6	122.35	-0.46	-0.93	0.34	121.90	-28.6	150.50	0.26
	2	9	8:24	4367	172.0	5828572	2506492		1362.7	1363.7	1363.1				1363.2	121.39	0.0	0.5	121.33	-0.24	-0.31	0.11	121.40	-29.4	150.80	0.56
	1 (Base)	10	8:14	4993	173.0	5828864	2505939	42.7492	1346.4	1345.8	1345.6				1345.7	119.83	0.0	0.4	119.83	0.00	0.00	0.00	120.23	-30.0	150.23	0.00
	19	11	1:09	5602	176.0	5829174	2505415		1335.4	1334.4	1336.1	1334.6			1334.5	118.84	0.0	0.4	118.45	0.25	0.93	-0.34	119.67	-30.8	150.47	0.24
	20	12	1:18	6079	180.0	5829427	2505010		1331.8	1328.8	1330.4	1328.5			1328.7	118.32	0.0	0.4	117.93	0.46	2.16	-0.78	120.13	-31.6	151.73	1.50
	21	13	1:31	6928	187.8	5829837	2504267		1310.3	1311.7	1312.3	1312.7	1311		1311.6	116.80	0.0	0.4	116.41	0.79	4.58	-1.66	120.46	-32.4	152.86	2.63
	22	14	1:42	7553	193.6	5830193	2503753		1286.2	1284.4	1285.2	1285.9			1285.4	114.47	0.0	0.3	114.07	1.07	6.36	-2.31	119.54	-33.1	152.64	2.41
	23	15	2:14	8135	199.0	5830494	2503255		1236.8	1238.4	1237.3				1237.5	110.20	0.0	0.3	109.86	1.32	8.02	-2.91	116.62	-33.9	150.52	0.28
	24	16	2:25	8718	199.0	5830805	2502762		1187	1187.6	1187.8				1187.5	105.74	0.0	0.3	105.44	1.57	8.02	-2.91	112.43	-34.5	146.93	-3.30
	25	17	2:43	9585	201.0	5831223	2502002	42.728	1148.9	1145.9	1146.6	1147.5	1149	1144.4	1149.0	102.32	0.0	0.3	102.07	1.91	8.64	-3.13	109.79	-36.2	145.99	-4.25
Base Station Readings			*8:14*		*183.0*	*5828864*	*2505939*		*1346.4*	*1345.8*	*1345.6*				*1345.7*	*119.83*										
			9:36						*1350.1*	*1351*	*1351.4*				*1351.2*	*120.32*										
			10:40						*1350.5*	*1348.3*	*1349.5*	*1351.2*	*1350.2*		*1350.4*	*120.25*										
			11:49						*1353.3*	*1350.8*	*1350.6*				*1350.7*	*120.28*										
			12:57						*1350*	*1349.8*	*1350.3*				*1350.0*	*120.22*										
			1:58						*1350.2*	*1350.3*	*1350*				*1350.2*	*120.23*										
			3:00						*1347.8*	*1347.8*	*1346.8*				*1347.8*	*120.02*										

FLINTOFT ROAD GRAVITY DATA

Date	Field Stations	Stations	Time	Position (m)	Elevation (m)	Northing	Easting	Latitude	Dial Readings						Av. Reading	Measured g (mgal)	Terrain Correction		Drift	Data Corrections		Bouguer	Corrected g (mgal)	Regional g (mgal)	Residual g (mgal)	Anomalies (mgal)
									Reading 1	Reading 2	Reading 3	Reading 4	Reading 5	Reading 6			Inner	Outer		Latitude	Free-air					
27/5/97	*1 (Base)*	1	7:50	0	192.0	5832326	2503277	42.718	1145.3	1146	1144.3				1145.2	101.98	0.0	0.3	101.98	0.00	0.00	0.00	102.28	-36.2	138.48	0.00
	2	2	8:02	499	195.2	5832320	2502778		1140.5	1142.1	1139.3	1140.6			1140.6	101.57	0.0	0.33	101.54	0.00	0.99	-0.36	102.50	-36.6	139.10	0.62
	3	3	8:10	966	198.2	5832280	2502312		1129.6	1127.4	1127.3				1128.1	100.46	0.0	0.35	100.41	-0.04	1.91	-0.69	101.94	-37.0	138.94	0.46
	4	4	8:23	1432	200.0	5832255	2501847		1114.2	1114.7	1116.5	1112.8	1112		1114.0	99.21	0.0	0.38	99.13	-0.06	2.47	-0.90	101.02	-37.4	138.42	-0.06
	5	5	8:35	2170	209	5832182	2501112		1099.3	1098.8	1099				1099.0	97.87	0.0	0.4	97.76	-0.12	5.25	-1.90	101.38	-37.8	139.18	0.70
	6	6	8:50	2783	211	5832123	2500501		1088.7	1087.5	1087.8				1088.0	96.89	0.0	0.46	96.74	-0.16	5.86	-2.13	100.77	-38.2	138.97	0.49
	7	7	9:23	3362	215	5832145	2499920		1085.4	1084.6	1085.8				1085.3	96.64	0.0	0.51	96.42	-0.15	7.10	-2.57	101.31	-38.6	139.91	1.43
	8	8	9:30	4118	220.0	5832191	2499161	42.7192	1090	1087.9	1086.5	1086.5			1087.7	96.86	0.0	0.57	96.62	-0.11	8.64	-3.13	102.60	-39.0	141.60	3.12
	9	9	9:42	4525	218.0	5832637	2498763		1097	1098.5	1098.8				1098.1	97.79	0.0	0.54	97.52	0.25	8.02	-2.91	103.42	-39.7	143.12	4.64
	10	10	9:50	4954	219.0	5832787	2498344		1102.8	1102.5	1102				1102.4	98.17	0.0	0.52	97.88	0.37	8.33	-3.02	104.09	-40.3	144.39	5.91
	14	11	10:45	5477	221.0	5833009	2497843		1106.9	1109.6	1110.1	1110.6			1110.1	98.85	0.0	0.5	98.51	0.55	8.95	-3.25	105.27	-41.0	146.27	7.79
	15	12	10:55	6050	227.0	5833135	2497281		1104.6	1104.5	1105.4				1104.8	98.39	0.0	0.49	98.04	0.65	10.80	-3.92	106.07	-41.6	147.67	9.19
	16	13	11:20	6537	224.0	5833340	2496819	42.7088	1093.5	1093.9	1094.2				1093.9	97.41	0.0	0.49	97.05	0.82	9.88	-3.58	104.65	-42.3	146.95	8.47
	17	14	11:28	7034	227.1	5833417	2496328		1081.2	1080.9	1080				1080.7	96.24	0.0	0.49	95.87	0.88	10.83	-3.93	104.14	-42.9	147.04	8.56
	18	15	11:37	7810	231.9	5833585	2495569		1076.1	1075.3	1075.4				1075.6	95.78	0.0	0.49	95.41	1.02	12.32	-4.47	104.77	-43.6	148.37	9.89
	19	16	11:45	8469	236.0	5833805	2494938		1082.6	1079.9	1085.5	1081	1079.7		1082.3	96.37	0.0	0.49	96.00	1.20	13.58	-4.92	106.34	-44.2	150.54	12.06
	20	17	11:55	8980	235.6	5834013	2494457	42.7027	1085.2	1084.1	1085.9				1085.1	96.63	0.0	0.62	96.25	1.36	13.45	-4.88	106.81	-44.9	151.71	13.23
	21	18	12:32	9652	235.1	5834371	2493844		1072.5	1071	1069.8	1067.5	1070		1070.2	95.30	0.0	0.75	94.83	1.65	13.29	-4.82	105.71	-45.5	151.21	12.73
	22	19	12:40	10109	234.7	5834863	2493492		1059	1058.5	1058.8				1058.8	94.28	0.0	0.88	93.79	2.05	13.18	-4.78	105.13	-46.2	151.33	12.85
	23	20	12:50	10415	237.8	5835314	2493300		1038	1036.3	1036.5				1036.4	92.29	0.0	0.85	91.76	2.42	14.14	-5.13	104.04	-46.8	150.84	12.36
	24	21	12:57	10957	243.3	5835652	2492837	42.6879	1029.9	1028.5	1029.9				1029.9	91.71	0.0	0.82	91.16	2.69	15.83	-5.74	104.76	-47.5	152.26	13.78
Base Station Readings			*7:50*		*192.0*	*5832326*	*2503277*		*1145.3*	*1146*	*1144.3*				*1145.2*	*101.98*										
			9:00						*1145.4*	*1146.9*	*1148.2*	*1148*			*1147.1*	*102.15*										
			10:00						*1150.6*	*1147*	*1148*	*1149.2*			*1148.7*	*102.29*										
			11:07						*1150.3*	*1149.8*	*1148.4*	*1148.2*			*1149.2*	*102.33*										
			12:07						*1151.6*	*1149.7*	*1149.3*				*1149.5*	*102.36*										
			13:12						*1153.3*	*1152.5*	*1150.5*	*1151.5*	*1150.9*		*1152.0*	*102.58*										

LOWRY PEAKS ROAD GRAVITY DATA

Date	Field Stations	Stations	Time	Position (m)	Elevation (m)	Northing	Easting	Latitude	Dial Readings							Measured g (mgal)	Terrain Correction		Data Corrections				Corrected g (mgal)	Regional g (mgal)	Residual g (mgal)	Anomalies (mgal)
									Reading 1	Reading 2	Reading 3	Reading 4	Reading 5	Reading 6	Av. Reading		Inner	Outer	Drift	Latitude	Free-air	Bouguer				
25/5/97	6	1	11:00	0	253.0	5822923	2507262	42.8027	1334.9	1338.3	1338.1				1338.2	119.17	0.0	0.8	119.07	-2.45	24.38	-8.84	132.91	-21.5	154.41	4.62
	5	2	10:53	516	224.0	5823230	2506847		1347.4	1346.7	1346.4				1346.8	119.94	0.0	0.7	119.85	-2.20	15.43	-5.60	128.19	-22.0	150.19	0.39
	4	3	10:40	1294	203.0	5823627	2506178		1358	1358.3	1357.9				1358.1	120.94	0.0	0.7	120.87	-1.88	8.95	-3.25	125.34	-22.5	147.84	-1.96
	3	4	10:25	2012	180.0	5823993	2505562		1386.7	1388.3	1382.5	1383.6	1385.1		1385.2	123.36	0.0	0.6	123.31	-1.59	1.85	-0.67	123.50	-23.3	146.80	-2.99
	2	5	10:10	2506	167.0	5824277	2505157		1402.1	1401.1	1401.4				1401.3	124.79	0.0	0.5	124.76	-1.36	-2.16	0.78	122.53	-24.1	146.63	-3.17
	9	6	12:03	3159	156.0	5824320	2504506		1415.1	1415.0					1415.05	126.01	0.0	0.4	124.51	-1.32	-5.55	2.01	120.05	-24.6	144.65	-5.15
	8	7	11:54	3681	159.0	5824363	2503986		1415.1	1415.1					1415.10	126.01	0.0	0.3	124.50	-1.29	-4.63	1.68	120.55	-25.1	145.65	-4.15
	7	8	11:46	4177	161.0	5824438	2503495		1401.4	1405.0					1403.20	124.95	0.0	0.2	123.44	-1.23	-4.01	1.46	119.89	-25.5	145.39	-4.41
	6	9	11:37	4604	161.0	5824514	2503075		1407.4	1405.7					1406.55	125.25	0.0	0.2	123.75	-1.17	-4.01	1.46	120.23	-26.0	146.23	-3.57
	5	10	11:28	5110	164.0	5824761	2502633		1400.5	1403.5					1402.00	124.85	0.0	0.2	123.37	-0.97	-3.09	1.12	120.62	-26.8	147.42	-2.38
	4	11	11:10	5619	167.0	5825060	2502221		1405.9	1405.0					1405.45	125.16	0.0	0.2	123.80	-0.72	-2.16	0.78	121.86	-27.6	149.46	-0.34
	3	12	11:02	6113	170.0	5825356	2501826		1374.2	1374.3					1374.25	122.38	0.0	0.2	121.09	-0.49	-1.23	0.45	119.97	-28.4	148.37	-1.43
	1 (Base)	13	9:55	7159	174.0	5825956	2500969	42.7754	1357.3	1352.5	1352.8				1352.7	120.46	0.0	0.1	120.46	0.00	0.00	0.00	120.60	-29.2	149.80	0.00
	7	14	11:30	7647	174.3	5825915	2500483		1349.9	1352.8	1349	1350.4			1350.5	120.26	0.0	0.1	120.08	-0.03	0.08	-0.03	120.23	-29.5	149.73	-0.07
	8	15	11:40	8131	174.5	5825887	2500000		1336.5	1347.4	1345.2	1343.7	1349.6	1348.2	1346.8	119.93	0.0	0.2	119.69	-0.06	0.16	-0.06	119.89	-29.8	149.69	-0.11
	9	16	11:50	8573	174.7	5825868	2499558		1348	1350.4	1350.8				1350.6	120.27	0.0	0.2	119.98	-0.07	0.23	-0.08	120.20	-30.1	150.30	0.50
	10	17	11:58	9073	175.0	5825842	2499059		1356.1	1355.1	1356.4				1356.3	120.78	0.0	0.2	120.44	-0.09	0.31	-0.11	120.71	-30.5	151.21	1.41
	11	18	12:10	9686	175.0	5826161	2498535		1344.1	1342.6	1342.2				1342.4	119.54	0.0	0.2	119.14	0.17	0.31	-0.11	119.68	-31.3	150.98	1.18
	12	19	12:15	10366	175.0	5826501	2497947		1325.8	1327.4	1320.1	1326.4			1326.5	118.13	0.0	0.2	117.70	0.44	0.31	-0.11	118.54	-32.0	150.54	0.74
	13	20	12:40	11467	177.0	5827246	2497136		1278.8	1278.6	1280.8	1280.3	1278.4		1279.4	113.93	0.0	0.3	113.52	1.04	0.93	-0.34	115.45	-33.9	149.35	-0.45
	14	21	12:50	12159	186.0	5827521	2496501		1261.4	1261.2	1260.9				1261.3	112.32	0.0	0.4	111.95	1.27	3.70	-1.34	115.98	-34.7	150.68	0.88
	15	22	12:58	12689	191.4	5827767	2496038		1241.7	1241.3	1241.6				1241.5	110.56	0.0	0.5	110.23	1.46	5.37	-1.95	115.61	-35.4	151.01	1.22
	16	23	1:10	13360	197.0	5828096	2495453		1215.9	1209.8	1225.4	1225.3			1225.4	109.12	0.0	0.6	108.84	1.73	7.10	-2.57	115.70	-36.2	151.90	2.10
	17	24	1:55	14385	198.0	5828493	2494508	42.7524	1205	1212.8	1202.2	1207.3	1212.4	1213.1	1212.8	108.00	0.0	0.5	107.80	2.05	7.41	-2.69	115.07	-36.4	151.47	1.67
Base Station Readings			*9:55*			*5825956*	*2500969*		*1357.3*	*1352.5*	*1352.8*				*1352.7*	*120.46*			*120.46*							
			11:18						*1354.1*	*1356.6*	*1353.4*	*1354*			*1354.1*	*120.58*			*120.46*							
			12:25						*1354.9*	*1357.8*	*1358.4*				*1358.1*	*120.94*			*120.46*							
			1:30						*1357*	*1354.7*	*1356*	*1354.8*			*1354.8*	*120.64*			*120.46*							
			2:45						*1354.8*	*1355.2*	*1355.8*				*1355.3*	*120.69*			*120.46*							
			4:20						*1357.9*	*1360.5*	*1351.8*	*1351.7*			*1351.8*	*120.38*			*120.46*							

KAIWARA ROAD GRAVITY DATA

Date	Field Stations	Stations	Time	Position (m)	Elevation (m)	Northing	Easting	Latitude	Dial Readings							Measured g (mgal)	Terrain Correction		Drift	Data Corrections			Corrected g (mgal)	Regional g (mgal)	Residual g (mgal)	Anomalies (mgal)
									Reading 1	Reading 2	Reading 3	Reading 4	Reading 5	Reading 6	Av. Reading		Inner	Outer		Latitude	Free-air	Bouguer				
29/5/97	18	1	12:40	0	175.0	5822265	2505223	42.8086	1529.5	1530.2	1531.1				1530.3	136.27			136.33	-2.14	-8.64	3.13	128.68	-21.6	150.28	7.29
	17	2	12:30	725	183.0	5822780	2505734		1460	1461.7	1459.5	1458.7			1460.0	130.01	0.0	0.0	130.06	-1.72	-6.17	2.24	124.40	-22.2	146.60	3.61
	16	3	11:19	1682	203.0	5823627	2506178		1379.5	1382.3	1381.4	1381.5			1381.2	122.99	0.0	0.8	123.03	-1.04	0.00	0.00	121.99	-22.5	144.49	1.50
	15	4	12:10	2350	209.0	5824073	2506676		1354.1	1353	1352.4				1353.2	120.50	0.0	0.7	120.53	-0.68	1.85	-0.67	121.03	-23.0	144.03	1.04
	11	5	10:27	3210	203.0	5824910	2506871	42.7848	1336	1335	1335.7				1335.6	118.93	0.0	0.7	119.00	0.00	0.00	0.00	119.00	-24.0	143.00	0.00
	10	6	10:19	3872	210.0	5825328	2507385		1315.9	1314.9	1317	1315.8			1315.9	117.18	0.0	0.7	117.23	0.34	2.16	-0.78	118.95	-24.4	143.35	0.35
	9	7	10:09	4706	225.0	5825776	2508088		1278.5	1278.8	1277.8				1278.4	113.84	0.0	0.7	113.88	0.70	6.79	-2.46	118.91	-24.6	143.51	0.51
	8	8	10:00	5408	231.0	5826184	2508660		1265.5	1265.8	1266				1265.8	112.72	0.0	0.7	112.75	1.03	8.64	-3.13	119.28	-24.7	143.98	0.99
	12	9	11:00	6065	223.0	5826596	2509171	42.7697	1285.5	1284.9	1285				1285.1	114.44	0.0	0.6	114.50	1.36	6.17	-2.24	119.80	-25.0	144.80	1.80
Base Station Readings			*9:36*			*5828864*	*2505939*		*1350.1*	*1351*	*1351.4*				*1350.8*	*120.29*										
(same base station as Iverachs			*10:40*						*1350.5*	*1348.3*	*1349.5*	*1351.2*	*1350.2*		*1349.9*	*120.21*										
Road)			*11:49*						*1353.3*	*1350.8*	*1350.6*				*1350.7*	*120.28*										
			12:57						*1350*	*1349.8*	*1350.3*				*1350.0*	*120.22*										

PAHAU RESERVE ROAD GRAVITY DATA

Date	Field Stations	Stations	Time	Position (m)	Elevation (m)	Northing	Easting	Latitude	Dial Readings							Measured g (mgal)	Terrain Correction		Drift	Data Corrections			Corrected g (mgal)	Regional g (mgal)	Residual g (mgal)	Anomalies (mgal)
									Reading 1	Reading 2	Reading 3	Reading 4	Reading 5	Reading 6	Av. Reading		Inner	Outer		Latitude	Free-air	Bouguer				
5/13/1997	10	1	1:00	0	137	5819795	2500175		1607	1607.5	1608.4	1607			1607.2	143.1181917	0	0.3	143.25	-3.01	-17.93	6.50	129.11	-21.0	150.11	1.72
	9	2	12:22	1300	148	5820914	2499514		1526	1524.6	1522	1523.4	1524.3		1523.8	135.69439	0	0.18	135.64	-2.11	-14.54	5.27	124.44	-22.7	147.14	-1.25
	8	3	12:10	2127	153	5821615	2499075		1501.1	1500.9	1501.6	1502			1501.4	133.69967	0	0.17	133.58	-1.54	-12.99	4.71	123.93	-24.1	148.03	-0.36
	7	4	11:56	3207	160	5822230	2498187		1457.1	1457.5	1464.5	1462.2	1457.2	1457.7	1457.4	129.7792438	0	0.16	129.59	-1.04	-10.83	3.93	121.80	-25.5	147.30	-1.09
	6	5	11:45	3914	166	5822361	2497492		1461.5	1460	1459.9	1458			1459.9	129.9996425	0	0.15	129.76	-0.94	-8.98	3.26	123.25	-26.1	149.35	0.96
	5	6	11:00	4963	171	5822712	2496504		1440.2	1440.5	1435	1435.7	1435.3	1435.2	1435.3	127.813465	0	0.15	127.57	-0.65	-7.44	2.70	122.32	-27.0	149.32	0.93
	4	7	10:45	5748	178.3	5822904	2495743		1417.5	1419.5	1417	1417.6			1417.4	126.2165017	0	0.15	126.03	-0.50	-5.18	1.88	122.38	-28.0	150.38	1.98
	3	8	10:30	6780	186	5823183	2494749		1387.7	1386.3	1388.8	1388.1			1388.2	123.61921	0	0.15	123.49	-0.27	-2.81	1.02	121.58	-28.9	150.48	2.08
	2	9	10:14	7564	192	5823414	2494000		1341.8	1340.7	1343.1	1343.1			1343.1	119.603055	0	0.18	119.53	-0.09	-0.96	0.35	119.02	-30.9	149.92	1.53
	1 (Base)	10	9:56	8222	195.1	5823520	2493350	42.7972	1318.3	1319.1	1318	1318.5			1318.3	117.3916467	0	0.2	117.39	0.00	0.00	0.00	117.59	-30.8	148.39	0.00
	11	11	1:35	9275	202	5824043	2492437		1270	1267.5	1266.4	1267.5			1267.5	112.870875	0	0.2	113.09	0.42	2.13	-0.77	115.07	-32.0	147.07	-1.32
	12	12	1:55	10112	211	5824274	2491632		1219.2	1221.3	1214.1	1220			1220.2	108.6558417	0	0.25	108.88	0.61	4.91	-1.78	112.86	-33.0	145.86	-2.53
	13	13	2:10	11076	220	5824523	2490701		1187	1187.9	1188.6	1188.3			1188.0	105.7869475	0	0.3	106.01	0.81	7.65	-2.79	112.02	-34.0	146.02	-2.37
	14	14	2:20	12178	234.7	5824846	2489647		1144	1142.9	1143.3	1140.9			1142.8	101.7641138	0	0.3	101.99	1.07	12.22	-4.43	111.15	-35.0	146.15	-2.25
	15	15	2:54	12909	242	5825040	2488942		1104	1103.6	1108.5	1107.7	1108	1110.2	1107.0	98.57835	0	0.35	98.76	1.23	14.47	-5.25	109.56	-36.0	145.56	-2.83
	16	16	3:17	13819	255	5825287	2488067		1056.6	1056	1052.5	1050.9	1055.6	1059.2	1055.1	93.95962333	0	0.4	94.09	1.43	18.43	-6.70	107.70	-37.0	144.70	-3.69
	17	17	3:36	14667	263	5825537	2487256		1017.7	1016.9	1019.8	1018.1			1018.1	90.66403125	0	0.55	90.75	1.63	20.95	-7.60	106.28	-38.0	144.28	-4.11
	18	18	3:50	16108	284	5826177	2485965		950.3	951	949.9	955			950.4	84.63312	0	0.7	84.69	2.15	27.43	-9.95	105.02	-39.0	144.02	-4.37
	Base Station Readings		*9:56*						*1318.3*	*1319.1*	*1318*	*1318.5*			*1318.3*	*117.3916467*										
			11:25						*1320.5*	*1321*	*1322.1*	*1322.1*			*1322.1*	*117.733005*										
			1:19						*1311.6*	*1311.4*	*1318*	*1317.7*	*1318*		*1315.8*	*117.1690217*										
			2:35						*1317.7*	*1318*	*1314*	*1315*	*1316*	*1314*	*1315.8*	*117.1705058*										
			4:10						*1318.2*	*1316.6*	*1312.4*	*1311.6*	*1319.5*	*1318.3*	*1318.2*	*117.3812575*										

STATE HIGHWAY 7 GRAVITY DATA

Date	Field Stations	Stations	Time	Position (m)	Elevation (m)	Northing	Easting	Latitude	Dial Readings							Measured g (mgal)	Terrain Correction		Drift	Data Corrections			Corrected g (mgal)	Regional g (mgal)	Residual g (mgal)	Anomalies (mgal)
									Reading 1	Reading 2	Reading 3	Reading 4	Reading 5	Reading 6	Av. Reading		Inner	Outer		Latitude	Free-air	Bouguer				
10/6/1997	15	1	12:00	0	187.0	5815630	2491382	42.8681	1581	1581					1581	140.79	0.0	0.5	140.53	-10.56	-2.22	0.81	129.05	-19.0	148.05	3.31
	14	2	11:47	1099	189.0	5816505	2492047		1556.1	1555.7	1557.6	1557.3			1557.5	138.70	0.0	0.4	138.54	-9.85	-1.60	0.58	128.07	-20.7	148.77	4.03
	13	3	11:37	2609	190.0	5817792	2492836		1517.5	1516.2	1516.6	1516.4			1516.4	135.04	0.0	0.2	134.96	-8.81	-1.30	0.47	125.53	-22.5	148.03	3.28
	12	4	11:28	4431	186.0	5819378	2493734		1504.5	1504.5					1504.5	133.98	0.0	0.2	133.98	-7.53	-2.53	0.92	125.01	-24.2	149.21	4.46
	11	5	10:57	6421	181.9	5821090	2494749		1474.4	1475.1	1473.6	1473	1472.9	1472.8	1473.6	131.22	0.0	0.2	131.37	-6.14	-3.81	1.38	122.97	-26.0	148.97	4.23
	10	6	10:49	7484	180.0	5821998	2495301		1466.3	1466.3					1466.3	130.57	0.0	0.2	130.72	-5.41	-4.37	1.59	122.69	-27.0	149.69	4.95
	9	7	10:40	8492	178.3	5822904	2495743		1448.8	1450.2	1450.2				1450.2	129.14	0.0	0.2	129.30	-4.68	-4.91	1.78	121.64	-28.0	149.64	4.90
	8	8	10:32	9440	177.3	5823679	2496288		1442.3	1442.1					1442.2	128.43	0.0	0.1	128.59	-4.05	-5.20	1.89	121.36	-28.8	150.16	5.41
	7	9	10:22	10272	176.5	5824417	2496672		1432.6	1433.2	1433.6				1433.4	127.64	0.0	0.1	127.81	-3.45	-5.46	1.98	120.98	-29.6	150.58	5.84
	6	10	9:59	10943	175.8	5824971	2497052		1425.8	1426.4	1426				1426.1	126.99	0.0	0.1	127.13	-3.00	-5.67	2.06	120.62	-30.4	151.02	6.28
	5	11	9:49	11745	175.0	5825691	2497405		1410.1	1408.8	1409.7				1409.9	125.55	0.0	0.1	125.66	-2.42	-5.93	2.15	119.58	-31.2	150.78	6.04
	4	12	9:41	12720	175.0	5826501	2497947		1359.7	1359.7					1359.7	121.08	0.0	0.2	121.16	-1.77	-5.93	2.15	115.82	-32.0	147.82	3.08
	3	13	9:34	13630	182.9	5827298	2498386		1312.2	1312.3					1312.3	116.86	0.0	0.2	116.92	-1.12	-3.49	1.26	113.77	-32.8	146.57	1.83
	2	14	9:24	14501	189.0	5828036	2498850		1271.3	1270.7	1270.8				1270.9	113.17	0.0	0.3	113.20	-0.53	-1.61	0.58	111.90	-33.5	145.40	0.66
	1 (Base)	15	9:15	15247	194.2	5828687	2499214	42.7508	1237.8	1239.4	1238.1				1238	110.24	0.0	0.3	110.24	0.00	0.00	0.00	110.54	-34.2	144.74	0.00
	16	16	12:27	15874	201.5	5829313	2499181		1220	1221	1220.1				1220.1	108.65	0.0	0.3	108.25	0.51	2.25	-0.82	110.46	-35.1	145.56	0.81
	17	17	12:35	16477	208.5	5829916	2499191		1192.1	1191.4	1191.9				1192	106.15	0.0	0.3	105.74	0.99	4.41	-1.60	109.80	-36.0	145.80	1.05
	18	18	12:42	17328	218.0	5830763	2499263		1150.7	1150.5	1150.3				1150.5	102.45	0.0	0.2	102.05	1.68	7.34	-2.66	108.62	-36.9	145.52	0.77
	19	19	12:51	18083	225.0	5831518	2499253		1113.2	1111.5	1113.4				1113.3	99.14	0.0	0.4	98.73	2.29	9.50	-3.45	107.47	-38.0	145.47	0.73
	20	20	12:59	18762	220.0	5832191	2499161	42.7192	1113.3	1113.5					1113.4	99.15	0.0	0.6	98.74	2.83	7.96	-2.89	107.22	-39.0	146.22	1.47
27/5/97	11	21		19561	212.0	5832987	2499097		1093.4	1090.5	1088.7	1089.8			1090.6	99.41	0.0	0.5	99.26	3.48	5.49	-1.99	106.74	-40.1	146.84	2.09
	12	22		19948	210.0	5833296	2498863		1092.5	1093.7	1093.7				1093.7	99.68	0.0	0.5	99.53	3.73	4.88	-1.77	106.84	-40.7	147.54	2.80
	13	23		20376	209.0	5833686	2498687	42.7057	1093.1	1093.5	1092.9				1093.2	99.64	0.0	0.5	99.47	4.04	4.57	-1.66	106.88	-41.3	148.18	3.44
Base Station Readings			*9:15*		*194.2*	*5828687*	*2499214*		*1237.8*	*1239.4*	*1238.1*				*1238*	*110.24*										
			10:12						*1236*	*1235.9*					*1236*	*110.07*										
			11:12						*1236.6*	*1236.4*					*1236.5*	*110.11*										
			12:17						*1241.6*	*1242.4*	*1242.5*				*1242.5*	*110.64*										
			13:07						*1241.6*	*1242.2*	*1242.6*	*1242.9*			*1242.6*	*110.65*										

STATE HIGHWAY 7 & 70 GRAVITY DATA

Date	Field Station	Station	Time	Position (m)	Elevation (m)	Northing	Easting	Latitude	Dial Readings							Measured g (mgal)	Terrain Correction		Data Corrections			Bouguer	Corrected g (mgal)	Regional g (mgal)	Residual g (mgal)	Anomalies (mgal)
									Reading 1	Reading 2	Reading 3	Reading 4	Reading 5	Reading 6	Av. Reading		Inner	Outer	Drift Corr.	Latitude	Free-air					
6/10/1997	15	1	12:00	0	187	5815630	2491382	42.8681	1581	1581					1581	140.79	0.0	0.5	140.53	-10.56	-2.22	0.81	129.05	-19.0	148.05	3.31
	14	2	11:47	1099	189	5816505	2492047		1556.1	1555.7	1557.6	1557.3			1557.5	138.70	0.0	0.4	138.54	-9.85	-1.60	0.58	128.07	-20.7	148.77	4.03
	13	3	11:37	2609	190.0	5817792	2492836		1517.5	1516.2	1516.6	1516.4			1516.4	135.04	0.0	0.2	134.96	-8.81	-1.30	0.47	125.53	-22.5	148.03	3.28
	12	4	11:28	4431	186.0	5819378	2493734		1504.5	1504.5					1504.5	133.98	0.0	0.2	133.98	-7.53	-2.53	0.92	125.01	-24.2	149.21	4.46
	11	5	10:57	6421	181.9	5821090	2494749		1474.4	1475.1	1473.6	1473	1472.9	1472.8	1473.6	131.22	0.0	0.2	131.37	-6.14	-3.80	1.38	122.98	-26.0	148.98	4.23
	10	6	10:49	7484	180.0	5821998	2495301		1466.3	1466.3					1466.3	130.57	0.0	0.2	130.72	-5.41	-4.38	1.59	122.68	-27.0	149.68	4.94
	9	7	10:40	8492	178.3	5822904	2495743		1448.8	1450.2	1450.2				1450.2	129.14	0.0	0.2	129.30	-4.68	-4.91	1.78	121.64	-28.0	149.64	4.90
	8	8	10:32	9440	177.3	5823679	2496288		1442.3	1442.1					1442.2	128.43	0.0	0.1	128.59	-4.05	-5.22	1.89	121.35	-28.8	150.15	5.40
	7	9	10:22	10272	176.5	5824417	2496672		1432.6	1433.2	1433.6				1433.4	127.64	0.0	0.1	127.81	-3.45	-5.46	1.98	120.98	-29.6	150.58	5.84
	6	10	9:59	10943	175.8	5824971	2497052		1425.8	1426.4	1426				1426.1	126.99	0.0	0.1	127.13	-3.00	-5.66	2.06	120.62	-30.4	151.02	6.27
	5	11	9:49	11745	175.0	5825691	2497405		1410.1	1408.8	1409.7				1409.9	125.55	0.0	0.1	125.66	-2.42	-5.93	2.15	119.58	-31.2	150.78	6.04
	4	12	9:41	12720	175.0	5826501	2497947		1359.7	1359.7					1359.7	121.08	0.0	0.2	121.16	-1.77	-5.93	2.15	115.82	-32.0	147.82	3.08
	3	13	9:34	13630	182.9	5827298	2498386		1312.2	1312.3					1312.3	116.86	0.0	0.2	116.92	-1.12	-3.49	1.26	113.77	-32.8	146.57	1.83
	2	14	9:24	14501	189.0	5828036	2498850		1271.3	1270.7	1270.8				1270.9	113.17	0.0	0.3	113.20	-0.53	-1.60	0.58	111.90	-33.5	145.40	0.66
	1 (Base)	15	9:15	15247	194.2	5828687	2499214	42.7508	1237.8	1239.4	1238.1				1238	110.24	0.0	0.3	110.24	0.00	0.00	0.00	110.54	-34.2	144.74	0.00
	2	16	13:19	16298	197.7	5829363	2500018		1215.2	1216.5	1215.5				1215.4	108.23	0.0	0.3	107.82	0.55	1.07	-0.39	109.35	-34.5	143.85	-0.90
	3	17	13:30	17195	200.6	5829962	2500686		1193.4	1194.4	1195.6	1196	1196.2		1195.9	106.49	0.0	0.3	106.09	1.03	1.97	-0.72	108.67	-34.9	143.57	-1.17
	4	18	13:37	18037	203.0	5830550	2501232		1177.1	1176.8	1176.5				1176.8	104.79	0.0	0.3	104.38	1.51	2.72	-0.98	107.92	-35.2	143.12	-1.62
	5	19	13:49	19060	202.0	5831223	2502002		1164.7	1162.8	1163.4	1164			1163.7	103.63	0.0	0.3	103.22	2.05	2.41	-0.87	107.10	-35.5	142.60	-2.14
	6	20	14:13	20112	197.0	5831941	2502771		1170.1	1170.8	1170.5				1170.5	104.23	0.0	0.3	103.82	2.63	0.86	-0.31	107.30	-35.9	143.20	-1.54
	7	21	14:33	20748	192.0	5832326	2503277		1175.6	1175.5					1175.6	104.69	0.0	0.3	104.30	2.94	-0.68	0.25	107.11	-36.2	143.31	-1.44
	8	22	14:42	22003	188.0	5833203	2504175		1162.4	1160.4	1161.3	1161.6			1161.4	103.42	0.0	0.2	103.05	3.65	-1.91	0.69	105.68	-36.4	142.08	-2.66
	9	23	14:50	23049	185.0	5833896	2504958		1140.5	1139	1139.2				1139.1	101.44	0.0	0.1	101.08	4.21	-2.84	1.03	103.58	-36.6	140.18	-4.56
	10	24	15:01	24010	181.5	5834590	2505623		1134.2	1132.1	1130.9	1136.6	1135.1	1135	1135.1	101.08	0.0	0.0	100.75	4.77	-3.92	1.42	103.05	-36.8	139.85	-4.89
	11	25	15:09	24407	181.5	5834944	2505803	42.6945	1130.1	1130.2					1130.2	100.64	0.0	0.0	100.32	5.06	-3.92	1.42	102.92	-37.0	139.92	-4.83
Base Station Readings			*9:15*		*194.2*	*5828687*	*2499214*		*1237.8*	*1239.4*	*1238.1*				*1238*	*110.24*										
			10:12						*1236*	*1235.9*					*1236*	*110.07*										
			11:12						*1236.6*	*1236.4*					*1236.5*	*110.11*										
			12:17						*1241.6*	*1242.4*	*1242.5*				*1242.5*	*110.64*										
			13:07		*194.2*	*5828687*	*2499214*		*1241.6*	*1242.2*	*1242.6*	*1242.9*			*1242.6*	*110.65*										
			14:23						*1242.7*	*1242.1*	*1243.2*	*1242.3*			*1242.6*	*110.65*										
			15:22						*1242.1*	*1240.3*	*1241.5*	*1240.8*	*1241.6*		*1241.3*	*110.54*										

Figure 2.9: Structure contours of the Lowry Peaks Anticline

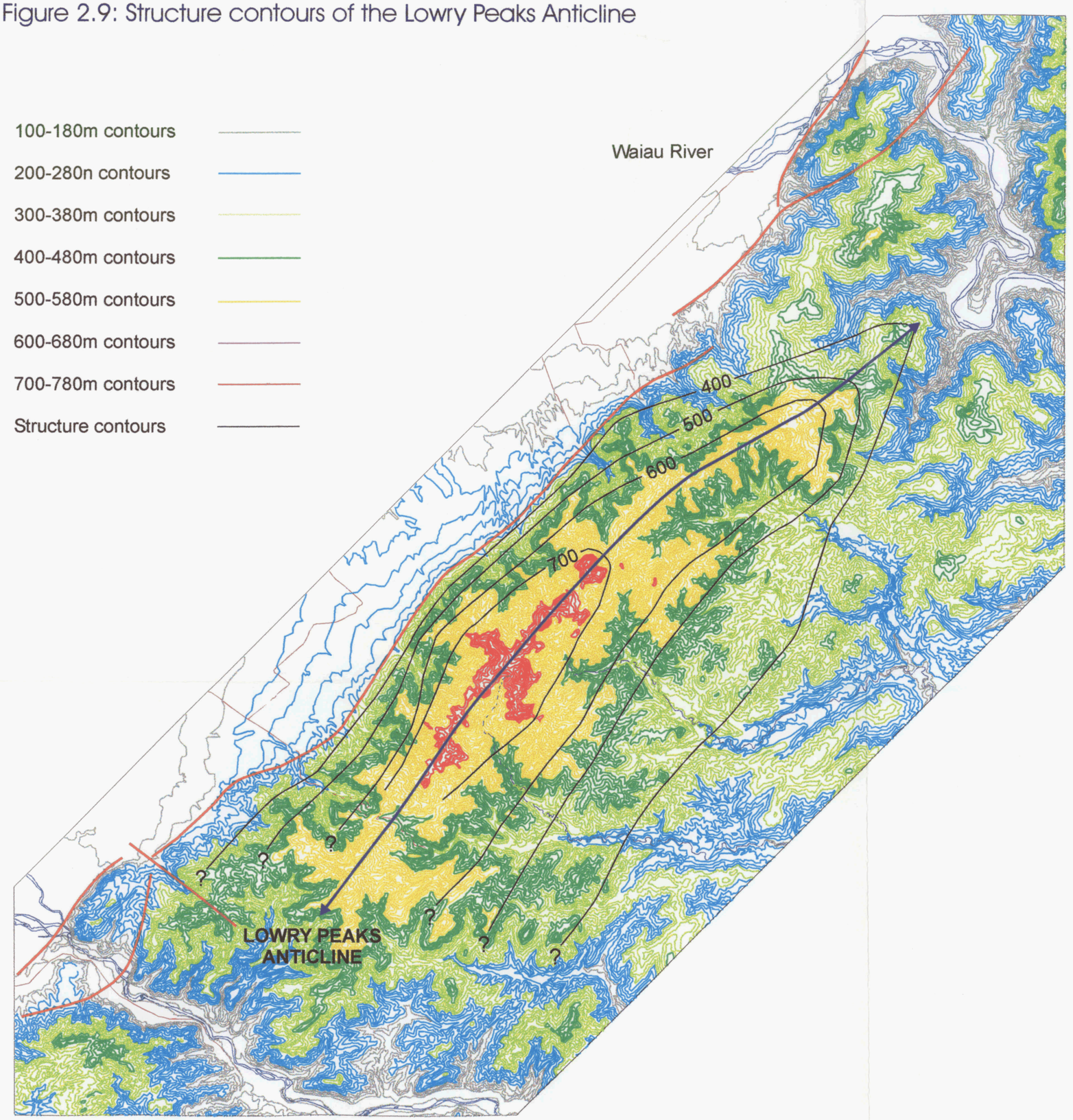

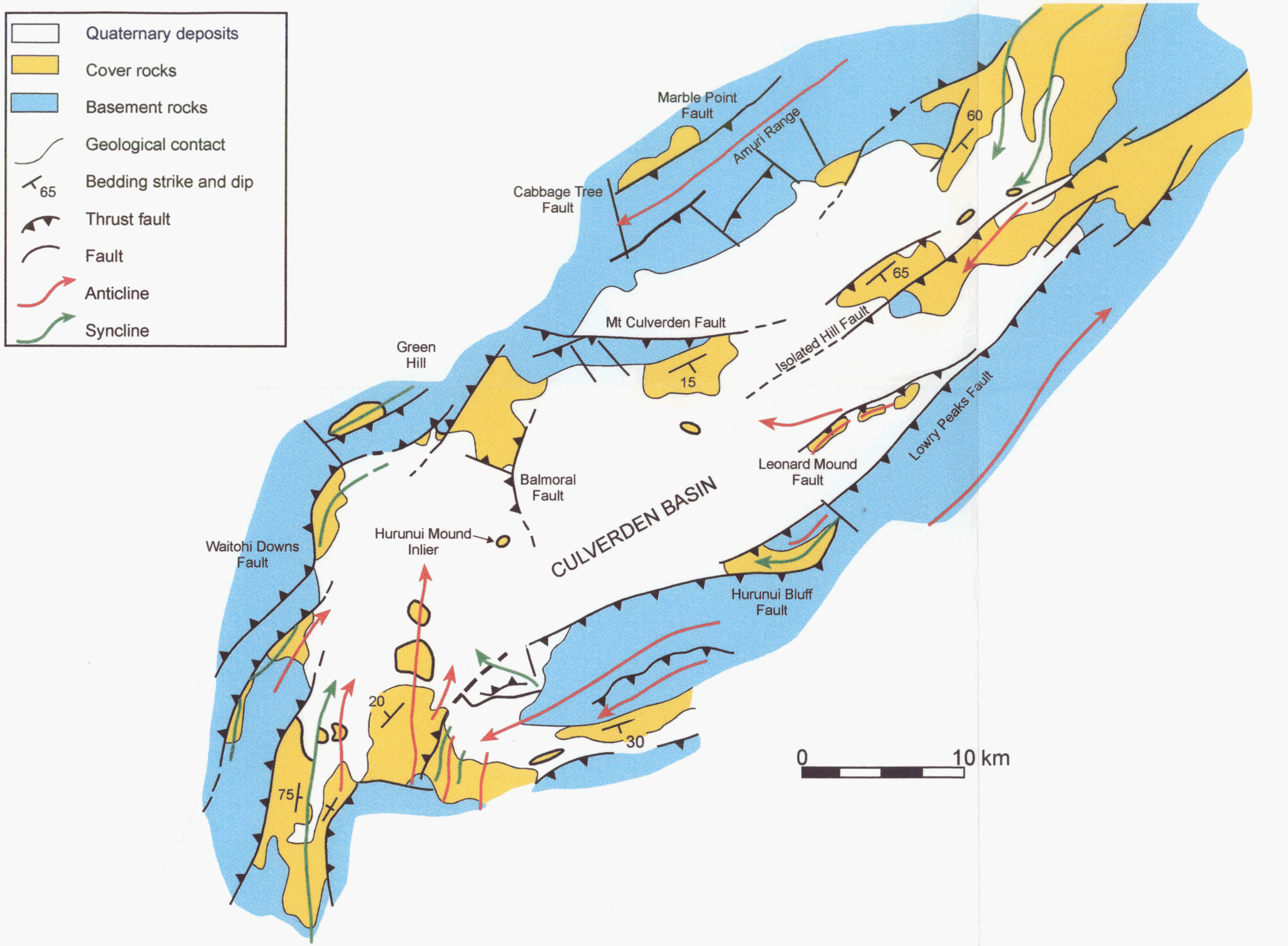

FIGURE 2.15: Summary map of the major structural elements of the western margin of Culverden Basinin relation to those along the eastern margin (after Nicol, 1991; Mould, 1992; Litchfield, 1995; this study)